LIGHTNING PHENOMENOLOGY NOTES
NOTE 3
5 February 1982

MEASUREMENTS OF ELECTROMAGNETIC PROPERTIES OF LIGHTNING WITH 10 NANOSECOND RESOLUTION (REVISED)

C.E. Baum, E.L. Breen, and J.P. O'Neill
Air Force Weapons Laboratory

C.B. Moore and D.L. Hall
New Mexico Institute of Mining and Technology

ABSTRACT

This paper presents electromagnetic data recorded from lightning strikes. The data analysis reveals general characteristics of fast electromagnetic fields measured at the ground including rise times, amplitudes, and time patterns. A look at the electromagnetic structure of lightning shows that the shortest rise times in the vicinity of 30 ns are associated with leader streamers. Lightning location is based on electromagnetic field characteristics and is compared to a nearby whole-sky camera. The fields from both leaders and return strokes have been measured and are discussed.

The data were obtained during 1978 and 1979 from lightning strikes occurring within 5 kilometers of an underground metal instrumentation room located on South Baldy peak near Langmuir Laboratory, New Mexico. The computer controlled instrumentation consisted of sensors previously used for measuring the nuclear electromagnetic pulse (EMP) and analog-digital recorders with 10 ns sampling, 256 levels of resolution, and 2 kilobytes of internal memory.

FOREWORD

This paper represents an expanded version of a previous paper with the same title appearing in a symposium proceedings in 1980 [6]. The purpose of this revision is primarily to include more of the data taken in the summers of 1978 and 1979 that were not prepared for the earlier version. Section 6 (the earlier section 5) now contains 9 analyzed waveform sets (compared to the previous 4 which are retained). In addition, the various pulses in the waveform sets are tabulated in digital format so that the reader may get a better understanding of the structure of these fast pulses. Also, the peak values of various parameters in the pulses are tabulated so that these numbers do not need to be read from the graphs. Finally, the graphical procedure for estimating direction to lightning pulses has been improved, and a new section 4 has been added to discuss this.

CONTENTS

I. INTRODUCTION

In the summers of 1978 and 1979 a set of measurements of the electromagnetic fields from natural lightning was made near the top of South Baldy peak (elevation 3275 m) which also houses Langmuir Laboratory near Socorro, New Mexico, U.S.A. As will be discussed in this paper the data consist of time waveforms of about 20 μs duration at a 10 ns sample spacing for the three electromagnetic field components (one electric and two magnetic) which exist adjacent to a conducting ground plane on top of the "iron Kiva" (or Kiva) (our screen room buried in the top of the mountain) and the surrounding earth surface (see fig. 1.1). The details of the instrumentation system are discussed in other papers [5,7].

As background, these measurements resulted from some interest in the difference between lightning and the nuclear electromagnetic pulse. For nuclear detection purposes it is desirable to reliably detect a nuclear EMP event without false triggering by lightning. The ARGUS-1A detector system was designed with the high altitude EMP environment in mind [2]. For this purpose magnetic (loop) sensors were used to avoid the low-frequency electric field from lightning and local static charging effects. In addition the sensors respond to the derivative of the field to emphasize the high frequencies present in the high-altitude nuclear EMP. Essentially one is looking for a pulse with 10 ns to 100 ns important characteristic times.

In order to understand the sensitivity of the ARGUS-1A to lightning two things were done. First the detectors were placed on South Baldy peak and their response to lightning monitored. Second, and more important for this paper, the fast transient characteristics of the transient electromagnetic fields (in time derivative form) were measured. It is these measurements and some analysis of them which are presented here.

The field sensors consist of two MGL-3 B-dot sensors and one ACD-5 D-dot sensor located on the roof (ground plane) of a buried shield enclosure (Kiva). The roof of the Kiva is flush with the earth surface and is electrically connected to the center of a 30 m × 30 m wire-mesh ground plane. Data recording is accomplished by Biomation 8100 waveform recorders controlled by an HP 9825 calculator. A more complete description of the instrumentation is presented in [5].

At first we had little idea of what to expect. We made some measurements (section 2) which showed us some of the signal levels and patterns in the waveforms of the field time derivatives, and in the time integral of these waveforms. Based on the kinds of pulses observed and their time patterns it appeared that these related to individual fast pulses along some leader formation process. This led to a model (sections 3 and 4) which with ranging information (section 5) allowed us to infer some of the characteristics of the current in the lightning streamer. Section 6 then applies this to some of the data obtained.

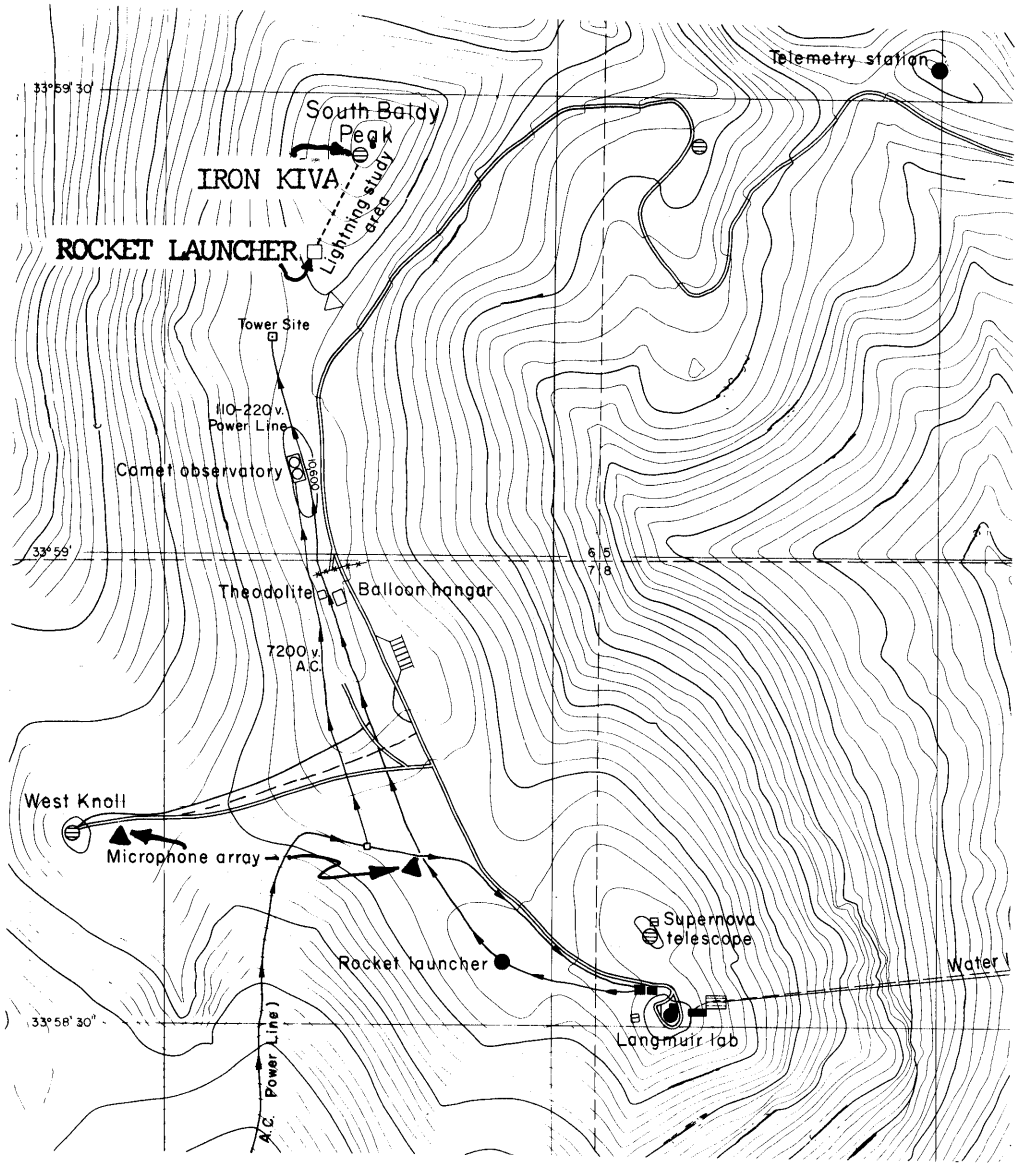

Iron Kiva altitude: 3275m. m.s.l.
map contour decrements: 13m

Figure 1.1 Top view of electromagnetic and related measurement layout around South Baldy Peak, New Mexico

II. GENERAL CHARACTERISTICS OF OBSERVED ELECTROMAGNETIC FIELDS

With the instrumentation at the Kiva discussed in [5,7] measurements were begun in the summer of 1978. For use in our data analysis the $\partial\vec{B}/\partial t$ sensors (MGL-3) had $A_{h_{eq}} = 0.1\ m^2$, and the $\partial\vec{D}/\partial t$ sensor (ACD-5) had $A_{e_{eq}} = 1.0\ m^2$ for use in the formulas

$$V_h = \vec{A}_{h_{eq}} \cdot \frac{\partial}{\partial t}\vec{B} \qquad \text{(open circuit voltage)}$$

$$I_e = -\vec{A}_{e_{eq}} \cdot \frac{\partial}{\partial t}\vec{D} \qquad \text{(short circuit current)} \qquad (2.1)$$

where the fields are those in the presence of the ground plane (i.e., including reflection). The response times (10-90 rise times of integrated output for step-function exciting field) into 50 Ω loads are short compared to our 10 ns sampling resolution and hence neglected.

The three sensors responded to the north and east components of $\partial\vec{B}/\partial t$ and to the vertical (up) component of $\partial\vec{D}/\partial t$. The signal from $\partial\vec{B}/\partial t$ north was attenuated a factor of 2 by a power splitter used to send this signal to an additional recorder for other purposes. These corrections and the equivalent areas are all removed for the displays of $\partial\vec{B}/\partial t$ and $\partial\vec{D}/\partial t$ in this paper. The $\vec{B}$ and $\vec{D}$ waveforms are determined by numerical integration of the digital data provided by the Biomation 8100 waveform recorders. Note that the integrated waveforms exhibit baseline slope which is at least partly due to errors in determining the baseline values for the original waveforms; this baseline shift is partly removed by estimating the baseline position near the beginning of the recording. The long-time variaton of the integrated waveforms should not be trusted, nevertheless; the purpose of the integration is to see the shape and amplitude of the fast pulses which are more reliable.

A nice property of the Biomation 8100 waveform recorder is that one has a significant length of recording time before the pulse which triggers the system is recorded. This pretrigger data time was set at about 4 μs. The self trigger was used on all three channels with the first trigger level being exceeded triggering all the recorders. Triggering in this case means freezing the data stream and transferring the 20 μs of information to magnetic disk.

Since the recording is digital there is also some limitation in the signal amplitude (voltage) resolution. The full scale is 256 uniformly spaced levels with zero approximately centered. Typical signals deviated about one third from baseline (zero) to the full level on one side or zero.

For some preliminary information let us now consider two examples of the kinds of waveforms we have seen. Detailed analysis of such waveforms is considered in section 6. A representative example of a leader waveform is given in figures 2.1 and 2.2. A representative

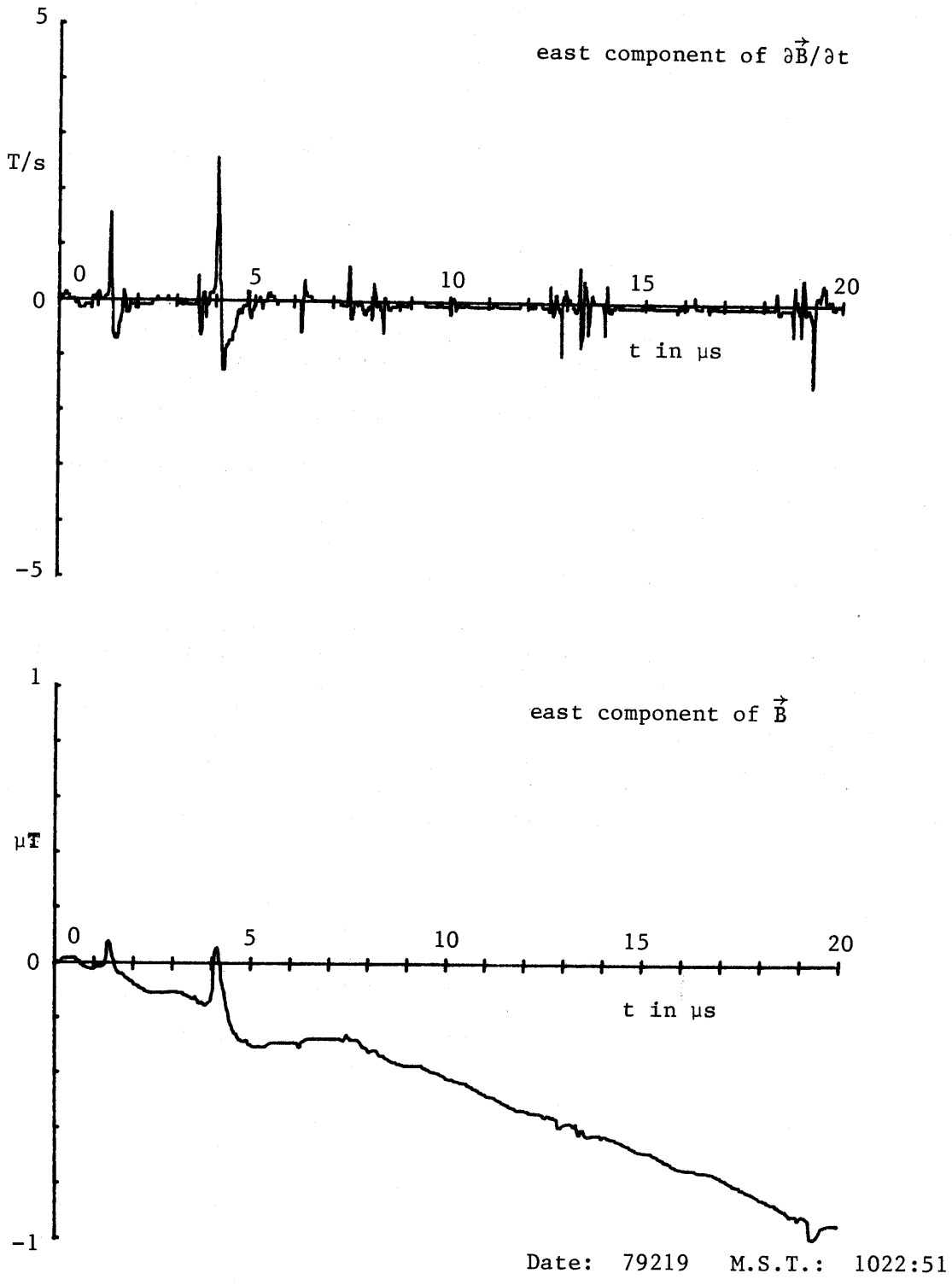

Figure 2.1 Leader example: 20 μs scale

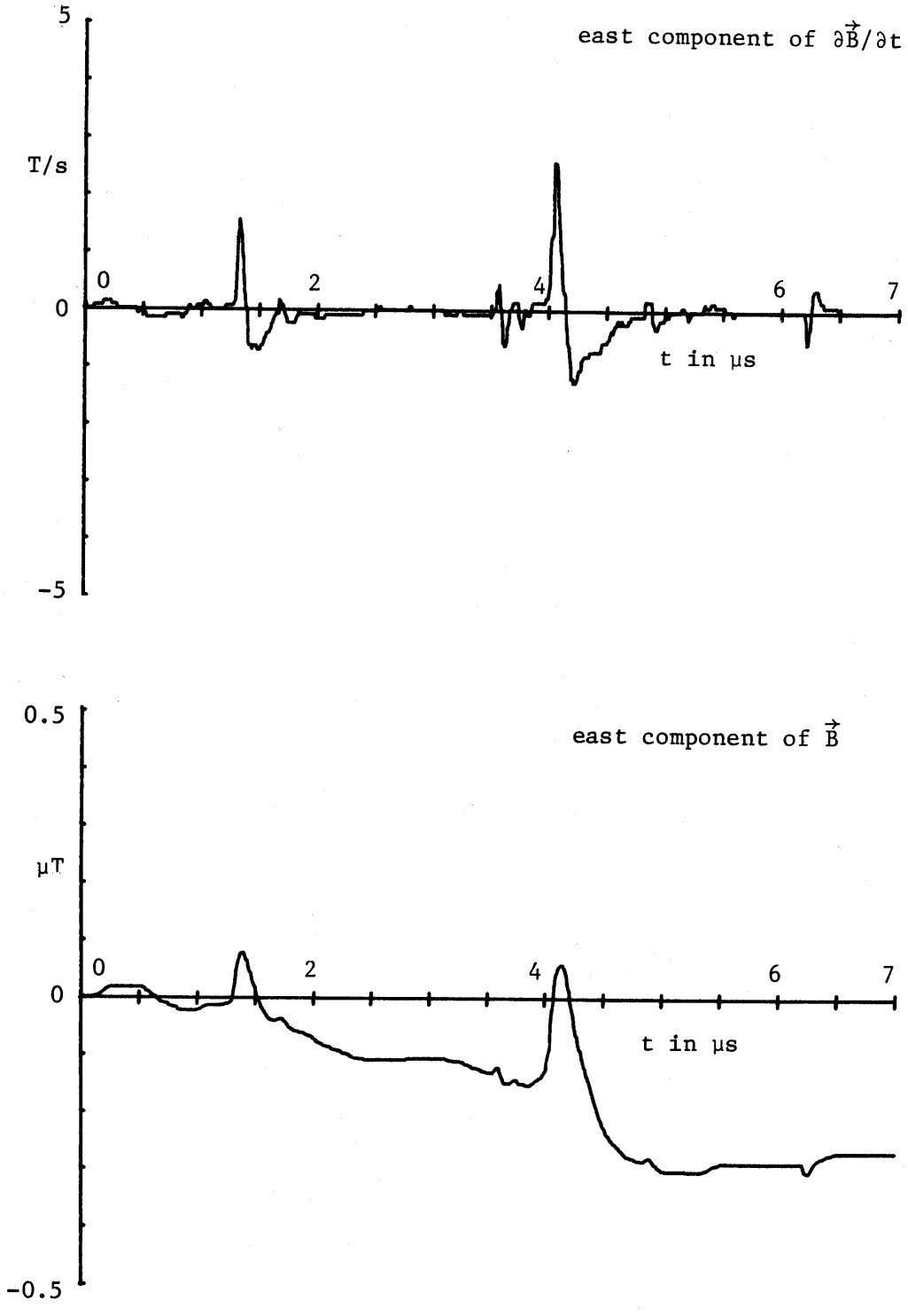

Figure 2.2 Same leader example: 7 μs scale

example of a return-stroke waveform is given in figures 2.3 and 2.4. In both cases only the east components of $\partial\vec{B}/\partial t$ and of $\vec{B}$ are exhibited.

Consider the leader waveform in figure 2.1. Note the complex structure with many individual pulses indicating the progression of the leader as a sequence of impulsive events. The horizontal distance (by flash to bang) to this stroke was about 350 m.

Note the large pulse at about 4 μs which triggered the recording. The first 7 μs of the record is expanded in figure 2.2. From a printout of the digital data this pulse has the approximate characteristics:

pulse at 4.0 μs

$$\frac{\partial}{\partial t} B_E \begin{cases} \text{peak} \simeq 2.42 \text{ T/s} \\ \text{zero to peak rise} \simeq 90 \text{ ns} \\ \text{10-90 rise} \simeq 50 \text{ ns} \end{cases} \qquad (2.2)$$

$$B_E \begin{cases} \text{baseline to peak} \simeq 0.169 \ \mu\text{T} \\ \text{baseline to peak rise} \simeq 150 \text{ ns} \\ \text{10-90 rise} \simeq 80 \text{ ns} \\ \text{width} \simeq 500 \text{ ns} \end{cases}$$

$\tau \simeq 70$ ns

Here τ has been defined as a characteristic time for the rise portion of the waveform with the formula

$$\tau \equiv \frac{\text{waveform peak}}{\text{derivative waveform peak}} \qquad (2.3)$$

Selecting a few more pulses from this waveform for comparison we have

pulse at 1.3 μs

$$\frac{\partial}{\partial t} B_E \begin{cases} \text{peak} \simeq 1.48 \text{ T/s} \\ \text{zero to peak rise} \simeq 50 \text{ ns} \\ \text{10-90 rise} \simeq 30 \text{ ns} \end{cases}$$

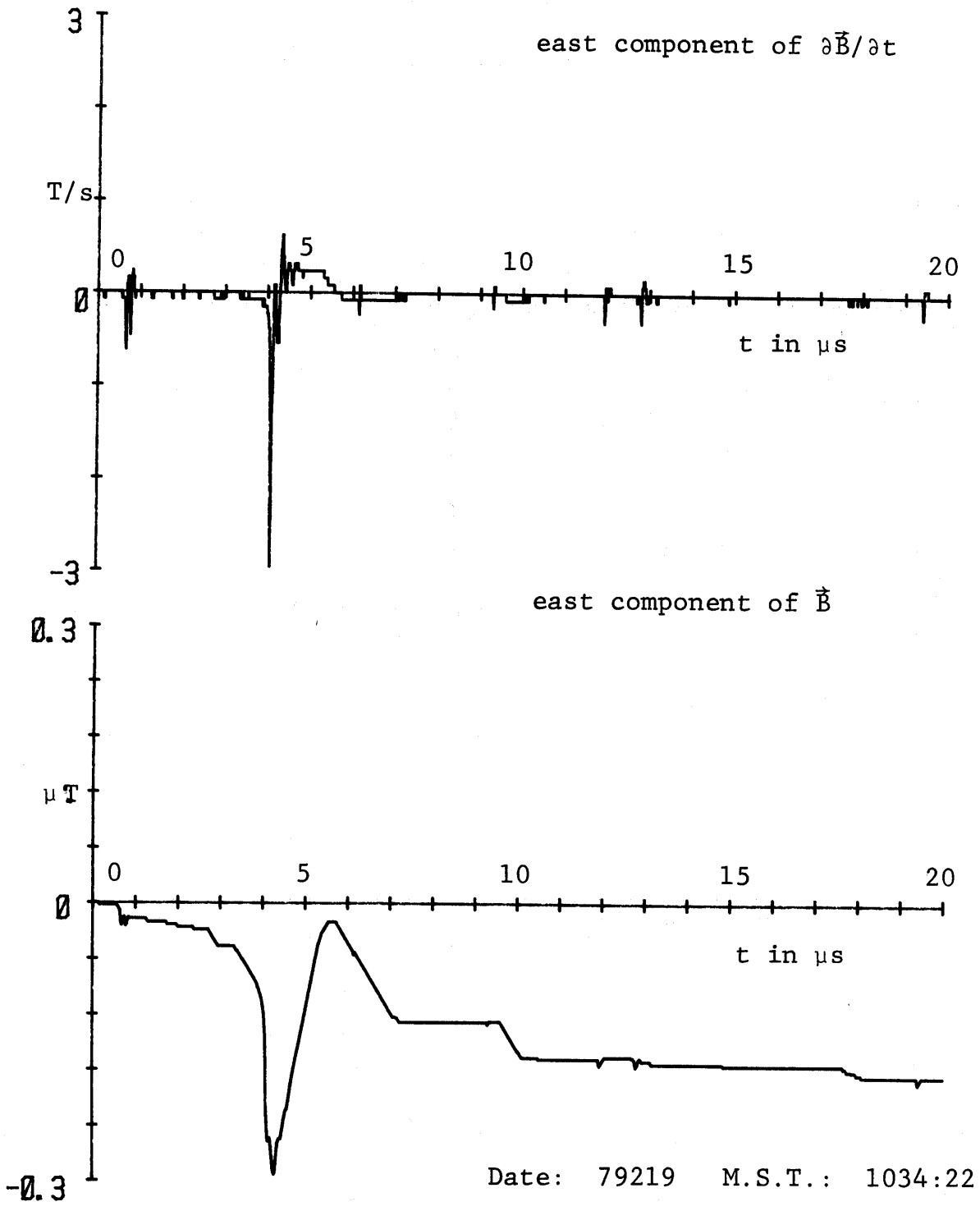

Figure 2.3 Return-stroke example: 20 µs scale

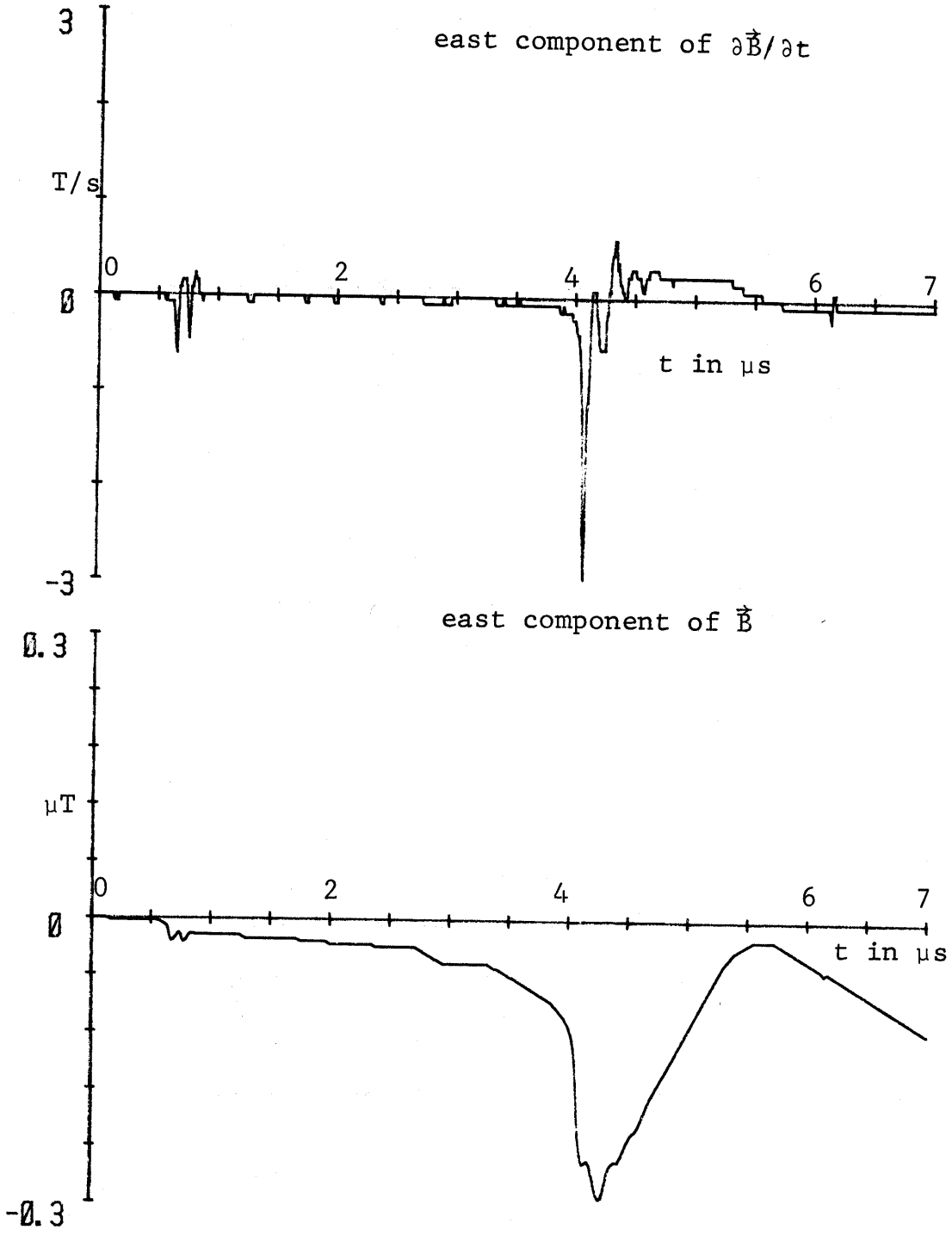

Figure 2.4 Same return-stroke example: 7 µs scale

$$B_E \begin{cases} \text{baseline to peak} \simeq .079\ \mu T \\ \text{baseline to peak rise} \simeq 100\ ns \\ \text{10-90 rise} \simeq 60\ ns \\ \text{width} \simeq 250\ ns \end{cases}$$

$$\tau \simeq 53\ ns$$

and another

pulse at 12.9 μs

$$\frac{\partial}{\partial t} B_E \begin{cases} \text{peak} \simeq -.86\ T/s \\ \text{zero to peak rise} \simeq 60\ ns \\ \text{10-90 rise} \simeq 30\ ns \end{cases}$$

(2.5)

$$B_E \begin{cases} \text{baseline to peak} \simeq -.03\ \mu T \\ \text{baseline to peak rise} \simeq 80\ ns \\ \text{10-90 rise} \simeq 40\ ns \\ \text{width} \simeq 160\ ns \end{cases}$$

$$\tau \simeq 35\ ns$$

and another

pulse at 14.0 μs

$$\frac{\partial}{\partial t} B_E \begin{cases} \text{peak} \simeq -.547\ T/s \\ \text{zero to peak rise} \simeq 40\ ns \\ \text{10-90 rise} \simeq 30\ ns \end{cases}$$

(2.6)

$$B_E \begin{cases} \text{baseline to peak} \simeq -.014\ \mu T \\ \text{baseline to peak rise} \simeq 50\ ns \\ \text{10-90 rise} \simeq 35\ ns \\ \text{width} \simeq 70\ ns \end{cases}$$

$$\tau \simeq 26\ ns$$

Comparing these individual pulses we have seen characteristic times for the rise ranging from about 70 ns to less than 30 ns. Also one can note that there seems to be a general trend in that smaller pulses have shorter characteristic times for the rise and shorter pulse widths. Pulse widths vary from about 500 ns to about 70 ns.

Now consider the return-stroke waveform in figure 2.3. The $\partial\vec{B}/\partial t$ structure is somewhat simplified by comparison to the previous leader example. The horizontal distance (by flash to bang) to this stroke was about 850 m. Comparing the peak derivative signals between return stroke (fig. 2.3) and leader (fig. 2.1) note that they are of comparable magnitude. Assuming that the leader is elevated somewhat above the ground, the inferred slant ranges to the sources for the two examples are crudely of the same order as well. It therefore seems that we may typically expect peak derivative waveforms from the larger leader pulses to have about the same strength as those for return strokes (at comparable distances).

The main pulse at about 4 μs which triggered the recording is expanded in figure 2.4 for the first 7 μs. Note the wide pulse characteristic of the return stroke as indicated in the east component of the $\vec{B}$ waveform. From a printout of the digital data this pulse has the approximate characteristics:

pulse at 4.0 μs

$$\frac{\partial}{\partial t} B_E \begin{cases} \text{peak} \simeq -2.81 \text{ T/s} \\ \text{zero to peak rise} \simeq 110 \text{ ns} \\ \text{10-90 rise} \simeq 35 \text{ ns} \end{cases}$$

$$B_E \begin{cases} \text{baseline to peak} \simeq -.129 \ \mu\text{T} \\ \text{baseline to peak rise} \simeq 160 \text{ ns} \\ \text{10-90 rise} \simeq 60 \text{ ns} \\ \text{width} \simeq 1000 \text{ ns} \end{cases} \qquad (2.7)$$

$\tau \simeq 46$ ns

It does seem that return strokes can be somewhat fast. We have looked at other return strokes and noticed similarly small values of τ. For this type of pulse of $\vec{B}$ the concept of width is somewhat problematical because of the current that continues in the arc after the fast part of the pulse has occurred.

III. FAST TRANSIENT ELECTROMAGNETIC FIELDS AT EARTH SURFACE RELATED TO INDIVIDUAL LIGHTNING CURRENT PULSES

Having seen some of the transient waveforms in section 2, and noting that many of the individual pulses are extremely fast with rise times of the order of some tens of ns, it appeared that one might be able to model these pulses as events somewhat localized in space. This concept uses the limitation of the speed of light on current propagation as compared to the distances of hundreds to thousands of meters from source to observer. As will appear later, this approach yields some valuable insight into the lightning streamer currents and propagation.

Let us begin by defining a spherical (r, θ, ϕ) coordinate system based on the Kiva as in figure 3.1A. For our purposes (r, θ, ϕ) signifies some position in space which is the source of the observed lightning signals at (near) $\vec{r} = \vec{0}$ (the Kiva). In addition to the spherical coordinates we have cylindrical (Ψ, ϕ, z) and cartesian (x,y,z) coordinates all related via

$$x = \Psi \cos(\phi) = r \sin(\theta) \cos(\phi)$$

$$y = \Psi \sin(\phi) = r \sin(\theta) \sin(\phi)$$

$$z = r \cos(\theta) \qquad (3.1)$$

$$r^2 = \Psi^2 + z^2$$

$$\Psi^2 = x^2 + y^2$$

$$\frac{\sin(\phi)}{y} = \frac{\cos(\phi)}{x}$$

with x and y taking the signs of $\cos(\phi)$ and $\sin(\phi)$ respectively. As indicated in figure 3.1A the coordinate system is oriented so that

x is north (geographical)

y is west

z is up (3.2)

θ is zenith angle

ϕ is counterclockwise from north

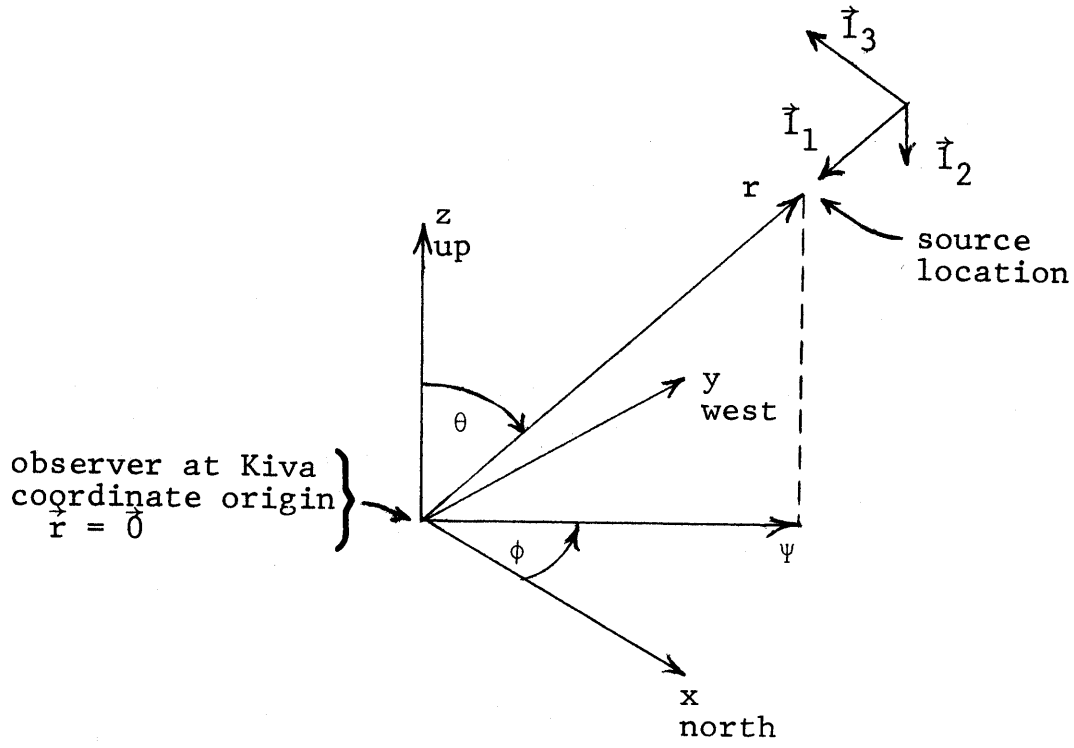

A. Coordinate systems

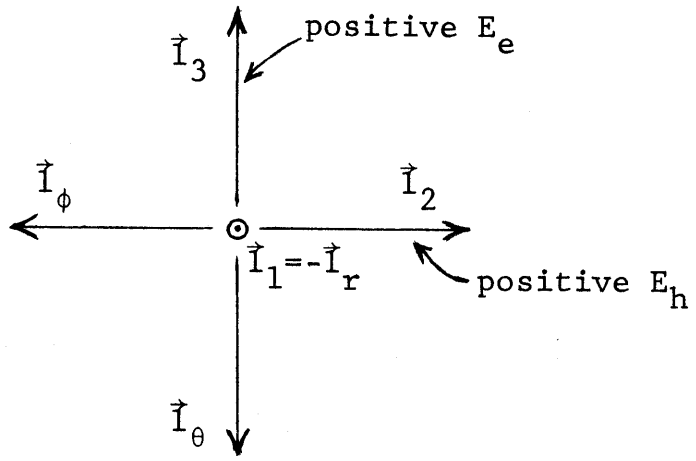

B. Reference directions seen by observer at $\vec{r} = \vec{0}$

Figure 3.1 Coordinates for lightning data analysis

Associated with these coordinates sets there are sets of unit vectors (right-handed) as

$$\vec{I}_x \times \vec{I}_y = \vec{I}_z \,,\ \vec{I}_y \times \vec{I}_z = \vec{I}_x \,,\ \vec{I}_z \times \vec{I}_x = \vec{I}_y$$
$$\vec{I}_\psi \times \vec{I}_\phi = \vec{I}_z \,,\ \vec{I}_\phi \times \vec{I}_z = \vec{I}_\psi \,,\ \vec{I}_z \times \vec{I}_\psi = \vec{I}_\phi \qquad (3.3)$$
$$\vec{I}_r \times \vec{I}_\theta = \vec{I}_\phi \,,\ \vec{I}_\theta \times \vec{I}_\phi = \vec{I}_r \,,\ \vec{I}_\phi \times \vec{I}_r = \vec{I}_\theta$$

which are related by

$$\vec{I}_\psi = \vec{I}_x \cos(\phi) + \vec{I}_y \sin(\phi)$$
$$\vec{I}_\phi = -\vec{I}_x \sin(\phi) + \vec{I}_y \cos(\phi)$$
$$\vec{I}_r = \vec{I}_\psi \sin(\theta) + \vec{I}_z \cos(\theta) \qquad (3.4)$$
$$\vec{I}_\theta = \vec{I}_\psi \cos(\theta) - \vec{I}_z \sin(\theta)$$

In addition to the coordinates for the source point with respect to the observation point let us define a set of unit vectors for describing the wave propagation to the observer. These are a right-handed system

$$\vec{I}_1 \times \vec{I}_2 = \vec{I}_3 \,,\ \vec{I}_2 \times \vec{I}_3 = \vec{I}_1 \,,\ \vec{I}_3 \times \vec{I}_1 = \vec{I}_2 \qquad (3.5)$$

which are related to our previously defined coordinate unit vectors as

$$\vec{I}_1 \equiv -\vec{I}_r$$
$$\vec{I}_2 \equiv -\vec{I}_\phi \qquad (3.6)$$
$$\vec{I}_3 \equiv -\vec{I}_\theta$$

Viewed from an observer at the Kiva one has the picture in figure 3.1B in which

$\vec{I}_1 \equiv$ direction of propagation
$\equiv$ pointing to observer

$\vec{I}_2 \equiv$ horizontal to right (3.7)

$\vec{I}_3 \equiv$ "up" as modified by being perpendicular to $\vec{I}_1$

Note that $\vec{1}_2$ and $\vec{1}_3$ are polarization vectors for the wave. The plane of incidence is defined by r and the z axis; it contains $\vec{1}_1$ and $\vec{1}_3$ as well as $\vec{1}_r$, $\vec{1}_\theta$, $\vec{1}_\psi$, and $\vec{1}_z$; $\vec{1}_2$ and $\vec{1}_\phi$ are perpendicular to the plane of incidence.

Next consider some distribution of current density $\vec{J}(\vec{r},t)$ in free space. The electromagnetic fields from this can be represented as [1]

$$\tilde{\vec{E}}_{inc}(\vec{r}',s) = -\left\langle \tilde{\overleftrightarrow{Z}}(\vec{r}',\vec{r}'';s) \;;\; \tilde{\vec{J}}(\vec{r}'',s) \right\rangle$$

$$\tilde{\vec{H}}_{inc}(\vec{r}',s) = \frac{1}{s\mu_o}\left\langle \nabla \times \tilde{\overleftrightarrow{Z}}(\vec{r}',\vec{r}'';s) \;;\; \tilde{\vec{J}}(\vec{r}'',s) \right\rangle \qquad (3.8)$$

with the subscript inc indicating incident at the observer at $\vec{r}' = \vec{0}$ and where $\vec{r}', \vec{r}''$ are now general coordinates (positions), s is the Laplace-transform variable (or complex frequency) with respect to time t (in general two sided) and the tilde $\sim$ indicates a Laplace-transformed quantity. The impedance kernel is

$$\tilde{\overleftrightarrow{Z}}(\vec{r}',\vec{r}'';s) = s\mu_o \tilde{\overleftrightarrow{G}}_o(\vec{r}',\vec{r}'';s)$$

$$\tilde{\overleftrightarrow{G}}_o(\vec{r}',\vec{r}'';s) = \left[\overleftrightarrow{1} - \gamma^{-2}\nabla'\nabla'\right] \tilde{G}_o(\vec{r}',\vec{r}'';s)$$

$\equiv$ dyadic Green's function of free space

$$\tilde{G}_o = \gamma \frac{e^{-\zeta}}{4\pi\zeta} \quad (\text{for } \vec{r}' \neq \vec{r}'')$$

$\equiv$ scalar Green's function of free space

$$\gamma \equiv \frac{s}{c} \equiv \text{free space propagation constant} \qquad (3.9)$$

$$c \equiv \frac{1}{\sqrt{\mu_o \varepsilon_o}} \simeq 3 \times 10^8 \text{ m/s}$$

$\equiv$ speed of light (in free space)

$$Z_o \equiv \sqrt{\frac{\mu_o}{\varepsilon_o}} \simeq 377\ \Omega$$

$\equiv$ wave impedance of free space

$$\zeta \equiv \gamma|\vec{r}' - \vec{r}''|$$

The symbol <,> indicates integration over the space coordinates common to the two terms (r" in (3.8)). The free-space dyadic Green's function has the explicit form

$$\overleftrightarrow{\tilde{G}}_o(\vec{r}',\vec{r}";s) = \frac{\gamma}{4\pi} e^{-\zeta}\left\{\left[-2\zeta^{-2} - 2\zeta^{-3}\right]\vec{I}_R\vec{I}_R + \left[\zeta^{-3} + \zeta^{-2} + \zeta^{-1}\right]\left[\overleftrightarrow{I} - \vec{I}_R\vec{I}_R\right]\right\} + \frac{1}{3\gamma^2}\delta(\vec{r}' - \vec{r}")\overleftrightarrow{I}$$

$\overleftrightarrow{I} \equiv$ identity dyad (3.10)

$$\vec{I}_R \equiv \frac{\vec{r}' - \vec{r}"}{|\vec{r}' - \vec{r}"|} \quad \text{for } \vec{r}' \neq \vec{r}"$$

where the delta function is introduced so that the remaining part can be handled in (3.8) as a principal value integral with a small spherical zone of exclusion centered on $\vec{r}' = \vec{r}"$ [3].

For our present purposes we assume that the distance from source to observer is large compared to the size of the source, i.e.,

$$\vec{r}' = \vec{0}$$

$$r" \equiv |\vec{r}"| \approx r >> |\vec{r}' - \vec{r}"| \tag{3.11}$$

where $\vec{r}$ is taken as some effective center of the source. Furthermore we assume that frequencies of interest are sufficiently high that only the leading term for large r" (the $|\vec{r}' - \vec{r}"|^{-1}$ or ζ^{-1} term in (3.10) need be included giving

$$\overleftrightarrow{\tilde{G}}_o(\vec{r}',\vec{r}";s) \approx \frac{e^{-\gamma|\vec{r}' - \vec{r}"|}}{4\pi|\vec{r}' - \vec{r}"|}\overleftrightarrow{I}_t \approx \frac{e^{\gamma\vec{I}_R\cdot\vec{r}"}}{4\pi r}\overleftrightarrow{I}_t \tag{3.12}$$

$\overleftrightarrow{I}_t \equiv \overleftrightarrow{I} - \vec{I}_R\vec{I}_R \equiv$ transverse dyad

Now referring to figure 3.1 we can approximate as

$$\vec{1}_R \approx \vec{1}_1 = -\vec{1}_r$$

$$\overleftrightarrow{1}_t \approx \overleftrightarrow{1} - \vec{1}_1\vec{1}_1 = \overleftrightarrow{1} - \vec{1}_r\vec{1}_r \tag{3.13}$$

This allows us to write (from 3.8))

$$\tilde{\vec{E}}_{inc}(0,s) \approx -\frac{\mu_o e^{-\gamma r}}{4\pi r}\overleftrightarrow{1}_t \cdot \tilde{\vec{T}}(s)$$

$$\tilde{\vec{T}}(s) \approx s\int_V e^{\gamma(r-\vec{1}_r\cdot r")}\,\tilde{\vec{J}}(\vec{r}",s)\,dV" \tag{3.14}$$

In time domain we have

$$\vec{T}(t) \approx \frac{\partial}{\partial t}\int_V \vec{J}(\vec{r}",t+\frac{1}{c}(r-\vec{1}_r\cdot\vec{r}"))\,dV" \tag{3.15}$$

This $\vec{T}$ can be thought of as a kind of effective source vector. Assuming that changes in $\vec{J}$ propagate over the source volume at velocities slow compared to c we have

$$\tilde{\vec{T}}(s) \approx s\int_V \tilde{\vec{J}}(\vec{r}",s)\,dV"$$

$$\vec{T}(t) \approx \frac{\partial}{\partial t}\int_V \vec{J}(\vec{r}",t)\,dV" \tag{3.16}$$

The magnetic field incident at $\vec{r}' = \vec{0}$ can be found by expanding from (3.8), or by simply noting that the far field ($|\vec{r}' - \vec{r}"|^{-1}$ term) has a plane-wave relation between the electric and magnetic field as

$$\tilde{\vec{H}}_{inc}(0,s) \approx \frac{1}{Z_o}\vec{1}_1 \times \tilde{\vec{E}}_{inc}(0,s)$$

$$\approx -\frac{e^{-\gamma r}}{4\pi rc}\vec{1}_1 \times \tilde{\vec{T}}(s) \tag{3.17}$$

In time domain the fields are

$$\vec{E}_{inc}(0,t) \approx -\frac{\mu_o}{4\pi r}\overleftrightarrow{1}_t \cdot \vec{T}(t-\frac{r}{c}) \tag{3.18}$$

$$\vec{H}_{inc}(0,t) \approx -\frac{1}{4\pi rc}\vec{1}_1 \times \vec{T}(t-\frac{r}{c})$$

Near $\vec{r}' = \vec{0}$ the incident field is an approximate plane wave propagating in the $\vec{1}_1$ direction; it can be represented as

$$\vec{E}_{inc}(\vec{r}',t) \simeq E_h(t - \frac{\vec{1}_1 \cdot \vec{r}'}{c})\,\vec{1}_2 + E_e(t - \frac{\vec{1}_1 \cdot \vec{r}'}{c})\,\vec{1}_3$$

$$\vec{H}_{inc}(\vec{r}',t) = \frac{1}{Z_o}\left\{E_h(t - \frac{\vec{1}_1 \cdot \vec{r}'}{c})\,\vec{1}_3 - E_e(t - \frac{\vec{1}_1 \cdot \vec{r}'}{c})\,\vec{1}_2\right\} \qquad (3.19)$$

This decomposes the fields incident at the observer into two parts, and E wave (or TM wave) denoted by a subscript e, and an H wave (or TE wave) denoted by a subscript h. This decomposition is based on the polarization with respect to the z axis (i.e., a TM wave has the magnetic field perpendicular to the z axis, and a TE wave has the electric field perpendicular to the z axis).

Now when the incident fields reach the ground plane (the x, y plane), the conducting ground plane reflects the fields so that (at least at the higher frequencies because of the finite dimension of the ground plane on the earth) approximately we have

$$E_z \simeq 2\vec{1}_z \cdot \vec{E}_{inc}$$

$$H_x \simeq 2\vec{1}_x \cdot \vec{H}_{inc} = H_N = -H_S \qquad (3.20)$$

$$H_y \simeq 2\vec{1}_y \cdot \vec{H}_{inc} = H_W = -H_E$$

The remaining three fields components are approximately zero. Note the orientation of the cartesian coordinates with respect to the (geographical) compass positions (north = N, east = E, south = S, west = W).

On the ground plane we then have

$$E_z = 2\sin(\theta)\,E_e$$

$$H_\phi = -H_2 = \frac{2}{Z_o}E_e \qquad (3.21)$$

$$H_\psi = -\cos(\theta)\,H_3 = -\frac{2}{Z_o}\cos(\theta)\,E_h$$

Then construct

$$\frac{1}{2} E_z = \sin(\theta)\, E_e$$

$$\frac{Z_o}{2} H_\phi = \frac{Z_o}{2} \{-H_x \sin(\phi) + H_y \cos(\phi)\} = E_e \qquad (3.22)$$

$$\frac{Z_o}{2} H_\psi = \frac{Z_o}{2} \{H_x \cos(\phi) + H_y \sin(\phi)\} = -\cos(\theta)\, E_h$$

From our measurements we have three pieces of information: E_z, H_x, and H_y. We have four unknowns: E_e, E_h, 0, and ϕ .

If we knew the source angles $(0,\phi)$, or at least one of these, then the two waves E_e and E_h could be constructed. Let us for the moment assume that θ and ϕ are known. From (3.18) and (3.19) together with E_e and E_h we can find

$$\overleftrightarrow{I}_t \cdot \vec{T}(t - \frac{r}{c}) = -\frac{4\pi r}{\mu_o} \vec{E}_{inc}(0,t)$$

$$= -\frac{4\pi r}{\mu_o} \{ E_h(t)\, \vec{I}_2 + E_e(t)\, \vec{I}_3 \} \qquad (3.23)$$

This shows that we can obtain the relative strength of the transverse (2 and 3) components of the source $\vec{T}$ by comparing E_h and E_e. Referring to figure 3.1B one can plot on such a diagram an angle that $\vec{T}$ makes with respect to say $\vec{I}_3$ as another vector on the plane perpendicular to $\vec{I}_1$. Note that the 1 component of $\vec{T}$ is not obtained in this technique since it does not appear in the far-field expansion at $\vec{r}' = \vec{0}$. If one knew r then the 2 and 3 components of $\vec{T}$ would be completely known. Techniques for estimating r are discussed in another section of this paper. Having r then one can use (3.23) to find T_2 and T_3; this is used for later plots of the transverse part of $\vec{T}$.

Figure 3.2 illustrates the components of $\overleftrightarrow{1}_t \cdot \vec{T}$ and its angle α (CCW) with respect to $\vec{1}_3$ as

$$\sin(\alpha) = \begin{cases} \dfrac{-T_h}{|\vec{T}|} \\ \text{or} \\ \dfrac{-\frac{\partial}{\partial t} T_h}{|\frac{\partial}{\partial t} \vec{T}|} \end{cases}$$

$$\cos(\alpha) = \begin{cases} \dfrac{T_e}{|\vec{T}|} \\ \text{or} \\ \dfrac{\frac{\partial}{\partial t} T_e}{|\frac{\partial}{\partial t} \vec{T}|} \end{cases} \qquad (3.24)$$

Angles away from 0° (or 360°) and 180° indicate the presence of an H (or TE) wave component. This kind of information can be used to infer the direction of the current at various times. This same kind of display also is used for $\overleftrightarrow{1}_t \cdot \frac{\partial \vec{T}}{\partial t}$ for the same purpose.

Having $\overleftrightarrow{1}_t \cdot \vec{T}$ one can also make some estimates concerning currents in the fast pulses in the source region near $\vec{r}$ by writing

$$\vec{T} \equiv \overrightarrow{(I\, v_{eff})} = \Delta\left\{\frac{\partial}{\partial t} \int_{V''} \vec{J}(\vec{r}'', t)\, dV''\right\} \qquad (3.25)$$

Here Δ indicates the change in the quantity; for later plots this is the change from the ambient value before a fast pulse to the peak of the pulse. (This convention is employed for $\partial \vec{T} / \partial t$ also.) An effective streamer speed v_{eff} can be used to obtain some indication of the current I, or at least some rough bound on it.

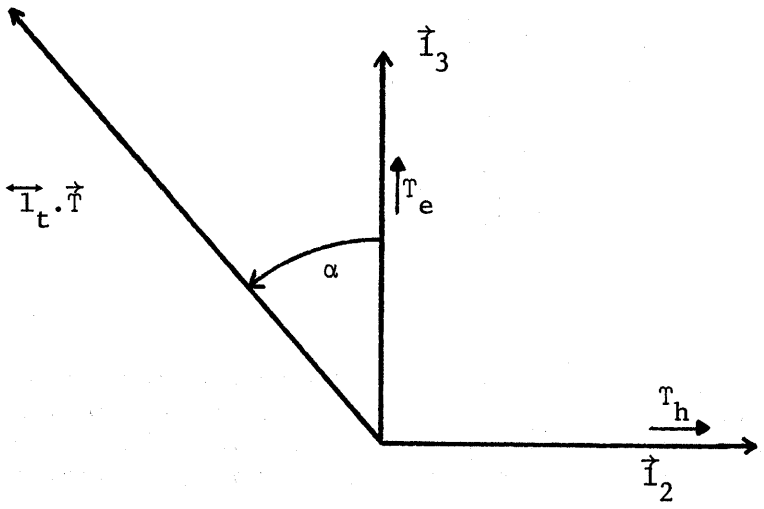

Fig 3.2 $\vec{T}$ components and angle as seen by observer.

IV. ESTIMATION OF DIRECTION TO LIGHTNING CURRENT PULSES

Now consider the determination of (θ,ϕ). Figure 4.1 shows a type of display of coordinates which is useful for our purposes. Superimposed on the horizontal (x,y) cartesian and compass coordinates we have a polar plot in which a function of θ as $\psi(\theta)$ is a radial coordinate with $0^{o} \leq \theta \leq \pi/2$. The azimuthal coordinate is ϕ with $0 \leq \phi < 2\pi$.

Returning to (3.22) our three measurements (E_z, H_x, H_y) can be used to find a relationship between θ and ϕ. Specifically the first two of (3.22) can be used to eliminate E_e giving

$$Z_o \left\{ -H_x \sin(\phi) + H_y \cos(\phi) \right\} = \frac{E_z}{\sin(\theta)} \qquad (4.1)$$

as our θ, ϕ relation. Constraining $0 \leq \theta \leq \pi/2$ and θ real gives a curve in the ($\psi(\theta)$, ϕ)"plane" of acceptable solutions of (4.1). For each pulse we can consider the change in the fields (ambient to peak) in (4.1) or some other aspect of the pulse waveforms. Besides the field change we have used the change in the time derivatives of the fields ($\partial E_z/\partial t$, $\partial H_x/\partial t$, $\partial H_y/\partial t$) in (4.1) to determine the θ,ϕ curves. Both the field changes and changes in field time derivatives (on the rise of the pulses) typically give comparable results, as will be seen later.

To place the relationship between $\psi(\theta)$ and ϕ in a convenient form construct cartesian (u,v) coordinates for the $(\psi(\theta),\phi)$ plane as

$$\begin{aligned} u &= \psi(\theta) \cos(\phi) \\ v &= \psi(\theta) \sin(\phi) \end{aligned} \qquad (4.2)$$

Substituting for $\sin(\phi)$ and $\cos(\phi)$ from (4.2) into (4.1) and rearranging terms gives

$$-H_x v + H_y u \equiv \frac{E_z}{Z_o} \frac{\psi(\theta)}{\sin(\theta)} \qquad (4.3)$$

Inspecting this equation gives the result that if

$$\psi(\theta) = \sin(\theta) \qquad (4.4)$$

then the solutions of (4.3), or equivalently (4.1) are straight lines in cartesian coordinates (u,v), or equivalently circular polar coordinates ($\sin(\theta)$, ϕ). We adopt the convention (4.4) and thereby characterize the display in Fig. 4.1. by

$$0 \leq \sin(\theta) \leq 1, \quad 0 \leq \phi < 2\pi \qquad (4.5)$$

This makes our domain of interest bounded by a unit circle $\sin(\theta) = 1$

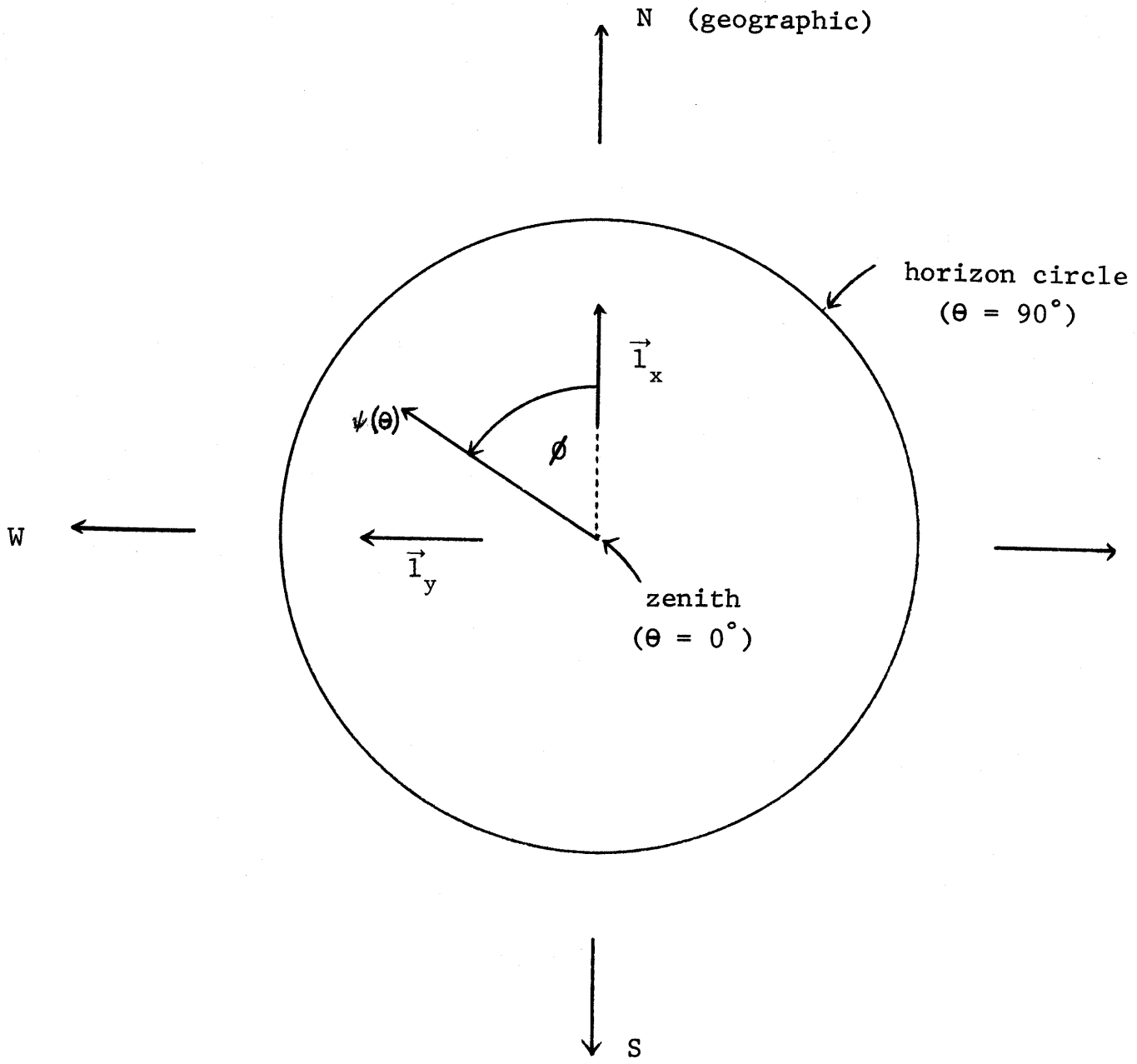

Figure 4.1 Polar plot for determining direction to source.

If we view a unit sphere with spherical polar coordinates (θ, ϕ) on it with its equator $\theta = \pi/2$ coincident with the unit circle in Fig. 4.1, then the curves (straight lines) on the plane are projections from the upper hemisphere of the θ, ϕ curves on the unit sphere. The curves on the unit sphere are circles because they correspond to the intersections of vertical planes with the unit sphere.

To solve for any particular u,v straight line from (4.3) and (4.4) one needs to find only two points to define the straight line. For this purpose define

$$H = \left[H_x^2 + H_y^2 \right]^{1/2} \tag{4.6}$$

and rewrite (4.1) as

$$\frac{H_x}{H} \sin(\phi) - \frac{H_y}{H} \cos(\phi) = - \frac{E_z}{Z_o H} \quad \frac{1}{\sin(\theta)} \tag{4.7}$$

This straight line intersects the unit circle at points given by

$$\sin(\theta) = 1$$

$$\frac{H_x}{H} \sin(\phi_n) - \frac{H_y}{H} \cos(\phi_n) = - \frac{E_z}{Z_o H} \tag{4.8}$$

which normally has one or two solutions except for errors in H_x, H_y, and E_z. Noting that

$$\left| \frac{H_x}{H} \right| \leq 1, \left| \frac{H_y}{H} \right| \leq 1 \tag{4.9}$$

with equality ideally achieved for special angles, we use the formula

$$\cos(\phi_n - \phi_o) = \cos(\phi_n) \cos(\phi_o) + \sin(\phi_n) \sin(\phi_o) \tag{4.10}$$

to identify

$$\cos(\phi_o) = - \frac{H_y}{H}$$

$$\sin(\phi_o) = \frac{H_x}{H} \tag{4.11}$$

giving

$$\cos(\phi_n - \phi_o) = - \frac{E_z}{Z_o H} \tag{4.12}$$

To solve first for ϕ_o one can observe the signs of $\cos(\phi_o)$ and $\sin(\phi_o)$ to find in which quadrant of the (u,v) plane ϕ_o lies. Use of any of several inverse trigonometric functions with (4.11) will give a ϕ_o which can be adjusted to lie in the proper quadrant. Next we find

$$\phi_n = \phi_o \pm \arccos \left(- \frac{E_z}{Z_o H} \right) \tag{4.13}$$

as our two solutions (or one if the arccos is zero). Note the minus sign in the argument of the arccos. This convention has been chosen because in our data analysis the electric field or electric-field derivatives are normally negative jumps corresponding to pulse rises for negative lightning (current positive upward). The arccos of the positive resulting argument then gives an angle less than $\pi/2$, making ϕ_o less than $\pi/2$ away from both ϕ_n. As the signal source reaches the horizon we have

$$\begin{aligned} \theta &\to \pi/2 \quad \text{from below} \\ \frac{-E_z}{Z_o H} &\to 1 \quad \text{from below} \\ \phi_n &\to \phi_o \quad \text{from both sides} \end{aligned} \tag{4.14}$$

Hence ϕ_o in the limit as $\theta \to \pi/2$ becomes the azimuth to the source.

In the rare case of positive lightning (negative vertical current) the situation is reversed. The jumps in the electric field or its derivative are then in general positive, and the argument of the arccos becomes negative. In the limit as $\theta \to \pi/2$ then $\phi_o \pm \pi$ becomes the azimuth. There is, of course, the possibility of seeing positive electric charges with negative lightning if the streamers are tortuous enough to occasionally turn up. The case of cloud to cloud lightning can have both signs for charges in electric fields and derivatives.

Having two ϕ_n on the unit circle, the straight line connecting them gives the possible (θ,ϕ) combinations solving (4.1). If there is only one ϕ_n then the one point on the unit circle is the (θ, ϕ) point of interest.

Since there is in general some error in each field-component measurement, and in our assumptions concerning how these measurements relate to the incident fields, there is some error in our determination of (θ, ϕ). If the electric fields are too large compared to the magnetic fields, the plane-wave character of the fields is violated and we can have $|E_z| > Z_o H$ which is occasionally observed.

Setting

$$\left| \frac{-E_z}{Z_o H} \right| = 1 + \delta \tag{4.15}$$

if $\delta > 0$ then the arccos does not give a real-valued $\phi_n - \phi_o$. This difficulty is remedied by setting

$$\arccos\left(\frac{-E_z}{Z_o H}\right) \simeq 0 \tag{4.16}$$

$\delta \equiv$ an error indicator

Generally for fields incident from near the horizon δ can sometimes be positive, but it is still small.

Having a straight-line contour in the $(\sin(\theta),\phi)$ "plane" resulting from a particular measured fast electromagnetic-field pulse (or its time derivative) one would like to find some point along that contour that represents the true angles (θ, ϕ) to the source. One way to do this uses an assumption that another pulse in a particular recording (about 20 μs wide in the presented data) comes from approximately the same source location. This is physically reasonable if one considers a leader propagating through the air to establish the lightning channel, and if the distance the streamer propagates during the pulse is small compared to the distance to the observer, then the change in (θ, ϕ) is small. Furthermore, if the two pulses under consideration have different polarizations (different proportions of E and H waves) due to different directions of $\vec{\vec{I}} \cdot \vec{T}$, then (4.1) will give in general different θ, ϕ contours for the two pulses. The intersection of the two contours can then be taken as an experimental determination of (θ, ϕ) for both pulses.

Going further, it will be observed in considering the data that the intersection of θ, ϕ contours is remarkably successful in determining (θ, ϕ) values. In some cases all the θ, ϕ contours (of the order of ten contours) can all pass quite near a common (θ, ϕ) approximate intersection. In other cases subsets of the contours for a particular waveform set form a few distinct approximate (θ, ϕ) values. Some cases are presented in the data illustrating some of the complexity that can be unravelled in this way.

Having determined the (θ, ϕ) values appropriate to particular pulses, and estimating the corresponding r, one goes back to (3.22) to find E_e and E_h (or their derivatives with respect to time). Then (3.23) gives the transverse components of $\vec{T}$ for plots with respect to the $\vec{I}_2$ and $\vec{I}_3$ directions as in figure 3.1B.

V. ESTIMATION OF RANGE TO LIGHTNING CURRENT PULSES

The electric field changes produced by lightning in this study were also sensed with a "slow antenna" field change meter and recorded onto FM magnetic tape, together with the IRIG B, 1 kHz time code that was distributed to coordinate the thunderstorm and lightning measurements. This time code was synchronized with Radio Station WWV and permitted the slow measurements to be correlated with a time resolution of 1 ms. A Globe 100 B microphone with an extended low frequency response was mounted on the metal mesh adjacent to the Kiva and was used to detect the arrival of thunder. The thunder signals were recorded on a second FM magnetic tape channel. In this manner, the time of occurrence, the nature of the lightning flash and the time from flash-to-thunder could be determined.

Two acoustic arrays, each consisting of three microphones at the vertices of 30 m, equilateral triangles were located in the meadow, south of the Kiva. (See Figure 1.1.) The time-difference of arrival of individual thunder peals across each of these triangular arrays permitted a determination of the direction cosines for the normal to the acoustic wave front. With these and the distance from each source to the array calculated from the speed of sound and the time interval from field change to peal arrival, a first estimate could be made for location of each source. Corrections were then made for the local winds and for thermal refraction in a second approximation for the source location using the technique described by Winn et al [4].

In addition to the use of these acoustic techniques for the location of lightning, the flashes in the vicinity of the Kiva were video-recorded with a time resolution of 16 ms per TV frame. One TV camera recorded the view from an all-sky reflecting, parabolic mirror located on top of South Baldy peak about 50 m north of the Kiva, while another TV system located at Langmuir Laboratory recorded the view of lightning over South Baldy peak as seen from 2 km to the SSE.

These video recordings have been played back, frame by frame, onto a video monitor where they were photographed together with an output displaying the IRIG B time code that was also recorded on the audio tracks of the video tape recorders.

All of the flashes reported in this study were "cloud-to-ground" discharges. Our first approximation for the slant range from the Kiva to the lightning current element of interest is based on the assumption that the time from flash to thunder multiplied by the speed of sound in air gives the horizontal distance from the Kiva microphone to the closest part of the lightning channel (that is striking the earth approximately vertically).

From section 4, the zenith angle θ and the azimuth angle ϕ can be estimated for the current element from the electromagnetic signal that it produced.

The approximate slant range r from the Kiva to the current element is therefore given by

$$r \simeq (336 \text{ m/s})(\Delta t)/\sin(\theta) \qquad (5.1)$$

The cartesian coordinates of the current element are therefore

$$x = (336 \text{ m/s})(\Delta t)\cos(\phi), \text{ toward the north}$$

$$y = (336 \text{ m/s})(\Delta t)\sin(\phi), \text{ toward the west}$$

$$z = r/\cos(\theta), \text{ above the Kiva} \qquad (5.2)$$

In the nine cases to date in which we have compared the thunder source maps with current element coordinates, there has been a fair agreement between the two somewhat independent location systems. If the range chosen from the horizontal distance assumption is too small, a better estimate for the range can be extracted from the intersection of the vector $\vec{r}$-- directed along the calculated values of θ and ϕ --with the thunder channels mapped by the acoustic technique.

VI. ANALYZED WAVEFORM SETS

In this section the techniques discussed in sections 3 through 5 are applied to nine selected waveform sets for which complete sets of waveforms and auxiliary data such as photographs and acoustic data exist. Each set of data is contained in a subsection 6.n for n = 1,2,...,9. Following the text in each subsection there is a set of figures; for convenience the figure numbers for section 6.n are all of the form 6.n.··· with tabular data also assigned a figure number. Each data set is given a descriptive name corresponding to the subsection title; note there is some repetition in the descriptions. Each data set or record is also decomposed into a set of events, each event corresponding to an identified pulse in the electromagnetic waveforms; each event is labelled according to its approximate time in the waveform set in μs. Since we use both the derivative waveforms and their numerical integrals to give the field waveforms we label figures based on the derivative waveforms with A at the end of the figure number, and we label figures based on the field waveforms with B at the end of the figure number.

The "figures" in each nth subsection are then organized as follows:

Fig. 6.n.1A	Derivative fields from ...
Fig. 6.n.1B	Fields from ...
Fig. 6.n.2.1	Digital data for event ...
⋮	⋮ ⋮ ⋮ ⋮ ⋮ ⋮
m	Digital data for event ...
⋮	⋮ ⋮ ⋮ ⋮ ⋮ ⋮
Fig. 6.n.3	Slow electric field change and thunder microphone record from ... (sometimes varies)
Fig. 6.n.4	Acoustic location of ...
Fig. 6.n.5A	$\sin(\theta), \phi$ contours for ... derivative waveform set and whole-sky videotape photograph
Fig. 6.n.5B	$\sin(\theta), \phi$ contours for ... waveform set and whole-sky videotape photograph
Fig. 6.n.6A	Tabulation of peak values for each event from derivative waveform set for ...
Fig. 6.n.6B	Tabulation of peak values for each event from waveform set for ...
Fig. 6.n.7A	$\partial\vec{T}/\partial t$ for ...
Fig. 6.n.7B	$\vec{T}$ for ...

6.1 Rocket-Triggered Lightning

Our first example is given in figures 6.1. ..., It is a good example of leader-like behavior and is associated with a triggered lightning event. The lightning stroke was triggered by a wire-trailing rocket launched from the position indicated in figure 1.1 which is 350 m in horizontal range at an azimuth of $\phi = 155^{o}$ with respect to the Kiva. The rocket was launched approximately vertically. Based on visual observations its height was estimated as about 600 m above the Kiva when it initiated a lightning discharge. This corresponds to a zenith angle of $\theta \simeq 30^{o}$ with respect to the Kiva. Based on the extreme electric-field enhancement at the rocket, it was expected that the streamer direction of interest was upward, beginning from the rocket. This polarity is assumed later in the data analysis.

Looking at figure 6.1.1A we see the leader-like behavior on the 20 μs waveform for the three derivative field components. For convenience 10 pulses are identified by numbers corresponding to their peak times of occurrence (within the record event) in microseconds; the north component of $\partial\vec{B}/\partial t$ had the generally largest pulses and was used for this labelling. Figure 6.1.1B results from the numerical integration of the digital data from which figure 6.1.1A was produced. Here the pulses are also identified (on the east component of $\vec{B}$ in this case). Note the general drift in the baseline which may be partially due to a little offset in the recording of the derivative data, but probably is a result of a continuing current flowing up the channel initiated by the rocket.

Figure 6.1.3 shows the slow changes in the electric field, first from the rising of the grounded wire, followed by the emission of upward-going positive streamers. Also shown is a recording of the narrowband RF power received centered on 34 MHz, as measured by a different experiment (Hayenga) with a complex antenna pattern. For our purposes it is interesting to note that the RF power emissions began at about 0.6 s after rocket launch indicating some corona-like discharges before the main lightning event.

The acoustically determined (per section 5) thunder sources are displayed in figure 6.1.4. This indicates that the lightning discharge turned south and extended about 4 km at a height of about 2 km. This can be compared to the whole-sky videotape photograph in figure 6.1.5A obtained at the balloon hangar (fig. 1.1) about 700 m south of the rocket launcher. This indicates the main streamer rising and propagating to the south near cloud-base level at a height of about 1 km. Figure 6.1.5B shows the same event at about 160 ms later. Note in the whole-sky photographs the TV camera in the center since it is above a paraboloidal mirror.

The θ, ϕ contours from the ten pulses identified for the derivative waveform in figure 6.1.1A are displayed in figure 6.1.5A. This shows a remarkably tight set of intersections in which all 10 contours pass through nearly the same point. The estimated angles from the Kiva to the source are $(\theta, \phi) \simeq (22.5^{o}, 172.7^{o})$.

This is in quite good agreement with the estimated rocket position. The major difference is in azimuth (173^{o} vs 155^{o}), but there are uncertainties in the exact position of the rocket because it impacted to the south near the comet observatory (fig. 1.1), despite its near vertical aiming. The slant range is estimated as $r \simeq 915$ m based on $\theta = 22.5^{o}$ and a horizontal distance of 350 m. The same contours, except now based on the field (numerically integrated) waveform are shown in figure 6.1.5B. Here the intersection is not so tightly clustered indicating that more accuracy is generally obtained from the derivative-format data. This is not surprising since the analysis is based on a high-frequency approximation and because the integration has some error. For comparison the estimated source location (based on the derivative data) is superimposed on the plot of acoustic source locations in figure 6.1.4.

Now we reconstruct the source. In figure 6.1.6A the derivative waveform with the estimated $\vec{r}$ (as discussed) is used to find the peak values of the $\partial \vec{T} / \partial t$ pulses. Figure 6.1.7A shows the individual vector pulses (as seen from the Kiva) oriented to the right and slightly downward. Assuming that the streamer velocity $\vec{v}_{eff}$ is parallel to $\vec{J}$ and in the same direction for this case we have the effective reconstruction of the positive streamer in figure 6.1.7A. For this type of assumed positive streamer, denoted by $\vec{v}_{eff} \uparrow\uparrow \vec{J}$ we take the individual vector pulses in their order of occurrence and lay them out from the graph origin sequentially in a cumulative manner (tail of vector coincident with head of previous vector). Figures 6.1.6B and 6.1.7B do the same thing for the $\vec{T}$ pulses from the field waveforms and give a comparable picture.

While this lightning event was a positive-going streamer, it is interesting to note that the impulsive nature of the fields is similar to that of natural negative step leaders.

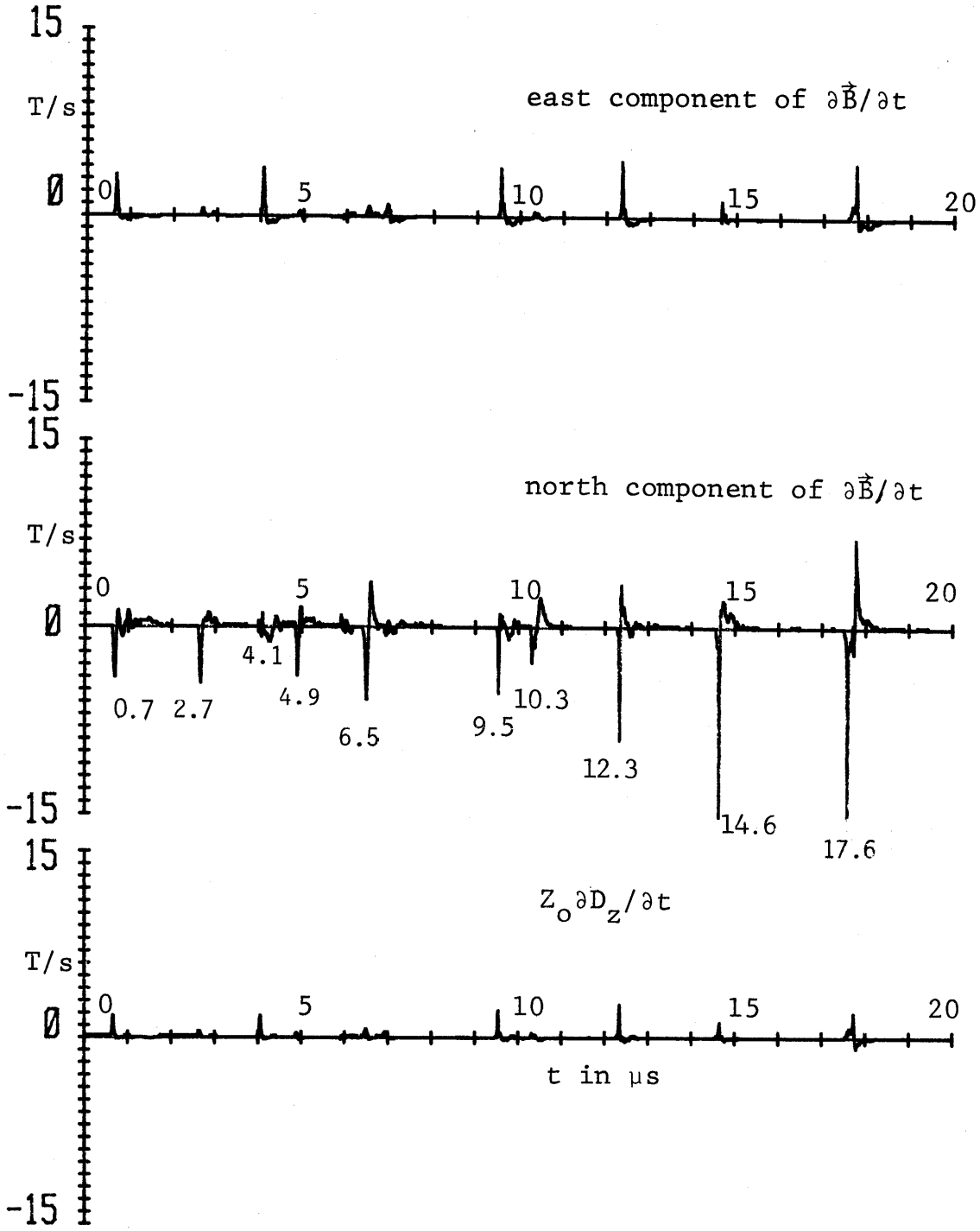

Date: 79228 M.S.T.: 1545:12

Figure 6.1.1A Derivative fields from rocket-triggered lightning

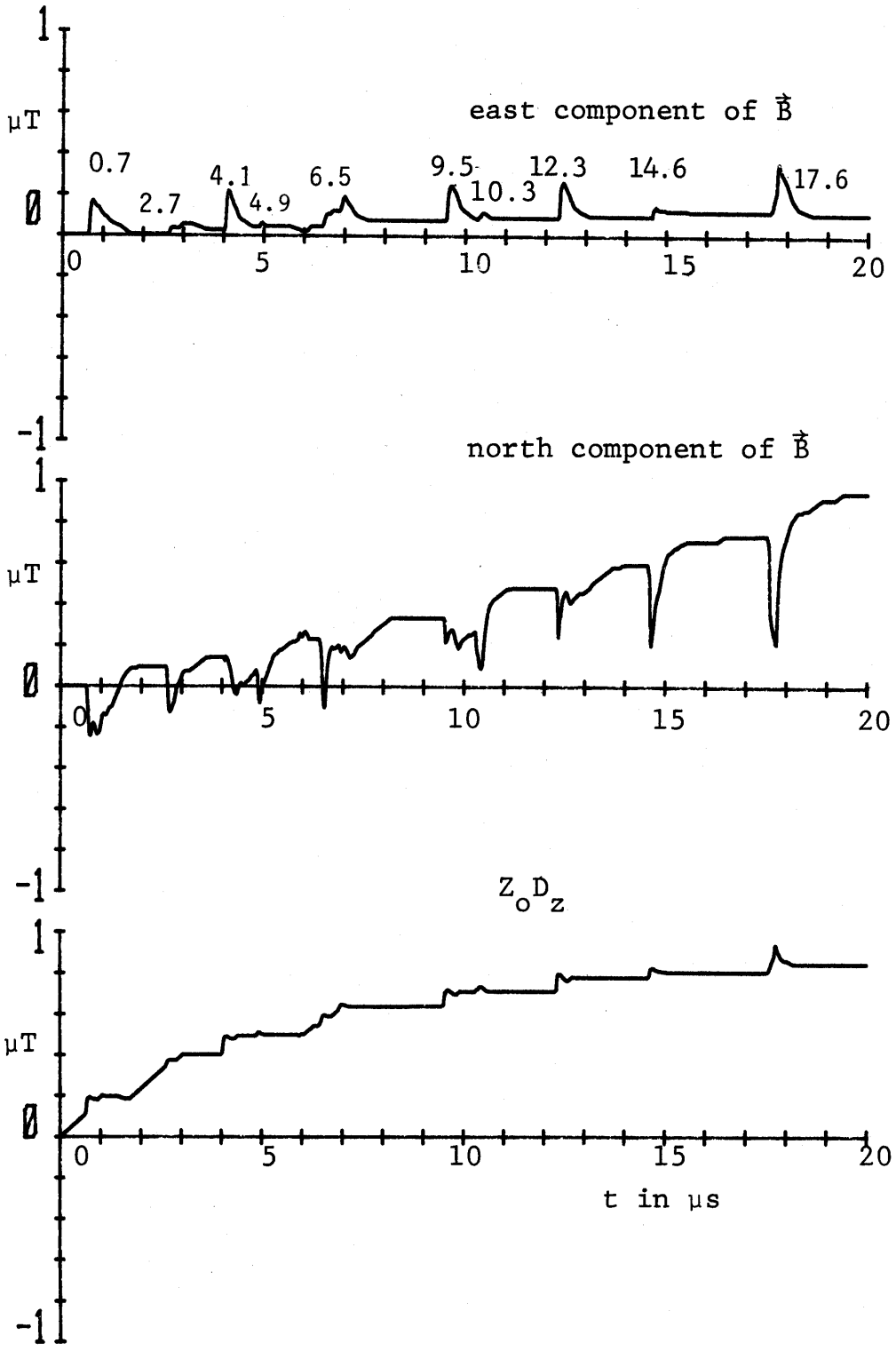

Date: 79228 M.S.T.: 1545:12

Figure 6.1.1B Fields from rocket-triggered lightning

Figure 6.1.2.1 Digital data for event 0.7

[ ] = baseline which is subtracted for peaks and numerical integration

Yeardate: 79228 Time: 15:45:12 M.S.T.

Time (μs)	$\partial B_E/\partial t$ (T/s)	$\partial B_N/\partial t$ (T/s)	$Z_o \partial D_z/\partial t$ (T/s)	B_E (μT)	B_N (μT)	$Z_o D_z$ (μT)
0.60	-0.156	0.156	0.118	-0.000	0.000	-0.000
0.61	-0.156	0.156	0.118	-0.000	0.000	-0.000
0.62	-0.156	0.156	0.177	-0.000	0.000	0.001
0.63	0.078	0.156	0.295	0.002	0.000	0.002
0.64	0.156	-0.469	0.530	0.005	-0.006	0.006
0.65	0.547	-1.250	1.414	0.012	-0.020	0.019
0.66	1.250	-2.500	1.708	0.027	-0.047	0.035
0.67	3.047	-3.125	1.649	0.059	-0.080	0.051
0.68	3.125	-3.281	1.001	0.091	-0.114	0.059
0.69	2.500	-3.906	0.530	0.118	-0.155	0.064
0.70	1.797	-3.906	0.295	0.137	-0.195	0.065
0.71	1.172	-2.656	0.059	0.151	-0.223	0.065
0.72	0.547	-1.406	0.059	0.158	-0.239	0.064
0.73	0.313	-0.156	0.059	0.162	-0.242	0.064
0.74	0.234	0.469	-0.177	0.166	-0.239	0.061
0.75	-0.313	1.250	-0.177	0.165	-0.228	0.058
0.76	-0.391	1.406	-0.177	0.163	-0.215	0.055
0.77	-0.391	1.406	-0.118	0.160	-0.203	0.053
0.78	-0.391	1.094	-0.177	0.158	-0.194	0.050
0.79	-0.391	0.781	-0.177	0.156	-0.187	0.047
0.80	-0.469	0.625	-0.177	0.152	-0.183	0.044
0.81	-0.469	0.000	-0.118	0.149	-0.184	0.041
0.82	-0.469	0.000	-0.118	0.146	-0.186	0.039
0.83	-0.469	-0.156	-0.118	0.143	-0.189	0.037
0.84	-0.391	-0.469	-0.059	0.141	-0.195	0.035
0.85	-0.313	-0.469	-0.059	0.139	-0.201	0.033
0.86	-0.313	-0.625	-0.059	0.138	-0.209	0.031
0.87	-0.234	-0.625	-0.059	0.137	-0.217	0.030
0.88	-0.234	-0.469	-0.059	0.136	-0.223	0.028
0.89	-0.234	-0.469	-0.118	0.135	-0.230	0.026
0.90	-0.391	-0.313	-0.118	0.133	-0.234	0.023
0.91	-0.391	0.156	-0.118	0.131	-0.234	0.021
0.92	-0.469	0.313	-0.059	0.127	-0.233	0.019
0.93	-0.547	0.313	-0.059	0.124	-0.231	0.017
0.94	-0.547	0.469	0.118	0.120	-0.228	0.017
0.95	-0.547	0.469	0.118	0.116	-0.225	0.017
0.96	-0.469	0.469	0.118	0.113	-0.222	0.017
0.97	-0.469	0.625	0.118	0.109	-0.217	0.017
0.98	-0.391	1.094	0.118	0.107	-0.208	0.017
0.99	-0.469	1.406	0.118	0.104	-0.195	0.017
1.00	-0.391	1.406	0.118	0.102	-0.183	0.017
1.01	-0.391	1.406	0.118	0.099	-0.170	0.017
1.02	-0.391	1.250	0.118	0.097	-0.159	0.017
1.03	-0.391	1.094	0.118	0.095	-0.150	0.017
1.04	-0.313	0.781	0.118	0.093	-0.144	0.017

Figure 6.1.2.1 Digital data for event 0.7 (continued)

Time (μs)	$\partial B_E/\partial t$ (T/s)	$\partial B_N/\partial t$ (T/s)	$Z_o \partial D_z/\partial t$ (T/s)	B_E (μT)	B_N (μT)	$Z_o D_z$ (μT)
1.05	-0.313	0.625	-0.059	0.091	-0.139	0.016
1.06	-0.234	0.469	-0.059	0.091	-0.136	0.014
1.07	-0.313	0.313	-0.059	0.089	-0.134	0.012
1.08	-0.313	0.000	-0.059	0.088	-0.136	0.010
1.09	-0.313	0.000	-0.118	0.086	-0.137	0.008
1.10	-0.313	0.000	-0.118	0.084	-0.139	0.006
1.11	-0.391	0.000	-0.118	0.082	-0.140	0.003
1.12	-0.391	0.313	-0.118	0.080	-0.139	0.001
1.13	-0.391	0.313	-0.118	0.077	-0.137	-0.002
1.14	-0.391	0.469	-0.059	0.075	-0.134	-0.003
1.15	-0.391	0.469	-0.059	0.073	-0.131	-0.005
1.16	-0.391	0.625	-0.059	0.070	-0.126	-0.007
1.17	-0.313	0.625	-0.059	0.069	-0.122	-0.009
1.18	-0.313	0.625	-0.059	0.067	-0.117	-0.010
1.19	-0.313	0.625	-0.059	0.066	-0.112	-0.012
1.20	-0.313	0.469	-0.059	0.064	-0.109	-0.014
1.21	-0.313	0.469	-0.059	0.063	-0.106	-0.016
1.22	-0.313	0.313	-0.059	0.061	-0.104	-0.017
1.23	-0.313	0.313	-0.059	0.059	-0.103	-0.019
1.24	-0.313	0.313	-0.059	0.058	-0.101	-0.021
1.25	-0.313	0.313	-0.059	0.056	-0.100	-0.023
1.26	-0.234	0.313	-0.059	0.055	-0.098	-0.025
1.27	-0.234	0.313	-0.059	0.055	-0.097	-0.026
1.28	-0.234	0.625	-0.059	0.054	-0.092	-0.028
1.29	-0.234	0.625	-0.059	0.053	-0.087	-0.030
1.30	-0.234	0.625	-0.059	0.052	-0.083	-0.032
1.31	-0.234	0.625	-0.059	0.052	-0.078	-0.033
1.32	-0.234	0.625	-0.059	0.051	-0.073	-0.035
1.33	-0.234	0.625	-0.059	0.050	-0.068	-0.037
1.34	-0.234	0.625	-0.059	0.049	-0.064	-0.039
1.35	-0.234	0.625	-0.059	0.048	-0.059	-0.040
1.36	-0.234	0.625	-0.059	0.048	-0.054	-0.042
1.37	-0.234	0.625	-0.059	0.047	-0.050	-0.044
1.38	-0.234	0.625	-0.059	0.046	-0.045	-0.046
1.39	-0.234	0.625	-0.059	0.045	-0.040	-0.048
1.40	-0.234	0.625	-0.059	0.045	-0.036	-0.049
1.41	-0.234	0.625	-0.118	0.044	-0.031	-0.052
1.42	-0.234	0.625	-0.118	0.043	-0.026	-0.054
1.43	-0.234	0.625	-0.118	0.042	-0.022	-0.056
1.44	-0.313	0.625	-0.118	0.041	-0.017	-0.059
1.45	-0.313	0.625	-0.118	0.039	-0.012	-0.061
1.46	-0.313	0.781	-0.118	0.037	-0.006	-0.063
1.47	-0.313	0.781	-0.118	0.036	0.000	-0.066
1.48	-0.313	0.781	-0.118	0.034	0.007	-0.068
1.49	-0.313	0.781	-0.118	0.033	0.013	-0.071
1.50	-0.313	0.781	-0.118	0.031	0.019	-0.073
1.51	-0.313	0.625	-0.118	0.030	0.024	-0.075
1.52	-0.313	0.625	-0.118	0.028	0.028	-0.078
1.53	-0.313	0.625	-0.118	0.027	0.033	-0.080
1.54	-0.313	0.625	-0.118	0.025	0.038	-0.082

Figure 6.1.2.1 Digital data for event 0.7 (continued)

Time (μs)	$\partial B_E/\partial t$ (T/s)	$\partial B_N/\partial t$ (T/s)	$Z_o \partial D_z/\partial t$ (T/s)	B_E (μT)	B_N (μT)	$Z_o D_z$ (μT)
1.55	-0.313	0.469	-0.118	0.023	0.041	-0.085
1.56	-0.313	0.469	-0.118	0.022	0.044	-0.087
1.57	-0.313	0.469	-0.118	0.020	0.047	-0.089
1.58	-0.313	0.469	-0.118	0.019	0.050	-0.092
1.59	-0.313	0.469	-0.118	0.017	0.053	-0.094
1.60	-0.313	0.469	-0.118	0.016	0.057	-0.096
1.61	-0.313	0.469	-0.059	0.014	0.060	-0.098
1.62	-0.313	0.469	-0.059	0.013	0.063	-0.100
1.63	-0.313	0.469	-0.059	0.011	0.066	-0.101
1.64	-0.313	0.469	-0.059	0.010	0.070	-0.103
1.65	-0.234	0.469	-0.059	0.009	0.073	-0.105
1.66	-0.234	0.313	-0.059	0.008	0.074	-0.107
1.67	-0.234	0.313	-0.059	0.007	0.076	-0.108
1.68	-0.234	0.313	-0.059	0.007	0.077	-0.110
1.69	-0.234	0.313	-0.059	0.006	0.079	-0.112
1.70	-0.234	0.313	-0.059	0.005	0.080	-0.114
1.71	-0.156	0.313	-0.059	0.005	0.082	-0.115
1.72	-0.156	0.313	-0.059	0.005	0.084	-0.117

Figure 6.1.2.2 Digital data for event 2.7

[ ] = baseline which is subtracted for peaks and numerical integration

Yeardate: 79228 Time: 15:45:12 M.S.T.

Time (μs)	$\partial B_E/\partial t$ (T/s)	$\partial B_N/\partial t$ (T/s)	$Z_o \partial D_z/\partial t$ (T/s)	B_E (μT)	B_N (μT)	$Z_o D_z$ (μT)
2.60	-0.156	0.156	0.118	-0.000	0.000	-0.000
2.61	-0.156	0.156	0.118	-0.000	0.000	-0.000
2.62	-0.156	-0.313	0.177	-0.000	-0.005	0.001
2.63	-0.156	-0.938	0.471	-0.000	-0.016	0.004
2.64	0.156	-2.500	0.471	0.003	-0.042	0.008
2.65	0.313	-3.750	0.471	0.008	-0.081	0.011
2.66	0.313	-3.906	0.471	0.012	-0.122	0.015
2.67	0.391	-4.375	0.295	0.018	-0.167	0.016
2.68	0.391	-2.656	0.236	0.023	-0.195	0.018
2.69	0.234	-1.406	0.059	0.027	-0.211	0.017
2.70	0.000	-0.625	0.059	0.029	-0.219	0.016
2.71	0.000	0.000	0.000	0.030	-0.220	0.015
2.72	-0.078	0.469	-0.059	0.031	-0.217	0.014
2.73	-0.156	0.625	-0.059	0.031	-0.212	0.012
2.74	-0.156	0.625	-0.059	0.031	-0.207	0.010
2.75	-0.156	0.625	-0.059	0.031	-0.203	0.008
2.76	-0.156	0.625	-0.059	0.031	-0.198	0.007
2.77	-0.234	0.781	-0.059	0.030	-0.192	0.005
2.78	-0.234	0.781	-0.059	0.029	-0.185	0.003
2.79	-0.234	0.625	-0.059	0.029	-0.181	0.001
2.80	-0.156	0.625	-0.059	0.029	-0.176	-0.000
2.81	-0.156	0.625	-0.059	0.029	-0.171	-0.002
2.82	-0.156	1.094	-0.059	0.029	-0.162	-0.004
2.83	-0.156	1.094	-0.059	0.029	-0.153	-0.006
2.84	-0.156	1.250	-0.059	0.029	-0.142	-0.007
2.85	-0.156	1.250	-0.059	0.029	-0.131	-0.009
2.86	-0.156	1.250	-0.059	0.029	-0.120	-0.011
2.87	-0.156	1.250	-0.059	0.029	-0.109	-0.013
2.88	-0.156	1.094	-0.059	0.029	-0.099	-0.015
2.89	-0.156	0.625	-0.059	0.029	-0.095	-0.016
2.90	0.078	0.625	0.118	0.031	-0.090	-0.016
2.91	0.078	0.469	0.118	0.033	-0.087	-0.016
2.92	0.078	0.469	0.118	0.036	-0.084	-0.016
2.93	0.078	0.469	0.118	0.038	-0.081	-0.016
2.94	0.078	0.625	0.118	0.040	-0.076	-0.016
2.95	0.078	0.625	0.118	0.043	-0.071	-0.016
2.96	0.078	0.625	0.118	0.045	-0.067	-0.016
2.97	0.078	0.625	0.118	0.047	-0.062	-0.016
2.98	0.078	0.625	0.118	0.050	-0.057	-0.016
2.99	-0.156	0.781	0.118	0.050	-0.051	-0.016
3.00	-0.156	0.781	0.118	0.050	-0.045	-0.016
3.01	-0.156	0.781	0.118	0.050	-0.038	-0.016
3.02	-0.156	0.625	0.118	0.050	-0.034	-0.016
3.03	-0.156	0.625	0.118	0.050	-0.029	-0.016
3.04	-0.156	0.469	0.118	0.050	-0.026	-0.016

Figure 6.1.2.2 Digital data for event 2.7 (continued)

Time (μs)	$\partial B_E/\partial t$ (T/s)	$\partial B_N/\partial t$ (T/s)	$Z_o \partial D_z/\partial t$ (T/s)	B_E (μT)	B_N (μT)	$Z_o D_z$ (μT)
3.05	-0.156	0.313	-0.059	0.050	-0.024	-0.018
3.06	-0.156	0.313	-0.059	0.050	-0.023	-0.020
3.07	-0.156	0.313	-0.059	0.050	-0.021	-0.022
3.08	-0.156	0.313	-0.059	0.050	-0.020	-0.023
3.09	-0.156	0.156	-0.059	0.050	-0.020	-0.025
3.10	-0.156	0.156	-0.059	0.050	-0.020	-0.027
3.11	-0.156	0.156	-0.059	0.050	-0.020	-0.029
3.12	-0.156	0.156	-0.059	0.050	-0.020	-0.030
3.13	-0.156	0.156	-0.059	0.050	-0.020	-0.032
3.14	-0.156	0.156	-0.059	0.050	-0.020	-0.034
3.15	-0.156	0.156	-0.059	0.050	-0.020	-0.036
3.16	-0.156	0.156	-0.059	0.050	-0.020	-0.038
3.17	-0.156	0.156	-0.059	0.050	-0.020	-0.039
3.18	-0.156	0.156	-0.059	0.050	-0.020	-0.041
3.19	-0.156	0.156	-0.059	0.050	-0.020	-0.043
3.20	-0.156	0.313	-0.059	0.050	-0.018	-0.045
3.21	-0.234	0.313	-0.059	0.049	-0.017	-0.046
3.22	-0.234	0.313	-0.059	0.048	-0.015	-0.048
3.23	-0.234	0.313	-0.059	0.047	-0.013	-0.050
3.24	-0.234	0.313	-0.059	0.046	-0.012	-0.052
3.25	-0.234	0.313	-0.059	0.046	-0.010	-0.053
3.26	-0.234	0.313	-0.059	0.045	-0.009	-0.055
3.27	-0.234	0.313	-0.059	0.044	-0.007	-0.057
3.28	-0.234	0.313	-0.059	0.043	-0.006	-0.059
3.29	-0.234	0.313	-0.059	0.042	-0.004	-0.061
3.30	-0.234	0.313	-0.059	0.041	-0.003	-0.063
3.31	-0.234	0.313	-0.059	0.041	-0.001	-0.064
3.32	-0.234	0.313	-0.059	0.040	0.000	-0.066
3.33	-0.234	0.313	-0.059	0.039	0.002	-0.068
3.34	-0.234	0.313	-0.059	0.038	0.003	-0.070
3.35	-0.234	0.313	-0.059	0.038	0.005	-0.071
3.36	-0.234	0.313	-0.059	0.037	0.007	-0.073
3.37	-0.234	0.313	-0.059	0.036	0.008	-0.075
3.38	-0.234	0.313	-0.059	0.035	0.010	-0.077
3.39	-0.234	0.313	-0.059	0.034	0.011	-0.078
3.40	-0.234	0.313	-0.059	0.034	0.013	-0.080
3.41	-0.234	0.313	-0.059	0.033	0.014	-0.082
3.42	-0.234	0.313	-0.059	0.032	0.016	-0.084
3.43	-0.234	0.313	-0.059	0.031	0.017	-0.086
3.44	-0.234	0.313	-0.059	0.030	0.019	-0.087
3.45	-0.234	0.313	-0.059	0.030	0.021	-0.089
3.46	-0.234	0.313	-0.059	0.029	0.022	-0.091
3.47	-0.234	0.313	-0.059	0.028	0.024	-0.093
3.48	-0.234	0.313	-0.059	0.027	0.025	-0.094
3.49	-0.234	0.313	-0.059	0.027	0.027	-0.096
3.50	-0.234	0.313	-0.059	0.026	0.028	-0.098
3.51	-0.234	0.313	-0.059	0.025	0.030	-0.100
3.52	-0.234	0.313	-0.059	0.024	0.031	-0.102
3.53	-0.234	0.313	-0.059	0.024	0.033	-0.103
3.54	-0.234	0.313	-0.059	0.023	0.034	-0.105
3.55	-0.234	0.313	-0.059	0.022	0.036	-0.107
3.56	-0.234	0.313	-0.059	0.021	0.037	-0.109
3.57	-0.156	0.313	-0.059	0.021	0.039	-0.110
3.58	-0.156	0.313	-0.059	0.021	0.041	-0.112

Figure 6.1.2.3 Digital data for event 4.1

[ ] = baseline which is subtracted for peaks and numerical integration

Yeardate: 79228 Time: 15:45:12 M.S.T.

Time (μs)	$\partial B_E/\partial t$ (T/s)	$\partial B_N/\partial t$ (T/s)	$Z_o \partial D_z/\partial t$ (T/s)	B_E (μT)	B_N (μT)	$Z_o D_z$ (μT)
4.00	-0.156	0.156	0.118	-0.000	0.000	-0.000
4.01	-0.156	0.156	0.118	-0.000	0.000	-0.000
4.02	-0.156	0.156	0.353	-0.000	0.000	0.002
4.03	0.391	0.156	0.943	0.005	0.000	0.011
4.04	1.172	0.156	1.414	0.019	0.000	0.024
4.05	2.500	0.156	1.708	0.045	0.000	0.039
4.06	3.438	-0.469	1.649	0.081	-0.006	0.055
4.07	3.672	-0.625	1.001	0.120	-0.014	0.064
4.08	3.125	0.625	0.530	0.152	-0.009	0.068
4.09	1.875	1.250	0.295	0.173	0.002	0.069
4.10	0.625	0.000	0.059	0.180	0.000	0.069
4.11	0.547	0.000	0.059	0.187	-0.002	0.068
4.12	0.000	-0.156	0.000	0.189	-0.005	0.067
4.13	-0.313	-0.313	-0.177	0.187	-0.009	0.064
4.14	-0.625	-0.313	-0.177	0.182	-0.014	0.061
4.15	-0.703	-0.313	-0.177	0.177	-0.018	0.058
4.16	-0.781	-0.469	-0.177	0.171	-0.025	0.055
4.17	-0.781	-0.469	-0.177	0.164	-0.031	0.052
4.18	-0.781	-0.469	-0.177	0.158	-0.037	0.049
4.19	-0.703	-0.469	-0.177	0.153	-0.043	0.046
4.20	-0.625	-0.469	-0.177	0.148	-0.050	0.043
4.21	-0.625	-0.781	-0.177	0.143	-0.059	0.040
4.22	-0.625	-0.781	-0.118	0.139	-0.068	0.038
4.23	-0.625	-0.781	-0.118	0.134	-0.078	0.036
4.24	-0.703	-1.094	-0.118	0.128	-0.090	0.033
4.25	-0.703	-1.094	-0.118	0.123	-0.103	0.031
4.26	-0.625	-1.250	-0.118	0.118	-0.117	0.029
4.27	-0.625	-1.250	-0.059	0.114	-0.131	0.027
4.28	-0.547	-1.250	-0.059	0.110	-0.145	0.025
4.29	-0.547	-0.781	-0.059	0.106	-0.154	0.023
4.30	-0.547	-0.625	-0.059	0.102	-0.162	0.022
4.31	-0.703	-0.625	-0.059	0.096	-0.170	0.020
4.32	-0.703	-0.156	-0.059	0.091	-0.173	0.018
4.33	-0.703	-0.156	0.118	0.085	-0.176	0.018
4.34	-0.703	0.000	0.118	0.080	-0.178	0.018
4.35	-0.703	0.000	0.118	0.074	-0.179	0.018
4.36	-0.625	0.000	0.118	0.070	-0.181	0.018
4.37	-0.625	0.469	0.118	0.065	-0.178	0.018
4.38	-0.469	0.625	0.118	0.062	-0.173	0.018
4.39	-0.469	0.938	0.118	0.059	-0.165	0.018
4.40	-0.469	0.938	0.118	0.056	-0.157	0.018
4.41	-0.391	0.938	0.118	0.053	-0.150	0.018
4.42	-0.391	0.781	-0.059	0.051	-0.143	0.016
4.43	-0.391	0.781	-0.059	0.049	-0.137	0.014
4.44	-0.313	0.625	-0.059	0.047	-0.132	0.013

Figure 6.1.2.3 Digital data for event 4.1 (continued)

Time (μs)	$\partial B_E/\partial t$ (T/s)	$\partial B_N/\partial t$ (T/s)	$Z_o \partial D_z/\partial t$ (T/s)	B_E (μT)	B_N (μT)	$Z_o D_z$ (μT)
4.45	-0.313	0.469	-0.059	0.046	-0.129	0.011
4.46	-0.313	0.469	-0.059	0.044	-0.126	0.009
4.47	-0.234	0.313	-0.059	0.043	-0.125	0.007
4.48	-0.234	0.000	-0.059	0.042	-0.126	0.006
4.49	-0.234	0.000	-0.059	0.042	-0.128	0.004
4.50	-0.234	-0.156	-0.059	0.041	-0.131	0.002
4.51	-0.234	-0.156	-0.059	0.040	-0.134	0.000
4.52	-0.234	-0.156	-0.059	0.039	-0.137	-0.001
4.53	-0.313	0.156	-0.059	0.038	-0.137	-0.003
4.54	-0.313	0.313	-0.059	0.036	-0.135	-0.005
4.55	-0.313	0.313	-0.059	0.035	-0.134	-0.007
4.56	-0.313	0.313	-0.059	0.033	-0.132	-0.009
4.57	-0.313	0.469	-0.059	0.031	-0.129	-0.010
4.58	-0.313	0.469	-0.059	0.030	-0.126	-0.012
4.59	-0.313	0.469	-0.059	0.028	-0.123	-0.014
4.60	-0.313	0.469	-0.059	0.027	-0.120	-0.016
4.61	-0.313	0.313	-0.059	0.025	-0.118	-0.017
4.62	-0.313	0.313	-0.059	0.024	-0.117	-0.019
4.63	-0.313	0.313	-0.059	0.022	-0.115	-0.021
4.64	-0.234	0.313	-0.059	0.021	-0.114	-0.023
4.65	-0.234	0.313	-0.059	0.021	-0.112	-0.024
4.66	-0.234	0.313	-0.059	0.020	-0.110	-0.026
4.67	-0.234	0.313	-0.059	0.019	-0.109	-0.028
4.68	-0.234	0.313	-0.059	0.018	-0.107	-0.030
4.69	-0.234	0.469	-0.059	0.017	-0.104	-0.032
4.70	-0.234	0.469	-0.059	0.017	-0.101	-0.033
4.71	-0.234	0.469	-0.059	0.016	-0.098	-0.035
4.72	-0.234	0.469	-0.059	0.015	-0.095	-0.037
4.73	-0.234	0.469	-0.059	0.014	-0.092	-0.039
4.74	-0.234	0.469	-0.059	0.013	-0.089	-0.040
4.75	-0.156	0.313	-0.059	0.013	-0.087	-0.042
4.76	-0.156	0.313	-0.059	0.013	-0.085	-0.044
4.77	-0.156	0.313	-0.059	0.013	-0.084	-0.046
4.78	-0.156	0.313	-0.059	0.013	-0.082	-0.047
4.79	-0.156	0.469	-0.059	0.013	-0.079	-0.049
4.80	-0.156	0.469	-0.059	0.013	-0.076	-0.051
4.81	-0.156	0.469	-0.059	0.013	-0.073	-0.053
4.82	-0.156	0.469	-0.059	0.013	-0.070	-0.055
4.83	-0.156	0.469	-0.059	0.013	-0.067	-0.056
4.84	-0.156	0.469	-0.059	0.013	-0.064	-0.058
4.85	-0.156	0.000	-0.059	0.013	-0.065	-0.060

Figure 6.1.2.4 Digital data for event 4.9

[ ] = baseline which is subtracted for peaks and numerical integration

Yeardate: 79228 Time: 15:45:12 M.S.T.

Time (μs)	$\partial B_E/\partial t$ (T/s)	$\partial B_N/\partial t$ (T/s)	$Z_o \partial D_z/\partial t$ (T/s)	B_E (μT)	B_N (μT)	$Z_o D_z$ (μT)
4.83	-0.156	0.469	-0.059	-0.000	-0.000	0.000
4.84	-0.156	0.469	-0.059	-0.000	-0.000	0.000
4.85	-0.156	0.000	-0.059	-0.000	-0.005	0.000
4.86	-0.156	-0.625	0.118	-0.000	-0.016	0.002
4.87	-0.156	-0.469	0.118	-0.000	-0.025	0.004
4.88	0.078	-0.781	0.177	0.002	-0.038	0.006
4.89	0.078	-2.500	0.295	0.005	-0.067	0.009
4.90	0.156	-3.750	0.295	0.008	-0.109	0.013
4.91	0.156	-3.281	0.236	0.011	-0.147	0.016
4.92	0.234	-1.406	0.059	0.015	-0.166	0.017
4.93	0.156	-0.625	0.000	0.018	-0.177	0.018
4.94	0.078	-0.625	-0.177	0.020	-0.188	0.017
4.95	-0.156	1.094	-0.177	0.020	-0.181	0.015
4.96	-0.234	1.719	-0.236	0.019	-0.169	0.013
4.97	-0.391	1.719	-0.236	0.017	-0.156	0.011
4.98	-0.391	1.719	-0.236	0.015	-0.144	0.010
4.99	-0.391	1.719	-0.177	0.012	-0.131	0.009
5.00	-0.313	1.250	-0.177	0.011	-0.123	0.007
5.01	-0.313	0.625	-0.118	0.009	-0.122	0.007
5.02	-0.313	0.625	-0.118	0.007	-0.120	0.006
5.03	-0.234	0.469	-0.118	0.007	-0.120	0.006
5.04	-0.234	0.469	-0.118	0.006	-0.120	0.005
5.05	-0.234	0.469	-0.118	0.005	-0.120	0.004
5.06	-0.234	0.625	-0.118	0.004	-0.119	0.004
5.07	-0.156	0.625	-0.059	0.004	-0.117	0.004
5.08	-0.156	0.625	-0.059	0.004	-0.115	0.004
5.09	-0.156	0.625	-0.059	0.004	-0.114	0.004
5.10	-0.156	0.781	-0.059	0.004	-0.111	0.004
5.11	-0.156	0.625	-0.059	0.004	-0.109	0.004
5.12	-0.156	0.625	-0.059	0.004	-0.108	0.004
5.13	-0.156	0.781	-0.059	0.004	-0.104	0.004
5.14	-0.156	0.781	-0.059	0.004	-0.101	0.004
5.15	-0.156	0.781	-0.059	0.004	-0.098	0.004
5.16	-0.156	0.781	-0.059	0.004	-0.095	0.004
5.17	-0.156	0.781	-0.059	0.004	-0.092	0.004
5.18	-0.156	0.781	-0.059	0.004	-0.089	0.004
5.19	-0.156	0.781	-0.059	0.004	-0.086	0.004
5.20	-0.156	0.625	-0.059	0.004	-0.084	0.004
5.21	-0.156	0.625	-0.059	0.004	-0.083	0.004
5.22	-0.156	0.625	-0.059	0.004	-0.081	0.004
5.23	-0.156	0.625	-0.059	0.004	-0.080	0.004
5.24	-0.156	0.781	-0.059	0.004	-0.076	0.004
5.25	-0.156	0.781	-0.059	0.004	-0.073	0.004
5.26	-0.156	0.625	-0.059	0.004	-0.072	0.004
5.27	-0.156	0.781	-0.059	0.004	-0.069	0.004
5.28	-0.156	0.625	-0.059	0.004	-0.067	0.004
5.29	-0.156	0.469	-0.059	0.004	-0.067	0.004

Figure 6.1.2.5 Digital data for event 6.5

[ ] = baseline which is subtracted for peaks and numerical integration

Yeardate: 79228 Time: 15:45:12 M.S.T.

Time (μs)	$\partial B_E/\partial t$ (T/s)	$\partial B_N/\partial t$ (T/s)	$Z_o \partial D_z/\partial t$ (T/s)	B_E (μT)	B_N (μT)	$Z_o D_z$ (μT)
6.40	-0.156	0.156	0.118	-0.000	0.000	-0.000
6.41	-0.156	0.156	0.118	-0.000	0.000	-0.000
6.42	-0.156	-0.313	0.118	-0.000	-0.005	-0.000
6.43	-0.156	-0.469	0.118	-0.000	-0.011	-0.000
6.44	-0.156	-0.781	0.177	-0.000	-0.020	0.001
6.45	0.078	-1.250	0.295	0.002	-0.034	0.002
6.46	0.156	-2.031	0.295	0.005	-0.056	0.004
6.47	0.156	-2.656	0.471	0.009	-0.084	0.008
6.48	0.313	-3.906	0.530	0.013	-0.125	0.012
6.49	0.547	-5.625	0.648	0.020	-0.183	0.017
6.50	0.625	-5.625	0.589	0.028	-0.241	0.022
6.51	0.625	-3.906	0.471	0.036	-0.281	0.025
6.52	0.547	-2.656	0.295	0.043	-0.309	0.027
6.53	0.391	-1.406	0.236	0.048	-0.325	0.028
6.54	0.313	-0.625	0.059	0.053	-0.333	0.028
6.55	0.234	0.625	0.059	0.057	-0.328	0.027
6.56	0.000	2.344	-0.177	0.059	-0.306	0.024
6.57	0.000	2.500	-0.177	0.060	-0.283	0.021
6.58	-0.078	3.594	-0.177	0.061	-0.248	0.018
6.59	-0.156	3.750	-0.177	0.061	-0.212	0.015
6.60	-0.156	3.125	-0.177	0.061	-0.182	0.012
6.61	-0.156	2.969	-0.118	0.061	-0.154	0.010
6.62	-0.156	2.344	-0.118	0.061	-0.132	0.007
6.63	-0.156	1.875	-0.118	0.061	-0.115	0.005
6.64	-0.156	1.719	-0.059	0.061	-0.099	0.003
6.65	0.078	1.250	-0.059	0.063	-0.089	0.001
6.66	0.078	1.250	-0.059	0.066	-0.078	-0.000
6.67	0.078	1.094	-0.059	0.068	-0.068	-0.002
6.68	0.078	0.781	-0.059	0.070	-0.062	-0.004
6.69	0.078	0.781	-0.059	0.073	-0.056	-0.006
6.70	0.078	0.781	-0.059	0.075	-0.049	-0.007
6.71	0.078	0.625	-0.059	0.077	-0.045	-0.009
6.72	-0.156	0.469	-0.059	0.077	-0.042	-0.011
6.73	-0.156	0.469	-0.059	0.077	-0.039	-0.013
6.74	-0.156	0.000	0.118	0.077	-0.040	-0.013
6.75	-0.156	0.000	0.118	0.077	-0.042	-0.013
6.76	-0.156	0.000	0.118	0.077	-0.043	-0.013
6.77	-0.156	0.000	0.118	0.077	-0.045	-0.013
6.78	-0.156	0.156	0.118	0.077	-0.045	-0.013
6.79	-0.156	0.156	0.118	0.077	-0.045	-0.013
6.80	-0.234	0.313	0.118	0.077	-0.043	-0.013
6.81	-0.234	0.313	0.118	0.076	-0.042	-0.013
6.82	-0.234	0.313	0.118	0.075	-0.040	-0.013
6.83	-0.234	0.313	0.118	0.074	-0.039	-0.013
6.84	-0.156	0.313	0.118	0.074	-0.037	-0.013

Figure 6.1.2.5 Digital data for event 6.5 (continued)

Time (μs)	$\partial B_E/\partial t$ (T/s)	$\partial B_N/\partial t$ (T/s)	$Z_o \partial D_z/\partial t$ (T/s)	B_E (μT)	B_N (μT)	$Z_o D_z$ (μT)
6.85	-0.156	0.313	0.118	0.074	-0.035	-0.013
6.86	-0.156	0.313	0.118	0.074	-0.034	-0.013
6.87	0.078	0.313	0.118	0.077	-0.032	-0.013
6.88	0.156	0.313	0.118	0.080	-0.031	-0.013
6.89	0.156	0.156	0.118	0.083	-0.031	-0.013
6.90	0.156	0.156	0.177	0.086	-0.031	-0.012
6.91	0.313	-0.313	0.295	0.091	-0.035	-0.010
6.92	0.547	-0.313	0.353	0.098	-0.040	-0.008
6.93	0.625	-0.313	0.412	0.105	-0.045	-0.005
6.94	0.781	-0.469	0.412	0.115	-0.051	-0.002
6.95	0.781	-0.469	0.353	0.124	-0.057	0.000
6.96	0.703	0.313	0.236	0.133	-0.056	0.001
6.97	0.313	0.313	0.059	0.137	-0.054	0.001
6.98	0.234	0.469	0.059	0.141	-0.051	0.000
6.99	0.000	0.469	0.000	0.143	-0.048	-0.001
7.00	-0.313	0.469	-0.118	0.141	-0.045	-0.003
7.01	-0.391	0.469	-0.118	0.139	-0.042	-0.006
7.02	-0.391	0.469	-0.118	0.137	-0.038	-0.008
7.03	-0.547	0.313	-0.118	0.133	-0.037	-0.010
7.04	-0.547	0.000	-0.118	0.129	-0.038	-0.013
7.05	-0.547	0.000	-0.118	0.125	-0.040	-0.015
7.06	-0.547	0.000	-0.118	0.121	-0.042	-0.017
7.07	-0.469	-0.156	-0.118	0.118	-0.045	-0.020
7.08	-0.469	-0.156	-0.118	0.115	-0.048	-0.022
7.09	-0.469	-0.156	-0.118	0.112	-0.051	-0.025
7.10	-0.469	-0.313	-0.118	0.109	-0.056	-0.027
7.11	-0.391	-0.313	-0.118	0.106	-0.060	-0.029
7.12	-0.391	-0.313	-0.118	0.104	-0.065	-0.032
7.13	-0.391	-0.313	-0.118	0.101	-0.070	-0.034
7.14	-0.391	-0.313	-0.118	0.099	-0.074	-0.036
7.15	-0.391	-0.313	-0.118	0.097	-0.079	-0.038
7.16	-0.469	-0.313	-0.118	0.094	-0.083	-0.041
7.17	-0.469	-0.313	-0.059	0.090	-0.088	-0.042
7.18	-0.469	0.156	-0.059	0.087	-0.088	-0.044
7.19	-0.469	0.313	-0.059	0.084	-0.086	-0.046
7.20	-0.547	0.313	-0.059	0.080	-0.085	-0.048
7.21	-0.547	0.313	-0.059	0.076	-0.083	-0.050
7.22	-0.469	0.313	-0.059	0.073	-0.082	-0.051
7.23	-0.469	0.313	-0.059	0.070	-0.080	-0.053
7.24	-0.469	0.313	-0.059	0.067	-0.079	-0.055
7.25	-0.469	0.313	-0.059	0.064	-0.077	-0.057
7.26	-0.391	0.313	-0.059	0.061	-0.076	-0.058
7.27	-0.391	0.469	-0.059	0.059	-0.072	-0.060
7.28	-0.391	0.469	-0.059	0.057	-0.069	-0.062
7.29	-0.313	0.469	-0.059	0.055	-0.066	-0.064
7.30	-0.313	0.625	-0.059	0.054	-0.061	-0.065
7.31	-0.313	0.625	-0.059	0.052	-0.057	-0.067
7.32	-0.313	0.625	-0.059	0.051	-0.052	-0.069
7.33	-0.313	0.625	-0.059	0.049	-0.047	-0.071
7.34	-0.234	0.469	-0.059	0.048	-0.044	-0.073

Figure 6.1.2.5 Digital data for event 6.5 (continued)

Time (μs)	$\partial B_E/\partial t$ (T/s)	$\partial B_N/\partial t$ (T/s)	$Z_o \partial D_z/\partial t$ (T/s)	B_E (μT)	B_N (μT)	$Z_o D_z$ (μT)
7.35	-0.234	0.469	-0.059	0.047	-0.041	-0.074
7.36	-0.234	0.469	-0.059	0.047	-0.038	-0.076
7.37	-0.234	0.469	-0.059	0.046	-0.035	-0.078
7.38	-0.234	0.313	-0.059	0.045	-0.033	-0.080
7.39	-0.234	0.313	-0.059	0.044	-0.032	-0.081
7.40	-0.234	0.313	-0.059	0.043	-0.030	-0.083
7.41	-0.234	0.313	-0.059	0.043	-0.029	-0.085
7.42	-0.234	0.313	-0.059	0.042	-0.027	-0.087
7.43	-0.234	0.313	-0.059	0.041	-0.025	-0.088
7.44	-0.234	0.313	-0.059	0.040	-0.024	-0.090
7.45	-0.234	0.313	-0.059	0.040	-0.022	-0.092
7.46	-0.234	0.313	-0.059	0.039	-0.021	-0.094
7.47	-0.234	0.313	-0.059	0.038	-0.019	-0.096
7.48	-0.234	0.313	-0.059	0.037	-0.018	-0.097
7.49	-0.234	0.313	-0.059	0.036	-0.016	-0.099
7.50	-0.234	0.313	-0.059	0.036	-0.015	-0.101

Figure 6.1.2.6 Digital data for event 9.5

[ ] = baseline which is subtracted for peaks and numerical integration

Yeardate: 79228 Time: 15:45:12 M.S.T.

Time (μs)	$\partial B_E/\partial t$ (T/s)	$\partial B_N/\partial t$ (T/s)	$Z_o \partial D_z/\partial t$ (T/s)	B_E (μT)	B_N (μT)	$Z_o D_z$ (μT)
9.49	[-0.156]	0.156	0.118	-0.000	0.000	-0.000
9.50	0.078	[0.156]	[0.118]	0.002	0.000	-0.000
9.51	0.078	-0.469	0.177	0.005	-0.006	0.001
9.52	0.156	-0.469	0.471	0.008	-0.012	0.004
9.53	0.547	-2.500	1.885	0.015	-0.039	0.022
9.54	2.500	-5.156	2.121	0.041	-0.092	0.042
9.55	3.750	-2.500	1.001	0.080	-0.119	0.051
9.56	3.125	0.625	0.059	0.113	-0.114	0.050
9.57	1.250	1.250	0.059	0.127	-0.103	0.049
9.58	0.625	0.000	0.295	0.135	-0.105	0.051
9.59	0.859	0.469	0.353	0.145	-0.102	0.054
9.60	0.938	1.094	0.236	0.156	-0.092	0.055
9.61	0.625	1.094	0.059	0.164	-0.083	0.054
9.62	0.234	0.625	0.059	0.168	-0.078	0.054
9.63	0.000	0.625	-0.177	0.169	-0.073	0.051
9.64	-0.078	0.625	-0.177	0.170	-0.069	0.048
9.65	-0.313	0.469	-0.177	0.169	-0.066	0.045
9.66	-0.313	0.313	-0.236	0.167	-0.064	0.041
9.67	-0.391	0.469	-0.236	0.165	-0.061	0.038
9.68	-0.625	0.313	-0.236	0.160	-0.060	0.034
9.69	-0.625	0.313	-0.236	0.156	-0.058	0.031
9.70	-0.469	0.156	-0.177	0.153	-0.058	0.028
9.71	-0.469	0.156	-0.177	0.149	-0.058	0.025
9.72	-0.469	0.156	-0.177	0.146	-0.058	0.022
9.73	-0.469	-0.313	-0.177	0.143	-0.063	0.019
9.74	-0.469	-0.313	-0.177	0.140	-0.068	0.016
9.75	-0.547	-0.469	-0.236	0.136	-0.074	0.013
9.76	-0.625	-0.469	-0.236	0.131	-0.080	0.009
9.77	-0.625	-0.781	-0.177	0.127	-0.089	0.006
9.78	-0.703	-0.781	-0.177	0.121	-0.099	0.003
9.79	-0.703	-0.625	-0.059	0.116	-0.107	0.001
9.80	-0.781	-0.469	0.000	0.110	-0.113	0.000
9.81	-0.781	-0.469	0.000	0.103	-0.119	-0.001
9.82	-0.703	-0.469	0.000	0.098	-0.125	-0.002
9.83	-0.703	-0.469	-0.059	0.092	-0.132	-0.004
9.84	-0.703	-0.313	-0.059	0.087	-0.136	-0.006
9.85	-0.703	-0.313	0.118	0.081	-0.141	-0.006
9.86	-0.703	-0.313	0.118	0.076	-0.146	-0.006
9.87	-0.625	0.156	0.118	0.071	-0.146	-0.006
9.88	-0.547	0.313	0.118	0.067	-0.144	-0.006
9.89	-0.469	0.625	0.118	0.064	-0.139	-0.006
9.90	-0.469	0.625	0.118	0.061	-0.135	-0.006
9.91	-0.391	0.781	0.118	0.059	-0.128	-0.006
9.92	-0.391	0.625	-0.059	0.056	-0.124	-0.007
9.93	-0.313	0.625	-0.059	0.055	-0.119	-0.009
9.94	-0.313	0.469	-0.059	0.053	-0.116	-0.011

Figure 6.1.2.6 Digital data for event 9.5 (continued)

Time (μs)	$\partial B_E/\partial t$ (T/s)	$\partial B_N/\partial t$ (T/s)	$Z_o \partial D_z/\partial t$ (T/s)	B_E (μT)	B_N (μT)	$Z_o D_z$ (μT)
9.95	-0.391	0.469	-0.059	0.051	-0.113	-0.01[illegible]
9.96	-0.391	0.313	-0.059	0.049	-0.111	-0.015
9.97	-0.313	0.469	-0.059	0.047	-0.108	-0.016
9.98	-0.313	0.469	-0.059	0.045	-0.105	-0.018
9.99	-0.313	0.313	-0.059	0.044	-0.103	-0.020
10.00	-0.313	0.313	-0.059	0.042	-0.102	-0.022
10.01	-0.234	0.313	-0.059	0.042	-0.100	-0.023
10.02	-0.234	0.313	-0.059	0.041	-0.099	-0.025
10.03	-0.313	0.313	-0.059	0.039	-0.097	-0.027
10.04	-0.313	0.313	-0.059	0.038	-0.096	-0.029
10.05	-0.313	0.313	-0.059	0.036	-0.094	-0.030
10.06	-0.313	0.313	-0.059	0.035	-0.092	-0.032
10.07	-0.313	0.313	-0.059	0.033	-0.091	-0.034
10.08	-0.313	0.313	-0.059	0.031	-0.089	-0.036
10.09	-0.313	0.313	-0.059	0.030	-0.088	-0.038
10.10	-0.313	0.313	-0.059	0.028	-0.086	-0.039
10.11	-0.313	0.313	-0.118	0.027	-0.085	-0.042
10.12	-0.313	0.313	-0.118	0.025	-0.083	-0.044
10.13	-0.313	0.156	-0.118	0.024	-0.083	-0.046
10.14	-0.313	0.156	-0.118	0.022	-0.083	-0.049
10.15	-0.313	0.156	-0.059	0.020	-0.083	-0.051
10.16	-0.313	0.156	-0.059	0.019	-0.083	-0.052
10.17	-0.313	0.156	-0.059	0.017	-0.083	-0.054
10.18	-0.313	0.313	-0.059	0.016	-0.081	-0.056
10.19	-0.313	0.313	-0.059	0.014	-0.080	-0.058
10.20	-0.234	0.313	-0.059	0.013	-0.078	-0.059
10.21	-0.234	0.313	-0.059	0.013	-0.077	-0.061
10.22	-0.234	0.313	-0.059	0.012	-0.075	-0.063
10.23	-0.234	0.313	-0.059	0.011	-0.074	-0.065
10.24	-0.234	0.313	-0.059	0.010	-0.072	-0.066
10.25	-0.234	0.313	-0.059	0.009	-0.071	-0.068
10.26	-0.234	0.313	-0.059	0.009	-0.069	-0.070
10.27	-0.234	0.313	-0.059	0.008	-0.067	-0.072
10.28	-0.234	0.156	-0.059	0.007	-0.067	-0.074
10.29	-0.156	-0.781	0.118	0.007	-0.077	-0.074

Figure 6.1.2.7 Digital data for event 10.3

[ ] = baseline which is subtracted for peaks and numerical integration

Yeardate: 79228 Time: 15:45:12 M.S.T.

Time (μs)	$\partial B_E/\partial t$ (T/s)	$\partial B_N/\partial t$ (T/s)	$Z_o \partial D_z/\partial t$ (T/s)	B_E (μT)	B_N (μT)	$Z_o D_z$ (μT)
10.26	-0.234	0.313	-0.059	-0.000	-0.000	0.000
10.27	-0.234	0.313	-0.059	-0.000	-0.000	0.000
10.28	-0.234	0.156	-0.059	-0.000	-0.002	0.000
10.29	-0.156	-0.781	0.118	0.001	-0.013	0.002
10.30	-0.156	-2.500	0.177	0.002	-0.041	0.004
10.31	0.156	-2.656	0.295	0.005	-0.070	0.008
10.32	0.234	-1.875	0.236	0.010	-0.092	0.011
10.33	0.156	-1.250	0.059	0.014	-0.108	0.012
10.34	0.000	-0.625	0.059	0.016	-0.117	0.013
10.35	0.000	-0.625	0.059	0.019	-0.127	0.014
10.36	0.000	-1.250	0.059	0.021	-0.142	0.015
10.37	0.078	-1.406	0.177	0.024	-0.159	0.018
10.38	0.078	-1.406	0.177	0.027	-0.177	0.020
10.39	0.156	-0.781	0.177	0.031	-0.188	0.022
10.40	0.156	-0.156	0.118	0.035	-0.192	0.024
10.41	0.078	-0.156	0.118	0.038	-0.197	0.026
10.42	0.078	0.000	-0.059	0.041	-0.200	0.026
10.43	-0.156	0.313	-0.059	0.042	-0.200	0.026
10.44	-0.156	0.625	-0.059	0.043	-0.197	0.026
10.45	-0.156	1.094	-0.118	0.044	-0.189	0.025
10.46	-0.156	1.250	-0.118	0.044	-0.180	0.025
10.47	-0.234	1.875	-0.177	0.044	-0.164	0.024
10.48	-0.234	2.344	-0.236	0.044	-0.144	0.022
10.49	-0.234	2.344	-0.236	0.044	-0.123	0.020
10.50	-0.313	2.500	-0.236	0.043	-0.102	0.019
10.51	-0.313	2.500	-0.236	0.042	-0.080	0.017
10.52	-0.313	2.344	-0.236	0.042	-0.059	0.015
10.53	-0.313	2.031	-0.236	0.041	-0.042	0.013
10.54	-0.313	2.031	-0.236	0.040	-0.025	0.012
10.55	-0.313	1.875	-0.236	0.039	-0.009	0.010
10.56	-0.313	1.719	-0.236	0.038	0.005	0.008
10.57	-0.313	1.563	-0.177	0.038	0.017	0.007
10.58	-0.313	1.250	-0.177	0.037	0.027	0.006
10.59	-0.313	1.250	-0.177	0.036	0.036	0.005
10.60	-0.313	1.250	-0.118	0.035	0.045	0.004
10.61	-0.234	1.094	-0.118	0.035	0.053	0.003
10.62	-0.234	0.781	-0.118	0.035	0.058	0.003
10.63	-0.234	0.781	-0.059	0.035	0.062	0.003

Figure 6.1.2.8 Digital data for event 12.3

[ ] = baseline which is subtracted for peaks and numerical integration

Yeardate: 79228 Time: 15:45:12 M.S.T.

Time (μs)	$\partial B_E/\partial t$ (T/s)	$\partial B_N/\partial t$ (T/s)	$Z_o \partial D_z/\partial t$ (T/s)	B_E (μT)	B_N (μT)	$Z_o D_z$ (μT)
12.25	-0.156	0.156	-0.059	-0.000	0.000	0.000
12.26	-0.156	0.156	[-0.059]	-0.000	0.000	0.000
12.27	-0.156	0.156	0.000	-0.000	0.000	0.001
12.28	-0.156	[0.156]	0.059	-0.000	0.000	0.002
12.29	[-0.156]	-0.313	0.118	-0.000	-0.005	0.004
12.30	0.078	-0.313	0.118	0.002	-0.009	0.005
12.31	0.078	-0.469	0.177	0.005	-0.016	0.008
12.32	0.156	-2.500	0.295	0.008	-0.042	0.011
12.33	0.547	-5.156	1.885	0.015	-0.095	0.031
12.34	2.422	-8.906	2.651	0.041	-0.186	0.058
12.35	4.375	-5.000	1.944	0.086	-0.237	0.078
12.36	3.750	2.344	0.530	0.125	-0.216	0.084
12.37	1.875	3.594	0.000	0.145	-0.181	0.084
12.38	0.625	2.500	-0.177	0.153	-0.158	0.083
12.39	0.234	1.250	-0.177	0.157	-0.147	0.082
12.40	0.234	1.250	0.059	0.161	-0.136	0.083
12.41	0.547	1.875	0.059	0.168	-0.119	0.084
12.42	0.313	1.875	-0.059	0.173	-0.102	0.084
12.43	0.000	1.875	-0.236	0.174	-0.084	0.082
12.44	-0.313	1.719	-0.236	0.173	-0.069	0.081
12.45	-0.391	1.250	-0.295	0.171	-0.058	0.079
12.46	-0.547	1.094	-0.295	0.167	-0.049	0.076
12.47	-0.547	0.781	-0.353	0.163	-0.042	0.073
12.48	-0.625	0.625	-0.353	0.158	-0.038	0.070
12.49	-0.625	0.625	-0.295	0.153	-0.033	0.068
12.50	-0.703	0.625	-0.295	0.148	-0.028	0.066
12.51	-0.703	0.625	-0.295	0.143	-0.024	0.063
12.52	-0.625	0.469	-0.236	0.138	-0.021	0.062
12.53	-0.547	0.469	-0.236	0.134	-0.017	0.060
12.54	-0.547	0.000	-0.236	0.130	-0.019	0.058
12.55	-0.547	0.000	-0.177	0.126	-0.021	0.057
12.56	-0.547	-0.156	-0.236	0.122	-0.024	0.055
12.57	-0.547	-0.469	-0.236	0.118	-0.030	0.053
12.58	-0.625	-0.469	-0.177	0.114	-0.036	0.052
12.59	-0.703	-0.469	0.000	0.108	-0.042	0.053
12.60	-0.703	-0.469	0.000	0.103	-0.049	0.053
12.61	-0.703	-0.469	0.059	0.097	-0.055	0.055
12.62	-0.625	-0.469	0.059	0.092	-0.061	0.056
12.63	-0.625	-0.313	0.118	0.088	-0.066	0.057
12.64	-0.625	-0.313	0.118	0.083	-0.071	0.059
12.65	-0.625	0.156	0.118	0.078	-0.071	0.061
12.66	-0.625	0.313	0.118	0.074	-0.069	0.063
12.67	-0.625	0.313	0.118	0.069	-0.067	0.065
12.68	-0.625	0.313	0.118	0.064	-0.066	0.066
12.69	-0.547	0.313	0.118	0.060	-0.064	0.068
12.70	-0.469	0.469	0.118	0.057	-0.061	0.070
12.71	-0.469	0.625	-0.059	0.054	-0.056	0.070

Figure 6.1.2.8 Digital data for event 12.3 (continued)

Time (μs)	$\partial B_E/\partial t$ (T/s)	$\partial B_N/\partial t$ (T/s)	$Z_o \partial D_z/\partial t$ (T/s)	B_E (μT)	B_N (μT)	$Z_o D_z$ (μT)
12.72	-0.313	0.625	-0.059	0.053	-0.052	0.070
12.73	-0.313	0.469	-0.059	0.051	-0.049	0.070
12.74	-0.313	0.313	-0.059	0.049	-0.047	0.070
12.75	-0.313	0.313	-0.059	0.048	-0.045	0.070
12.76	-0.313	0.313	-0.059	0.046	-0.044	0.070
12.77	-0.313	0.313	-0.118	0.045	-0.042	0.069
12.78	-0.313	0.313	-0.118	0.043	-0.041	0.069
12.79	-0.313	0.313	-0.059	0.042	-0.039	0.069
12.80	-0.313	0.469	-0.059	0.040	-0.036	0.069
12.81	-0.313	0.469	-0.059	0.039	-0.033	0.069
12.82	-0.313	0.469	-0.059	0.037	-0.030	0.069
12.83	-0.313	0.313	-0.059	0.035	-0.028	0.069
12.84	-0.313	0.313	-0.059	0.034	-0.027	0.069
12.85	-0.313	0.313	-0.059	0.032	-0.025	0.069
12.86	-0.313	0.313	-0.059	0.031	-0.024	0.069
12.87	-0.313	0.313	-0.059	0.029	-0.022	0.069
12.88	-0.313	0.156	-0.059	0.028	-0.022	0.069
12.89	-0.234	0.156	-0.059	0.027	-0.022	0.069
12.90	-0.234	0.156	-0.059	0.026	-0.022	0.069
12.91	-0.234	0.156	-0.059	0.025	-0.022	0.069
12.92	-0.234	0.156	-0.059	0.024	-0.022	0.069
12.93	-0.234	0.156	-0.059	0.024	-0.022	0.069
12.94	-0.234	0.156	-0.059	0.023	-0.022	0.069
12.95	-0.234	0.156	-0.059	0.022	-0.022	0.069
12.96	-0.234	0.156	-0.059	0.021	-0.022	0.069
12.97	-0.234	0.156	-0.059	0.021	-0.022	0.069
12.98	-0.313	0.313	-0.059	0.019	-0.020	0.069
12.99	-0.313	0.313	-0.059	0.017	-0.019	0.069
13.00	-0.234	0.313	-0.059	0.017	-0.017	0.069
13.01	-0.234	0.313	-0.059	0.016	-0.016	0.069
13.02	-0.234	0.313	-0.059	0.015	-0.014	0.069
13.03	-0.234	0.313	-0.059	0.014	-0.013	0.069
13.04	-0.234	0.313	-0.059	0.013	-0.011	0.069
13.05	-0.234	0.313	-0.059	0.013	-0.009	0.069
13.06	-0.234	0.313	-0.059	0.012	-0.008	0.069
13.07	-0.234	0.313	-0.059	0.011	-0.006	0.069
13.08	-0.234	0.313	-0.059	0.010	-0.005	0.069
13.09	-0.156	0.313	-0.059	0.010	-0.003	0.069
13.10	-0.156	0.313	-0.059	0.010	-0.002	0.069
13.11	-0.156	0.313	-0.059	0.010	-0.000	0.069

Figure 6.1.2.9 Digital data for event 14.6

[ ] = baseline which is subtracted for peaks and numerical integration

Yeardate: 79228 Time: 15:45:12 M.S.T.

Time (μs)	$\partial B_E/\partial t$ (T/s)	$\partial B_N/\partial t$ (T/s)	$Z_o \partial D_z/\partial t$ (T/s)	B_E (μT)	B_N (μT)	$Z_o D_z$ (μT)
14.55	-0.156	0.156	-0.059	-0.000	0.000	0.000
14.56	-0.156	0.156	-0.059	-0.000	0.000	0.000
14.57	-0.156	-0.469	-0.059	-0.000	-0.006	0.000
14.58	-0.156	-1.250	-0.059	-0.000	-0.020	0.000
14.59	-0.156	-1.250	0.118	-0.000	-0.034	0.002
14.60	-0.156	-0.781	0.118	-0.000	-0.044	0.004
14.61	-0.156	-1.250	0.118	-0.000	-0.058	0.005
14.62	-0.156	-5.156	0.118	-0.000	-0.111	0.007
14.63	-0.156	-15.000	0.471	-0.000	-0.262	0.012
14.64	-0.391	-10.000	1.001	-0.002	-0.364	0.023
14.65	0.547	-2.656	1.178	0.005	-0.392	0.035
14.66	1.250	1.250	0.530	0.019	-0.381	0.041
14.67	0.625	1.250	0.059	0.027	-0.370	0.042
14.68	0.313	1.719	0.059	0.031	-0.355	0.044
14.69	0.234	1.719	0.059	0.035	-0.339	0.045
14.70	0.000	1.719	0.059	0.037	-0.323	0.046
14.71	0.000	1.875	0.118	0.038	-0.306	0.048
14.72	0.234	2.344	-0.059	0.042	-0.284	0.048
14.73	0.234	2.344	-0.118	0.046	-0.262	0.047
14.74	-0.313	2.188	-0.177	0.044	-0.242	0.046
14.75	-0.313	2.188	-0.236	0.042	-0.222	0.044
14.76	-0.313	2.031	-0.236	0.041	-0.203	0.042
14.77	-0.313	1.250	-0.295	0.039	-0.192	0.040
14.78	-0.391	1.250	-0.177	0.037	-0.181	0.039
14.79	-0.313	1.250	-0.177	0.035	-0.170	0.038
14.80	-0.234	1.094	-0.177	0.035	-0.161	0.037
14.81	-0.234	1.094	-0.177	0.034	-0.151	0.035
14.82	-0.234	0.781	-0.177	0.033	-0.145	0.034
14.83	-0.234	0.781	-0.118	0.032	-0.139	0.034
14.84	-0.156	0.781	-0.118	0.032	-0.133	0.033
14.85	-0.156	0.938	-0.118	0.032	-0.125	0.032
14.86	-0.156	1.094	-0.059	0.032	-0.115	0.032
14.87	-0.156	1.094	-0.059	0.032	-0.106	0.032
14.88	-0.156	1.250	-0.118	0.032	-0.095	0.032
14.89	-0.156	1.406	-0.118	0.032	-0.083	0.031
14.90	-0.156	1.250	-0.118	0.032	-0.072	0.031
14.91	-0.156	1.250	-0.059	0.032	-0.061	0.031
14.92	-0.156	1.250	-0.059	0.032	-0.050	0.031
14.93	-0.156	1.250	-0.059	0.032	-0.039	0.031
14.94	-0.156	1.250	-0.118	0.032	-0.028	0.030
14.95	-0.234	1.094	-0.118	0.031	-0.019	0.030
14.96	-0.234	1.094	-0.118	0.031	-0.009	0.029
14.97	-0.234	0.781	-0.059	0.030	-0.003	0.029
14.98	-0.234	0.781	-0.059	0.029	0.003	0.029
14.99	-0.234	0.781	-0.059	0.028	0.010	0.029
15.00	-0.234	0.781	-0.059	0.028	0.016	0.029
15.01	-0.234	0.781	-0.059	0.027	0.022	0.029
15.02	-0.156	0.781	-0.059	0.027	0.028	0.029

Figure 6.1.2.10 Digital data for event 17.6

[ ] = baseline which is subtracted for peaks and numerical integration

Yeardate: 79228 Time: 15:45:12 M.S.T.

Time (μs)	$\partial B_E/\partial t$ (T/s)	$\partial B_N/\partial t$ (T/s)	$Z_o \partial D_z/\partial t$ (T/s)	B_E (μT)	B_N (μT)	$Z_o D_z$ (μT)
17.50	-0.156	0.156	-0.059	-0.000	0.000	0.000
17.51	-0.156	0.156	-0.059	-0.000	0.000	0.000
17.52	-0.156	-0.313	-0.059	-0.000	-0.005	0.000
17.53	-0.156	-0.469	-0.059	-0.000	-0.011	0.000
17.54	-0.156	-0.469	0.118	-0.000	-0.017	0.002
17.55	-0.156	-0.781	0.118	-0.000	-0.027	0.004
17.56	-0.156	-1.250	0.118	-0.000	-0.041	0.005
17.57	-0.156	-2.656	0.118	-0.000	-0.069	0.007
17.58	0.078	-10.156	0.118	0.002	-0.172	0.009
17.59	0.078	-15.000	0.353	0.005	-0.323	0.013
17.60	0.078	-5.156	0.530	0.007	-0.377	0.019
17.61	0.078	-1.406	0.530	0.009	-0.392	0.025
17.62	0.391	-1.250	0.295	0.015	-0.406	0.028
17.63	0.313	-1.250	0.471	0.019	-0.420	0.034
17.64	0.547	-1.406	0.707	0.027	-0.436	0.041
17.65	0.938	-0.781	0.707	0.037	-0.445	0.049
17.66	0.938	-0.781	0.471	0.048	-0.455	0.054
17.67	0.625	-1.250	0.412	0.056	-0.469	0.059
17.68	0.625	-0.781	0.412	0.064	-0.478	0.064
17.69	0.547	-0.625	0.412	0.071	-0.486	0.068
17.70	0.547	0.000	0.412	0.078	-0.487	0.073
17.71	0.625	0.469	0.412	0.086	-0.484	0.078
17.72	0.859	-1.250	0.530	0.096	-0.498	0.084
17.73	1.250	-1.875	1.885	0.110	-0.519	0.103
17.74	3.672	-0.156	1.944	0.148	-0.522	0.123
17.75	4.297	0.000	1.001	0.193	-0.523	0.134
17.76	2.500	2.500	0.059	0.219	-0.500	0.135
17.77	1.172	7.344	-0.412	0.233	-0.428	0.131
17.78	0.234	6.719	-0.707	0.237	-0.362	0.125
17.79	-0.391	5.000	-0.884	0.234	-0.314	0.117
17.80	-0.938	4.844	-0.707	0.226	-0.267	0.111
17.81	-0.938	4.375	-0.648	0.218	-0.225	0.105
17.82	-0.938	3.750	-0.471	0.211	-0.189	0.101
17.83	-0.859	2.344	-0.471	0.204	-0.167	0.096
17.84	-0.859	1.875	-0.530	0.196	-0.150	0.092
17.85	-0.781	1.875	-0.471	0.190	-0.133	0.088
17.86	-0.625	1.719	-0.471	0.186	-0.117	0.083
17.87	-0.625	1.250	-0.471	0.181	-0.106	0.079
17.88	-0.469	1.250	-0.412	0.178	-0.095	0.076
17.89	-0.469	1.094	-0.353	0.175	-0.086	0.073
17.90	-0.469	1.094	-0.295	0.171	-0.076	0.070
17.91	-0.547	1.094	-0.295	0.168	-0.067	0.068
17.92	-0.547	1.094	-0.236	0.164	-0.058	0.066
17.93	-0.547	0.781	-0.177	0.160	-0.051	0.065
17.94	-0.547	0.781	-0.177	0.156	-0.045	0.064

Figure 6.1.2.10 Digital data for event 17.6 (continued)

Time (μs)	$\partial B_E/\partial t$ (T/s)	$\partial B_N/\partial t$ (T/s)	$Z_o \partial D_z/\partial t$ (T/s)	B_E (μT)	B_N (μT)	$Z_o D_z$ (μT)
17.95	-0.547	0.781	-0.177	0.152	-0.039	0.063
17.96	-0.547	0.781	-0.177	0.148	-0.033	0.062
17.97	-0.547	0.781	-0.177	0.144	-0.026	0.060
17.98	-0.625	0.781	-0.177	0.139	-0.020	0.059
17.99	-0.703	0.781	-0.118	0.134	-0.014	0.059
18.00	-0.781	0.781	-0.059	0.128	-0.008	0.059
18.01	-0.781	0.938	0.000	0.121	0.000	0.059
18.02	-0.781	0.938	-0.059	0.115	0.008	0.059
18.03	-0.781	0.781	-0.118	0.109	0.014	0.059
18.04	-0.781	0.781	-0.118	0.103	0.020	0.058
18.05	-0.781	0.938	-0.118	0.096	0.028	0.058
18.06	-0.781	0.938	-0.177	0.090	0.036	0.056
18.07	-0.781	0.781	-0.177	0.084	0.042	0.055
18.08	-0.781	0.781	-0.177	0.078	0.049	0.054
18.09	-0.703	0.781	-0.177	0.072	0.055	0.053
18.10	-0.625	0.625	-0.177	0.068	0.060	0.052
18.11	-0.625	0.625	-0.177	0.063	0.064	0.050
18.12	-0.625	0.625	-0.177	0.058	0.069	0.049
18.13	-0.469	0.625	-0.177	0.055	0.074	0.048
18.14	-0.469	0.469	-0.177	0.052	0.077	0.047
18.15	-0.469	0.469	-0.177	0.049	0.080	0.046
18.16	-0.469	0.469	-0.177	0.046	0.083	0.045
18.17	-0.469	0.469	-0.177	0.042	0.086	0.043
18.18	-0.469	0.469	-0.118	0.039	0.089	0.043
18.19	-0.469	0.469	-0.118	0.036	0.092	0.042
18.20	-0.469	0.469	-0.118	0.033	0.095	0.042
18.21	-0.469	0.469	-0.118	0.030	0.099	0.041
18.22	-0.469	0.469	-0.059	0.027	0.102	0.041
18.23	-0.391	0.469	-0.059	0.025	0.105	0.041
18.24	-0.391	0.469	-0.059	0.022	0.108	0.041
18.25	-0.391	0.469	-0.059	0.020	0.111	0.041
18.26	-0.391	0.313	-0.059	0.017	0.113	0.041
18.27	-0.313	0.313	-0.059	0.016	0.114	0.041
18.28	-0.313	0.313	-0.059	0.014	0.116	0.041
18.29	-0.313	0.313	-0.059	0.013	0.117	0.041
18.30	-0.234	0.313	-0.059	0.012	0.119	0.041
18.31	-0.234	0.156	-0.059	0.011	0.119	0.041
18.32	-0.234	0.156	-0.059	0.010	0.119	0.041
18.33	-0.234	0.156	-0.059	0.010	0.119	0.041
18.34	-0.234	0.156	-0.059	0.009	0.119	0.041
18.35	-0.234	0.156	-0.059	0.008	0.119	0.041
18.36	-0.234	0.156	-0.059	0.007	0.119	0.041
18.37	-0.234	0.156	-0.059	0.007	0.119	0.041
18.38	-0.234	0.156	-0.059	0.006	0.119	0.041
18.39	-0.234	0.313	-0.059	0.005	0.121	0.041
18.40	-0.234	0.313	-0.059	0.004	0.122	0.041
18.41	-0.234	0.313	-0.059	0.003	0.124	0.041
18.42	-0.234	0.313	-0.059	0.003	0.125	0.041
18.43	-0.234	0.156	-0.059	0.002	0.125	0.041
18.44	-0.234	0.156	-0.059	0.001	0.125	0.041
18.45	-0.234	0.313	-0.059	0.000	0.127	0.041

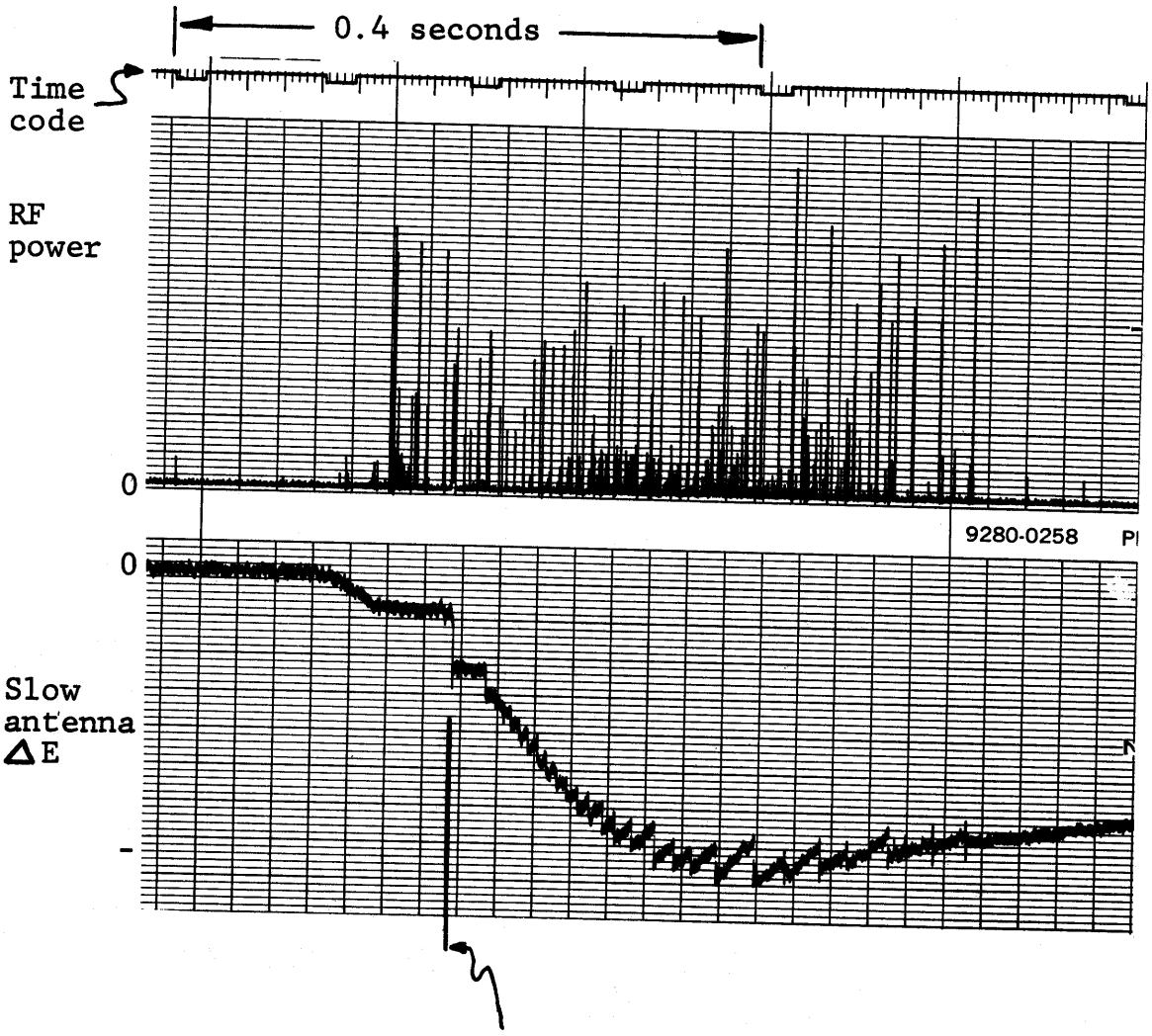

Horizontal range from Kiva to rocket launcher : 350 m

Date: 79228 M.S.T.: 1545:12

Figure 6.1.3 Slow electric field change and RF power received at 34 MHz from rocket-triggered lightning

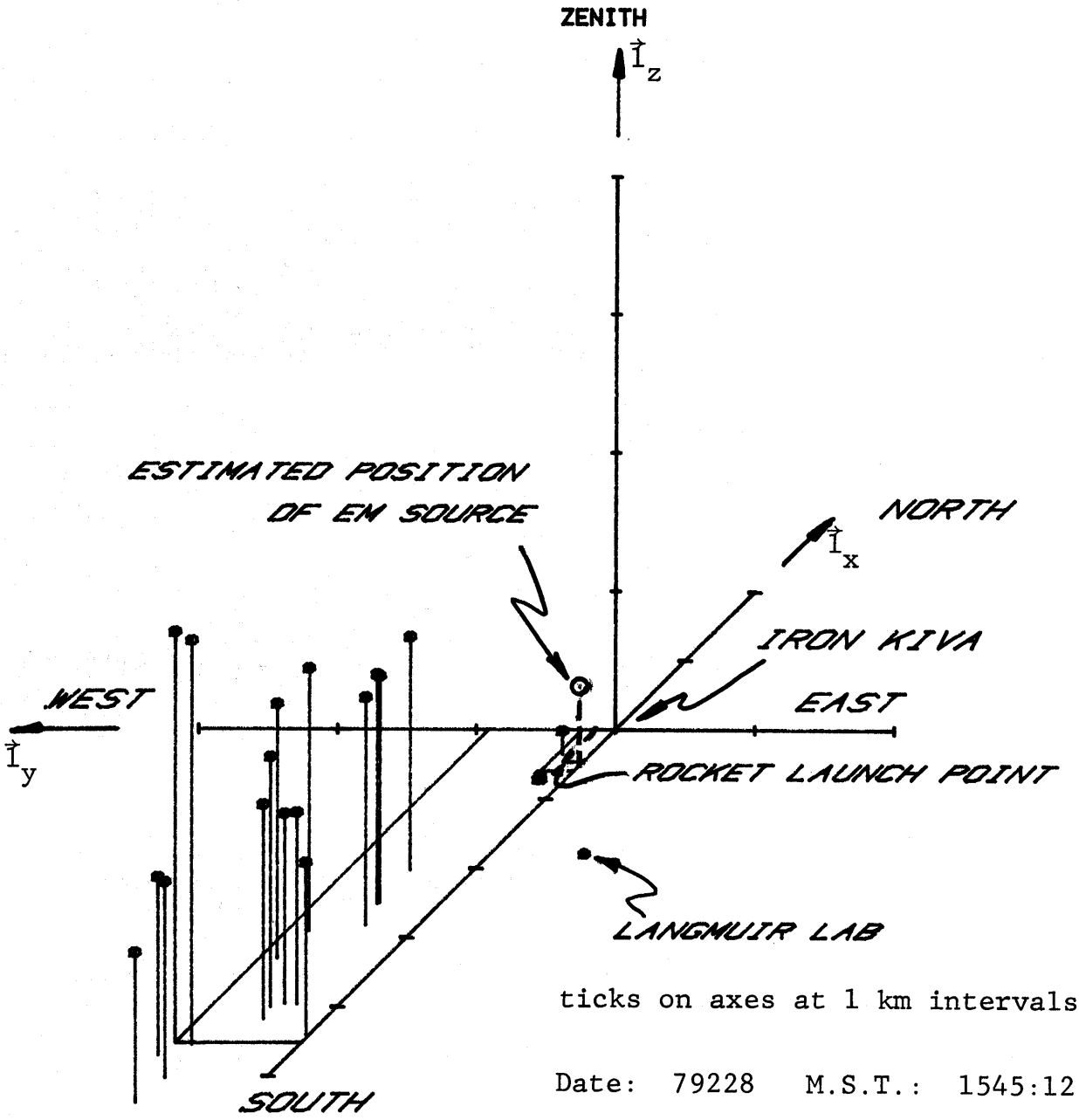

Figure 6.1.4 Acoustic location of rocket-triggered lightning

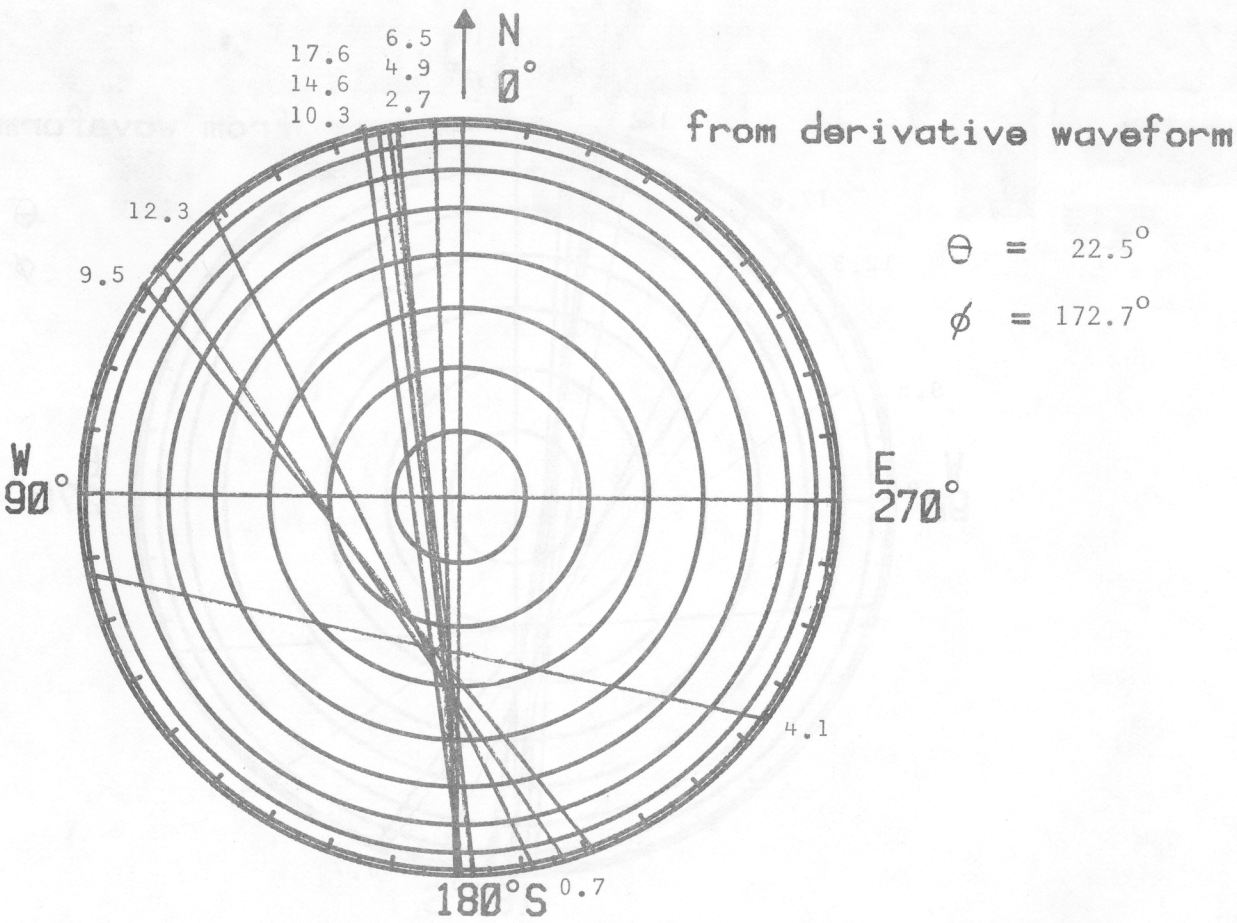

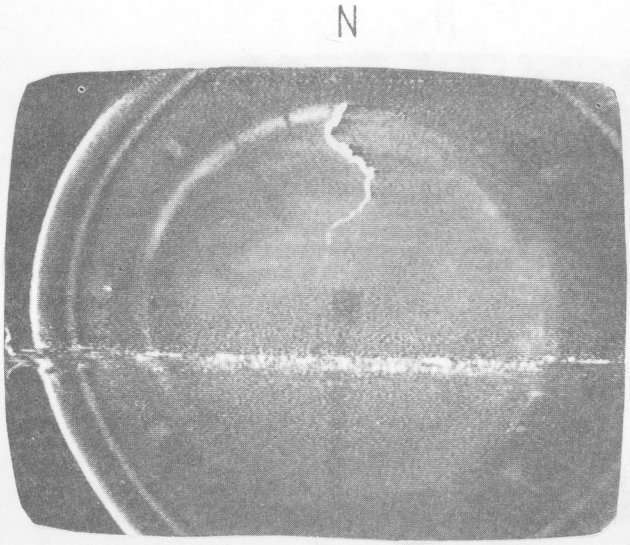

Figure 6.1.5 A sin(θ),ϕ contours for rocket-triggered lightning derivative waveform and whole-sky videotape photograph

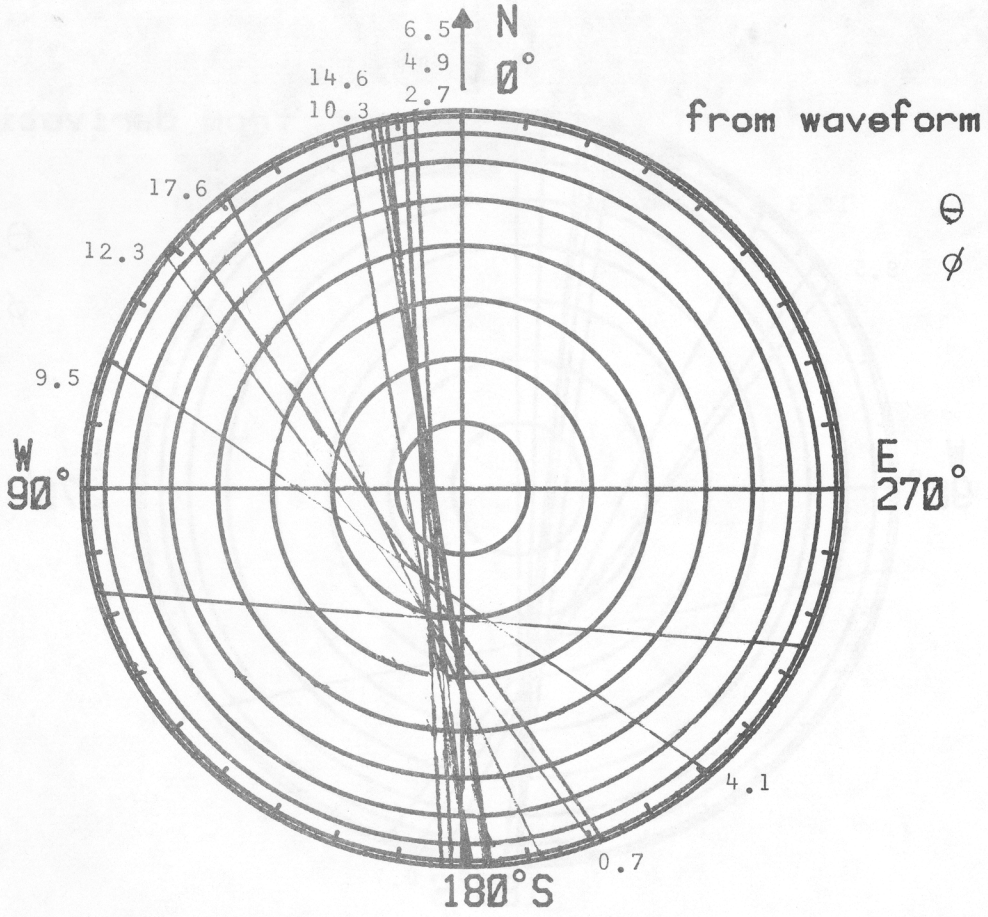

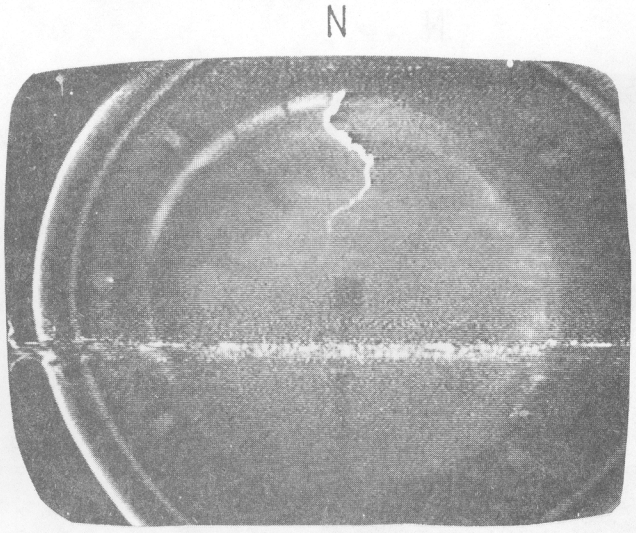

Whole Sky Photograph From Hangar
DATE : 79228 M.S.T.: 1545.12

Figure 6.1.5B sin(θ),ϕ contours for rocket-triggered lightning waveform and whole-sky videotape photograph

Figure 6.1.6A Tabulation of peak values for each event from derivative waveform set for rocket-triggered lightning

Yeardate: 79228 M.S.T.:1545.12

$\phi = 172.7^{o} \pm 0.6^{o}$, $\theta = 22.5^{o} \pm 1.9^{o}$, $r = 915$ m

Event Number	Time (μs)	$Z_o \Delta\partial D_z/\partial t$ (T/s)	$\Delta\partial B_E/\partial t$ (T/s)	$\Delta\partial B_N/\partial t$ (T/s)	$\Delta\partial B_h/\partial t$ (T/s)	$\Delta\partial B_e/\partial t$ (T/s)	$\lvert\Delta\partial\vec{B}/\partial t\rvert$ (T/s)
0.7	0.69	1.59	3.28	-4.06	-2.45	1.42	2.83
2.7	2.67	0.35	0.55	-4.53	-2.55	0.04	2.55
4.1	4.07	1.59	3.83	-0.78	-0.66	1.86	1.98
4.9	4.90	0.35	0.39	-4.22	-2.36	-0.03	2.37
6.5	6.49	0.53	0.78	-5.78	-3.25	0.09	3.26
9.5	9.54	2.00	3.67	-5.31	-3.16	1.55	3.52
10.3	10.31	0.35	0.39	-2.81	-1.58	0.05	1.58
12.3	12.34	2.59	4.53	-9.06	-5.30	1.78	5.59
14.6	14.63	1.24	1.41	-15.16	-8.50	-0.09	8.50
17.6	17.59	0.59	0.55	-15.16	-8.45	-0.52	8.46

CALCULATED VALUES FOR $\partial\vec{T}/\partial t$

Event Number	$\partial T_2/\partial t$ (10^{15} Am/s^2)	$\partial T_3/\partial t$ (10^{15} Am/s^2)	$\lvert\partial\vec{T}/\partial t\rvert$ (10^{15} Am/s^2)	α (deg)
0.7	5777	-3351	6679	240
2.7	6015	-83	6016	269
4.1	1551	-4399	4664	199
4.9	5585	63	5585	271
6.5	7686	-204	7689	268
9.5	7470	-3656	8317	244
10.3	3740	-111	3742	268
12.3	12505	-4202	13192	251
14.6	20063	220	20064	271
17.6	19945	1228	19983	274

Figure 6.1.6B Tabulation of peak values for each event from waveform set for rocket-triggered lightning

Yeardate: 79228 M.S.T.:1545.12

$\phi = 165.8^{o} \pm 0.1^{o}$, $\theta = 16.1^{o} \pm 2.5^{o}$, $r = 1262$ m

Event Number	Time (μs)	$Z_o \Delta D_s$ (μT)	ΔB_E (μT)	ΔB_N (μT)	ΔB_h (μT)	ΔB_e (μT)	$\lvert\Delta\vec{B}\rvert$ (μT)
0.7	0.73	0.07	0.17	-0.24	-0.14	0.06	0.16
2.7	2.71	0.02	0.03	-0.22	-0.12	-0.00	0.12
4.1	4.07	0.07	0.12	-0.01	-0.02	0.06	0.06
4.9	4.94	0.02	0.02	-0.19	-0.10	-0.00	0.10
6.5	6.54	0.03	0.05	-0.33	-0.18	0.00	0.18
9.5	9.55	0.05	0.06	-0.12	-0.07	0.02	0.07
10.3	10.42	0.03	0.03	-0.18	-0.10	0.00	0.10
12.3	12.35	0.07	0.13	-0.24	-0.14	0.04	0.14
14.6	14.65	0.04	0.02	-0.39	-0.21	-0.02	0.21
17.6	17.59	0.03	0.02	-0.32	-0.17	-0.02	0.18

CALCULATED VALUES FOR $\vec{I}_t . \vec{T}$

Event Number	T_2 (10^9 Am/s)	T_3 (10^9 Am/s)	$\lvert\vec{T}\rvert$ (10^9 Am/s)	α (deg)
0.7	388	-174	425	246
2.7	326	3	327	270
4.1	46	-158	165	196
4.9	278	11	278	272
6.5	496	-4	496	269
9.5	187	-62	197	252
10.3	261	-4	261	269
12.3	372	-120	391	252
14.6	574	53	576	275
17.6	473	45	475	275

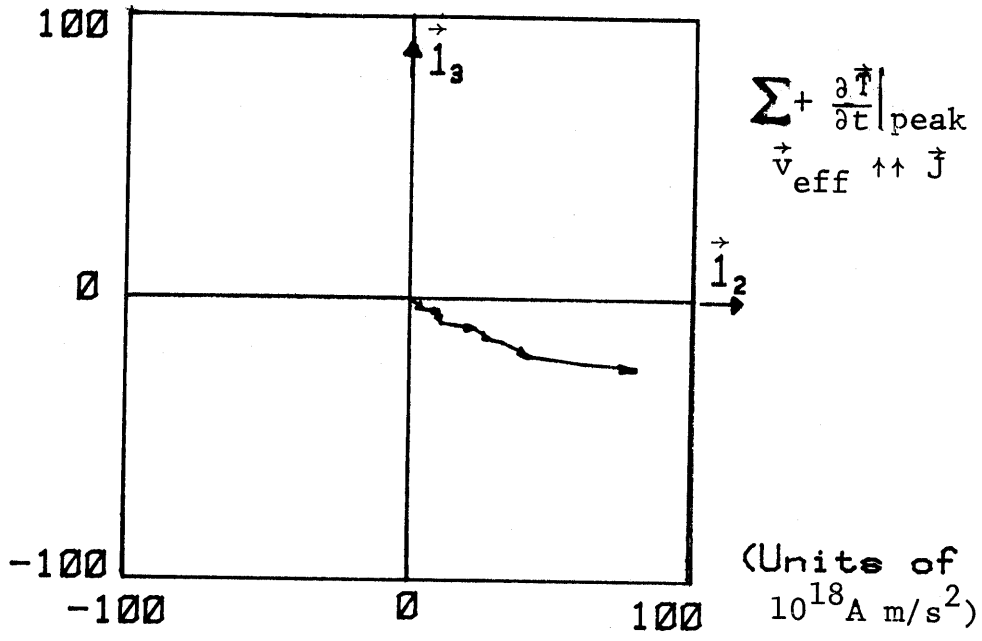

Effective reconstruction of positive streamer

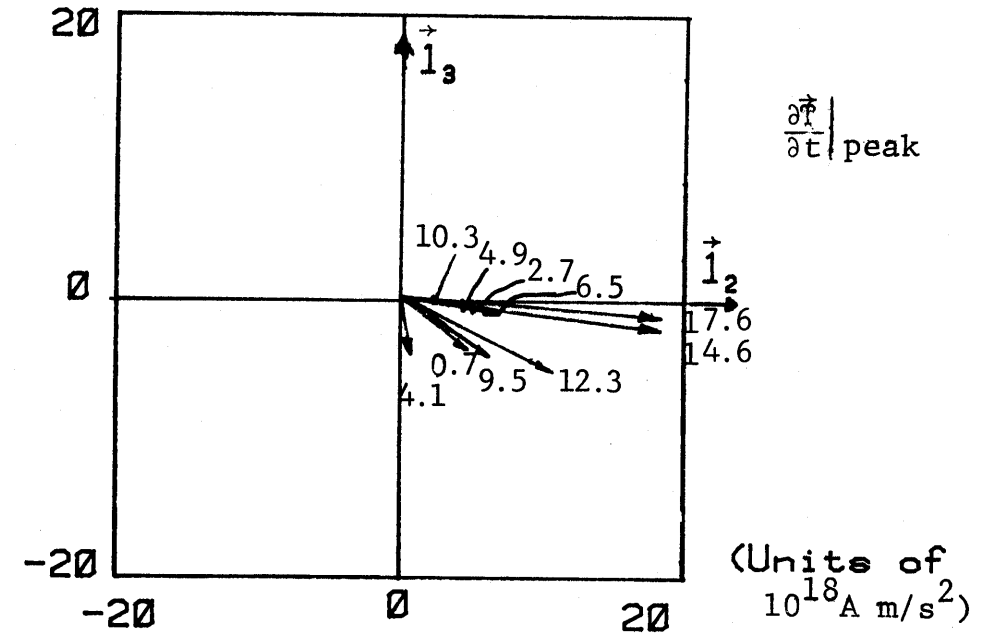

Peaks of $\partial \vec{I}/\partial t$

$\phi = 172.7^{o}$, $\theta = 22.5^{o}$, $r = 915$ m

Date : 79228 M. S. T. : 1545: 12

Figure 6.1.7 A $\partial \vec{I}/\partial t$ for rocket-triggered lightning

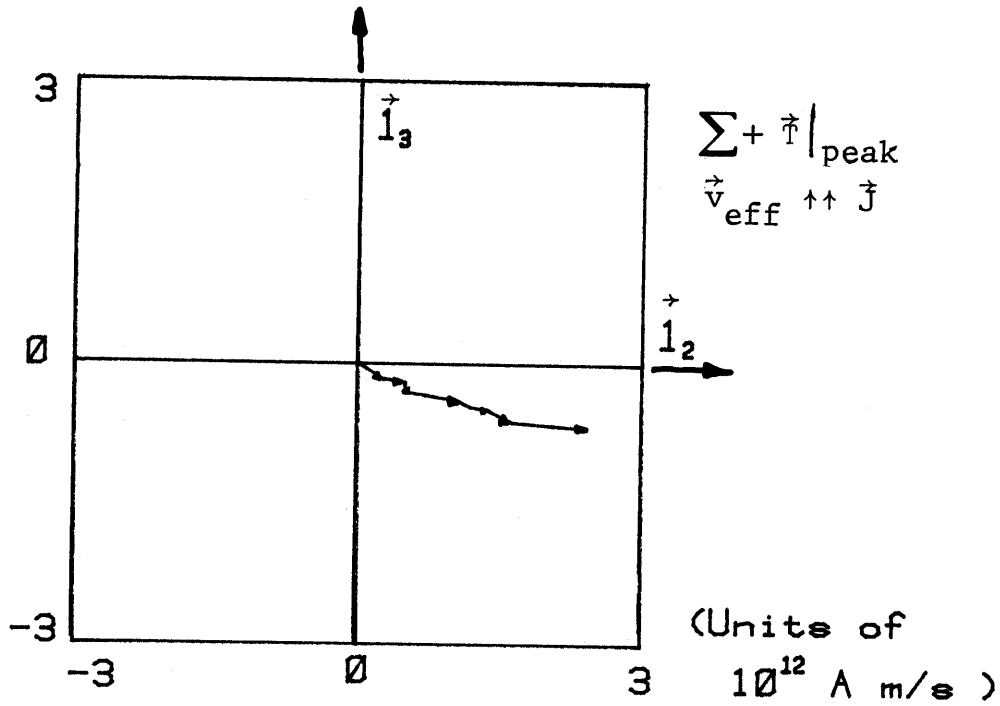

Effective reconstruction of positive streamer

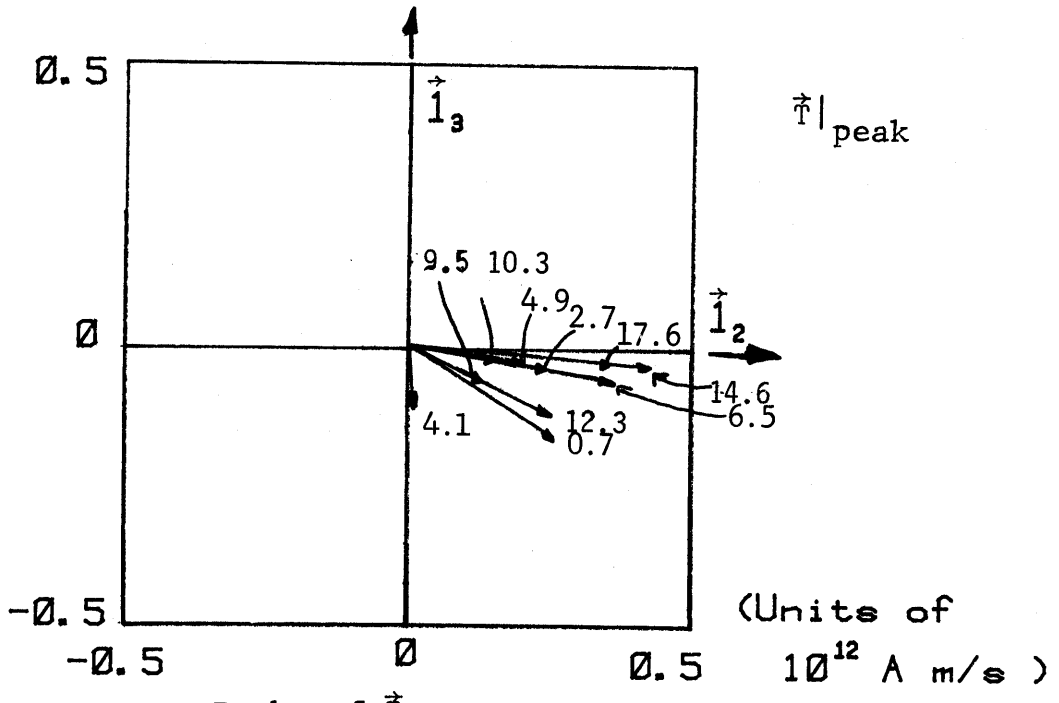

Peaks of $\vec{\mathcal{T}}$

$\phi = 165.8^{o}$, $\theta = 16.1^{o}$, $r = 1262$ m

Date : 79228 M. S. T. : 1545: 12

Figure 6.1.7B $\vec{\mathcal{T}}$ for rocket-triggered lightning

6.2 Midrange Leader(s)

Our second example is given in figures 6.2.***. As will be seen this is a case of significant branching. For sake of a label let us refer to this case as "midrange leader(s)." Figures 6.2.1A and 6.2.1B show the derivative fields and fields for the 20 μs record indicating leader-like behavior.

Figure 6.2.3 shows the slow electric field and thunder microphone records from which a horizontal range of 400 m is estimated. Figure 6.2.4 gives the acoustic source reconstruction indicating an interesting streamer-path structure. Extending from about 3 km height, about 3 km to the east (slightly north of east), the pattern divides at about 2.5 km above the Kiva and descends to the mountain in at least three major channels. On this is superimposed three EM source locations determined from the derivative waveform.

The whole-sky videotape photographs in figures 6.2.5A and 6.2.5B show these three channels quite clearly as seen from the Kiva. Figure 6.2.5B corresponds to 32 ms later than figure 6.2.5A.

Looking at the θ, ϕ contours in figure 6.2.5A from the derivative waveform in figure 6.2.1A, we do not see all the contours passing near a common (θ,ϕ). It appears that several sources are located above the Kiva. From figure 6.2.5A three (θ , ϕ) values were found as indicated on the figure. These angles are combined with the horizontal range of 400 m to give the estimated EM source locations in figure 6.2.4. As an aid in identifying the three sets of pulses corresponding to the three locations, the directions of $\partial\vec{T}/\partial t$ were considered so as to have all the $\partial\vec{T}/\partial t$ pulses in a particular set have the same general direction (as in figure 6.2.7A).

Considering the field waveform in figure 6.2.1B the plot of contours in figure 6.2.5B was made. Here four sets of pulses were identified. Sets 1, 2, and 3 correspond reasonably to those from the derivative waveforms as do the directions of the $\vec{T}$ pulses as compared to the corresponding $\partial\vec{T}/\partial t$ pulses. Set 4 in Figure 6.2.5B was defined based on a disagreement in the direction of $\vec{T}$ pulses from those in set 1 as based on the directions in figures 6.2.7B.1 and 6.2.7B.4. However, noting the small θ values for this case the change in ϕ still corresponds to only a small distance change on the unit sphere, but a large rotation of the unit vectors $\vec{I}_2$, $\vec{I}_3$. Identifying these set 4 $\vec{T}$ pulses with the corresponding $\partial\vec{T}/\partial t$ pulses it appears that set 4 pulses likely belong combined with set 1.

Since set 1 corresponds to small θ an estimate of slant range based on 400 m horizontal range is likely in error because the lightning arc is not exactly vertical. Based on figure 6.2.4 the lower heights as in figure 6.2.7A for $\theta = 32^{o}$ are more reasonable. This is consistent with relying more on $\partial\vec{T}/\partial t$ data for θ , ϕ determination.

For this negative step leader we have $\vec{v}_{eff} \downarrow\uparrow \vec{J}$ (antiparallel). So in the effective streamer reconstruction in figures 6.2.7A and 6.2.7B the vectors for the sequential pulses are started from the graph origin with each vector head placed at the previous vector tail.

Note that values of $\vec{T}$ pulses depend on choice of r. For sets 1 and 4 r is clearly overestimated indicating the true values are somewhat less (by perhaps a factor of 2) than indicated in figures 6.2.7B.

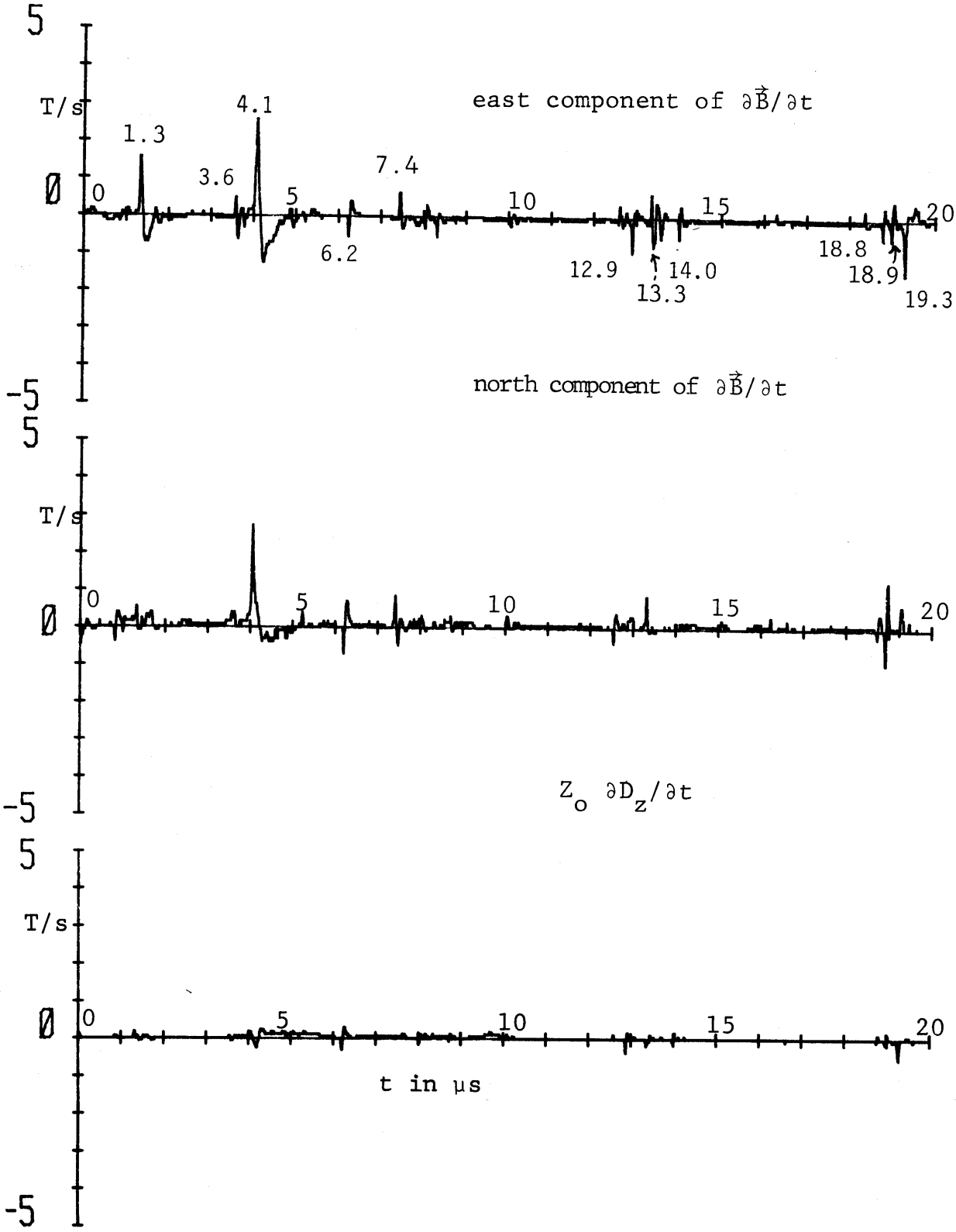

Date: 79219 M.S.T.: 1022:51

Figure 6.2.1 A Derivative fields from midrange leader(s)

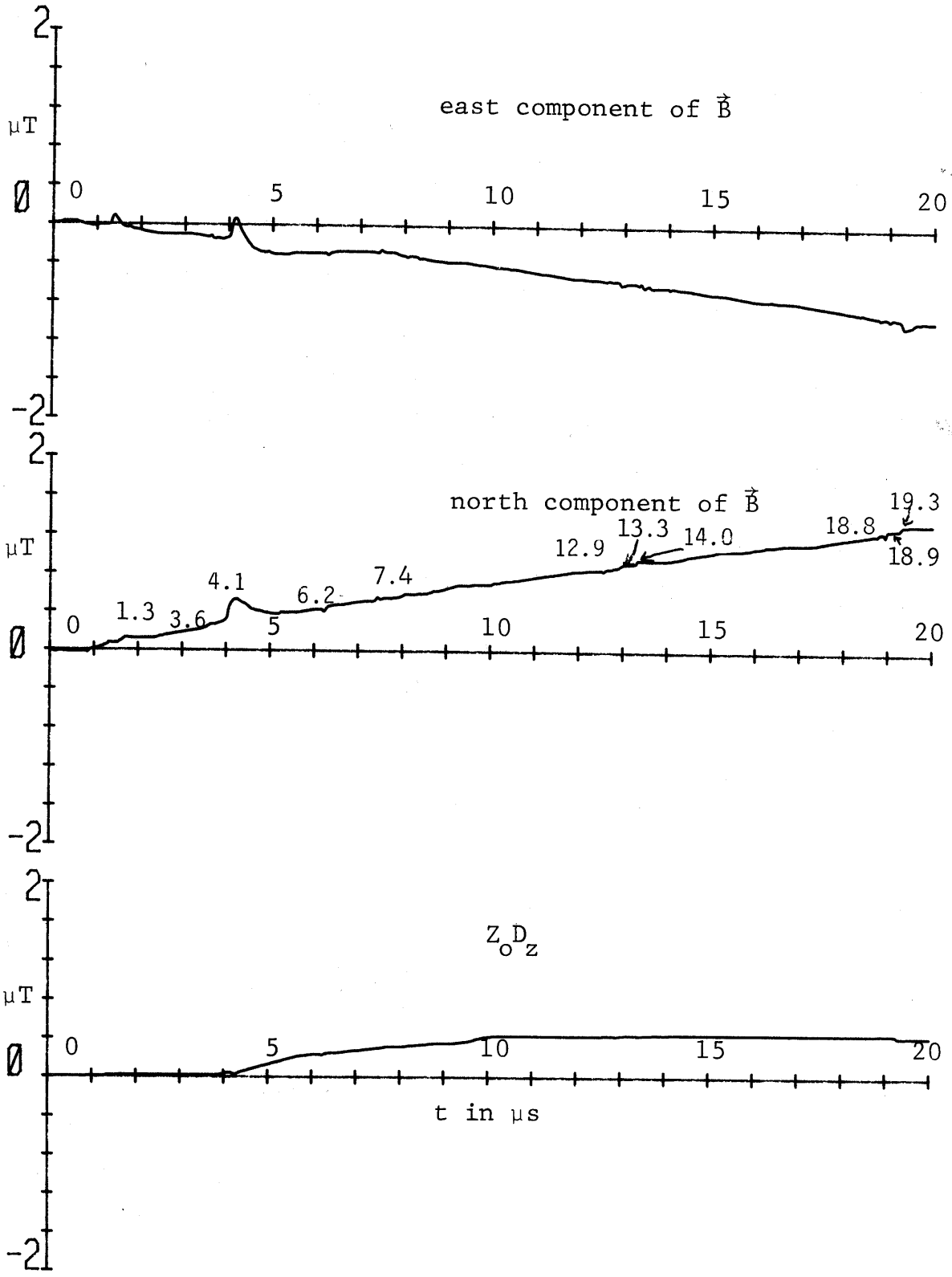

Date: 79219 M.S.T.: 1022:51

Figure 6.2.1B Fields from midrange leader(s)

Figure 6.2.2.1 Digital data for event 1.3

[ ] = baseline which is subtracted for peaks and numerical integration

Yeardate: 79219 Time: 10:22:51 M.S.T.

Time (μs)	$\partial B_E/\partial t$ (T/s)	$\partial B_N/\partial t$ (T/s)	$Z_o \partial D_z/\partial t$ (T/s)	B_E (μT)	B_N (μT)	$Z_o D_z$ (μT)
1.27	0.000	0.234	0.059	0.000	0.000	-0.000
1.28	0.000	0.234	0.059	0.000	0.000	-0.000
1.29	0.078	0.234	0.118	0.001	0.000	0.001
1.30	0.234	0.234	0.177	0.003	0.000	0.002
1.31	0.547	0.313	0.236	0.009	0.001	0.004
1.32	1.172	0.547	0.236	0.020	0.004	0.005
1.33	1.484	0.547	0.236	0.035	0.007	0.007
1.34	1.484	0.313	0.118	0.050	0.008	0.008
1.35	1.250	0.000	0.059	0.063	0.006	0.008
1.36	0.859	-0.078	0.059	0.071	0.002	0.008
1.37	0.547	-0.078	0.118	0.077	-0.001	0.008
1.38	0.234	-0.078	0.118	0.079	-0.004	0.009
1.39	0.000	-0.078	0.118	0.079	-0.007	0.009
1.40	-0.078	-0.078	0.059	0.078	-0.010	0.009
1.41	-0.625	-0.078	0.059	0.072	-0.013	0.009
1.42	-0.703	-0.078	0.000	0.065	-0.016	0.008
1.43	-0.703	-0.078	0.000	0.058	-0.019	0.008
1.44	-0.781	0.000	0.000	0.050	-0.022	0.007
1.45	-0.703	0.234	0.000	0.043	-0.022	0.007
1.46	-0.703	0.156	0.000	0.036	-0.022	0.006
1.47	-0.703	0.156	0.000	0.029	-0.023	0.005
1.48	-0.703	0.000	0.000	0.022	-0.026	0.005
1.49	-0.781	0.000	0.000	0.014	-0.028	0.004
1.50	-0.781	0.000	0.059	0.006	-0.030	0.004
1.51	-0.781	0.000	0.059	-0.002	-0.033	0.004

Figure 6.2.2.2 Digital data for event 3.6

[ ] = baseline which is subtracted for peaks and numerical integration

Yeardate: 79219 Time: 10:22:51 M.S.T.

Time (μs)	$\partial B_E/\partial t$ (T/s)	$\partial B_N/\partial t$ (T/s)	$Z_o \partial D_z/\partial t$ (T/s)	B_E (μT)	B_N (μT)	$Z_o D_z$ (μT)
3.52	[-0.156]	0.156	0.059	-0.000	0.000	-0.000
3.53	-0.078	0.156	[0.059]	0.001	0.000	-0.000
3.54	-0.078	[0.156]	0.118	0.002	0.000	0.001
3.55	0.000	0.313	0.118	0.003	0.002	0.001
3.56	0.234	0.313	0.118	0.007	0.003	0.002
3.57	0.313	0.391	0.118	0.012	0.005	0.002
3.58	0.391	0.234	0.059	0.017	0.006	0.002
3.59	0.000	0.234	0.000	0.019	0.007	0.002
3.60	-0.313	0.234	0.000	0.017	0.008	0.001
3.61	-0.625	0.234	0.000	0.012	0.009	0.001
3.62	-0.625	0.313	0.000	0.008	0.010	-0.000
3.63	-0.703	0.391	0.000	0.002	0.013	-0.001
3.64	-0.625	0.313	0.059	-0.002	0.014	-0.001
3.65	-0.391	0.234	0.059	-0.005	0.015	-0.001
3.66	-0.313	0.000	0.059	-0.006	0.013	-0.001
3.67	-0.078	0.000	0.059	-0.005	0.011	-0.001
3.68	-0.078	0.000	0.118	-0.004	0.010	-0.000
3.69	0.000	0.000	0.118	-0.003	0.008	0.000
3.70	0.078	0.000	0.118	-0.001	0.007	0.001
3.71	0.078	0.000	0.118	0.002	0.005	0.001
3.72	0.078	0.000	0.118	0.004	0.004	0.002
3.73	0.078	0.000	0.118	0.006	0.002	0.003
3.74	0.078	0.000	0.059	0.009	0.001	0.003
3.75	-0.156	0.156	0.059	0.009	0.001	0.003
3.76	-0.234	0.156	0.059	0.008	0.001	0.003
3.77	-0.313	0.156	0.059	0.006	0.001	0.003
3.78	-0.391	0.156	0.118	0.004	0.001	0.003
3.79	-0.313	0.078	0.118	0.003	-0.000	0.004

Figure 6.2.2.3 Digital data for event 4.1

[ ] = baseline which is subtracted for peaks and numerical integration

Yeardate: 79219 Time: 10:22:51 M.S.T.

Time (μs)	$\partial B_E/\partial t$ (T/s)	$\partial B_N/\partial t$ (T/s)	$Z_o \partial D_z/\partial t$ (T/s)	B_E (μT)	B_N (μT)	$Z_o D_z$ (μT)
3.91	0.078	0.156	0.118	0.000	0.000	-0.000
3.92	0.078	0.156	0.118	0.000	0.000	-0.000
3.93	0.078	0.234	0.118	0.000	0.001	-0.000
3.94	0.078	0.313	0.118	0.000	0.002	-0.000
3.95	0.078	0.313	0.118	0.000	0.004	-0.000
3.96	0.078	0.313	0.118	0.000	0.005	-0.000
3.97	0.078	0.313	0.118	0.000	0.007	-0.000
3.98	0.156	0.313	0.118	0.001	0.009	-0.000
3.99	0.156	0.391	0.118	0.002	0.011	-0.000
4.00	0.156	0.469	0.177	0.002	0.014	0.001
4.01	0.313	0.625	0.236	0.005	0.019	0.002
4.02	0.625	0.938	0.236	0.010	0.027	0.003
4.03	1.172	1.797	0.236	0.021	0.043	0.004
4.04	1.250	2.500	0.236	0.033	0.066	0.005
4.05	1.875	2.734	0.236	0.051	0.092	0.006
4.06	2.500	1.875	0.236	0.075	0.109	0.008
4.07	2.500	1.563	0.177	0.099	0.123	0.008
4.08	2.109	1.250	0.118	0.120	0.134	0.008
4.09	1.797	1.172	0.118	0.137	0.145	0.008
4.10	1.484	0.938	0.059	0.151	0.152	0.008
4.11	0.938	0.859	0.059	0.159	0.159	0.007
4.12	0.625	0.703	0.000	0.165	0.165	0.006
4.13	0.313	0.625	0.000	0.167	0.170	0.005
4.14	0.234	0.625	-0.059	0.169	0.174	0.003
4.15	0.000	0.625	-0.059	0.168	0.179	0.001
4.16	-0.313	0.547	-0.118	0.164	0.183	-0.001
4.17	-0.625	0.391	-0.118	0.157	0.185	-0.004
4.18	-0.703	0.313	-0.177	0.149	0.187	-0.007
4.19	-0.938	0.234	-0.177	0.139	0.188	-0.009
4.20	-1.250	0.234	-0.177	0.126	0.188	-0.012
4.21	-1.250	0.000	-0.118	0.113	0.187	-0.015
4.22	-1.328	0.000	-0.059	0.099	0.185	-0.017
4.23	-1.328	0.000	0.000	0.085	0.184	-0.018
4.24	-1.328	-0.078	0.000	0.071	0.182	-0.019
4.25	-1.250	-0.078	0.059	0.058	0.179	-0.020
4.26	-1.172	-0.234	0.059	0.045	0.175	-0.020
4.27	-1.094	-0.313	0.236	0.033	0.171	-0.019
4.28	-1.094	-0.391	0.236	0.022	0.165	-0.018
4.29	-0.938	-0.313	0.295	0.011	0.160	-0.016
4.30	-0.938	-0.313	0.295	0.001	0.156	-0.014
4.31	-0.859	-0.313	0.295	-0.008	0.151	-0.013
4.32	-0.859	-0.313	0.295	-0.017	0.146	-0.011
4.33	-0.859	-0.313	0.295	-0.027	0.142	-0.009
4.34	-0.859	-0.313	0.295	-0.036	0.137	-0.007
4.35	-0.859	-0.313	0.295	-0.046	0.132	-0.006

Figure 6.2.2.3 Digital data for event 4.1 (continued)

Time (μs)	$\partial B_E/\partial t$ (T/s)	$\partial B_N/\partial t$ (T/s)	$Z_o \partial D_z/\partial t$ (T/s)	B_E (μT)	B_N (μT)	$Z_o D_z$ (μT)
4.36	-0.781	-0.234	0.295	-0.054	0.128	-0.004
4.37	-0.781	-0.234	0.236	-0.063	0.125	-0.003
4.38	-0.781	-0.234	0.236	-0.071	0.121	-0.001
4.39	-0.781	-0.156	0.236	-0.080	0.118	-0.000
4.40	-0.781	-0.156	0.177	-0.089	0.114	0.000
4.41	-0.781	-0.156	0.177	-0.097	0.111	0.001
4.42	-0.781	-0.234	0.177	-0.106	0.107	0.001
4.43	-0.781	-0.313	0.177	-0.114	0.103	0.002
4.44	-0.781	-0.391	0.177	-0.123	0.097	0.003
4.45	-0.781	-0.391	0.177	-0.132	0.092	0.003
4.46	-0.703	-0.313	0.177	-0.139	0.087	0.004
4.47	-0.625	-0.391	0.177	-0.146	0.082	0.004
4.48	-0.625	-0.391	0.177	-0.153	0.076	0.005
4.49	-0.625	-0.391	0.177	-0.160	0.071	0.006
4.50	-0.625	-0.313	0.177	-0.167	0.066	0.006
4.51	-0.625	-0.313	0.177	-0.174	0.061	0.007
4.52	-0.547	-0.313	0.177	-0.181	0.057	0.007
4.53	-0.547	-0.391	0.177	-0.187	0.051	0.008
4.54	-0.469	-0.391	0.236	-0.192	0.046	0.009
4.55	-0.391	-0.313	0.177	-0.197	0.041	0.010
4.56	-0.469	-0.313	0.177	-0.203	0.036	0.010
4.57	-0.391	-0.313	0.236	-0.207	0.032	0.011
4.58	-0.313	-0.313	0.236	-0.211	0.027	0.013
4.59	-0.313	-0.078	0.236	-0.215	0.025	0.014
4.60	-0.234	-0.078	0.236	-0.218	0.022	0.015
4.61	-0.234	-0.156	0.177	-0.221	0.019	0.016
4.62	-0.313	-0.078	0.177	-0.225	0.017	0.016
4.63	-0.313	-0.078	0.177	-0.229	0.014	0.017
4.64	-0.234	-0.313	0.177	-0.232	0.010	0.017
4.65	-0.313	-0.313	0.177	-0.236	0.005	0.018
4.66	-0.313	-0.078	0.177	-0.240	0.003	0.018
4.67	-0.313	-0.078	0.177	-0.244	0.000	0.019

Figure 6.2.2.4 Digital data for event 6.2

[ ] = baseline which is subtracted for peaks and numerical integration

Yeardate: 79219 Time: 10:22:51 M.S.T.

Time (μs)	$\partial B_E/\partial t$ (T/s)	$\partial B_N/\partial t$ (T/s)	$Z_o \partial D_z/\partial t$ (T/s)	B_E (μT)	B_N (μT)	$Z_o D_z$ (μT)
6.16	-0.078	0.000	0.059	-0.000	0.000	-0.000
6.17	-0.078	0.000	0.059	-0.000	0.000	-0.000
6.18	-0.078	-0.078	0.059	-0.000	-0.001	-0.000
6.19	-0.078	-0.625	-0.177	-0.000	-0.007	-0.002
6.20	-0.078	-0.703	-0.236	-0.000	-0.014	-0.005
6.21	-0.391	-0.391	-0.236	-0.003	-0.018	-0.008
6.22	-0.625	-0.078	0.000	-0.009	-0.019	-0.009
6.23	-0.625	-0.078	0.000	-0.014	-0.020	-0.009
6.24	-0.391	0.234	0.236	-0.017	-0.017	-0.008
6.25	-0.313	0.547	0.295	-0.020	-0.012	-0.005
6.26	-0.078	0.625	0.353	-0.020	-0.005	-0.002
6.27	0.234	0.703	0.353	-0.017	0.002	0.001
6.28	0.313	0.703	0.353	-0.013	0.009	0.004
6.29	0.313	0.703	0.236	-0.009	0.016	0.006
6.30	0.313	0.625	0.236	-0.005	0.022	0.007
6.31	0.313	0.313	0.177	-0.001	0.025	0.009
6.32	0.234	0.313	0.177	0.002	0.029	0.010

Figure 6.2.2.5 Digital data for event 7.4

[ ] = baseline which is subtracted for peaks and numerical integration

Yeardate: 79219 Time: 10:22:51 M.S.T.

Time (μs)	$\partial B_E/\partial t$ (T/s)	$\partial B_N/\partial t$ (T/s)	$Z_o \partial D_z/\partial t$ (T/s)	B_E (μT)	B_N (μT)	$Z_o D_z$ (μT)
7.33	-0.156	0.000	0.118	-0.000	0.000	-0.000
7.34	-0.156	0.000	0.118	-0.000	0.000	-0.000
7.35	-0.156	0.078	0.118	-0.000	0.001	-0.000
7.36	-0.156	0.156	0.118	-0.000	0.002	-0.000
7.37	-0.156	0.156	0.118	-0.000	0.004	-0.000
7.38	-0.156	0.156	0.118	-0.000	0.005	-0.000
7.39	-0.156	0.547	0.118	-0.000	0.011	-0.000
7.40	-0.156	0.625	0.118	-0.000	0.017	-0.000
7.41	0.078	0.859	0.118	0.002	0.026	-0.000
7.42	0.234	0.625	0.118	0.006	0.032	-0.000
7.43	0.547	0.313	0.118	0.013	0.035	-0.000
7.44	0.547	0.000	0.118	0.020	0.035	-0.000
7.45	0.547	-0.078	0.118	0.027	0.034	-0.000
7.46	0.234	-0.391	0.059	0.031	0.030	-0.001
7.47	0.000	-0.391	0.059	0.033	0.027	-0.001
7.48	-0.313	-0.469	0.118	0.031	0.022	-0.001
7.49	-0.391	-0.313	0.118	0.029	0.019	-0.001
7.50	-0.391	-0.078	0.118	0.027	0.018	-0.001
7.51	-0.391	0.000	0.118	0.024	0.018	-0.001
7.52	-0.391	0.234	0.118	0.022	0.020	-0.001
7.53	-0.313	0.234	0.118	0.020	0.023	-0.001
7.54	-0.313	0.234	0.118	0.019	0.025	-0.001
7.55	-0.234	0.234	0.118	0.018	0.027	-0.001
7.56	-0.156	0.156	0.118	0.018	0.029	-0.001
7.57	-0.156	0.156	0.118	0.018	0.031	-0.001
7.58	-0.078	0.156	0.118	0.019	0.032	-0.001
7.59	-0.078	0.078	0.118	0.019	0.033	-0.001
7.60	-0.078	0.000	0.118	0.020	0.033	-0.001
7.61	-0.078	0.000	0.118	0.021	0.033	-0.001
7.62	-0.078	0.000	0.118	0.022	0.033	-0.001
7.63	-0.078	0.000	0.177	0.022	0.033	-0.000

Figure 6.2.2.6 Digital data for event 12.9

[ ] = baseline which is subtracted for peaks and numerical integration

Yeardate: 79219 Time: 10:22:51 M.S.T.

Time (μs)	$\partial B_E/\partial t$ (T/s)	$\partial B_N/\partial t$ (T/s)	$Z_o \partial D_z/\partial t$ (T/s)	B_E (μT)	B_N (μT)	$Z_o D_z$ (μT)
12.82	-0.156	0.078	0.059	-0.000	0.000	-0.000
12.83	-0.156	0.078	0.059	-0.000	0.000	-0.000
12.84	-0.234	0.078	0.059	-0.001	0.000	-0.000
12.85	-0.234	0.000	0.059	-0.002	-0.001	-0.000
12.86	-0.234	0.000	0.000	-0.002	-0.002	-0.001
12.87	-0.313	0.000	-0.236	-0.004	-0.002	-0.004
12.88	-0.625	0.234	-0.295	-0.009	-0.001	-0.007
12.89	-1.016	0.234	0.000	-0.017	0.001	-0.008
12.90	-0.938	0.234	0.059	-0.025	0.002	-0.008
12.91	-0.625	0.234	0.236	-0.030	0.004	-0.006
12.92	-0.078	0.234	0.236	-0.029	0.005	-0.004
12.93	-0.078	0.234	0.177	-0.028	0.007	-0.003
12.94	0.000	0.313	0.118	-0.027	0.009	-0.002
12.95	0.078	0.313	0.059	-0.024	0.012	-0.002
12.96	0.000	0.313	0.118	-0.023	0.014	-0.002
12.97	0.000	0.313	0.177	-0.021	0.016	-0.001
12.98	0.000	0.313	0.177	-0.020	0.019	0.001
12.99	0.156	0.313	0.177	-0.016	0.021	0.002
13.00	0.156	0.234	0.177	-0.013	0.023	0.003
13.01	0.078	0.234	0.118	-0.011	0.024	0.004
13.02	0.078	0.000	0.118	-0.009	0.023	0.004
13.03	0.078	0.000	0.059	-0.007	0.022	0.004
13.04	0.000	0.000	0.059	-0.005	0.021	0.004
13.05	0.000	0.000	0.059	-0.004	0.021	0.004
13.06	0.000	0.000	0.059	-0.002	0.020	0.004
13.07	-0.078	0.000	0.118	-0.001	0.019	0.005
13.08	-0.078	0.000	0.118	-0.000	0.018	0.005
13.09	-0.078	0.000	0.118	0.000	0.018	0.006
13.10	0.000	0.000	0.118	0.002	0.017	0.006
13.11	0.000	0.000	0.059	0.003	0.016	0.006
13.12	0.000	0.000	0.059	0.005	0.015	0.006
13.13	-0.078	0.000	0.059	0.006	0.014	0.006
13.14	-0.078	0.000	0.059	0.007	0.014	0.006
13.15	-0.078	0.000	0.059	0.007	0.013	0.006
13.16	-0.078	0.000	0.059	0.008	0.012	0.006
13.17	-0.078	0.000	0.059	0.009	0.011	0.006
13.18	-0.078	0.078	0.059	0.010	0.011	0.006
13.19	-0.156	0.078	0.059	0.010	0.011	0.006
13.20	-0.156	0.000	0.059	0.010	0.011	0.006
13.21	-0.156	0.000	0.059	0.010	0.010	0.006
13.22	-0.156	0.078	0.059	0.010	0.010	0.006
13.23	-0.156	0.078	0.059	0.010	0.010	0.006

Figure 6.2.2.7 Digital data for event 13.3

[ ] = baseline which is subtracted for peaks and numerical integration

Yeardate: 79219 Time: 10:22:51 M.S.T.

Time (μs)	$\partial B_E/\partial t$ (T/s)	$\partial B_N/\partial t$ (T/s)	$Z_o \partial D_z/\partial t$ (T/s)	B_E (μT)	B_N (μT)	$Z_o D_z$ (μT)
13.28	-0.234	0.156	0.059	-0.000	0.000	-0.000
13.29	-0.234	0.156	0.059	-0.000	0.000	-0.000
13.30	-0.234	0.547	0.059	-0.000	0.004	-0.000
13.31	-0.156	0.859	0.059	0.001	0.011	-0.000
13.32	-0.156	0.859	0.059	0.002	0.018	-0.000
13.33	0.078	0.547	0.059	0.005	0.022	-0.000
13.34	0.547	0.234	0.000	0.012	0.023	-0.001
13.35	0.547	0.000	0.000	0.020	0.021	-0.001
13.36	0.000	0.000	-0.118	0.023	0.020	-0.003
13.37	-0.625	-0.078	-0.059	0.019	0.017	-0.004
13.38	-0.703	-0.078	-0.059	0.014	0.015	-0.005
13.39	-0.859	-0.078	0.000	0.008	0.012	-0.006
13.40	-0.781	-0.078	0.000	0.003	0.010	-0.006
13.41	-0.703	-0.078	0.000	-0.002	0.008	-0.007
13.42	-0.703	0.000	0.000	-0.007	0.006	-0.008
13.43	-0.625	0.000	0.059	-0.011	0.005	-0.008
13.44	-0.078	0.078	0.177	-0.009	0.004	-0.006
13.45	0.000	0.078	0.177	-0.007	0.003	-0.005
13.46	0.313	0.000	0.177	-0.001	0.001	-0.004
13.47	0.313	0.000	0.118	0.004	-0.000	-0.003
13.48	0.313	0.000	0.118	0.010	-0.002	-0.003
13.49	0.234	-0.078	0.118	0.014	-0.004	-0.002
13.50	0.234	-0.078	0.118	0.019	-0.006	-0.002
13.51	0.156	-0.078	0.118	0.023	-0.009	-0.001
13.52	0.078	-0.078	0.118	0.026	-0.011	-0.000

Figure 6.2.2.8 Digital data for event 14.0

[ ] = baseline which is subtracted for peaks and numerical integration

Yeardate: 79219 Time: 10:22:51 M.S.T.

Time (μs)	$\partial B_E/\partial t$ (T/s)	$\partial B_N/\partial t$ (T/s)	$Z_o \partial D_z/\partial t$ (T/s)	B_E (μT)	B_N (μT)	$Z_o D_z$ (μT)
13.94	-0.078	0.000	0.059	-0.000	0.000	-0.000
13.95	[-0.078]	0.000	0.059	-0.000	0.000	-0.000
13.96	-0.156	0.000	[0.059]	-0.001	0.000	-0.000
13.97	-0.156	0.000	0.000	-0.002	0.000	-0.001
13.98	-0.234	[0.000]	0.000	-0.003	0.000	-0.001
13.99	-0.625	0.156	-0.059	-0.009	0.002	-0.002
14.00	-0.625	0.156	0.059	-0.014	0.003	-0.002
14.01	-0.078	0.156	0.236	-0.014	0.005	-0.001
14.02	-0.078	0.156	0.236	-0.014	0.006	0.001
14.03	0.234	0.000	0.236	-0.011	0.006	0.003
14.04	0.234	0.000	0.059	-0.008	0.006	0.003
14.05	0.234	0.000	0.059	-0.005	0.006	0.003
14.06	0.000	0.000	0.059	-0.004	0.006	0.003
14.07	-0.078	0.000	0.059	-0.004	0.006	0.003
14.08	-0.078	0.000	0.059	-0.004	0.006	0.003

Figure 6.2.2.9 Digital data for event 18.8

[ ] = baseline which is subtracted for peaks and numerical integration

Yeardate: 79219 Time: 10:22:51 M.S.T.

Time (μs)	$\partial B_E/\partial t$ (T/s)	$\partial B_N/\partial t$ (T/s)	$Z_o \partial D_z/\partial t$ (T/s)	B_E (μT)	B_N (μT)	$Z_o D_z$ (μT)
18.69	-0.156	0.000	0.059	-0.000	0.000	-0.000
18.70	-0.156	0.000	0.059	-0.000	0.000	-0.000
18.71	-0.156	-0.078	0.059	-0.000	-0.001	-0.000
18.72	-0.156	-0.234	0.059	-0.000	-0.003	-0.000
18.73	-0.156	-0.156	0.059	-0.000	-0.005	-0.000
18.74	-0.234	0.000	0.059	-0.001	-0.005	-0.000
18.75	-0.234	0.234	0.000	-0.002	-0.002	-0.001
18.76	-0.391	0.313	0.000	-0.004	0.001	-0.001
18.77	-0.625	0.391	0.059	-0.009	0.005	-0.001
18.78	-0.313	0.391	0.177	-0.010	0.009	-0.000
18.79	-0.078	0.391	0.177	-0.009	0.013	0.001
18.80	0.000	0.391	0.177	-0.008	0.016	0.002
18.81	0.234	0.313	0.118	-0.004	0.020	0.003
18.82	0.234	0.234	0.059	-0.000	0.022	0.003
18.83	0.000	0.156	0.059	0.002	0.023	0.003
18.84	0.000	0.000	0.059	0.003	0.023	0.003
18.85	0.000	0.000	0.059	0.005	0.023	0.003
18.86	0.000	0.000	0.059	0.006	0.023	0.003
18.87	0.000	0.000	0.059	0.008	0.023	0.003
18.88	-0.078	-0.078	0.059	0.008	0.022	0.003
18.89	-0.078	-0.078	0.059	0.009	0.021	0.003
18.90	-0.156	-0.313	0.059	0.009	0.018	0.003
18.91	-0.156	-0.938	0.059	0.009	0.009	0.003
18.92	-0.234	-0.938	0.059	0.008	-0.000	0.003
18.93	-0.234	-0.625	0.059	0.008	-0.007	0.003
18.94	-0.234	0.000	0.000	0.007	-0.007	0.002
18.95	-0.234	1.172	0.000	0.006	0.005	0.002
18.96	-0.391	1.172	-0.059	0.004	0.017	0.001
18.97	-0.625	1.250	0.000	-0.001	0.029	0.000

Figure 6.2.2.10 Digital data for event 18.9

[ ] = baseline which is subtracted for peaks and numerical integration

Yeardate: 79219 Time: 10:22:51 M.S.T.

Time (μs)	$\partial B_E/\partial t$ (T/s)	$\partial B_N/\partial t$ (T/s)	$Z_o \partial D_z/\partial t$ (T/s)	B_E (μT)	B_N (μT)	$Z_o D_z$ (μT)
18.86	0.000	0.000	0.059	0.000	0.000	-0.000
18.87	0.000	0.000	0.059	0.000	0.000	-0.000
18.88	-0.078	-0.078	0.059	-0.001	-0.001	-0.000
18.89	-0.078	-0.078	0.059	-0.002	-0.002	-0.000
18.90	-0.156	-0.313	0.059	-0.003	-0.005	-0.000
18.91	-0.156	-0.938	0.059	-0.005	-0.014	-0.000
18.92	-0.234	-0.938	0.059	-0.007	-0.023	-0.000
18.93	-0.234	-0.625	0.059	-0.009	-0.030	-0.000
18.94	-0.234	0.000	0.000	-0.012	-0.030	-0.001
18.95	-0.234	1.172	0.000	-0.014	-0.018	-0.001
18.96	-0.391	1.172	-0.059	-0.018	-0.006	-0.002
18.97	-0.625	1.250	0.000	-0.024	0.006	-0.003
18.98	-0.625	0.938	0.059	-0.030	0.016	-0.003
18.99	-0.391	0.625	0.236	-0.034	0.022	-0.001
19.00	-0.078	0.313	0.177	-0.035	0.025	-0.000
19.01	0.234	0.234	0.177	-0.033	0.027	0.001
19.02	0.313	0.000	0.118	-0.030	0.027	0.002
19.03	0.391	0.000	0.059	-0.026	0.027	0.002
19.04	0.391	0.000	0.059	-0.022	0.027	0.002
19.05	0.234	0.000	0.059	-0.020	0.027	0.002
19.06	0.000	0.000	0.059	-0.020	0.027	0.002
19.07	0.000	0.000	0.059	-0.020	0.027	0.002
19.08	-0.078	0.078	0.059	-0.021	0.028	0.002
19.09	-0.234	0.078	0.059	-0.023	0.029	0.002
19.10	-0.234	0.078	0.059	-0.025	0.029	0.002
19.11	-0.234	0.078	0.059	-0.028	0.030	0.002
19.12	-0.234	0.000	0.059	-0.030	0.030	0.002
19.13	-0.156	0.000	0.000	-0.031	0.030	0.001
19.14	-0.156	0.000	0.000	-0.033	0.030	0.000

Figure 6.2.2.11 Digital data for event 19.3

[ ] = baseline which is subtracted for peaks and numerical integration

Yeardate: 79219 Time: 10:22:51 M.S.T.

Time (μs)	$\partial B_E/\partial t$ (T/s)	$\partial B_N/\partial t$ (T/s)	$Z_o \partial D_z/\partial t$ (T/s)	B_E (μT)	B_N (μT)	$Z_o D_z$ (μT)
19.18	-0.156	0.078	0.000	-0.000	0.000	0.000
19.19	[-0.156]	0.078	0.000	-0.000	0.000	0.000
19.20	-0.234	0.078	0.000	-0.001	0.000	0.000
19.21	-0.234	[0.078]	0.000	-0.002	0.000	0.000
19.22	-0.234	0.000	0.000	-0.002	-0.001	0.000
19.23	-0.313	0.000	[0.000]	-0.004	-0.002	0.000
19.24	-0.391	-0.078	-0.118	-0.006	-0.003	-0.001
19.25	-0.391	0.000	-0.236	-0.009	-0.004	-0.004
19.26	-0.625	0.313	-0.412	-0.013	-0.002	-0.008
19.27	-1.016	0.547	-0.471	-0.022	0.003	-0.012
19.28	-1.563	0.625	-0.236	-0.036	0.009	-0.015
19.29	-1.563	0.625	-0.177	-0.050	0.014	-0.016
19.30	-1.250	0.625	0.000	-0.061	0.020	-0.016
19.31	-0.703	0.547	0.000	-0.066	0.024	-0.016
19.32	-0.391	0.313	0.059	-0.069	0.027	-0.016
19.33	-0.313	0.313	0.059	-0.070	0.029	-0.015
19.34	-0.078	0.234	0.059	-0.070	0.030	-0.015
19.35	0.000	0.000	0.059	-0.068	0.030	-0.014
19.36	0.078	0.000	0.059	-0.066	0.029	-0.013
19.37	0.078	0.000	0.059	-0.063	0.028	-0.013
19.38	0.078	0.000	0.059	-0.061	0.028	-0.012
19.39	0.078	0.000	0.059	-0.059	0.027	-0.012
19.40	0.078	0.000	0.059	-0.056	0.026	-0.011
19.41	0.078	0.000	0.059	-0.054	0.025	-0.010
19.42	0.078	0.000	0.059	-0.052	0.025	-0.010
19.43	0.078	0.000	0.059	-0.049	0.024	-0.009
19.44	0.078	0.000	0.059	-0.047	0.023	-0.009
19.45	0.000	0.000	0.118	-0.045	0.022	-0.008
19.46	0.078	0.156	0.118	-0.043	0.023	-0.006
19.47	0.078	0.234	0.118	-0.041	0.025	-0.005
19.48	0.078	0.234	0.118	-0.038	0.026	-0.004
19.49	0.156	0.000	0.118	-0.035	0.025	-0.003
19.50	0.156	0.000	0.118	-0.032	0.025	-0.002
19.51	0.234	0.000	0.118	-0.028	0.024	-0.000
19.52	0.313	0.000	0.059	-0.024	0.023	0.000
19.53	0.313	0.000	0.059	-0.019	0.022	0.001
19.54	0.234	0.000	0.059	-0.015	0.021	0.001
19.55	0.234	0.000	0.059	-0.011	0.021	0.002
19.56	0.156	0.000	0.059	-0.008	0.020	0.002
19.57	0.234	0.000	0.059	-0.004	0.019	0.003
19.58	0.234	0.000	0.059	-0.000	0.018	0.004
19.59	0.234	0.000	0.059	0.004	0.018	0.004
19.60	0.000	0.000	0.000	0.005	0.017	0.004
19.61	0.000	0.000	0.000	0.007	0.016	0.004
19.62	-0.078	0.000	0.000	0.008	0.015	0.004
19.63	-0.078	0.000	0.059	0.008	0.014	0.005
19.64	-0.078	0.000	0.059	0.009	0.014	0.005

Figure 6.2.2.11 Digital data for event 19.3 (continued)

Time (μs)	$\partial B_E/\partial t$ (T/s)	$\partial B_N/\partial t$ (T/s)	$Z_o \partial D_z/\partial t$ (T/s)	B_E (μT)	B_N (μT)	$Z_o D_z$ (μT)
19.65	-0.078	0.078	0.059	0.010	0.014	0.006
19.66	-0.078	0.000	0.059	0.011	0.013	0.007
19.67	-0.078	0.000	0.059	0.012	0.012	0.007
19.68	0.000	0.000	0.059	0.013	0.011	0.008
19.69	0.000	0.000	0.059	0.015	0.011	0.008
19.70	0.000	0.000	0.059	0.016	0.010	0.009
19.71	0.000	0.000	0.059	0.018	0.009	0.010
19.72	0.000	0.000	0.059	0.019	0.008	0.010
19.73	0.000	0.000	0.059	0.021	0.007	0.011
19.74	0.000	0.000	0.059	0.023	0.007	0.011
19.75	-0.078	0.000	0.059	0.023	0.006	0.012
19.76	-0.078	0.000	0.059	0.024	0.005	0.013
19.77	-0.078	0.000	0.059	0.025	0.004	0.013
19.78	-0.156	0.000	0.059	0.025	0.003	0.014
19.79	-0.156	0.000	0.059	0.025	0.003	0.014
19.80	-0.156	0.000	0.059	0.025	0.002	0.015
19.81	-0.156	0.000	0.059	0.025	0.001	0.016
19.82	-0.156	0.000	0.059	0.025	0.000	0.016

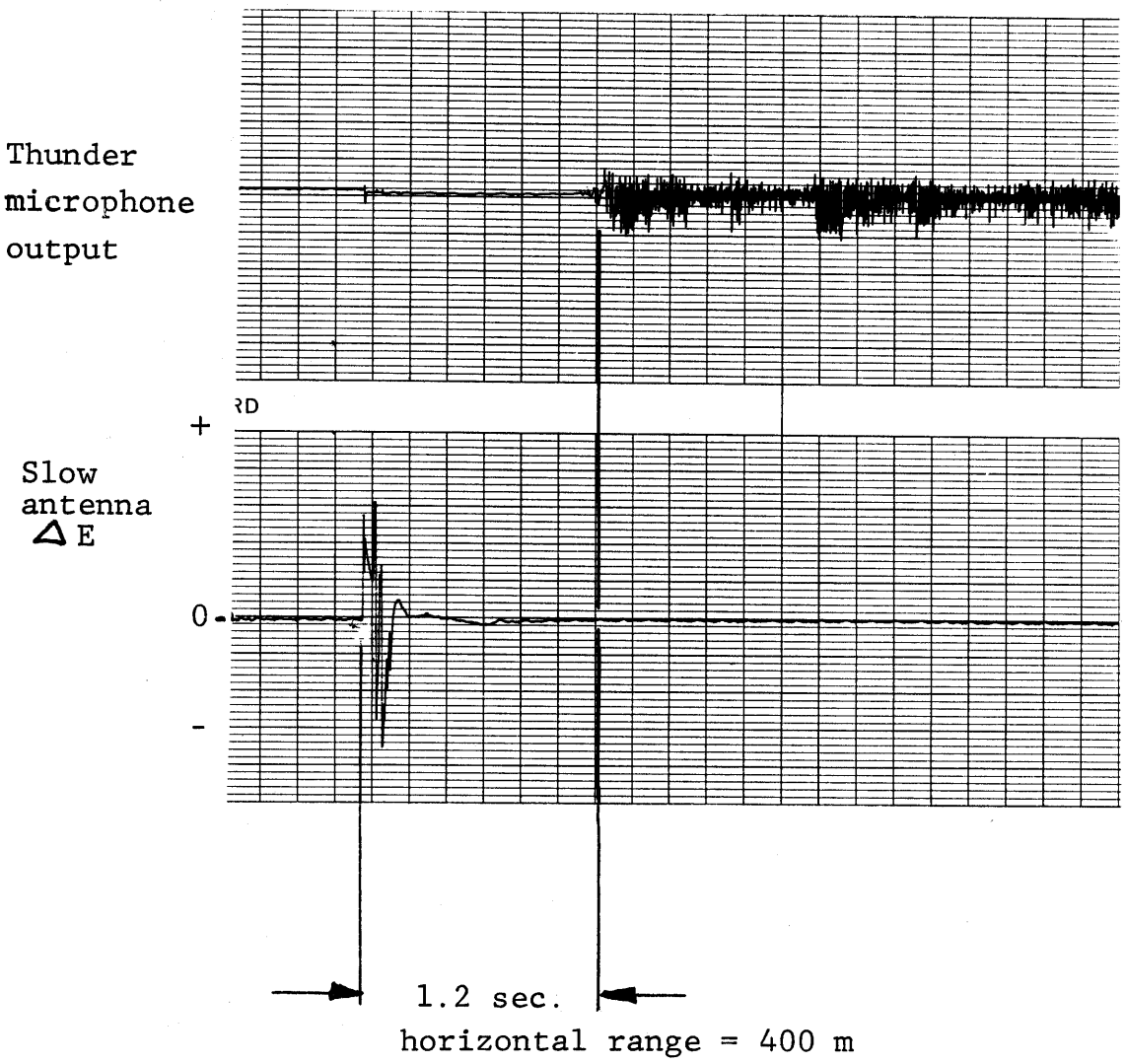

Date: 79219 M.S.T.: 1022:51

Figure 6.2.3 Slow E field change and thunder microphone record of midrange leader

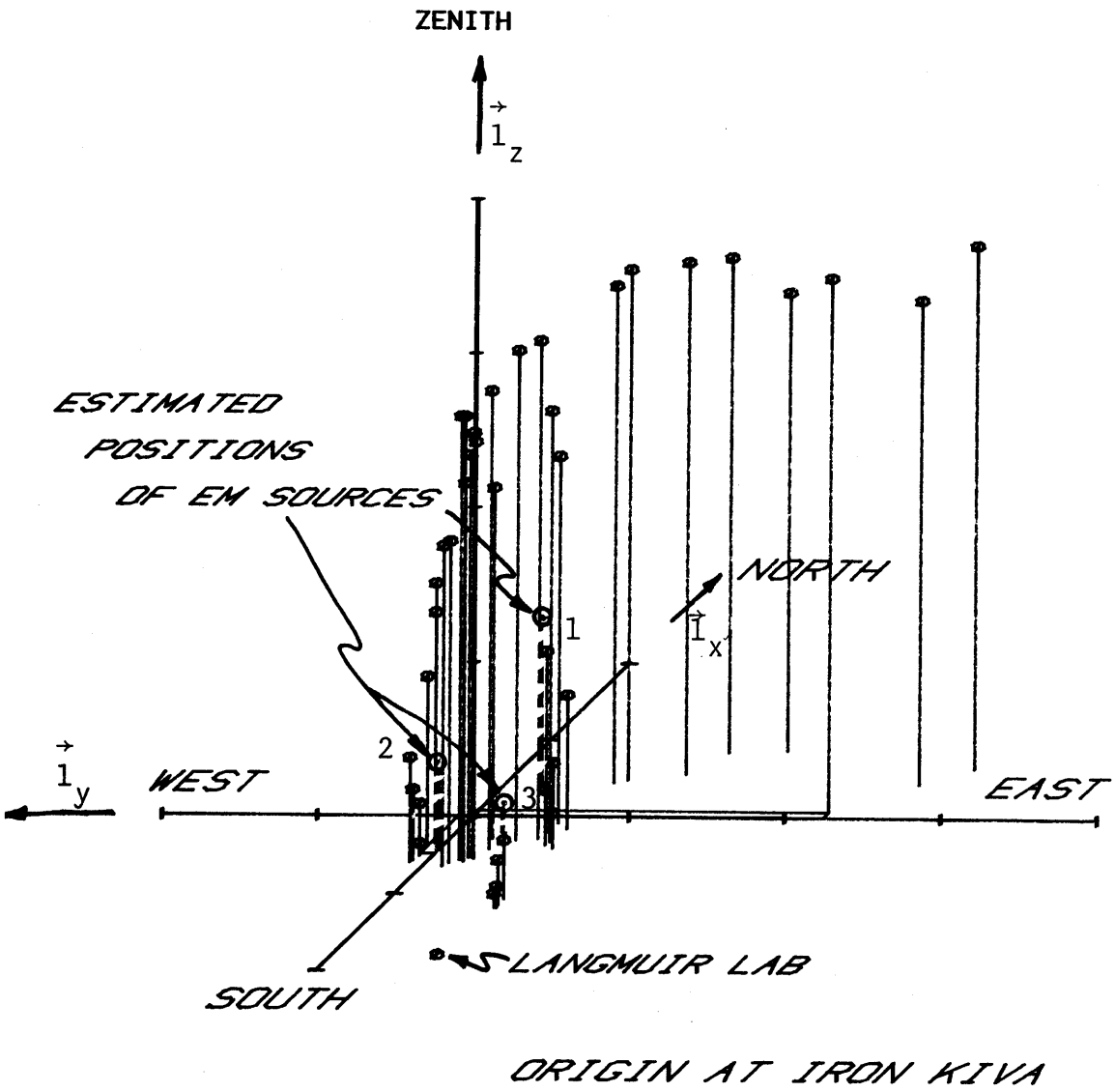

ticks on axes at 1 km intervals.

Date : 79219 M.S.T. : 1022:51

Note: Three lightning channels to earth
1,2,3 indicate set numbers of $\partial\vec{I}/\partial t$ pulses.

Figure 6.2.4 Acoustic location of midrange leader(s)

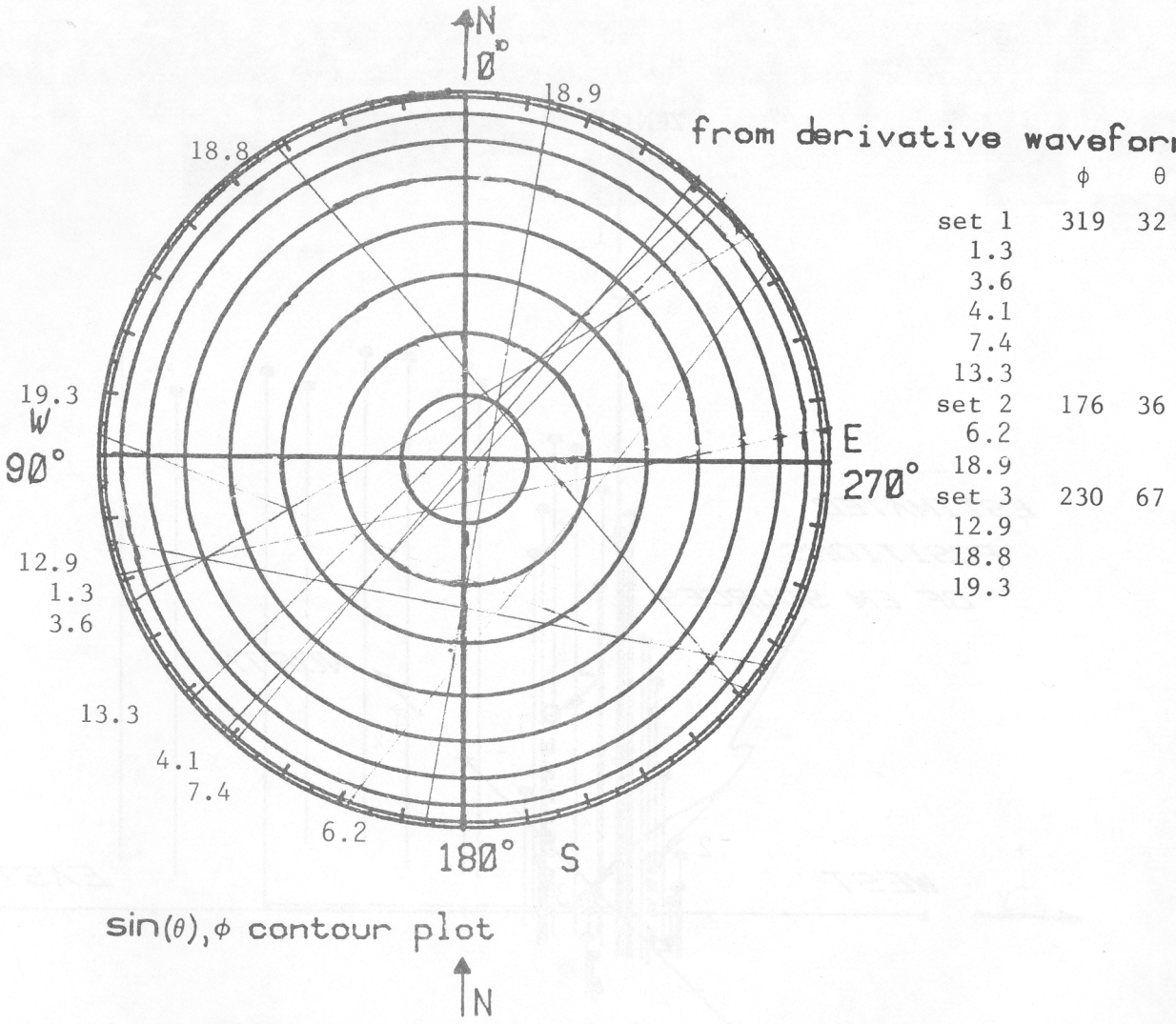

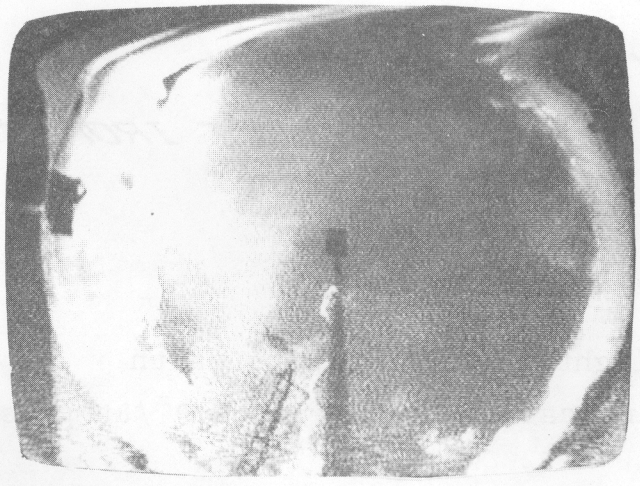

Whole-sky photograph from Kiva

Date: 79219 M.S.T.: 10:22:51

Figure 6.2.5A sin(θ),ϕ contours for midrange leader(s) derivative waveform and whole-sky videotape photograph

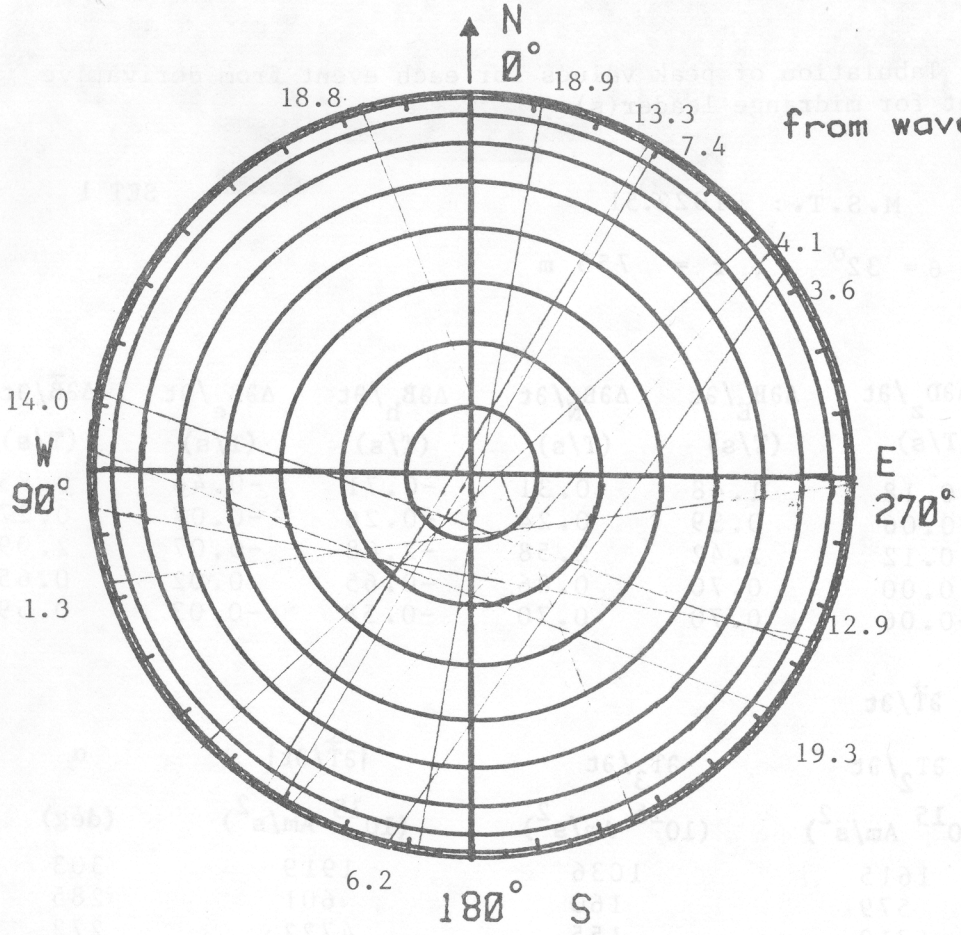

from waveform

	ϕ	θ
set 1	340	6
7.4		
13.3		
18.8		
set 2	172	55
6.2		
18.9		
set 3	242	55
12.9		
14.0		
19.3		
set 4	195	11
1.3		
3.6		
4.1		

sin(θ),ϕ contour plot

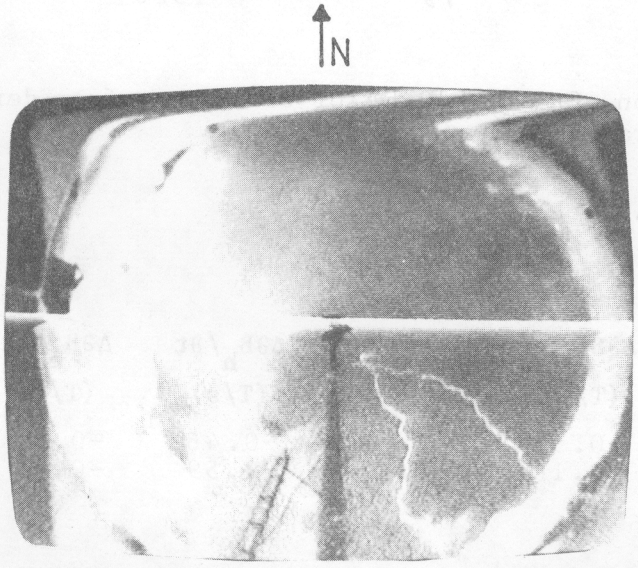

Whole-sky photograph from Kiva

Date: 79219 M.S.T.: 10:22:51

Figure 6.2.5B sin(θ),ϕ contours for midrange leader(s) waveform and whole-sky videotape photograph

Figure 6.2.6A.1 Tabulation of peak values for each event from derivative waveform set for midrange leader(s)

Yeardate: 79219 M.S.T.: 1022.51 SET 1

$\phi = 319^{\circ}$; $\theta = 32^{\circ}$; r = 755 m

Event Number	Time (μs)	$Z_o \Delta\partial D_z/\partial t$ (T/s)	$\Delta\partial B_E/\partial t$ (T/s)	$\Delta\partial B_N/\partial t$ (T/s)	$\Delta\partial B_h/\partial t$ (T/s)	$\Delta\partial B_e/\partial t$ (T/s)	$\lvert\Delta\partial\vec{B}/\partial t\rvert$ (T/s)
1.3	1.33	0.18	1.48	0.31	-0.71	-0.46	0.85
3.6	3.58	-0.06	0.39	0.24	-0.26	-0.07	0.27
4.1	4.05	0.12	2.42	2.58	-2.08	-0.07	2.09
7.4	7.41	0.00	0.70	0.86	-0.65	0.02	0.65
13.3	13.32	-0.06	0.70	0.70	-0.58	-0.03	0.59

CALCULATED VALUES FOR $\partial\vec{T}/\partial t$

Event Number	$\partial T_2/\partial t$ (10^{15} Am/s^2)	$\partial T_3/\partial t$ (10^{15} Am/s^2)	$\lvert\partial\vec{T}/\partial t\rvert$ (10^{15} Am/s^2)	α (deg)
1.3	1615	1036	1919	303
3.6	579	160	601	285
4.1	4719	155	4722	272
7.4	1481	-37	1482	269
13.3	1324	79	1326	273

Figure 6.2.6A.2 Tabulation of peak values for each event from derivative waveform set for midrange leader(s)

Yeardate: 79219 M.S.T.: 1022.51 SET 2

$\phi = 176^{\circ}$; $\theta = 36^{\circ}$; r = 681 m

Event Number	Time (μs)	$Z_o \Delta\partial D_z/\partial t$ (T/s)	$\Delta\partial B_E/\partial t$ (T/s)	$\Delta\partial B_N/\partial t$ (T/s)	$\Delta\partial B_h/\partial t$ (T/s)	$\Delta\partial B_e/\partial t$ (T/s)	$\lvert\Delta\partial\vec{B}/\partial t\rvert$ (T/s)
6.2	6.23	-0.30	-0.55	-0.70	-0.46	-0.25	0.52
18.9	18.92	-0.06	-0.16	-0.94	-0.59	-0.05	0.59

CALCULATED VALUES FOR $\partial\vec{T}/\partial t$

Event Number	$\partial T_2/\partial t$ (10^{15} Am/s^2)	$\partial T_3/\partial t$ (10^{15} Am/s^2)	$\lvert\partial\vec{T}/\partial t\rvert$ (10^{15} Am/s^2)	α (deg)
6.2	933	507	1062	299
18.9	1194	92	1198	274

Figure 6.2.6A.3 Tabulation of peak values for each event from derivative waveform set for midrange leader(s)

Yeardate: 79219 M.S.T.: 1022.51 SET 3

ϕ = 230° ; θ = 67° ; r = 435 m

Event Number	Time (μs)	$Z_o \Delta\partial D_z/\partial t$ (T/s)	$\Delta\partial B_E/\partial t$ (T/s)	$\Delta\partial B_N/\partial t$ (T/s)	$\Delta\partial B_h/\partial t$ (T/s)	$\Delta\partial B_e/\partial t$ (T/s)	$\lvert\Delta\partial\vec{B}/\partial t\rvert$ (T/s)
12.9	12.89	-0.35	-0.86	0.16	0.97	-0.22	1.00
18.8	18.77	0.12	-0.47	0.55	0.91	0.06	0.91
19.3	19.28	-0.47	-1.41	0.55	1.83	-0.24	1.85

CALCULATED VALUES FOR $\partial\vec{T}/\partial t$

Event Number	$\partial T_2/\partial t$ (10^{15} Am/s^2)	$\partial T_3/\partial t$ (10^{15} Am/s^2)	$\lvert\partial\vec{T}/\partial t\rvert$ (10^{15} Am/s^2)	α (deg)
12.9	-1266	282	1297	77
18.8	-1186	-77	1188	94
19.3	-2385	316	2405	82

Figure 6.2.6B.1 Tabulation of peak values for each event from waveform set for midrange leader(s)

Yeardate: 79219 M.S.T.:1022.51 SET 1

$\phi = 340^{\circ}$; $\theta = 6^{\circ}$; r =3827 m

Event Number	Time (μs)	$Z_o \Delta D_s$ (μT)	ΔB_E (μT)	ΔB_N (μT)	ΔB_h (μT)	ΔB_e (μT)	$\lvert\Delta\vec{B}\rvert$ (μT)
7.4	7.43	0.00	0.02	0.04	-0.02	-0.00	0.02
13.3	13.34	-0.00	0.01	0.02	-0.01	-0.00	0.01
18.8	18.78	0.00	-0.01	0.03	-0.01	0.01	0.01

CALCULATED VALUES FOR $\vec{I}_t.\vec{T}$

Event Number	T_2 (10^9 Am/s)	T_3 (10^9 Am/s)	$\lvert\vec{T}\rvert$ (10^9 Am/s)	α (deg)
7.4	229	39	233	280
13.3	152	30	155	281
18.8	121	-105	160	229

Figure 6.2.6B.2 Tabulation of peak values for each event from waveform set for midrange leader(s)

Yeardate: 79219 M.S.T.:1022.51 SET 2

$\phi = 172^{\circ}$; $\theta = 55^{\circ}$; r = 488 m

Event Number	Time (μs)	$Z_o \Delta D_s$ (μT)	ΔB_E (μT)	ΔB_N (μT)	ΔB_h (μT)	ΔB_e (μT)	$\lvert\Delta\vec{B}\rvert$ (μT)
6.2	6.23	-0.01	-0.01	-0.02	-0.02	-0.01	0.02
18.9	18.94	-0.00	-0.01	-0.03	-0.03	-0.00	0.03

CALCULATED VALUES FOR $\vec{I}_t.\vec{T}$

Event Number	T_2 (10^9 Am/s)	T_3 (10^9 Am/s)	$\lvert\vec{T}\rvert$ (10^9 Am/s)	α (deg)
6.2	28	8	29	286
18.9	39	1	39	271

Figure 6.2.6B.3 Tabulation of peak values for each event from waveform set for midrange leader(s)

Yeardate: 79219 M.S.T.:1022.51 SET 3

$\phi = 242^{\circ}$; $\theta = 55^{\circ}$; r = 488 m

Event Number	Time (μs)	$Z_o \Delta D_z$ (μT)	ΔB_E (μT)	ΔB_N (μT)	ΔB_h (μT)	ΔB_e (μT)	$\lvert\Delta\vec{B}\rvert$ (μT)
12.9	12.91	-0.01	-0.03	0.01	0.03	-0.00	0.03
14.0	14.00	-0.00	-0.01	0.01	0.01	-0.00	0.01
19.3	19.29	-0.02	-0.05	0.02	0.05	-0.00	0.05

CALCULATED VALUES FOR $\vec{I}_t \cdot \vec{T}$

Event Number	T_2 (10^9 Am/s)	T_3 (10^9 Am/s)	$\lvert\vec{T}\rvert$ (10^9 Am/s)	α (deg)
12.9	-37	7	37	79
14.0	-19	2	19	85
19.3	-68	5	68	86

Figure 6.2.6B.4 Tabulation of peak values for each event from waveform set for midrange leader(s)

Yeardate: 79219 M.S.T.:1022.51 SET 4

$\phi = 195^{\circ}$; $\theta = 11^{\circ}$; r =2096 m

Event Number	Time (μs)	$Z_o \Delta D_z$ (μT)	ΔB_E (μT)	ΔB_N (μT)	ΔB_h (μT)	ΔB_e (μT)	$\lvert\Delta\vec{B}\rvert$ (μT)
1.3	1.34	0.01	0.05	0.01	-0.00	0.03	0.03
3.6	3.58	0.00	0.01	0.01	0.00	0.00	0.00
4.1	4.05	0.01	0.10	0.09	0.03	0.06	0.07

CALCULATED VALUES FOR $\vec{I}_t \cdot \vec{T}$

Event Number	T_2 (10^9 Am/s)	T_3 (10^9 Am/s)	$\lvert\vec{T}\rvert$ (10^9 Am/s)	α (deg)
1.3	20	-158	159	187
3.6	-17	-24	29	145
4.1	-203	-376	427	152

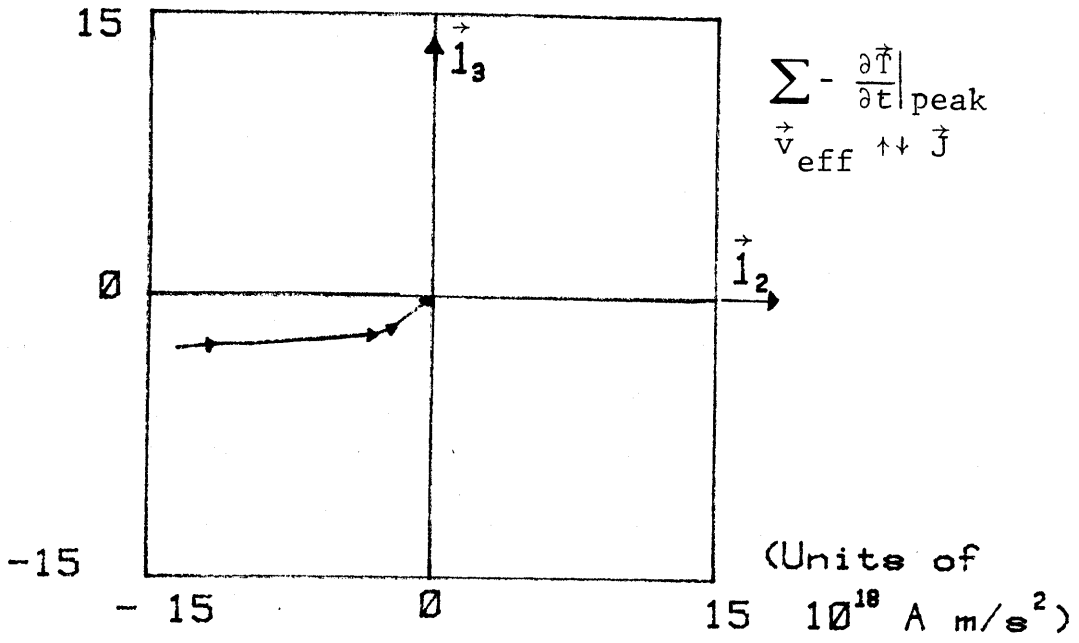

Effective reconstruction of negative streamer

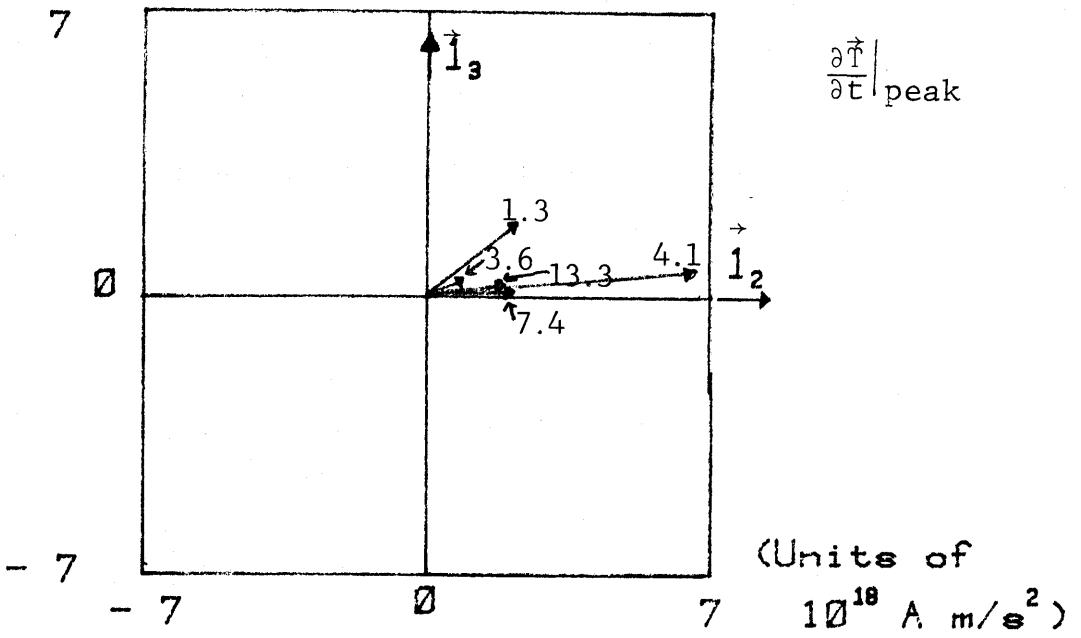

Peaks of $\partial\vec{T}/\partial t$

ϕ = 319° θ = 32°, r = 755 m

Date : 79219 M. S. T. : 1022.51

Figure 6.2.7A.1 $\partial\vec{T}/\partial t$ for midrange leader(set 1)

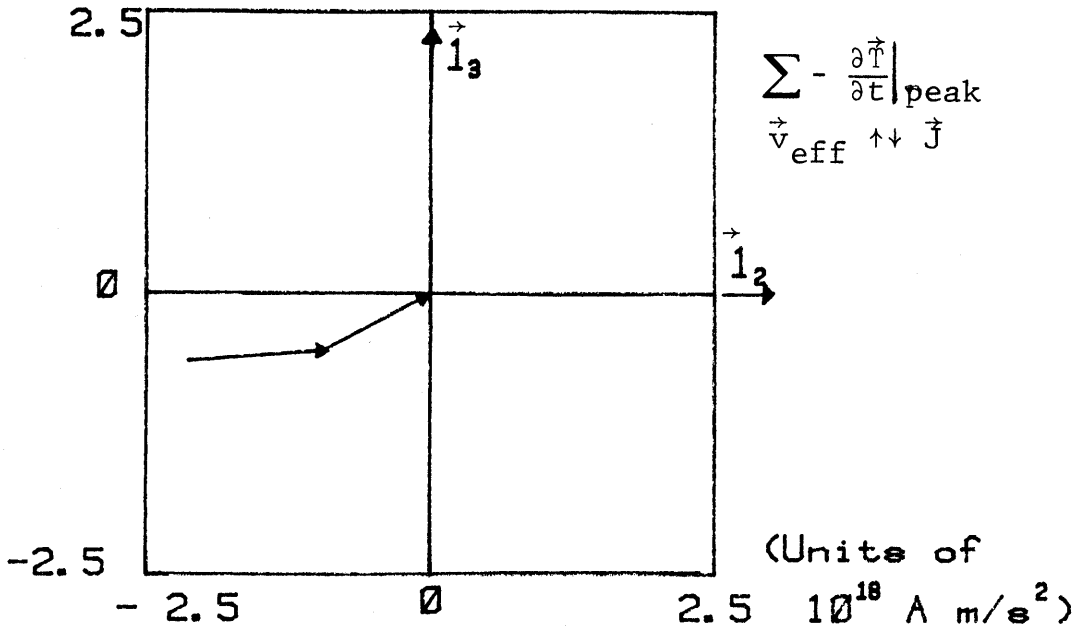

Effective reconstruction of negative streamer

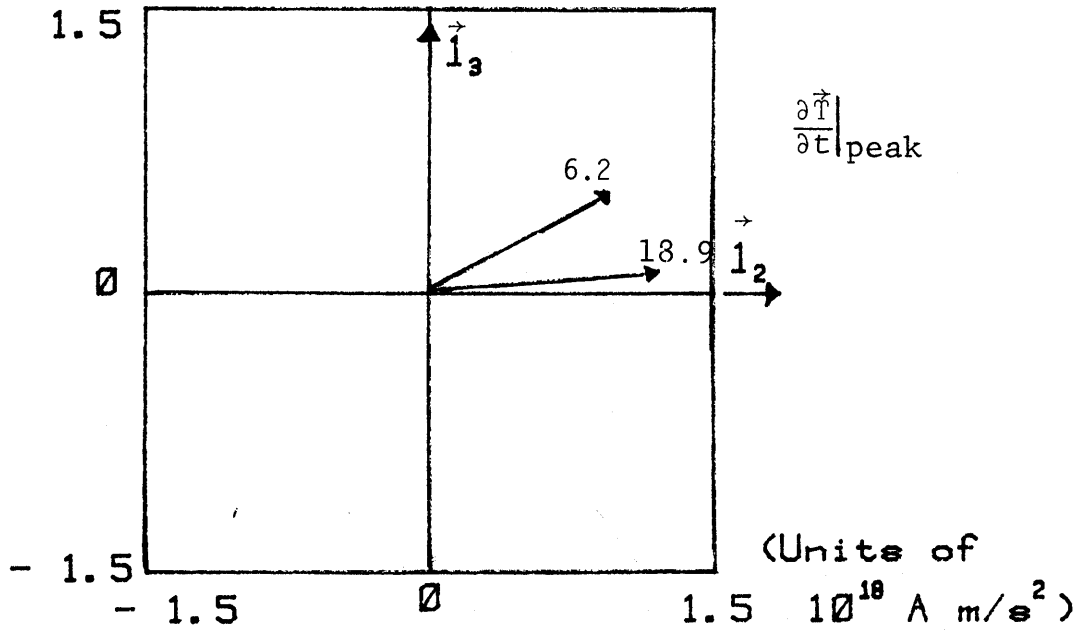

Peaks of $\partial\vec{T}/\partial t$

$\phi = 176^{\circ}$, $\theta = 36^{\circ}$, $r = 681$ m

Date : 79219 M.S.T.: 1022.51

Figure 6.2.7A.2 $\partial\vec{T}/\partial t$ for midrange leader (set 2)

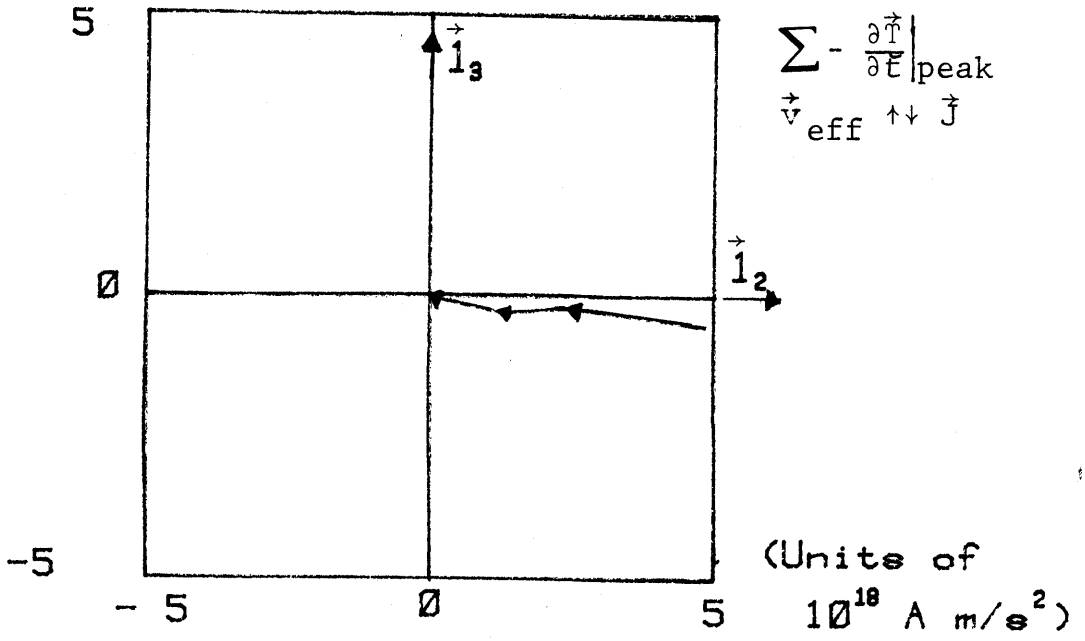

Effective reconstruction of negative streamer

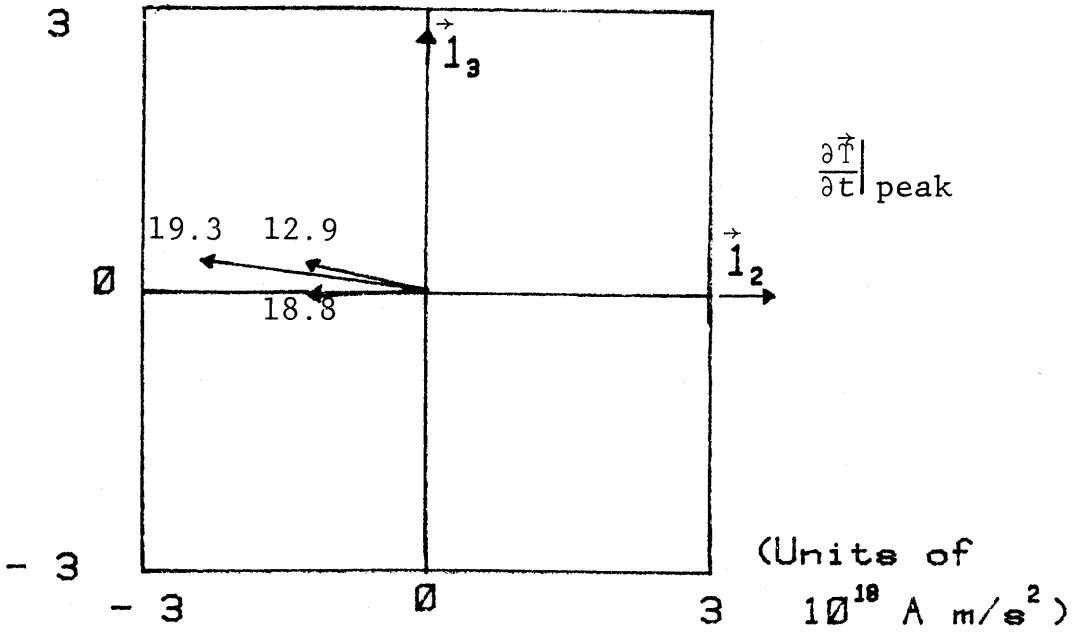

Peaks of $\partial \vec{T}/\partial t$

$\phi = 230^o$, $\theta = 67^o$, r = 435 m

Date : 79219 M. S. T. : 1022.51

Figure 6.2.7A.3 $\partial \vec{T}/\partial t$ for midrange leader (set 3)

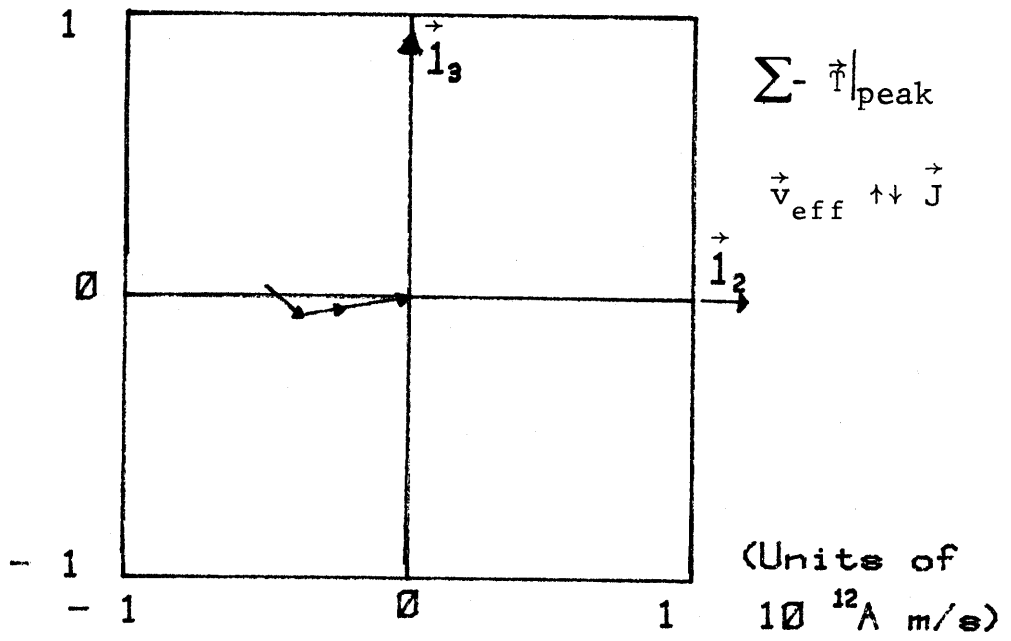

Effective reconstruction of negative streamer

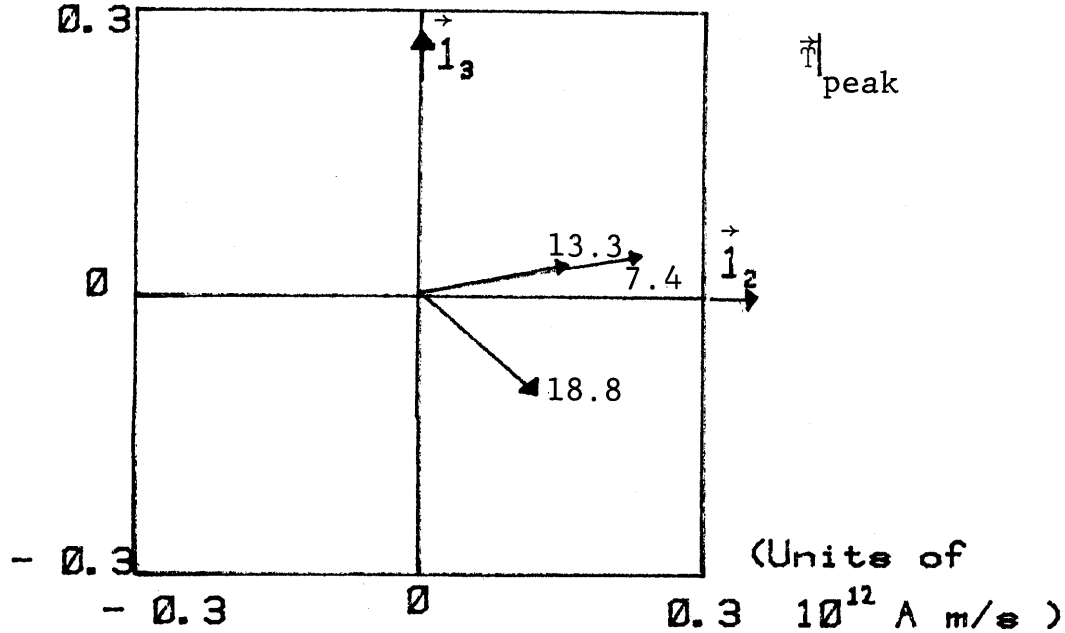

Peaks of $\vec{T}$

$\phi = 340^{o}$, $\theta = 6^{o}$, r = 3827 m

Date : 79219 M. S. T. : 1022.51

Figure 6.2.7B.1 $\vec{T}$ for midrange leader (set 1)

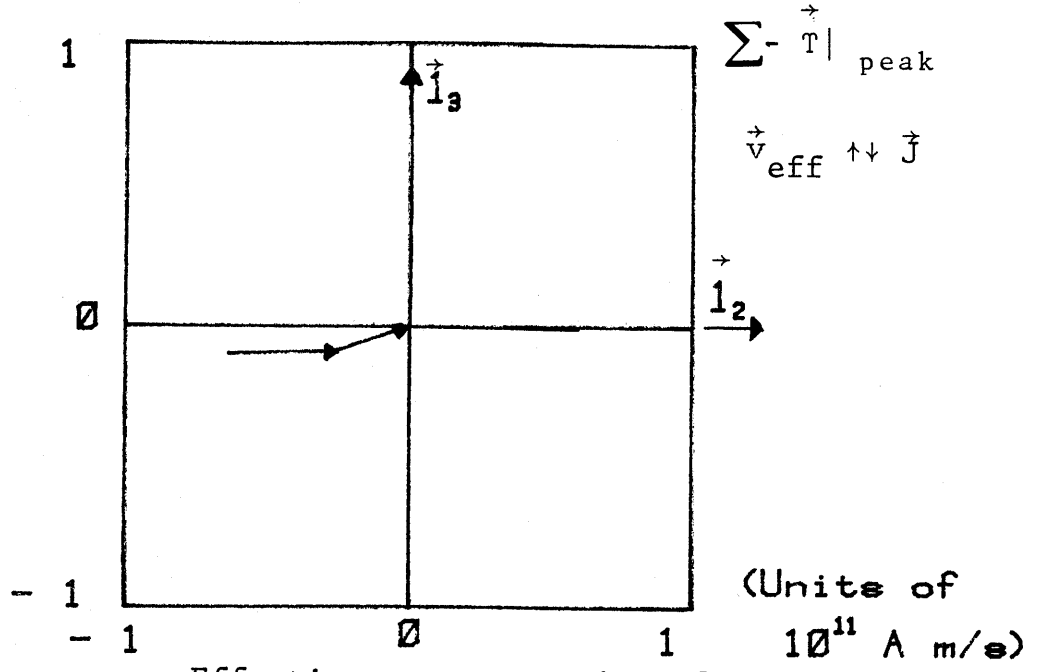

Effective reconstruction of negative streamer

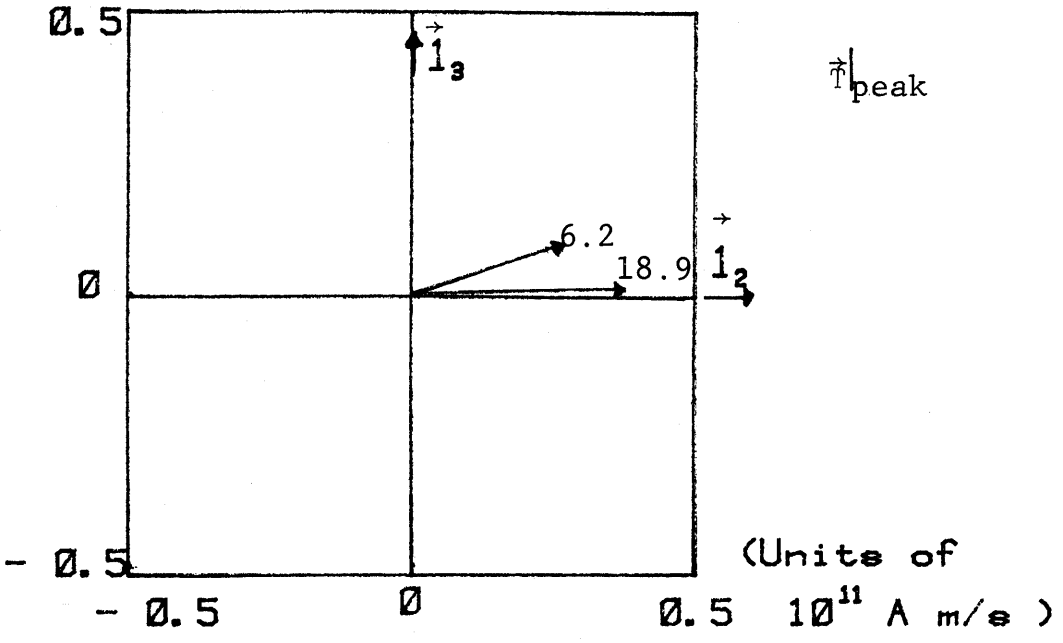

Peaks of $\vec{T}$

$\phi = 172^{o}$, $\theta = 55^{o}$, r = 488 m

Date : 79219 M.S.T.: 1022.51

Figure 6.2.7B.2 $\vec{T}$ for midrange leader (set 2)

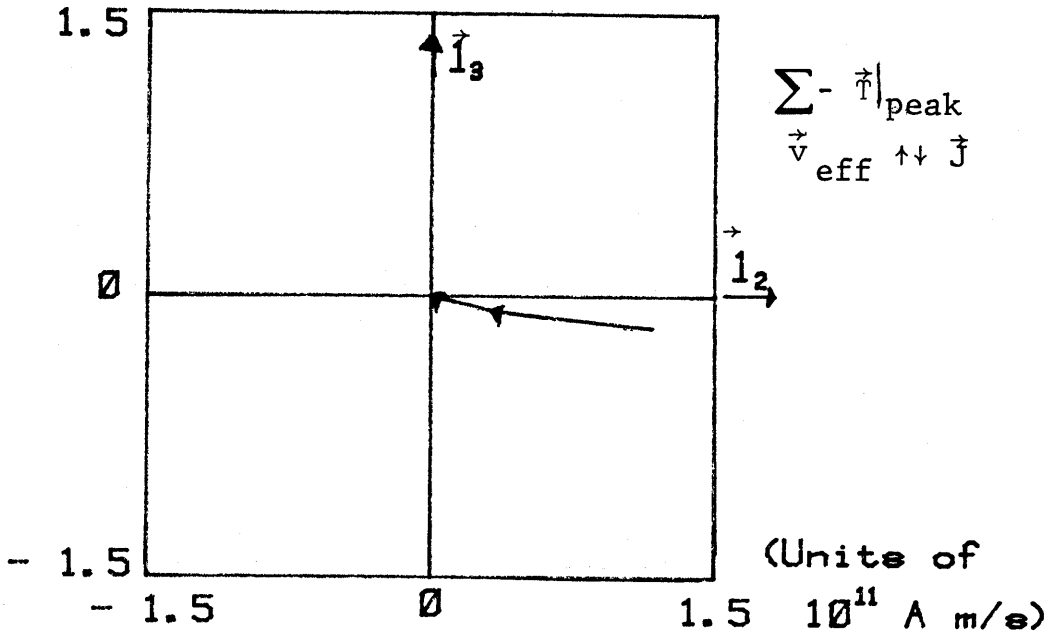

Effective reconstruction of negative streamer

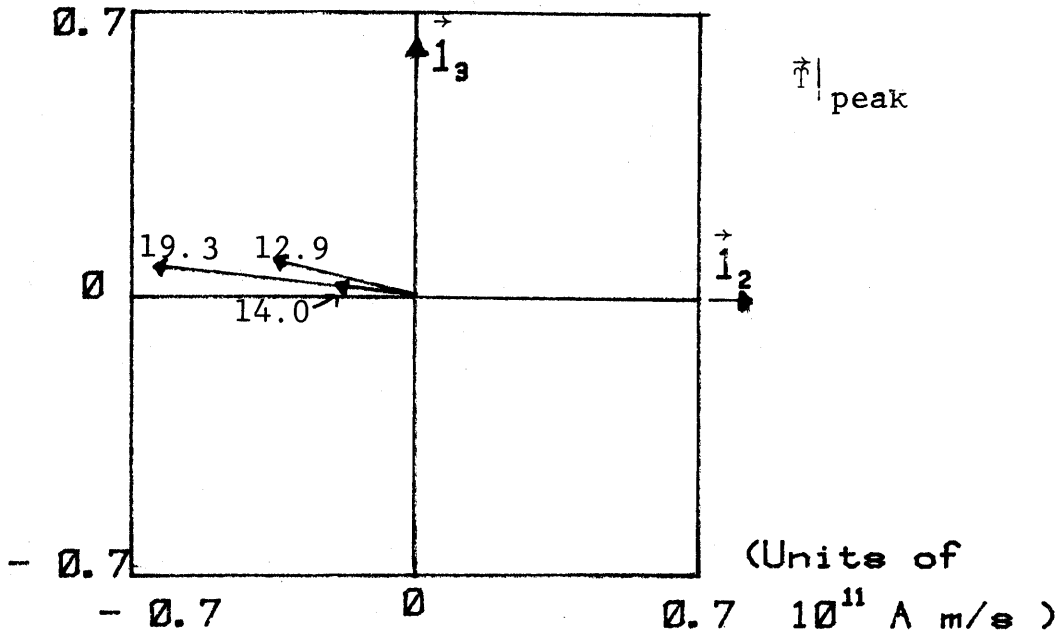

Peaks of $\vec{T}$

$\phi = 242^{o}$, $\theta = 55^{o}$, r = 488 m

Date : 79219 M.S.T.: 1022.51

Figure 6.2.7B.3 $\vec{T}$ for midrange leader (set 3)

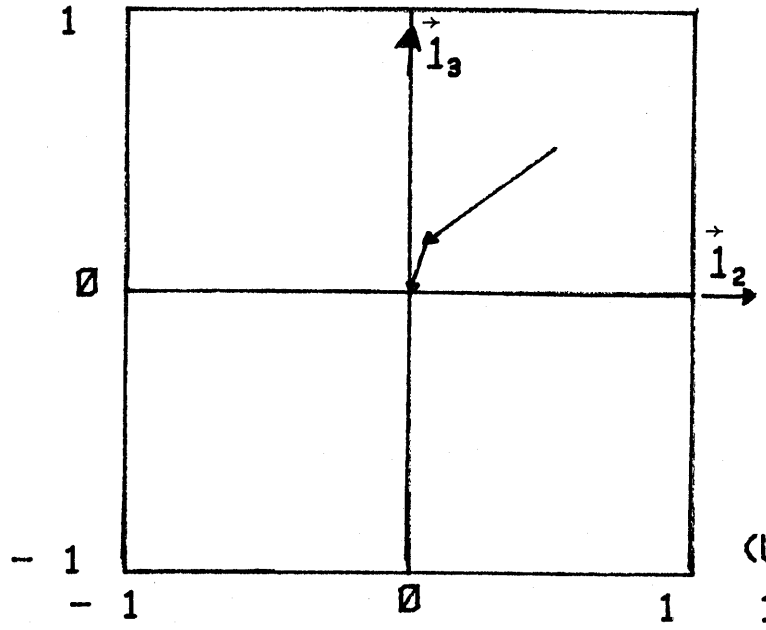

Effective reconstruction of negative streamer

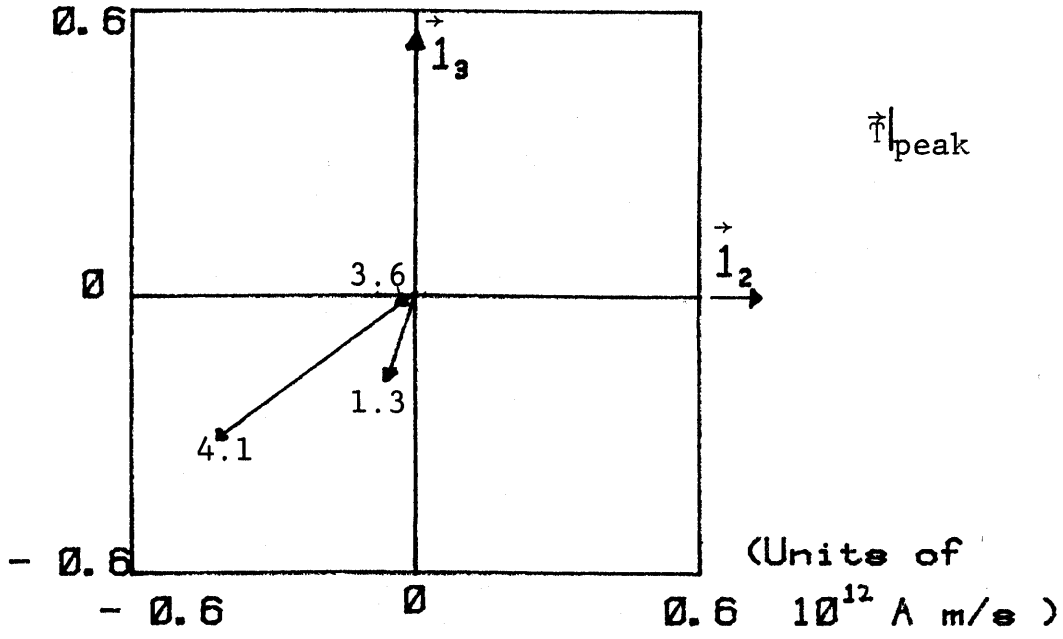

Peaks of $\vec{T}$

$\phi = 195^{\circ}$, $\theta = 11^{\circ}$, r = 2096 m

Date : 79219 M.S.T.: 1022.51

Figure 6.2.7B.4 $\vec{T}$ for midrange leader (set 4)

6.3 Nearby Leader

Our third example is given in figures 6.3.••••. This is labelled "nearby leader." Figures 6.3.1A and 6.3.1B show the derivative fields and fields for the 20 μs record.

Figure 6.3.3 shows the slow electric field and thunder microphone records, from which a horizontal range of 95 m is estimated. Figure 6.3.4 gives the acoustic source reconstruction indicating one principal streamer channel near the Kiva. Extending from about 5 km height there is some branching also collecting charge about 1.5 km a little north of west. On this is superimposed the location of the two EM sources which were very close together on this scale. Figures 6.3.5A and 6.3.5B show the same whole-sky videotape photograph indicating a channel to the west. Noting that this whole-sky camera is not exactly at the Kiva, but about 50 m north of it on the highest point of South Baldy peak (see fig. 1.1), the several channel location techniques give quite good agreement.

Looking at the θ, ϕ contours for derivative data in figure 6.3.5A we find two approximate sets of contour intersections. This was aided by noting the direction of $\partial\vec{T}/\partial t$ pulses in figure 6.3.7A. Figure 6.3.5B does the same for the field waveform pulses with good agreement, including the directions of the pulses in figures 6.3.7B.

Noting the two sources approximately above and below each other, these appear to be on or near the same main channel. It is conceivable that the lower source is a positive streamer and the upper streamer a negative one with the two streamers heading toward each other. For the plots of the $\partial\vec{T}/\partial t$ and $\vec{T}$ pulses in figures 6.3.7A and 6.3.7B we have chosen the convention $\vec{v}_{eff} \uparrow\downarrow \vec{J}$ since such an above possibility is difficult to confirm.

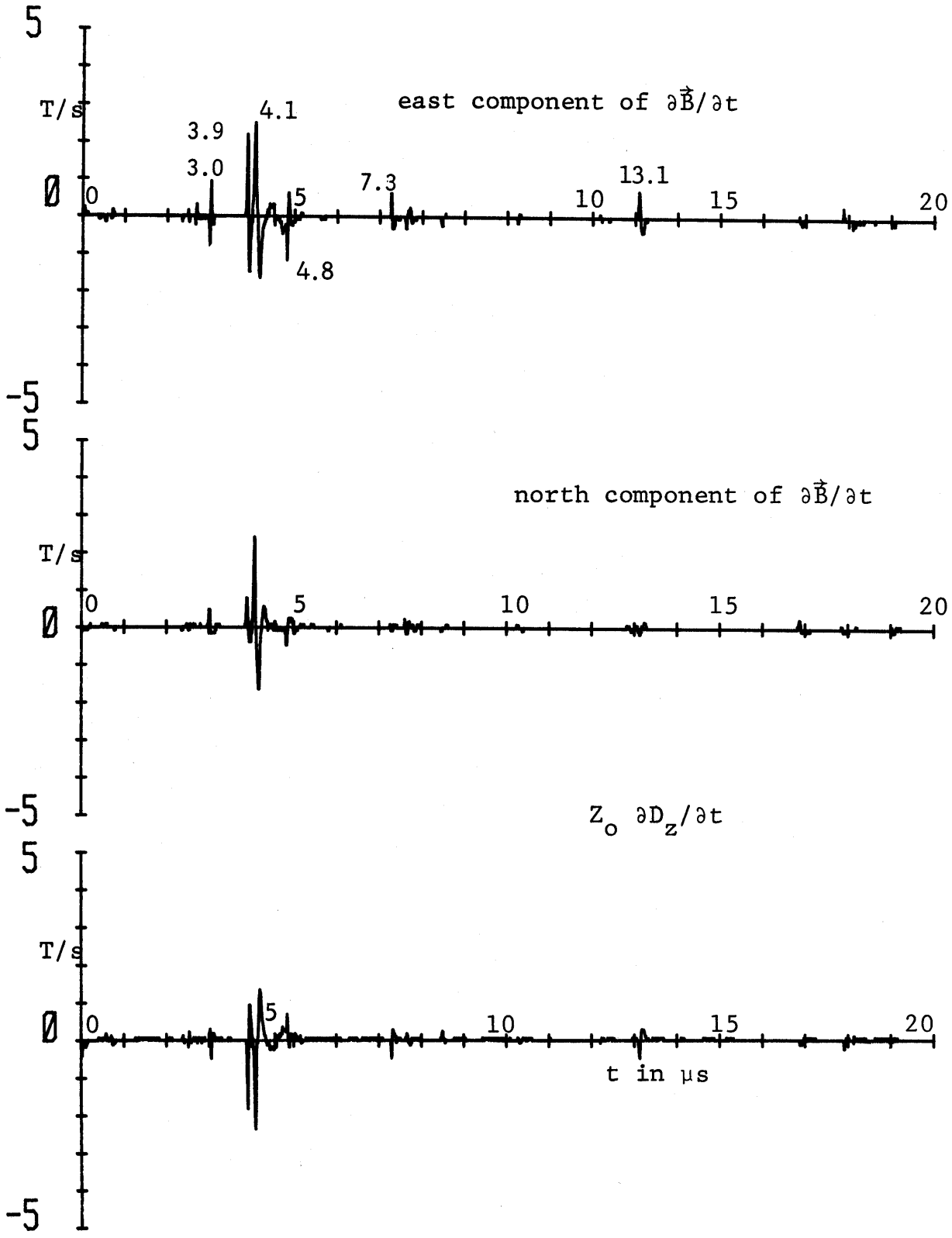

Figure 6.3.1A Derivative fields from nearby leader

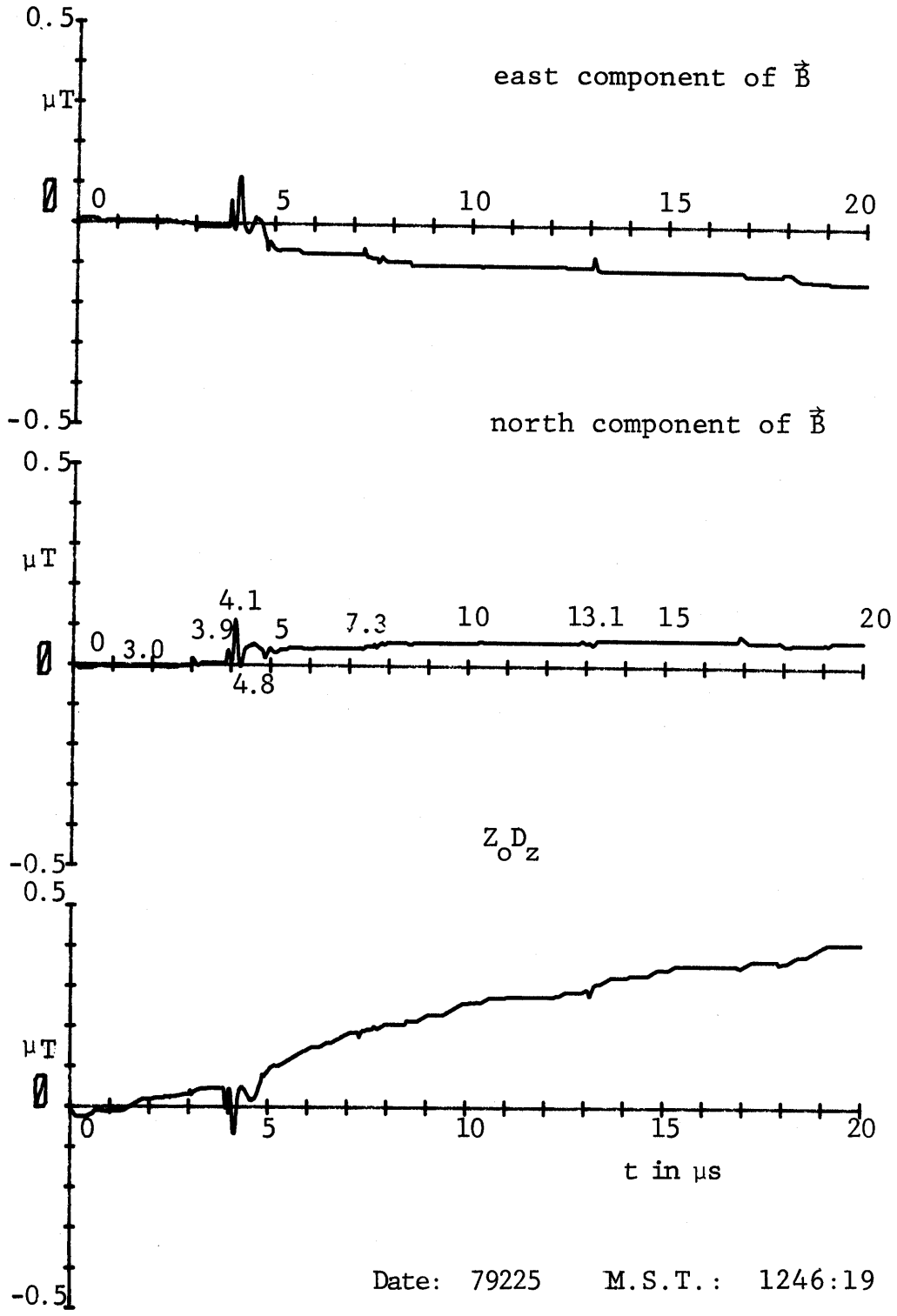

Figure 6.3.1B Fields from nearby leader

Figure 6.3.2.1 Digital data for event 3.0

[ ] = baseline which is subtracted for peaks and numerical integration

Yeardate: 79225 Time: 12:46:19 M.S.T.

Time (μs)	$\partial B_E/\partial t$ (T/s)	$\partial B_N/\partial t$ (T/s)	$Z_o \partial D_z/\partial t$ (T/s)	B_E (μT)	B_N (μT)	$Z_o D_z$ (μT)
2.93	-0.078	0.078	0.000	-0.000	0.000	0.000
2.94	[-0.078]	0.078	0.000	-0.000	0.000	0.000
2.95	-0.156	0.078	0.000	-0.001	0.000	0.000
2.96	-0.156	[0.078]	0.000	-0.002	0.000	0.000
2.97	-0.234	0.156	0.000	-0.003	0.001	0.000
2.98	-0.625	0.156	0.000	-0.009	0.002	0.000
2.99	-0.938	0.156	0.000	-0.017	0.002	0.000
3.00	-0.078	0.547	[0.000]	-0.017	0.007	0.000
3.01	0.547	0.547	0.059	-0.011	0.012	0.001
3.02	0.859	0.547	0.236	-0.002	0.016	0.003
3.03	0.000	0.234	0.295	-0.001	0.018	0.006
3.04	0.000	0.000	0.236	-0.000	0.017	0.008
3.05	-0.078	-0.078	-0.412	-0.000	0.016	0.004
3.06	-0.313	-0.078	-0.471	-0.002	0.014	-0.001
3.07	-0.313	-0.078	0.000	-0.005	0.013	-0.001
3.08	-0.313	-0.078	0.059	-0.007	0.011	-0.000
3.09	-0.078	-0.078	0.059	-0.007	0.010	0.000
3.10	-0.078	-0.078	0.118	-0.007	0.008	0.002
3.11	-0.078	-0.078	0.177	-0.007	0.007	0.003
3.12	-0.078	-0.078	0.177	-0.007	0.005	0.005
3.13	-0.078	-0.078	0.118	-0.007	0.004	0.006
3.14	-0.078	-0.078	0.059	-0.007	0.002	0.007
3.15	-0.078	0.000	0.000	-0.007	0.001	0.007
3.16	-0.078	0.000	0.000	-0.007	0.000	0.007

Figure 6.3.2.2 Digital data for event 3.9

[ ] = baseline which is subtracted for peaks and numerical integration

Yeardate: 79225 Time: 12:46:19 M.S.T.

Time (μs)	$\partial B_E/\partial t$ (T/s)	$\partial B_N/\partial t$ (T/s)	$Z_o \partial D_z/\partial t$ (T/s)	B_E (μT)	B_N (μT)	$Z_o D_z$ (μT)
3.83	0.000	0.078	0.000	0.000	0.000	0.000
3.84	0.000	0.078	0.000	0.000	0.000	0.000
3.85	0.313	0.156	0.000	0.003	0.001	0.000
3.86	1.172	0.156	0.000	0.015	0.002	0.000
3.87	2.109	0.234	0.000	0.036	0.003	0.000
3.88	1.875	0.547	-0.059	0.055	0.008	-0.001
3.89	0.547	0.859	-0.236	0.060	0.016	-0.003
3.90	-0.391	0.859	-0.884	0.056	0.023	-0.012
3.91	-1.250	0.625	-1.414	0.044	0.029	-0.026
3.92	-1.563	0.313	-1.826	0.028	0.031	-0.044
3.93	-1.563	0.000	-0.471	0.013	0.030	-0.049
3.94	-1.250	-0.078	0.000	0.000	0.029	-0.049
3.95	-0.703	-0.313	0.530	-0.007	0.025	-0.044
3.96	-0.625	-0.313	0.943	-0.013	0.021	-0.034
3.97	-0.313	-0.313	0.943	-0.016	0.017	-0.025
3.98	-0.078	-0.313	0.766	-0.017	0.013	-0.017
3.99	-0.078	-0.313	0.530	-0.018	0.009	-0.012
4.00	0.234	-0.078	0.471	-0.016	0.008	-0.007
4.01	0.313	-0.078	0.295	-0.013	0.006	-0.004
4.02	0.547	0.000	0.059	-0.007	0.006	-0.004
4.03	1.172	0.313	0.059	0.005	0.008	-0.003
4.04	1.797	0.625	0.000	0.023	0.013	-0.003

Figure 6.3.2.3 Digital data for event 4.1

[ ] = baseline which is subtracted for peaks and numerical integration

Yeardate: 79225 Time: 12:46:19 M.S.T.

Time (μs)	$\partial B_E/\partial t$ (T/s)	$\partial B_N/\partial t$ (T/s)	$Z_o \partial D_z/\partial t$ (T/s)	B_E (μT)	B_N (μT)	$Z_o D_z$ (μT)
4.00	0.234	-0.078	0.471	0.000	-0.000	0.000
4.01	0.313	-0.078	0.295	0.001	-0.000	-0.002
4.02	0.547	0.000	0.059	0.004	0.001	-0.006
4.03	1.172	0.313	0.059	0.013	0.005	-0.010
4.04	1.797	0.625	0.000	0.029	0.012	-0.015
4.05	2.188	1.250	-0.236	0.048	0.025	-0.022
4.06	2.422	1.875	-0.412	0.070	0.045	-0.031
4.07	1.875	2.500	-0.884	0.087	0.070	-0.044
4.08	0.625	2.422	-1.826	0.091	0.095	-0.067
4.09	0.547	1.250	-2.297	0.094	0.109	-0.095
4.10	0.234	0.547	-2.356	0.094	0.115	-0.123
4.11	0.000	0.000	-1.885	0.091	0.116	-0.147
4.12	-0.078	-0.391	-0.943	0.088	0.112	-0.161
4.13	-0.625	-0.625	-0.177	0.080	0.107	-0.167
4.14	-1.250	-0.938	0.000	0.065	0.098	-0.172
4.15	-1.563	-1.016	-0.059	0.047	0.089	-0.177
4.16	-1.641	-1.328	0.118	0.028	0.077	-0.181
4.17	-1.719	-1.563	0.471	0.009	0.062	-0.181
4.18	-1.641	-1.563	0.766	-0.010	0.047	-0.178
4.19	-1.328	-1.328	1.178	-0.025	0.035	-0.171
4.20	-1.016	-0.938	1.237	-0.038	0.026	-0.163
4.21	-0.938	-0.391	1.355	-0.050	0.023	-0.154
4.22	-0.703	-0.313	1.296	-0.059	0.021	-0.146
4.23	-0.625	-0.078	1.178	-0.068	0.021	-0.139
4.24	-0.391	0.000	0.943	-0.074	0.021	-0.134
4.25	-0.391	0.234	0.707	-0.080	0.024	-0.132
4.26	-0.313	0.313	0.530	-0.085	0.028	-0.131
4.27	-0.313	0.469	0.471	-0.091	0.034	-0.131

Figure 6.3.2.4 Digital data for event 4.8

[ ] = baseline which is subtracted for peaks and numerical integration

Yeardate: 79225 Time: 12:46:19 M.S.T.

Time (μs)	$\partial B_E/\partial t$ (T/s)	$\partial B_N/\partial t$ (T/s)	$Z_o \partial D_z/\partial t$ (T/s)	B_E (μT)	B_N (μT)	$Z_o D_z$ (μT)
4.77	-0.313	0.000	0.295	0.000	0.000	-0.000
4.78	[-0.313]	0.000	0.295	0.000	0.000	-0.000
4.79	-0.391	[0.000]	0.295	-0.001	0.000	-0.000
4.80	-0.703	-0.078	[0.295]	-0.005	-0.001	-0.000
4.81	-1.250	-0.078	0.236	-0.014	-0.002	-0.001
4.82	-0.703	-0.391	0.295	-0.018	-0.005	-0.001
4.83	-0.078	-0.391	0.295	-0.016	-0.009	-0.001
4.84	0.547	-0.313	0.471	-0.007	-0.013	0.001
4.85	0.547	-0.078	0.707	0.002	-0.013	0.005
4.86	0.313	0.000	0.530	0.008	-0.013	0.008
4.87	0.234	0.234	0.059	0.013	-0.011	0.005
4.88	0.000	0.313	0.000	0.016	-0.008	0.002
4.89	-0.078	0.313	-0.177	0.018	-0.005	-0.003
4.90	-0.313	0.313	-0.177	0.018	-0.002	-0.007
4.91	-0.234	0.234	0.000	0.019	0.001	-0.010

Figure 6.3.2.5 Digital data for event 7.3

[ ] = baseline which is subtracted for peaks and numerical integration

Yeardate: 79225 Time: 12:46:19 M.S.T.

Time (μs)	$\partial B_E/\partial t$ (T/s)	$\partial B_N/\partial t$ (T/s)	$Z_o \partial D_z/\partial t$ (T/s)	B_E (μT)	B_N (μT)	$Z_o D_z$ (μT)
7.23	-0.078	0.078	0.000	-0.000	0.000	0.000
7.24	[-0.078]	0.078	0.000	-0.000	0.000	0.000
7.25	0.547	[0.078]	0.000	0.006	0.000	0.000
7.26	0.547	0.156	0.000	0.012	0.001	0.000
7.27	0.000	0.156	0.000	0.013	0.002	0.000
7.28	-0.313	0.078	[0.000]	0.011	0.002	0.000
7.29	-0.391	0.000	-0.177	0.008	0.001	-0.002
7.30	-0.391	0.000	-0.471	0.005	0.000	-0.006
7.31	-0.391	0.000	-0.412	0.002	-0.001	-0.011
7.32	-0.391	0.000	0.059	-0.002	-0.002	-0.010
7.33	-0.313	0.078	0.295	-0.004	-0.002	-0.007
7.34	-0.313	0.156	0.295	-0.007	-0.001	-0.004
7.35	-0.156	0.156	0.236	-0.007	-0.000	-0.002
7.36	-0.078	0.156	0.177	-0.007	0.000	0.000

Figure 6.3.2.6 Digital data for event 13.1

[ ] = baseline which is subtracted for peaks and numerical integration

Yeardate: 79225 Time: 12:46:19 M.S.T.

Time (μs)	$\partial B_E/\partial t$ (T/s)	$\partial B_N/\partial t$ (T/s)	$Z_o \partial D_z/\partial t$ (T/s)	B_E (μT)	B_N (μT)	$Z_o D_z$ (μT)
13.02	-0.078	0.078	0.059	-0.000	0.000	-0.000
13.03	-0.078	0.078	0.059	-0.000	0.000	-0.000
13.04	-0.078	0.156	0.059	-0.000	0.001	-0.000
13.05	0.000	0.156	0.059	0.001	0.002	-0.000
13.06	0.234	0.156	0.000	0.004	0.002	-0.001
13.07	0.313	0.156	0.000	0.008	0.003	-0.001
13.08	0.625	0.078	0.000	0.015	0.003	-0.002
13.09	0.547	0.000	0.000	0.021	0.002	-0.002
13.10	0.234	0.000	-0.118	0.024	0.002	-0.004
13.11	0.000	0.000	-0.236	0.025	0.001	-0.007
13.12	-0.313	-0.078	-0.412	0.023	-0.001	-0.012
13.13	-0.391	-0.078	-0.471	0.020	-0.002	-0.017
13.14	-0.391	0.000	-0.236	0.016	-0.003	-0.020
13.15	-0.469	0.000	0.000	0.012	-0.004	-0.021
13.16	-0.469	0.000	0.059	0.009	-0.005	-0.021
13.17	-0.469	0.156	0.236	0.005	-0.004	-0.019
13.18	-0.469	0.156	0.295	0.001	-0.003	-0.017
13.19	-0.391	0.156	0.295	-0.002	-0.003	-0.015
13.20	-0.313	0.156	0.295	-0.004	-0.002	-0.012
13.21	-0.156	0.156	0.295	-0.005	-0.001	-0.010
13.22	-0.156	0.156	0.295	-0.006	-0.000	-0.007
13.23	-0.078	0.234	0.236	-0.006	0.001	-0.006
13.24	-0.078	0.234	0.236	-0.006	0.003	-0.004
13.25	-0.078	0.234	0.177	-0.006	0.004	-0.003
13.26	-0.156	0.234	0.118	-0.007	0.006	-0.002
13.27	-0.156	0.156	0.118	-0.007	0.007	-0.002
13.28	-0.078	0.156	0.059	-0.007	0.008	-0.002

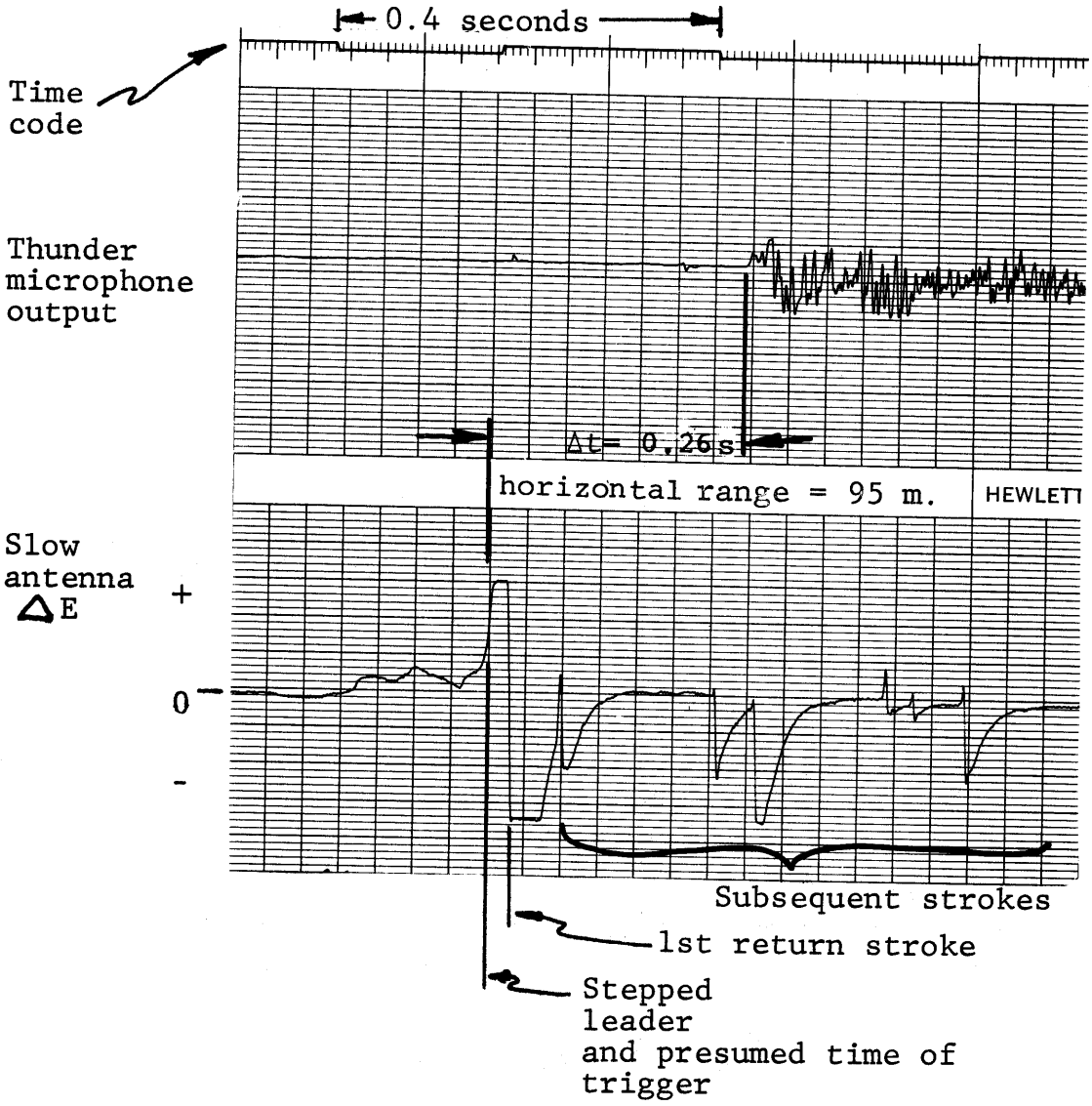

Date: 79225 M.S.T.: 1246:19

Figure 6.3.3 Slow electric field change and thunder microphone record from nearby leader streamer

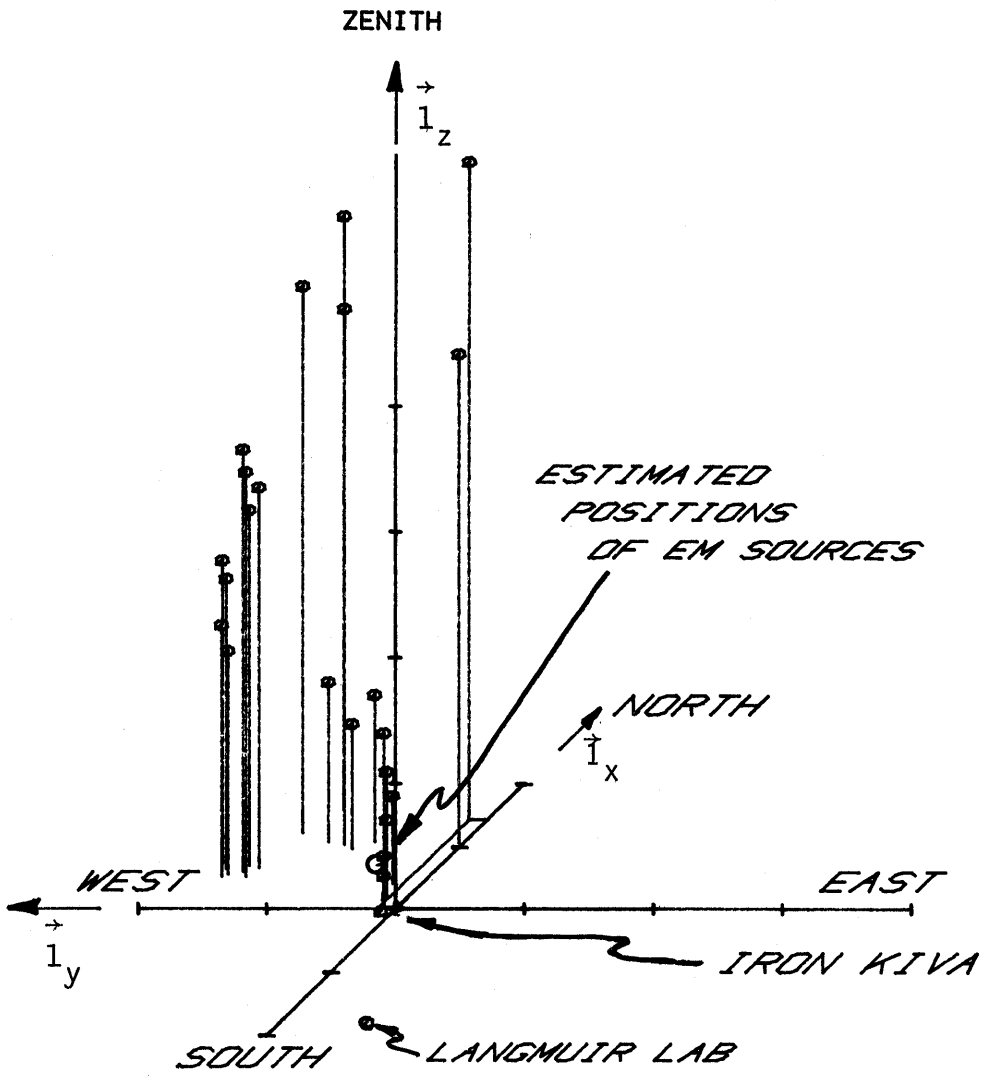

ticks on axes at 1 km intervals

Date :79225 M.S.T. : 1246·19

Figure 6.3.4 Acoustic location of lightning with nearby leader streamer

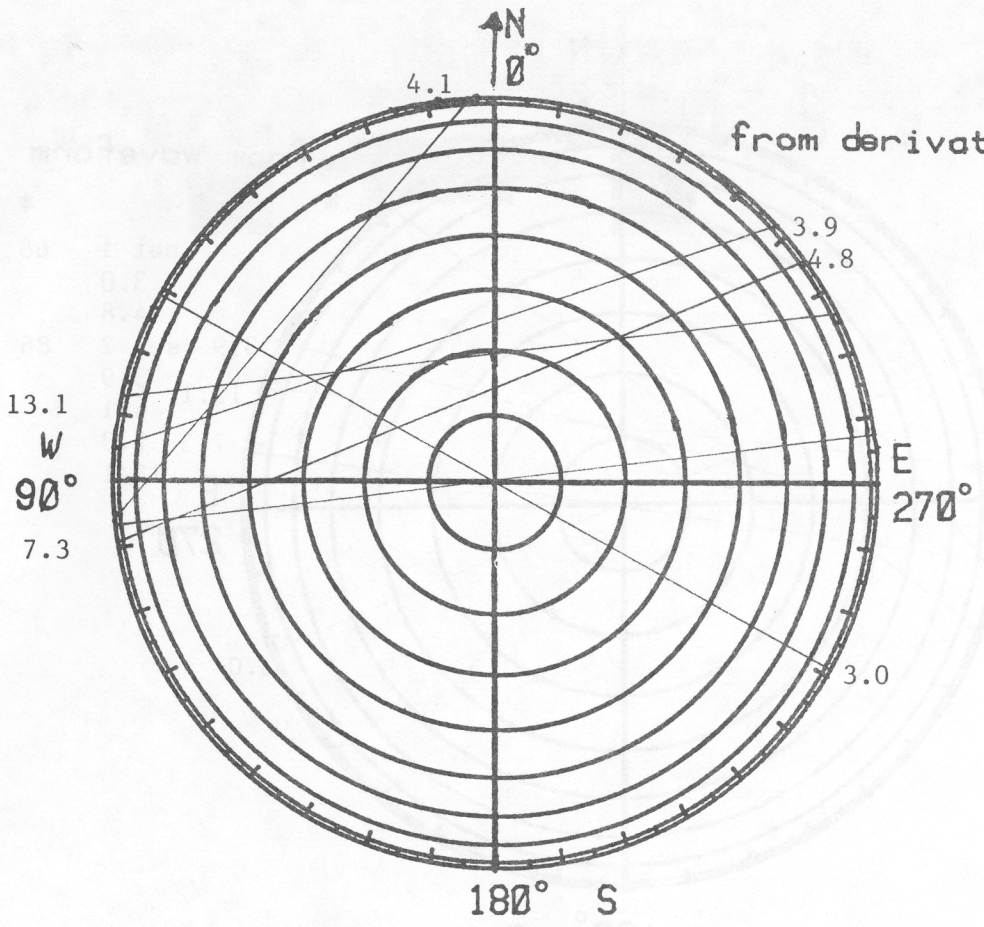

from derivative waveform

	ϕ	θ
set 1	61	18
3.0		
4.8		
set 2	74	50
3.9		
4.1		
7.3		
13.1		

$\sin(\theta),\phi$ contour plot

N

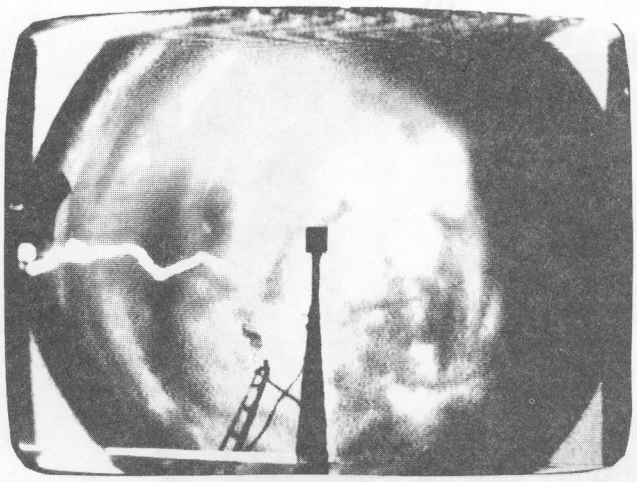

Whole-sky photograph from Kiva

Date: 79225 M.S.T.: 12:46:19

Figure 6.3.5 A $\sin(\theta),\phi$ contours for nearby leader derivative waveform and whole-sky videotape photograph

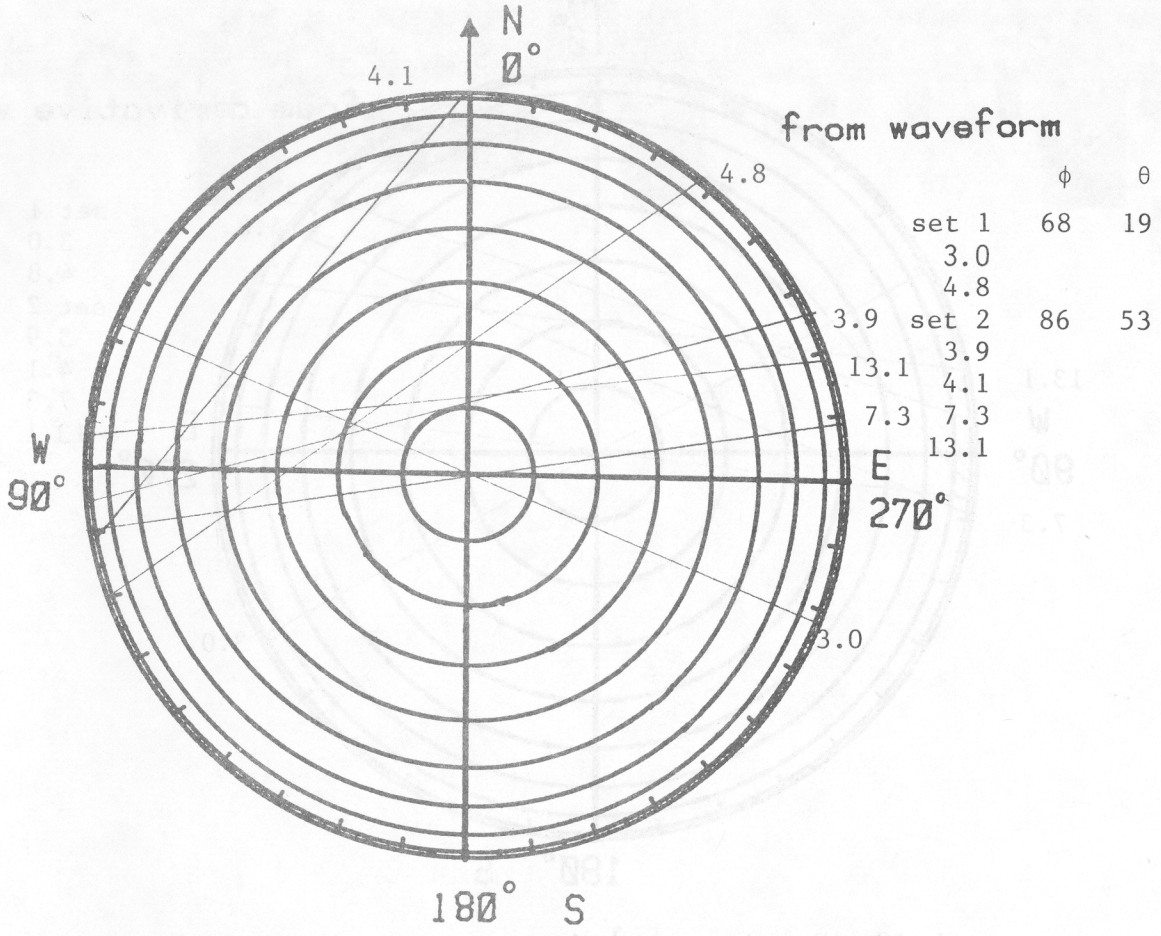

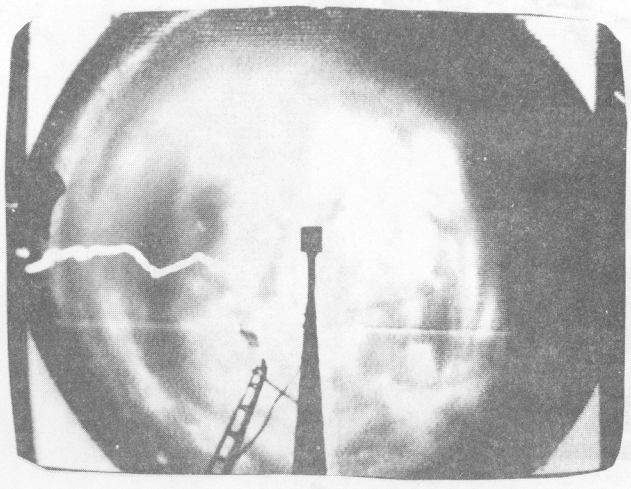

Whole-sky photograph from Kiva

Date: 79225 M.S.T.: 12:46:19

Figure 6.3.5B sin(θ),φ contours for nearby leader waveform and whole-sky videotape photograph

Figure 6.3.6A.1 Tabulation of peak values for each event from derivative waveform set for nearby leader

Yeardate: 79225 M.S.T.: 1246.19 SET 1

ϕ = 61° ; θ = 18° ; r = 307 m

Event Number	Time (μs)	$Z_o \Delta\partial D_z/\partial t$ (T/s)	$\Delta\partial B_E/\partial t$ (T/s)	$\Delta\partial B_N/\partial t$ (T/s)	$\Delta\partial B_h/\partial t$ (T/s)	$\Delta\partial B_e/\partial t$ (T/s)	$\lvert\Delta\partial\vec{B}/\partial t\rvert$ (T/s)
3.0	2.99	0.00	-0.86	0.47	-0.51	0.00	0.51
4.8	4.81	0.24	-0.94	-0.39	-0.33	0.40	0.52

CALCULATED VALUES FOR $\partial\vec{T}/\partial t$

Event Number	$\partial T_2/\partial t$ (10^{15} Am/s^2)	$\partial T_3/\partial t$ (10^{15} Am/s^2)	$\lvert\partial\vec{T}/\partial t\rvert$ (10^{15} Am/s^2)	α (deg)
3.0	475	-3	475	270
4.8	305	-367	478	220

Figure 6.3.6A.2 Tabulation of peak values for each event from derivative waveform set for nearby leader

Yeardate: 79225 M.S.T.: 1246.19 SET 2

ϕ = 74° ; θ = 50° ; r = 124 m

Event Number	Time (μs)	$Z_o \Delta\partial D_z/\partial t$ (T/s)	$\Delta\partial B_E/\partial t$ (T/s)	$\Delta\partial B_N/\partial t$ (T/s)	$\Delta\partial B_h/\partial t$ (T/s)	$\Delta\partial B_e/\partial t$ (T/s)	$\lvert\Delta\partial\vec{B}/\partial t\rvert$ (T/s)
3.9	3.87	-0.88	2.11	0.70	1.43	-0.63	1.56
4.1	4.06	-2.36	2.19	2.58	1.08	-1.54	1.88
7.3	7.26	0.00	0.63	0.08	0.45	-0.12	0.47
13.1	13.08	-0.24	0.70	0.08	0.51	-0.13	0.53

CALCULATED VALUES FOR $\partial\vec{T}/\partial t$

Event Number	$\partial T_2/\partial t$ (10^{15} Am/s^2)	$\partial T_3/\partial t$ (10^{15} Am/s^2)	$\lvert\partial\vec{T}/\partial t\rvert$ (10^{15} Am/s^2)	α (deg)
3.9	-531	234	580	66
4.1	-403	573	701	35
7.3	-168	46	174	75
13.1	-189	50	196	75

Figure 6.3.6B.1 Tabulation of peak values for each event from waveform set for nearby leader

Yeardate: 79225 M.S.T.:1246.19 SET 1

ϕ = 68° ; θ = 19° ; r = 292 m

Event Number	Time (μs)	$Z_o \Delta D_s$ (μT)	ΔB_E (μT)	ΔB_N (μT)	ΔB_h (μT)	ΔB_e (μT)	$\lvert\Delta\vec{B}\rvert$ (μT)
3.0	2.99	0.00	-0.02	0.01	-0.01	-0.00	0.01
4.8	4.82	0.01	-0.02	-0.01	-0.01	0.01	0.01

CALCULATED VALUES FOR $\vec{I}_t . \vec{T}$

Event Number	T_2 (10^9 Am/s)	T_3 (10^9 Am/s)	$\lvert\vec{T}\rvert$ (10^9 Am/s)	α (deg)
3.0	9	0	9	270
4.8	5	-8	10	214

Figure 6.3.6B.2 Tabulation of peak values for each event from waveform set for nearby leader

Yeardate: 79225 M.S.T.:1246.19 SET 2

ϕ = 86° ; θ = 53° ; r = 119 m

Event Number	Time (μs)	$Z_o \Delta D_s$ (μT)	ΔB_E (μT)	ΔB_N (μT)	ΔB_h (μT)	ΔB_e (μT)	$\lvert\Delta\vec{B}\rvert$ (μT)
3.8	3.89	-0.01	0.06	0.02	0.05	-0.01	0.05
4.1	4.11	-0.09	0.09	0.11	0.07	-0.06	0.09
7.3	7.27	0.00	0.01	0.00	0.01	-0.00	0.01
13.1	13.11	-0.01	0.03	0.00	0.02	-0.00	0.02

CALCULATED VALUES FOR $\vec{I}_t . \vec{T}$

Event Number	T_2 (10^9 Am/s)	T_3 (10^9 Am/s)	$\lvert\vec{T}\rvert$ (10^9 Am/s)	α (deg)
3.8	-17	4	18	78
4.1	-25	21	32	49
7.3	-4	1	4	82
13.1	-7	1	7	83

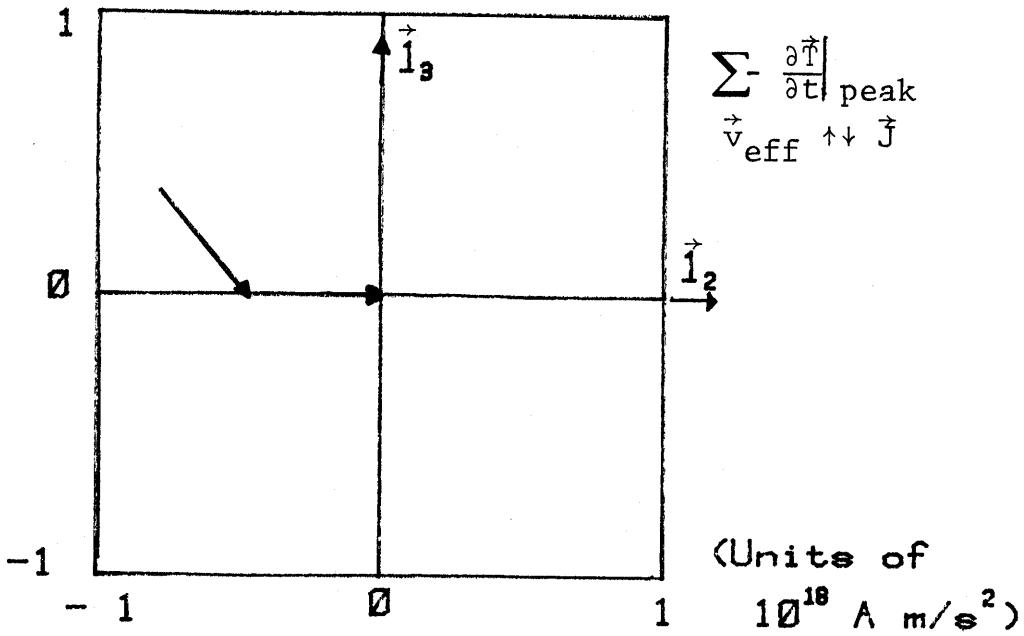

Effective reconstruction of negative streamer

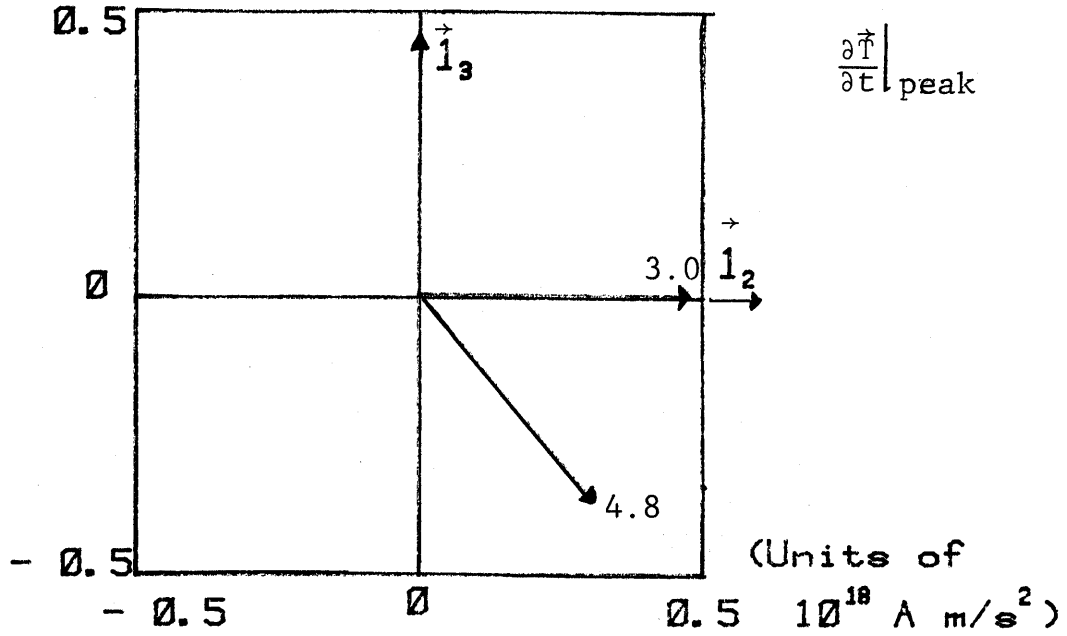

Peaks of $\partial\vec{T}/\partial t$

$\phi = 61^{o}$, $\theta = 18^{o}$, r = 307 m

Date : 79225 M. S. T. : 1246.19

Figure 6.3.7A.1 $\partial\vec{T}/\partial t$ for nearby leader (set 1)

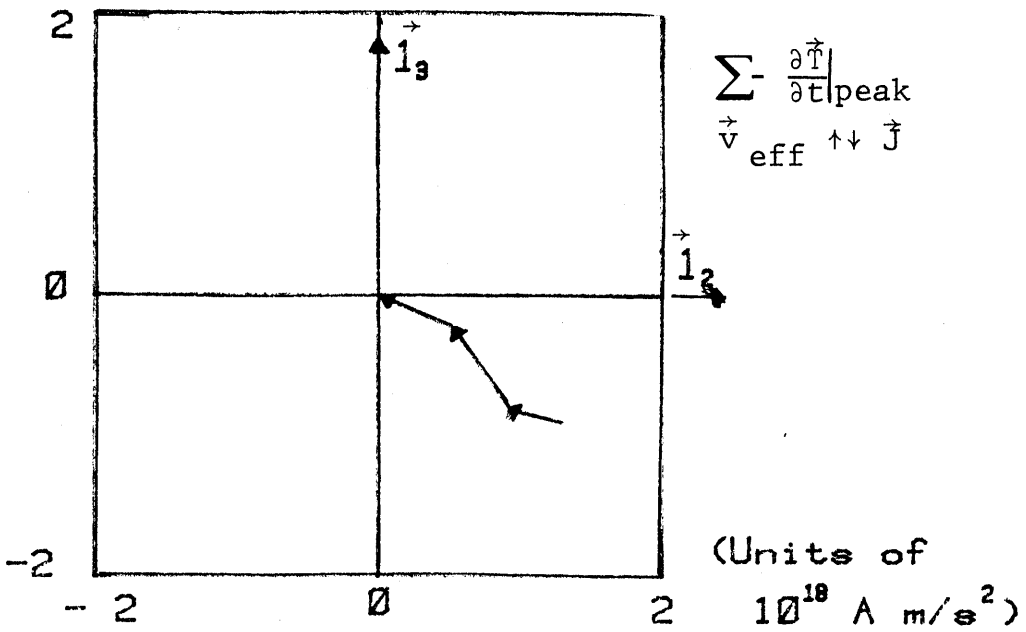

Effective reconstruction of negative streamer

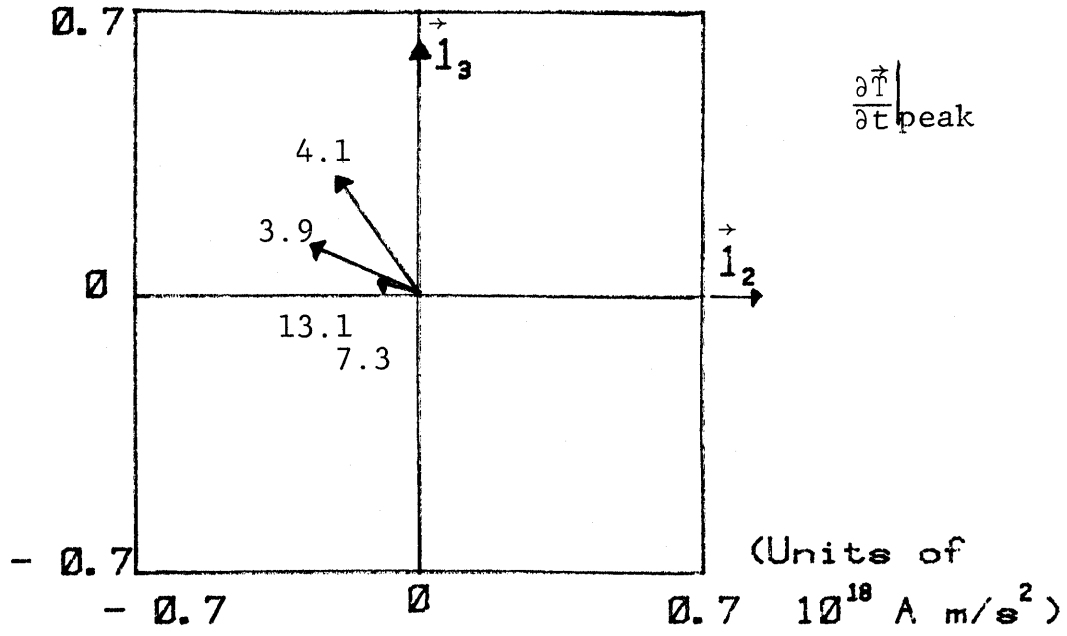

Peaks of $\partial\vec{T}/\partial t$

$\phi = 74^{\circ}$, $\theta = 50^{\circ}$, r = 124 m

Date : 79225 M. S. T. : 1246. 19

Figure 6.3.7A.2 $\partial\vec{T}/\partial t$ for nearby leader (set 2)

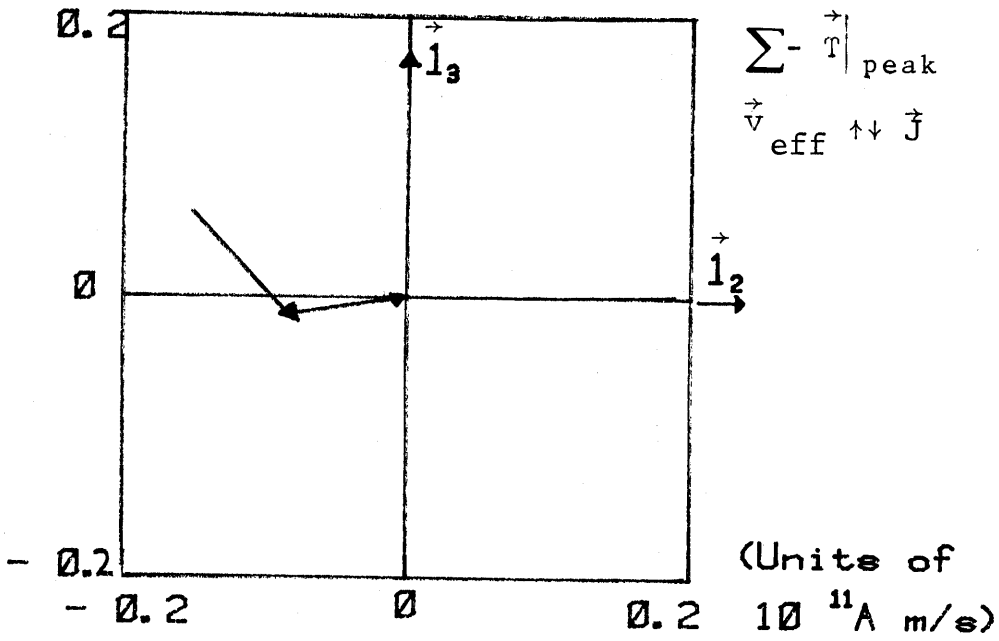

Effective reconstruction of negative streamer

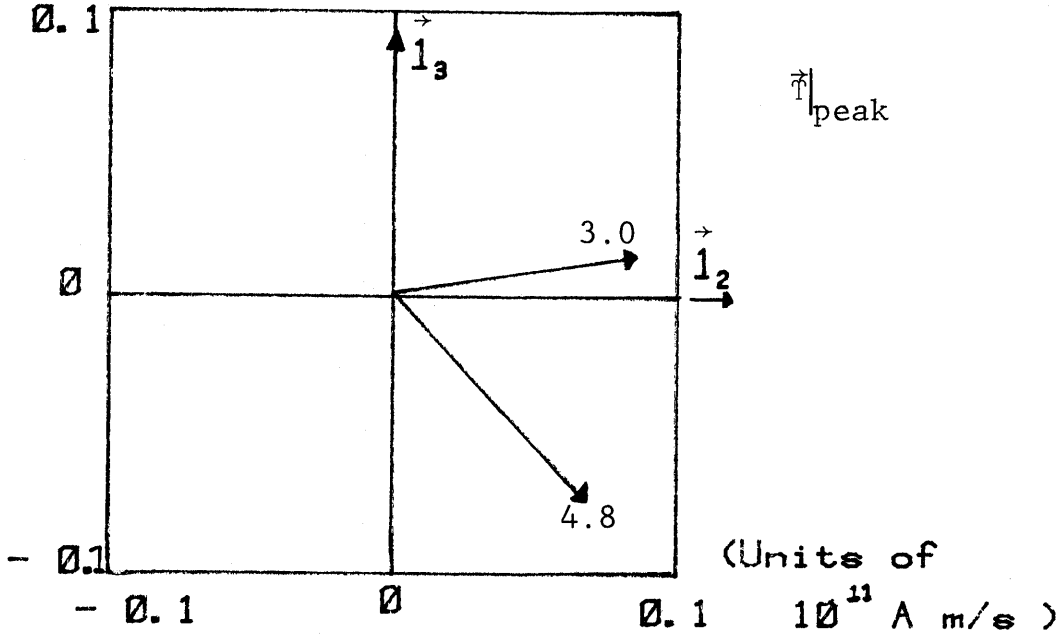

Peaks of $\hat{T}$

$\phi = 68^{o}$, $\theta = 19^{o}$, $r = 292$ m

Date : 79225 M. S. T. : 1246.19

Figure 6.3.7B.1 $\hat{T}$ for nearby leader (set 1)

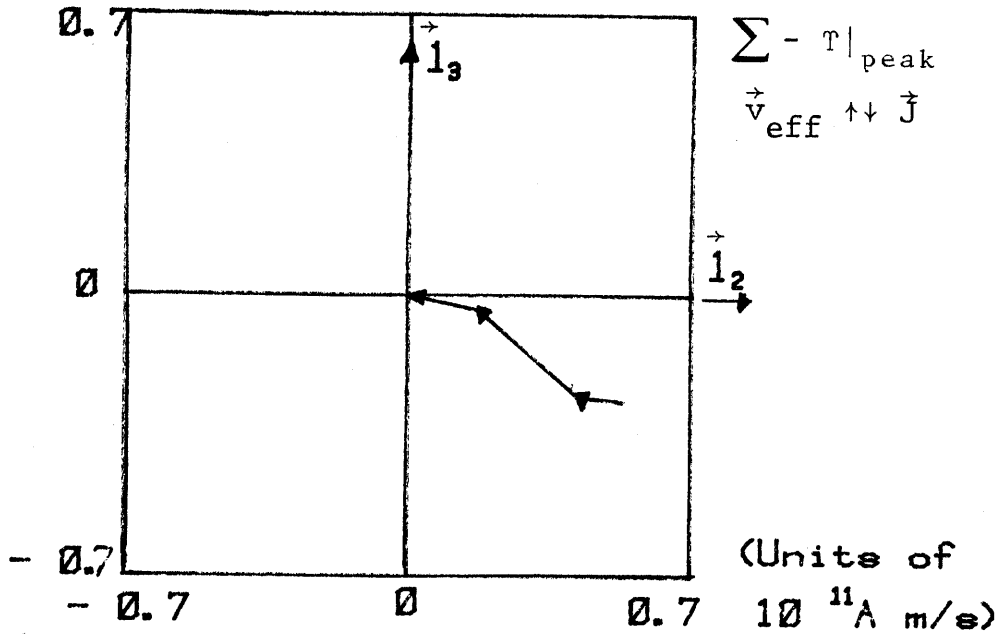

Effective reconstruction of negative streamer

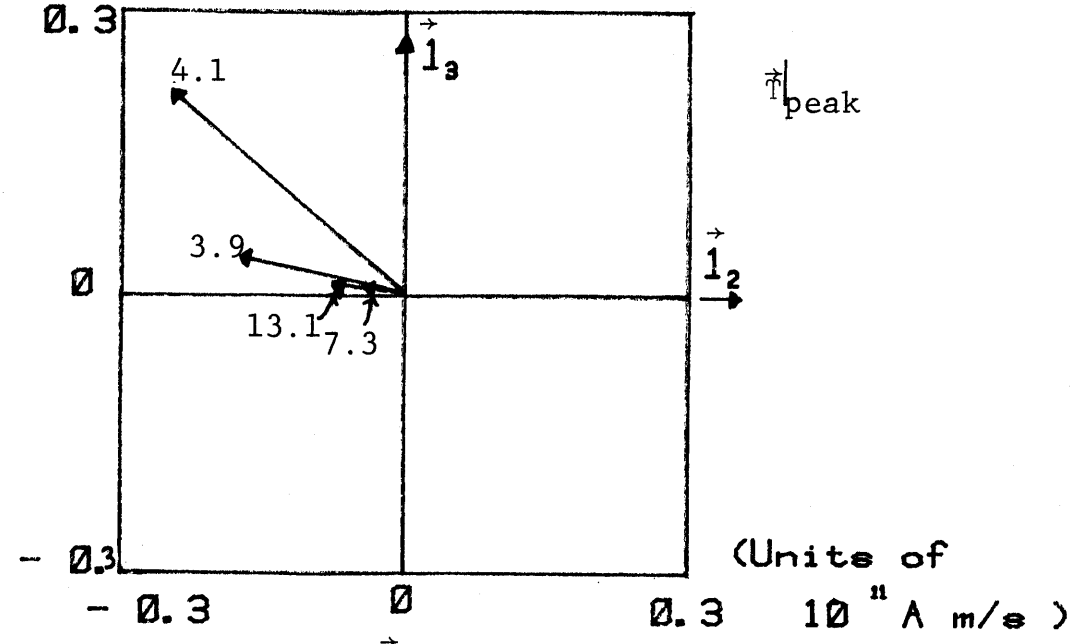

Peaks of $\hat{T}$

$\phi = 86^{\circ}$, $\theta = 53^{\circ}$, r = 119 m

Date : 79225 M.S.T.: 1246.19

Figure 6.3.7B.2 $\hat{T}$ for nearby leader (set 2)

6.4 Distant Return Stroke

Our fourth example is given in figures 6.4.•••. This is labelled "return stroke" based on the wide (1 μs) pulses as indicated in figure 6.4.1B, as well as the sustained deviation of the later-time portions of the waveform. Figures 6.4.1A and 6.4.1B show the derivative fields and fields for the 20 μs records.

Figure 6.4.3 shows the slow electric field and thunder microphone records, from which a horizontal range of 1775 m is estimated. Figure 6.4.4 gives the acoustic source reconstruction indicating two possible closures to ground. Extending from about 4 km height a little north of east of the Kiva the channel approaches the Kiva striking the ground about 2 km due east. On this is superimposed the estimated locations of the EM source, one each for the derivative waveform and the field waveform. Figures 6.4.5A and 6.4.5B show the same whole-sky videotape photograph indicating a channel to the east, in agreement with the acoustic source location.

Looking at the θ, ϕ contours for derivative data in figure 6.4.5A we find a single approximate contour intersection somewhat north of east and at a high elevation. Similar results are found from the field waveform pulses in figure 6.4.5B. These two (θ, ϕ) values are combined with the horizontal range to give the two estimates for the source location in figure 6.4.4. Note, however, that the lightning channel is not vertical and the true source location is likely to be farther to the east, and at a high elevation, unless some branching occurs back toward the west.

Figures 6.4.7A and 6.4.7B give the rough streamer reconstruction based on $\partial\vec{T}/\partial t$ and $\vec{T}$ respectively. The streamer is assumed positive, i.e., $\vec{v}_{eff} \uparrow\uparrow \vec{J}$, in keeping with the character of a return stroke. Note, however, the high elevation. This return-stroke corresponds to a large and wide current pulse in the clouds. A larger range (as is possible) would give larger $\partial\vec{T}/\partial t$ and $\vec{T}$ pulses than indicated in figures 6.4.7A and 6.5.7B.

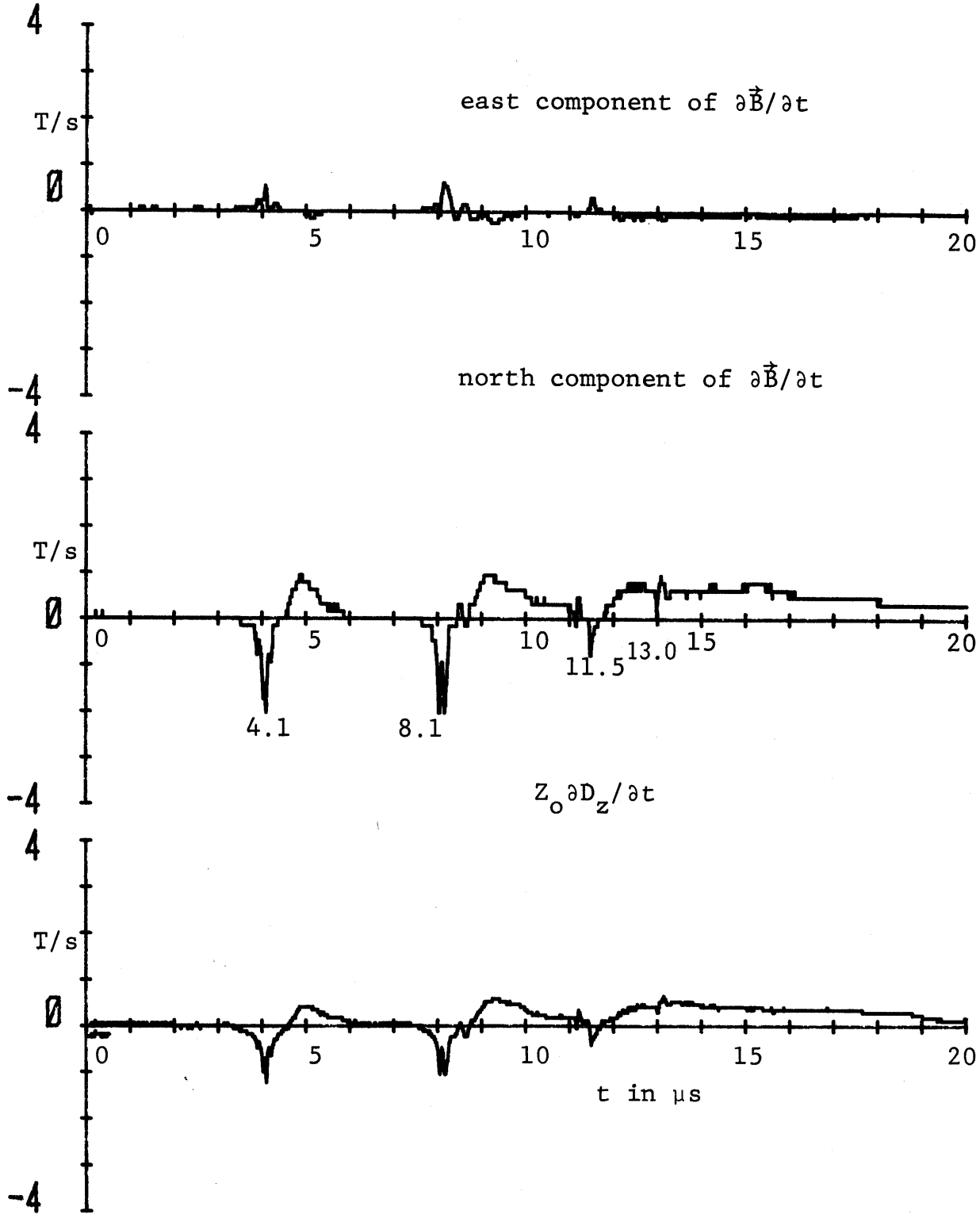

Date: 79219 M.S.T.: 1013:04

Figure 6.4.1A Derivative fields from distant return-stroke

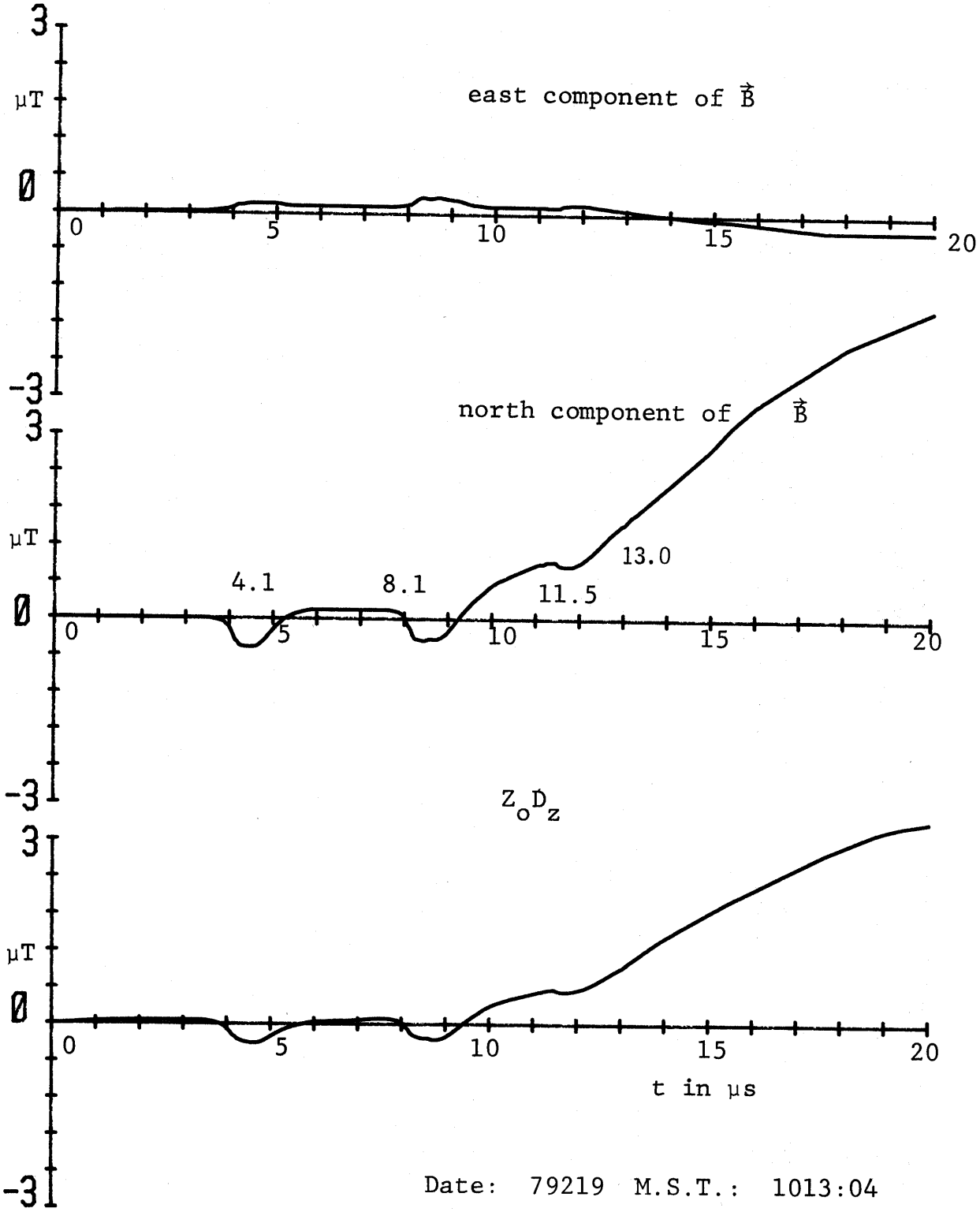

Figure 6.4.1B **Fields from distant return-stroke**

Figure 6.4.2.1 Digital data for event 4.1

[ ] = baseline which is subtracted for peaks and numerical integration

Yeardate: 79219 Time: 10:13:04 M.S.T.

Time (μs)	$\partial B_E/\partial t$ (T/s)	$\partial B_N/\partial t$ (T/s)	$Z_o \partial D_z/\partial t$ (T/s)	B_E (μT)	B_N (μT)	$Z_o D_z$ (μT)
3.81	0.000	-0.078	-0.353	0.000	0.001	-0.000
3.82	0.000	-0.078	-0.353	0.000	0.002	-0.000
3.83	0.000	-0.078	-0.353	0.000	0.002	-0.000
3.84	0.000	-0.156	-0.412	0.000	0.002	-0.001
3.85	0.000	-0.234	-0.412	0.000	0.002	-0.001
3.86	0.078	-0.156	-0.412	0.001	0.002	-0.002
3.87	0.156	-0.234	-0.471	0.002	0.001	-0.003
3.88	0.156	-0.313	-0.530	0.004	-0.001	-0.005
3.89	0.156	-0.391	-0.589	0.005	-0.003	-0.007
3.90	0.156	-0.391	-0.589	0.007	-0.005	-0.009
3.91	0.156	-0.313	-0.530	0.009	-0.007	-0.011
3.92	0.078	-0.313	-0.530	0.009	-0.009	-0.013
3.93	0.078	-0.234	-0.471	0.010	-0.009	-0.014
3.94	0.078	-0.234	-0.471	0.011	-0.010	-0.015
3.95	0.078	-0.313	-0.589	0.012	-0.012	-0.018
3.96	0.078	-0.313	-0.589	0.013	-0.013	-0.020
3.97	0.156	-0.313	-0.589	0.014	-0.015	-0.022
3.98	0.156	-0.391	-0.648	0.016	-0.017	-0.025
3.99	0.156	-0.391	-0.707	0.017	-0.020	-0.029
4.00	0.156	-0.547	-0.825	0.019	-0.023	-0.034
4.01	0.156	-0.625	-0.884	0.020	-0.028	-0.039
4.02	0.156	-0.703	-1.119	0.022	-0.034	-0.047
4.03	0.156	-0.859	-1.119	0.023	-0.041	-0.054
4.04	0.313	-0.781	-0.943	0.027	-0.047	-0.060
4.05	0.313	-0.703	-0.884	0.030	-0.052	-0.065
4.06	0.391	-0.703	-0.825	0.034	-0.058	-0.070
4.07	0.469	-0.703	-0.884	0.038	-0.063	-0.076
4.08	0.391	-0.703	-0.943	0.042	-0.069	-0.081
4.09	0.391	-0.938	-1.178	0.046	-0.077	-0.090
4.10	0.234	-1.016	-1.355	0.048	-0.085	-0.100
4.11	0.000	-0.938	-1.178	0.048	-0.093	-0.108
4.12	0.000	-0.703	-0.943	0.048	-0.099	-0.114
4.13	0.000	-0.625	-0.707	0.048	-0.103	-0.117
4.14	-0.078	-0.469	-0.648	0.048	-0.106	-0.120
4.15	-0.078	-0.391	-0.648	0.047	-0.109	-0.123
4.16	-0.078	-0.391	-0.589	0.046	-0.111	-0.126
4.17	-0.078	-0.391	-0.589	0.045	-0.113	-0.128
4.18	-0.078	-0.391	-0.648	0.045	-0.116	-0.131
4.19	0.000	-0.391	-0.707	0.045	-0.118	-0.134
4.20	0.000	-0.469	-0.766	0.045	-0.121	-0.139
4.21	0.000	-0.469	-0.766	0.045	-0.124	-0.143
4.22	0.000	-0.469	-0.707	0.045	-0.127	-0.146
4.23	0.000	-0.391	-0.648	0.045	-0.130	-0.149

Figure 6.4.2.1 Digital data for event 4.1 (continued)

Time (μs)	$\partial B_E/\partial t$ (T/s)	$\partial B_N/\partial t$ (T/s)	$Z_o \partial D_z/\partial t$ (T/s)	B_E (μT)	B_N (μT)	$Z_o D_z$ (μT)
4.24	0.000	-0.313	-0.589	0.045	-0.133	-0.155
4.25	0.000	-0.313	-0.530	0.045	-0.136	-0.160
4.26	0.078	-0.078	-0.530	0.046	-0.137	-0.165
4.27	0.078	-0.078	-0.471	0.047	-0.138	-0.170
4.28	0.078	-0.078	-0.412	0.047	-0.139	-0.174
4.29	0.078	-0.078	-0.412	0.048	-0.139	-0.178
4.30	0.078	-0.078	-0.412	0.049	-0.140	-0.183
4.31	0.078	-0.078	-0.412	0.050	-0.141	-0.187
4.32	0.078	-0.078	-0.412	0.050	-0.142	-0.191
4.33	0.078	-0.078	-0.412	0.051	-0.143	-0.195
4.34	0.078	-0.078	-0.412	0.052	-0.143	-0.199
4.35	0.000	-0.078	-0.353	0.052	-0.144	-0.203
4.36	0.000	-0.078	-0.353	0.052	-0.144	-0.203
4.37	0.000	0.000	-0.295	0.052	-0.143	-0.202
4.38	0.000	0.000	-0.295	0.052	-0.142	-0.202
4.39	0.000	0.000	-0.295	0.052	-0.142	-0.201
4.40	0.000	0.000	-0.295	0.052	-0.141	-0.201
4.41	-0.078	0.000	-0.295	0.051	-0.140	-0.200
4.42	-0.078	0.000	-0.295	0.050	-0.139	-0.199
4.43	-0.078	0.000	-0.295	0.050	-0.139	-0.199
4.44	-0.078	0.000	-0.295	0.049	-0.138	-0.198
4.45	-0.078	0.000	-0.236	0.048	-0.137	-0.197
4.46	-0.078	0.000	-0.236	0.047	-0.136	-0.196
4.47	-0.078	0.000	-0.236	0.047	-0.135	-0.195
4.48	-0.078	0.000	-0.236	0.046	-0.135	-0.194
4.49	-0.078	0.000	-0.177	0.045	-0.134	-0.192
4.50	-0.078	0.000	-0.177	0.044	-0.133	-0.190
4.51	-0.078	0.000	-0.177	0.043	-0.132	-0.188
4.52	-0.078	0.000	-0.177	0.043	-0.132	-0.187
4.53	-0.078	0.000	-0.177	0.042	-0.131	-0.185
4.54	-0.078	0.000	-0.177	0.041	-0.130	-0.183
4.55	-0.078	0.000	-0.177	0.040	-0.129	-0.181
4.56	-0.078	0.078	-0.177	0.040	-0.128	-0.180
4.57	-0.078	0.078	-0.118	0.039	-0.126	-0.177
4.58	-0.078	0.078	-0.177	0.038	-0.124	-0.175
4.59	-0.078	0.000	-0.177	0.037	-0.124	-0.174
4.60	-0.078	0.156	-0.177	0.036	-0.121	-0.172
4.61	-0.078	0.156	-0.118	0.036	-0.119	-0.170
4.62	-0.078	0.156	-0.059	0.035	-0.117	-0.167
4.63	-0.078	0.156	-0.059	0.034	-0.114	-0.164
4.64	-0.078	0.156	-0.059	0.033	-0.112	-0.161
4.65	-0.078	0.234	-0.059	0.032	-0.109	-0.158
4.66	-0.078	0.234	0.000	0.032	-0.106	-0.154
4.67	-0.078	0.234	0.000	0.031	-0.103	-0.151
4.68	-0.078	0.234	0.000	0.030	-0.100	-0.147
4.69	-0.078	0.313	0.000	0.029	-0.096	-0.144
4.70	-0.078	0.313	0.059	0.029	-0.092	-0.140
4.71	-0.078	0.313	0.059	0.028	-0.088	-0.135
4.72	-0.078	0.313	0.059	0.027	-0.084	-0.131

Figure 6.4.2.1 Digital data for event 4.1 (continued)

Time (μs)	$\partial B_E/\partial t$ (T/s)	$\partial B_N/\partial t$ (T/s)	$Z_o \partial D_z/\partial t$ (T/s)	B_E (μT)	B_N (μT)	$Z_o D_z$ (μT)
4.73	-0.078	0.313	0.059	0.026	-0.080	-0.127
4.74	-0.078	0.313	0.059	0.025	-0.076	-0.123
4.75	-0.078	0.313	0.059	0.025	-0.072	-0.119
4.76	-0.078	0.313	0.118	0.024	-0.068	-0.114
4.77	-0.078	0.313	0.059	0.023	-0.064	-0.110
4.78	-0.078	0.313	0.118	0.022	-0.060	-0.105
4.79	-0.078	0.391	0.177	0.022	-0.056	-0.100
4.80	-0.078	0.391	0.177	0.021	-0.051	-0.095
4.81	-0.078	0.391	0.177	0.020	-0.046	-0.090
4.82	-0.078	0.391	0.236	0.019	-0.042	-0.084
4.83	-0.078	0.391	0.236	0.018	-0.037	-0.078
4.84	-0.078	0.391	0.236	0.018	-0.032	-0.072
4.85	-0.078	0.391	0.236	0.017	-0.028	-0.066
4.86	-0.078	0.469	0.295	0.016	-0.022	-0.059
4.87	-0.078	0.469	0.295	0.015	-0.017	-0.053
4.88	-0.078	0.469	0.295	0.015	-0.011	-0.047
4.89	-0.078	0.469	0.295	0.014	-0.006	-0.040
4.90	-0.078	0.469	0.295	0.013	-0.000	-0.034
4.91	-0.078	0.469	0.295	0.012	0.005	-0.027
4.92	-0.078	0.469	0.295	0.011	0.011	-0.021
4.93	-0.078	0.391	0.295	0.011	0.015	-0.014
4.94	-0.078	0.391	0.295	0.010	0.020	-0.008
4.95	-0.078	0.391	0.295	0.009	0.025	-0.001
4.96	-0.156	0.391	0.295	0.007	0.029	0.005
4.97	-0.156	0.391	0.295	0.006	0.034	0.012
4.98	-0.156	0.391	0.295	0.004	0.039	0.018
4.99	-0.156	0.391	0.295	0.003	0.043	0.025
5.00	-0.156	0.391	0.295	0.001	0.048	0.031
5.01	-0.156	0.391	0.295	-0.000	0.053	0.038

Figure 6.4.2.2 Digital data for event 8.1

[ ] = baseline which is subtracted for peaks and numerical integration

Yeardate: 79219 Time: 10:13:04 M.S.T.

Time (μs)	$\partial B_E/\partial t$ (T/s)	$\partial B_N/\partial t$ (T/s)	$Z_o \partial D_z/\partial t$ (T/s)	B_E (μT)	B_N (μT)	$Z_o D_z$ (μT)
7.91	0.078	-0.234	-0.353	0.000	0.002	-0.000
7.92	0.078	-0.234	[-0.353]	0.000	0.005	-0.000
7.93	0.078	-0.234	-0.412	0.000	0.007	-0.001
7.94	0.078	-0.234	-0.412	0.000	0.009	-0.001
7.95	0.078	[-0.234]	-0.471	0.000	0.012	-0.002
7.96	0.078	-0.313	-0.471	0.000	0.013	-0.004
7.97	0.078	-0.391	-0.471	0.000	0.014	-0.005
7.98	0.078	-0.391	-0.530	0.000	0.015	-0.007
7.99	0.078	-0.469	-0.589	0.000	0.015	-0.009
8.00	0.078	-0.547	-0.648	0.000	0.014	-0.012
8.01	0.078	-0.703	-0.707	0.000	0.012	-0.015
8.02	0.078	-0.703	-0.884	0.000	0.009	-0.021
8.03	[0.078]	-1.016	-0.943	0.000	0.004	-0.027
8.04	-0.156	-1.016	-1.119	-0.002	-0.002	-0.034
8.05	-0.156	-1.016	-1.178	-0.005	-0.007	-0.042
8.06	0.078	-0.938	-1.119	-0.005	-0.012	-0.050
8.07	0.234	-0.703	-0.884	-0.003	-0.014	-0.055
8.08	0.313	-0.625	-0.707	-0.001	-0.016	-0.059
8.09	0.313	-0.469	-0.648	0.002	-0.016	-0.062
8.10	0.391	-0.469	-0.589	0.005	-0.016	-0.064
8.11	0.469	-0.469	-0.648	0.009	-0.016	-0.067
8.12	0.547	-0.547	-0.707	0.013	-0.016	-0.071
8.13	0.547	-0.625	-0.884	0.018	-0.018	-0.076
8.14	0.547	-0.703	-0.943	0.023	-0.020	-0.082
8.15	0.469	-0.859	-1.119	0.027	-0.024	-0.090
8.16	0.469	-1.016	-1.178	0.031	-0.030	-0.098
8.17	0.469	-0.938	-1.178	0.034	-0.034	-0.106
8.18	0.469	-0.938	-1.178	0.038	-0.039	-0.114
8.19	0.469	-0.781	-1.119	0.042	-0.042	-0.122
8.20	0.469	-0.703	-1.001	0.046	-0.044	-0.129
8.21	0.469	-0.703	-0.943	0.050	-0.047	-0.134
8.22	0.391	-0.625	-0.884	0.053	-0.048	-0.140
8.23	0.391	-0.469	-0.884	0.056	-0.048	-0.145
8.24	0.313	-0.391	-0.766	0.059	-0.048	-0.149
8.25	0.313	-0.313	-0.648	0.061	-0.046	-0.152
8.26	0.234	-0.078	-0.471	0.063	-0.042	-0.153
8.27	0.234	-0.078	-0.471	0.064	-0.038	-0.154
8.28	0.234	-0.078	-0.471	0.066	-0.034	-0.156
8.29	0.156	-0.078	-0.412	0.066	-0.030	-0.156
8.30	0.078	-0.078	-0.353	0.066	-0.026	-0.156
8.31	0.000	-0.078	-0.353	0.065	-0.024	-0.156
8.32	0.000	-0.078	-0.353	0.064	-0.023	-0.156
8.33	0.000	-0.078	-0.353	0.064	-0.021	-0.156
8.34	-0.078	-0.078	-0.353	0.062	-0.020	-0.156
8.35	-0.156	-0.078	-0.353	0.060	-0.018	-0.156
8.36	-0.156	-0.078	-0.353	0.057	-0.017	-0.156
8.37	-0.234	-0.078	-0.353	0.054	-0.015	-0.156

Figure 6.4.2.2 Digital data for event 8.1 (continued)

Time (μs)	$\partial B_E/\partial t$ (T/s)	$\partial B_N/\partial t$ (T/s)	$Z_o \partial D_z/\partial t$ (T/s)	B_E (μT)	B_N (μT)	$Z_o D_z$ (μT)
8.38	-0.234	-0.078	-0.353	0.051	-0.014	-0.156
8.39	-0.234	-0.078	-0.353	0.048	-0.012	-0.156
8.40	-0.234	-0.078	-0.353	0.045	-0.010	-0.156
8.41	-0.234	-0.078	-0.295	0.042	-0.009	-0.155
8.42	-0.234	-0.078	-0.295	0.039	-0.007	-0.155
8.43	-0.234	-0.078	-0.295	0.036	-0.006	-0.154
8.44	-0.234	0.000	-0.295	0.032	-0.003	-0.154
8.45	-0.234	0.000	-0.236	0.029	-0.001	-0.153
8.46	-0.156	0.000	-0.177	0.027	0.001	-0.151
8.47	-0.156	0.156	-0.177	0.025	0.005	-0.149
8.48	-0.156	0.156	-0.118	0.022	0.009	-0.147
8.49	-0.078	0.156	-0.118	0.021	0.013	-0.144
8.50	-0.078	0.156	-0.118	0.019	0.017	-0.142
8.51	-0.078	0.156	-0.059	0.018	0.021	-0.139
8.52	0.000	0.156	-0.059	0.017	0.025	-0.136
8.53	0.000	0.156	-0.059	0.016	0.029	-0.133
8.54	0.000	0.156	-0.118	0.015	0.033	-0.131
8.55	0.000	0.156	-0.118	0.014	0.036	-0.128
8.56	0.078	0.078	-0.118	0.014	0.040	-0.126
8.57	0.078	0.000	-0.177	0.014	0.042	-0.124
8.58	0.078	0.000	-0.236	0.014	0.044	-0.123
8.59	0.078	0.000	-0.236	0.014	0.047	-0.122
8.60	0.078	0.000	-0.295	0.014	0.049	-0.121
8.61	0.078	0.000	-0.353	0.014	0.051	-0.121
8.62	0.078	-0.078	-0.353	0.014	0.053	-0.121
8.63	0.078	-0.078	-0.353	0.014	0.054	-0.121
8.64	0.078	-0.078	-0.353	0.014	0.056	-0.121
8.65	0.078	-0.078	-0.353	0.014	0.057	-0.121
8.66	0.000	-0.078	-0.353	0.014	0.059	-0.121
8.67	0.000	-0.078	-0.353	0.013	0.061	-0.121
8.68	0.000	-0.078	-0.295	0.012	0.062	-0.121
8.69	-0.078	0.000	-0.295	0.011	0.064	-0.120
8.70	-0.078	0.000	-0.236	0.009	0.067	-0.119
8.71	-0.078	0.000	-0.177	0.007	0.069	-0.117
8.72	-0.156	0.000	-0.177	0.005	0.071	-0.116
8.73	-0.234	0.156	-0.118	0.002	0.075	-0.113
8.74	-0.234	0.156	-0.118	-0.001	0.079	-0.111
8.75	-0.234	0.156	-0.059	-0.004	0.083	-0.108
8.76	-0.234	0.156	-0.059	-0.007	0.087	-0.105
8.77	-0.234	0.156	0.000	-0.011	0.091	-0.101
8.78	-0.234	0.156	-0.059	-0.014	0.095	-0.098
8.79	-0.234	0.156	0.000	-0.017	0.099	-0.095
8.80	-0.234	0.156	0.000	-0.020	0.103	-0.091
8.81	-0.234	0.156	0.000	-0.023	0.107	-0.088
8.82	-0.234	0.156	0.000	-0.026	0.111	-0.084
8.83	-0.234	0.156	0.000	-0.029	0.114	-0.081
8.84	-0.234	0.156	0.000	-0.032	0.118	-0.077
8.85	-0.234	0.156	0.000	-0.035	0.122	-0.074

Figure 6.4.2.2 Digital data for event 8.1 (continued)

Time (μs)	$\partial B_E/\partial t$ (T/s)	$\partial B_N/\partial t$ (T/s)	$Z_o \partial D_z/\partial t$ (T/s)	B_E (μT)	B_N (μT)	$Z_o D_z$ (μT)
8.86	-0.234	0.234	0.059	-0.039	0.127	-0.070
8.87	-0.234	0.234	0.059	-0.042	0.132	-0.066
8.88	-0.234	0.234	0.059	-0.045	0.136	-0.061
8.89	-0.234	0.234	0.118	-0.048	0.141	-0.057
8.90	-0.234	0.234	0.118	-0.051	0.146	-0.052
8.91	-0.156	0.313	0.118	-0.053	0.151	-0.047
8.92	-0.156	0.313	0.177	-0.056	0.157	-0.042
8.93	-0.156	0.313	0.177	-0.058	0.162	-0.037
8.94	-0.156	0.313	0.177	-0.060	0.168	-0.031
8.95	-0.156	0.313	0.177	-0.063	0.173	-0.026
8.96	-0.156	0.313	0.177	-0.065	0.178	-0.021
8.97	-0.156	0.391	0.236	-0.068	0.185	-0.015
8.98	-0.156	0.391	0.236	-0.070	0.191	-0.009
8.99	-0.156	0.391	0.236	-0.072	0.197	-0.003
9.00	-0.156	0.391	0.236	-0.075	0.203	0.003

Figure 6.4.2.3 Digital data for event 11.5

[ ] = baseline which is subtracted for peaks and numerical integratio

Yeardate: 79219 Time: 10:13:04 M.S.T.

Time (μs)	$\partial B_E/\partial t$ (T/s)	$\partial B_N/\partial t$ (T/s)	$Z_o \partial D_z/\partial t$ (T/s)	B_E (μT)	B_N (μT)	$Z_o D_z$ (μT)
11.43	0.000	0.000	0.000	0.000	0.000	0.000
11.44	0.000	-0.078	-0.059	0.000	-0.001	-0.001
11.45	0.000	-0.078	-0.118	0.000	-0.002	-0.002
11.46	0.078	-0.313	-0.177	0.001	-0.005	-0.004
11.47	0.156	-0.391	-0.236	0.002	-0.009	-0.006
11.48	0.234	-0.391	-0.412	0.005	-0.013	-0.010
11.49	0.234	-0.391	-0.471	0.007	-0.016	-0.015
11.50	0.234	-0.313	-0.530	0.009	-0.020	-0.020
11.51	0.234	-0.234	-0.471	0.012	-0.022	-0.025
11.52	0.234	-0.234	-0.412	0.014	-0.024	-0.029
11.53	0.234	-0.156	-0.412	0.016	-0.026	-0.033
11.54	0.234	-0.156	-0.412	0.019	-0.027	-0.037
11.55	0.156	-0.156	-0.353	0.020	-0.029	-0.041
11.56	0.078	-0.156	-0.353	0.021	-0.030	-0.044
11.57	0.078	-0.078	-0.353	0.022	-0.031	-0.048
11.58	0.000	-0.078	-0.353	0.022	-0.032	-0.051
11.59	0.000	-0.078	-0.295	0.022	-0.033	-0.054
11.60	0.000	-0.078	-0.295	0.022	-0.034	-0.057
11.61	0.000	-0.078	-0.295	0.022	-0.034	-0.060
11.62	0.000	-0.078	-0.295	0.022	-0.035	-0.063
11.63	0.000	-0.078	-0.177	0.022	-0.036	-0.065
11.64	0.000	-0.078	-0.177	0.022	-0.037	-0.067
11.65	0.000	0.000	-0.177	0.022	-0.037	-0.068
11.66	0.000	0.000	-0.118	0.022	-0.037	-0.070
11.67	0.000	0.000	-0.177	0.022	-0.037	-0.071
11.68	0.000	0.000	-0.118	0.022	-0.037	-0.072
11.69	0.000	0.000	-0.118	0.022	-0.037	-0.074
11.70	0.000	0.000	-0.177	0.022	-0.037	-0.075
11.71	0.000	0.000	-0.118	0.022	-0.037	-0.077
11.72	-0.078	0.000	-0.118	0.021	-0.037	-0.078
11.73	-0.078	0.000	-0.059	0.020	-0.037	-0.078
11.74	-0.078	0.000	0.000	0.020	-0.037	-0.078
11.75	-0.078	0.000	-0.059	0.019	-0.037	-0.079
11.76	-0.078	0.000	-0.059	0.018	-0.037	-0.079
11.77	-0.078	0.000	-0.059	0.018	-0.037	-0.080
11.78	-0.078	0.000	-0.059	0.017	-0.037	-0.080
11.79	-0.078	0.078	-0.059	0.016	-0.036	-0.081
11.80	-0.078	0.078	0.000	0.015	-0.035	-0.081
11.81	-0.078	0.000	0.000	0.015	-0.035	-0.081
11.82	-0.078	0.000	0.000	0.014	-0.035	-0.081
11.83	-0.078	0.156	0.000	0.013	-0.034	-0.081
11.84	-0.078	0.078	0.000	0.012	-0.033	-0.081
11.85	-0.078	0.078	0.000	0.011	-0.032	-0.081
11.86	-0.078	0.156	0.000	0.011	-0.031	-0.081
11.87	-0.078	0.156	0.000	0.010	-0.029	-0.081

Figure 6.4.2.3 Digital data for event 11.5 (continued)

Time (μs)	$\partial B_E/\partial t$ (T/s)	$\partial B_N/\partial t$ (T/s)	$Z_o \partial D_z/\partial t$ (T/s)	B_E (μT)	B_N (μT)	$Z_o D_z$ (μT)
11.88	-0.078	0.156	0.000	0.009	-0.028	-0.081
11.89	-0.078	0.156	0.000	0.008	-0.026	-0.081
11.90	-0.078	0.156	0.000	0.008	-0.025	-0.081
11.91	-0.078	0.156	0.000	0.007	-0.023	-0.081
11.92	-0.078	0.156	0.000	0.006	-0.021	-0.081
11.93	-0.078	0.156	0.059	0.005	-0.020	-0.080
11.94	-0.078	0.156	0.059	0.004	-0.018	-0.080
11.95	-0.078	0.156	0.059	0.004	-0.017	-0.079
11.96	-0.078	0.156	0.059	0.003	-0.015	-0.079
11.97	-0.078	0.156	0.059	0.002	-0.014	-0.078
11.98	-0.078	0.156	0.059	0.001	-0.012	-0.077
11.99	-0.078	0.156	0.059	0.000	-0.010	-0.077
12.00	-0.078	0.156	0.059	-0.000	-0.009	-0.076
12.01	-0.078	0.234	0.059	-0.001	-0.007	-0.076
12.02	-0.078	0.234	0.059	-0.002	-0.004	-0.075
12.03	-0.156	0.234	0.059	-0.003	-0.002	-0.074
12.04	-0.156	0.234	0.059	-0.005	0.001	-0.074
12.05	-0.156	0.234	0.059	-0.007	0.003	-0.073
12.06	-0.156	0.234	0.059	-0.008	0.005	-0.073
12.07	-0.156	0.234	0.059	-0.010	0.008	-0.072
12.08	-0.156	0.234	0.059	-0.011	0.010	-0.072
12.09	-0.078	0.313	0.059	-0.012	0.013	-0.071
12.10	-0.156	0.313	0.118	-0.014	0.016	-0.070
12.11	-0.156	0.313	0.118	-0.015	0.019	-0.069
12.12	-0.234	0.313	0.177	-0.018	0.022	-0.067
12.13	-0.234	0.234	0.118	-0.020	0.025	-0.066
12.14	-0.234	0.234	0.118	-0.022	0.027	-0.064
12.15	-0.234	0.234	0.118	-0.025	0.029	-0.063
12.16	-0.234	0.234	0.118	-0.027	0.032	-0.062
12.17	-0.234	0.313	0.118	-0.029	0.035	-0.061
12.18	-0.234	0.313	0.177	-0.032	0.038	-0.059
12.19	-0.234	0.313	0.177	-0.034	0.041	-0.057
12.20	-0.234	0.313	0.177	-0.036	0.044	-0.056
12.21	-0.234	0.313	0.236	-0.039	0.047	-0.053
12.22	-0.156	0.313	0.236	-0.040	0.051	-0.051
12.23	-0.156	0.313	0.236	-0.042	0.054	-0.049
12.24	-0.156	0.313	0.236	-0.043	0.057	-0.046
12.25	-0.156	0.313	0.177	-0.045	0.060	-0.044
12.26	-0.156	0.313	0.177	-0.046	0.063	-0.043
12.27	-0.156	0.313	0.177	-0.048	0.066	-0.041
12.28	-0.156	0.313	0.177	-0.050	0.069	-0.039
12.29	-0.156	0.313	0.177	-0.051	0.072	-0.037
12.30	-0.156	0.313	0.177	-0.053	0.076	-0.036
12.31	-0.156	0.313	0.236	-0.054	0.079	-0.033
12.32	-0.156	0.313	0.236	-0.056	0.082	-0.031
12.33	-0.156	0.391	0.177	-0.057	0.086	-0.029
12.34	-0.156	0.313	0.295	-0.059	0.089	-0.026
12.35	-0.156	0.313	0.236	-0.060	0.092	-0.024

Figure 6.4.2.3 Digital data for event 11.5 (continued)

Time (μs)	$\partial B_E/\partial t$ (T/s)	$\partial B_N/\partial t$ (T/s)	$Z_o \partial D_z/\partial t$ (T/s)	B_E (μT)	B_N (μT)	$Z_o D_z$ (μT)
12.36	-0.156	0.391	0.236	-0.062	0.096	-0.021
12.37	-0.156	0.391	0.236	-0.064	0.100	-0.019
12.38	-0.156	0.313	0.295	-0.065	0.103	-0.016
12.39	-0.156	0.313	0.236	-0.067	0.106	-0.014
12.40	-0.156	0.391	0.236	-0.068	0.110	-0.011
12.41	-0.156	0.391	0.295	-0.070	0.114	-0.008
12.42	-0.156	0.391	0.295	-0.071	0.118	-0.006
12.43	-0.156	0.313	0.295	-0.073	0.121	-0.003
12.44	-0.234	0.313	0.295	-0.075	0.124	0.000

Figure 6.4.2.4 Digital data for event 13.0

[ ] = baseline which is subtracted for peaks and numerical integration

Yeardate: 79219 Time: 10:13:04 M.S.T.

Time (μs)	$\partial B_E/\partial t$ (T/s)	$\partial B_N/\partial t$ (T/s)	$Z_o \partial D_z/\partial t$ (T/s)	B_E (μT)	B_N (μT)	$Z_o D_z$ (μT)
12.93	-0.156	0.313	0.295	-0.000	-0.000	-0.000
12.94	-0.156	0.313	0.295	-0.000	-0.000	-0.000
12.95	-0.156	0.234	0.295	-0.000	-0.001	-0.000
12.96	-0.156	0.234	0.295	-0.000	-0.002	-0.000
12.97	-0.078	0.234	0.295	0.001	-0.002	-0.000
12.98	-0.078	0.000	0.295	0.002	-0.005	-0.000
12.99	-0.078	0.000	0.236	0.002	-0.009	-0.001
13.00	-0.078	0.234	0.177	0.003	-0.009	-0.002
13.01	-0.156	0.234	0.177	0.003	-0.010	-0.003
13.02	-0.156	0.313	0.177	0.003	-0.010	-0.004
13.03	-0.156	0.313	0.295	0.003	-0.010	-0.004
13.04	-0.156	0.391	0.295	0.003	-0.009	-0.004
13.05	-0.156	0.391	0.412	0.003	-0.008	-0.003
13.06	-0.156	0.391	0.412	0.003	-0.008	-0.002
13.07	-0.156	0.391	0.412	0.003	-0.007	-0.000
13.08	-0.234	0.469	0.412	0.002	-0.005	0.001
13.09	-0.234	0.391	0.412	0.001	-0.005	0.002
13.10	-0.234	0.391	0.412	0.001	-0.004	0.003
13.11	-0.234	0.391	0.471	-0.000	-0.003	0.005
13.12	-0.234	0.391	0.471	-0.001	-0.002	0.007
13.13	-0.234	0.391	0.471	-0.002	-0.001	0.008
13.14	-0.234	0.391	0.530	-0.002	-0.001	0.011
13.15	-0.234	0.391	0.530	-0.003	0.000	0.013

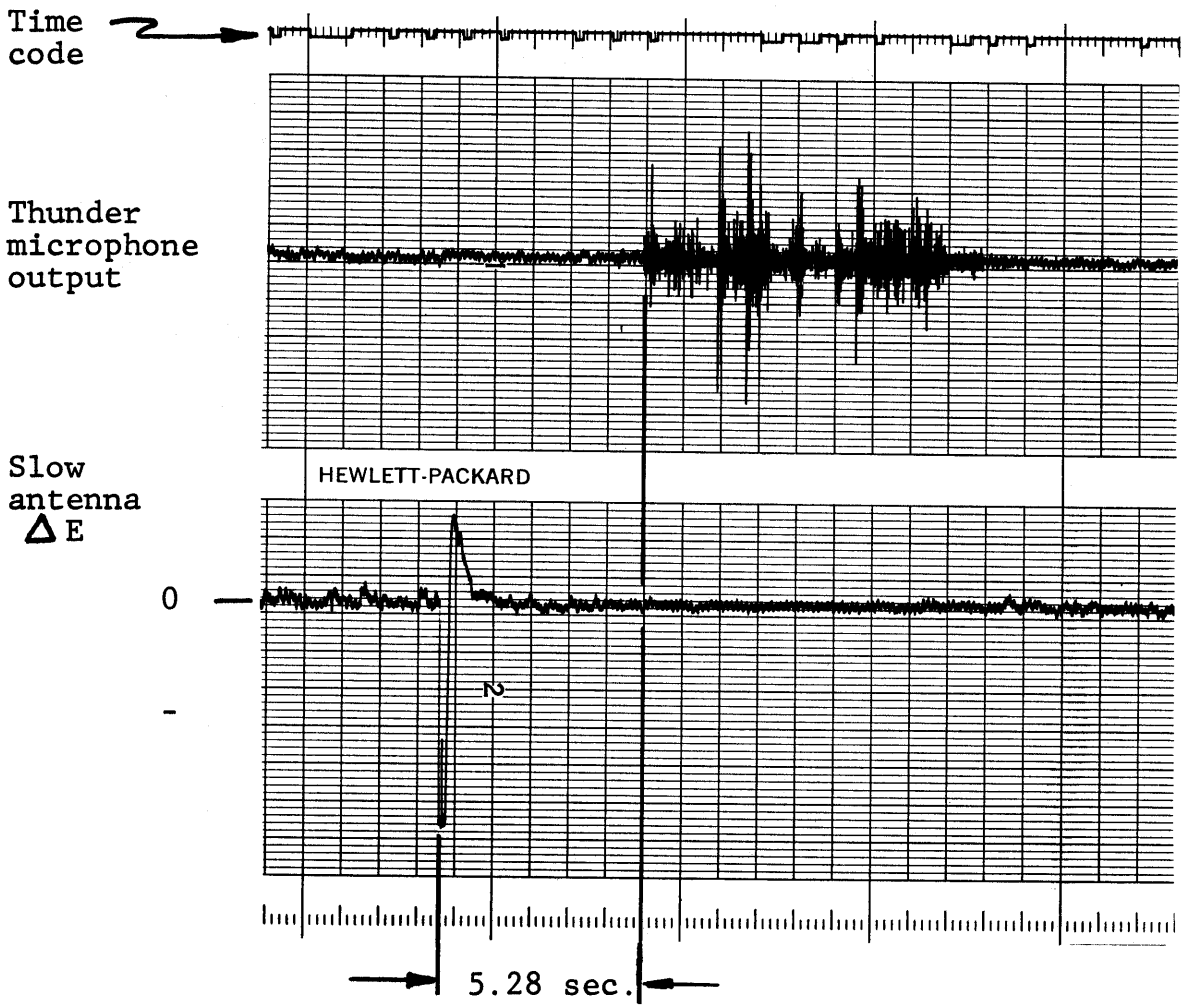

Figure 6.4.3 Slow E field change and thunder microphone record of distant return-stroke

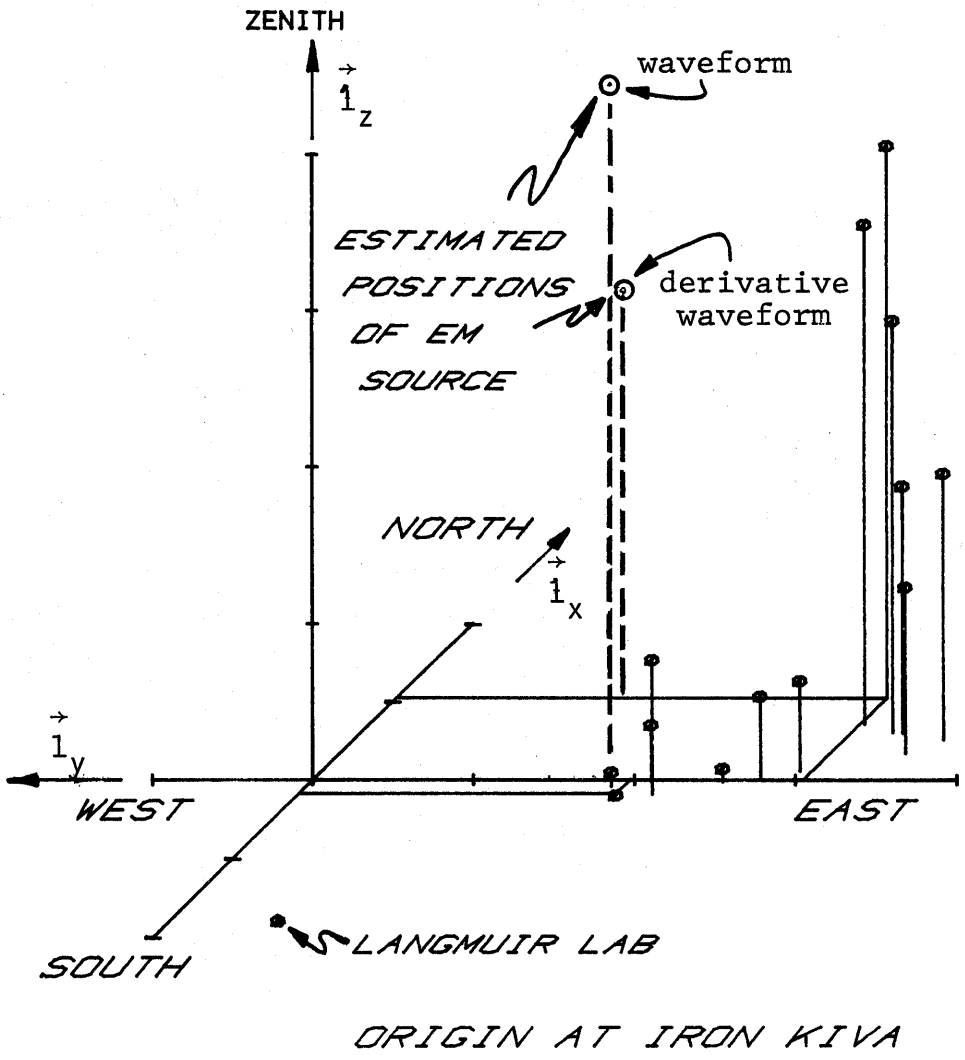

ticks on axes at 1 km intervals

Date : 79219 M.S.T. : 1013:04

Figure 6.4.4 Acoustic location of distant return stroke

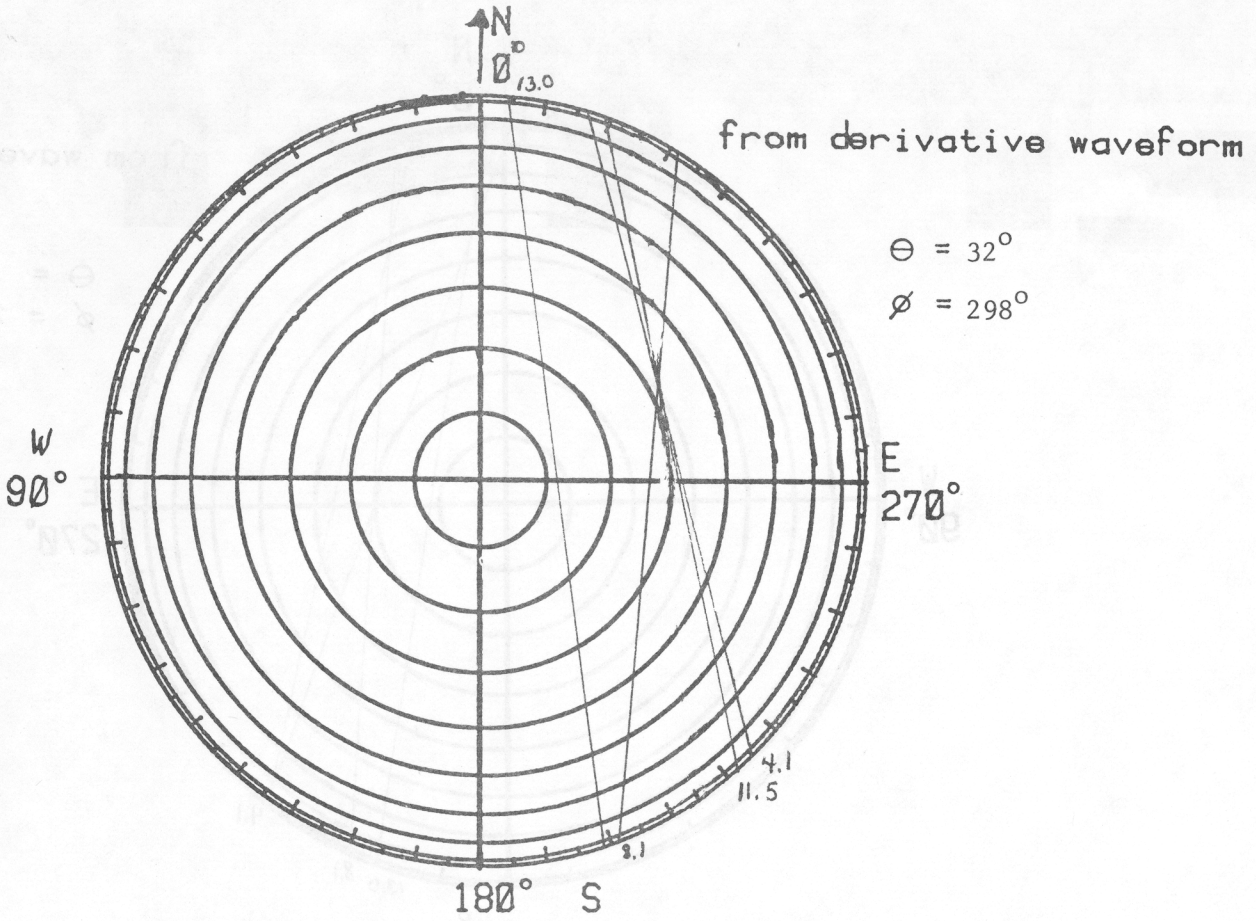

sin(θ),φ contour plot

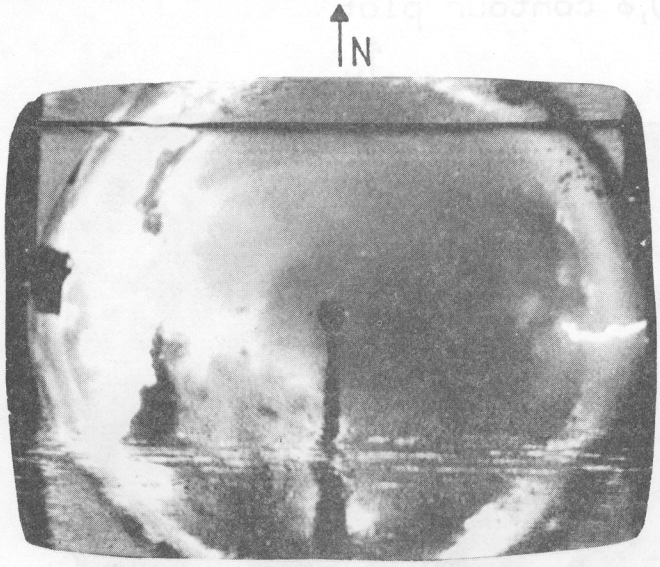

Whole-sky photograph from Kiva

Date: 79219 M.S.T.: 10:13:04

Figure 6.4.5A sin(θ),φ contours for distant return stroke derivative waveform and whole-sky videotape photograph

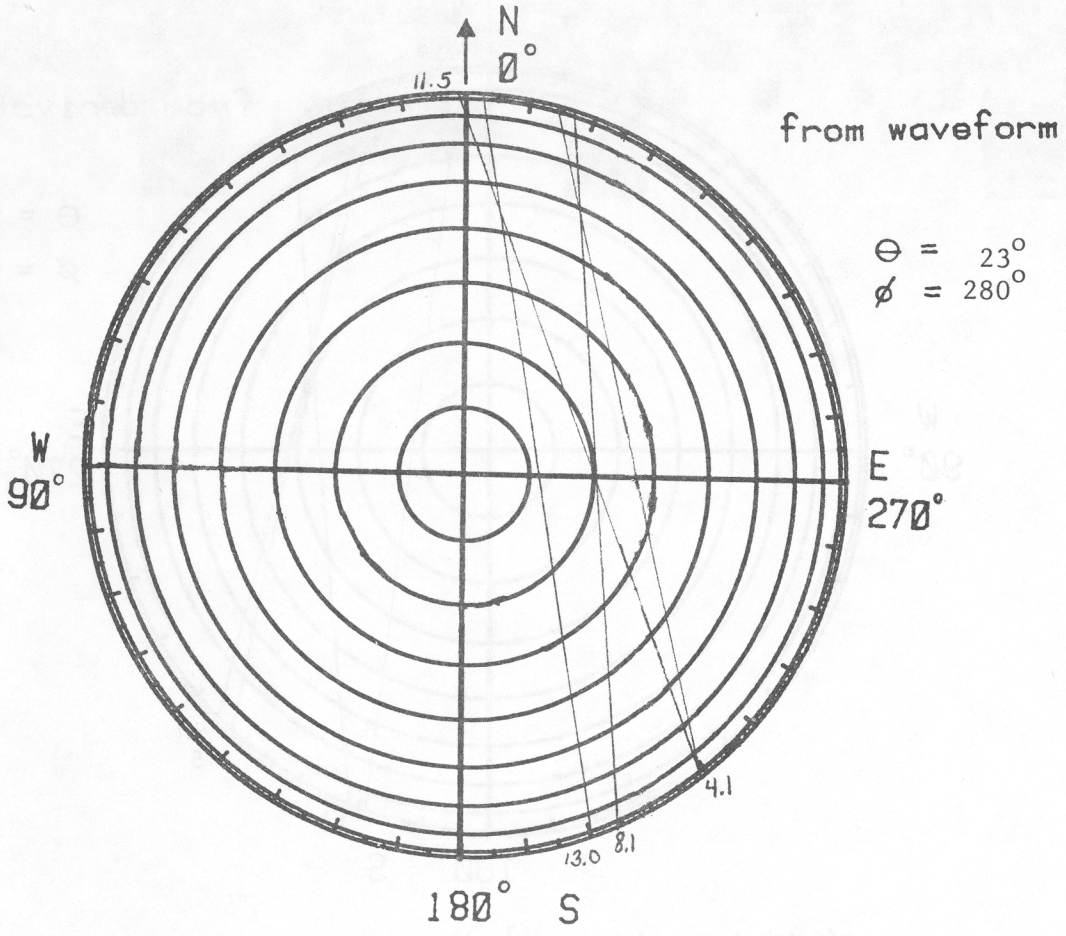

sin(θ),ϕ contour plot

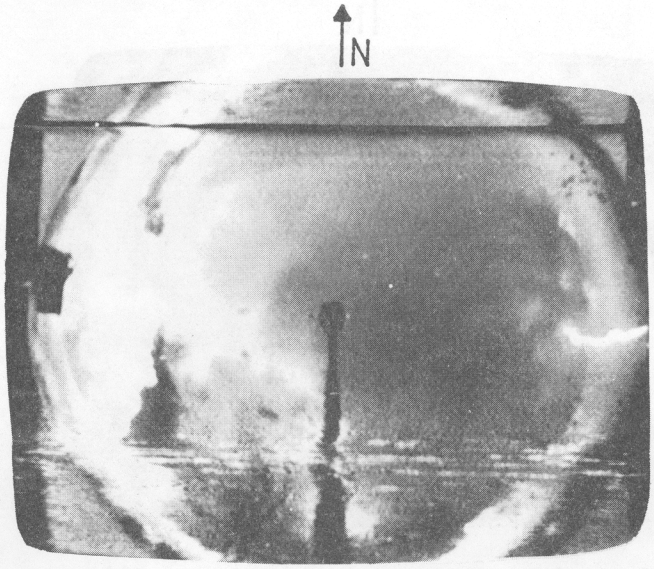

Whole-sky photograph from Kiva

Date: 79219 M.S.T.: 10:13:04

Figure 6.4.5B sin(θ),ϕ contours for distant return stroke waveform and whole-sky videotape photograph

Figure 6.4.6A Tabulation of peak values for each event from derivative waveform set for distant return stroke

Yeardate: 79219 M.S.T.: 1013.04

$\phi = 298^{\circ}$; $\theta = 32^{\circ}$; r = 3350 m

Event Number	Time (μs)	$Z_o \Delta \partial D_z/\partial t$ (T/s)	$\Delta \partial B_E/\partial t$ (T/s)	$\Delta \partial B_N/\partial t$ (T/s)	$\Delta \partial B_h/\partial t$ (T/s)	$\Delta \partial B_e/\partial t$ (T/s)	$\lvert \Delta \partial \vec{B}/\partial t \rvert$ (T/s)
4.1	4.10	-1.00	0.47	-0.94	0.02	-0.53	0.53
8.1	8.05	-0.94	0.47	-0.78	-0.03	-0.45	0.46
11.5	11.49	-0.53	0.23	-0.39	-0.01	-0.23	0.23
13.0	12.99	0.12	0.08	-0.31	0.05	-0.16	0.16

CALCULATED VALUES FOR $\partial \vec{I}/\partial t$

Event Number	$\partial T_2/\partial t$ (10^{15} Am/s^2)	$\partial T_3/\partial t$ (10^{15} Am/s^2)	$\lvert \partial \vec{I}/\partial t \rvert$ (10^{15} Am/s^2)	α (deg)
4.1	-161	5276	5279	2
8.1	289	4569	4578	356
11.5	139	2282	2286	357
13.0	-454	1559	1624	16

Figure 6.4.6B Tabulation of peak values for each event from waveform set for distant return stroke

Yeardate: 79219 M.S.T.: 1013.04

$\phi = 280^{o}$; $\theta = 23^{o}$; r = 4543 m

Event Number	Time (μs)	$Z_o \Delta D_s$ (μT)	ΔB_E (μT)	ΔB_N (μT)	ΔB_h (μT)	ΔB_e (μT)	$\lvert\Delta\vec{B}\rvert$ (μT)
4.1	4.10	-0.16	0.05	-0.13	-0.01	-0.07	0.07
8.1	8.05	-0.16	0.07	-0.05	-0.03	-0.03	0.04
11.5	11.49	-0.01	0.02	-0.04	-0.01	-0.02	0.02
13.0	13.02	-0.00	0.00	-0.01	-0.00	-0.01	0.01

CALCULATED VALUES FOR $\overleftrightarrow{1}_t \cdot \vec{T}$

Event Number	T_2 (10^9 Am/s)	T_3 (10^9 Am/s)	$\lvert\vec{T}\rvert$ (10^9 Am/s)	α (deg)
4.1	183	929	947	349
8.1	446	418	612	313
11.5	94	292	307	342
13.0	9	71	71	353

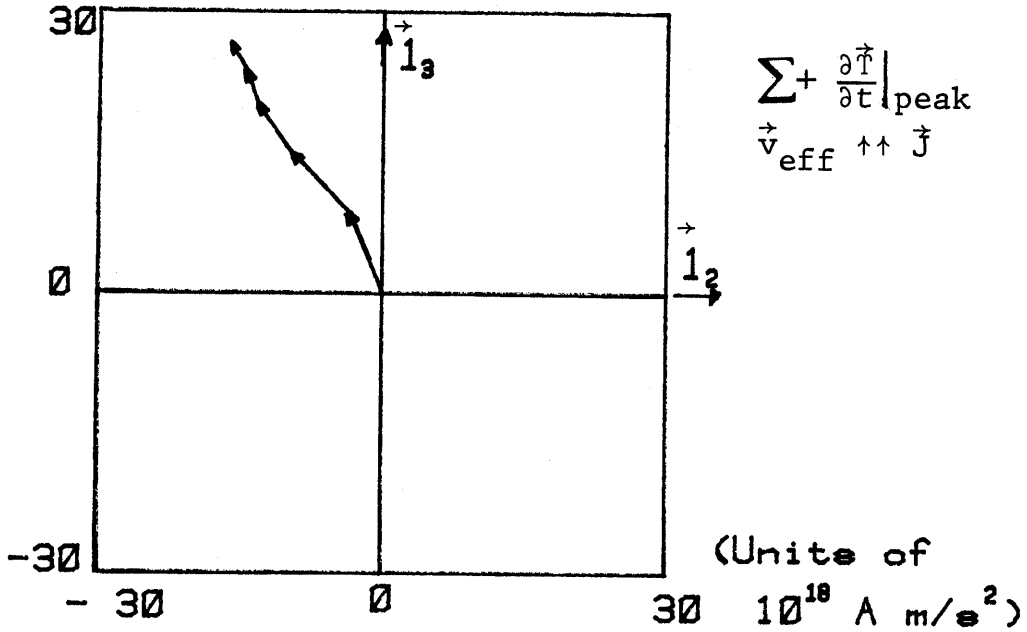

Effective reconstruction of positive streamer

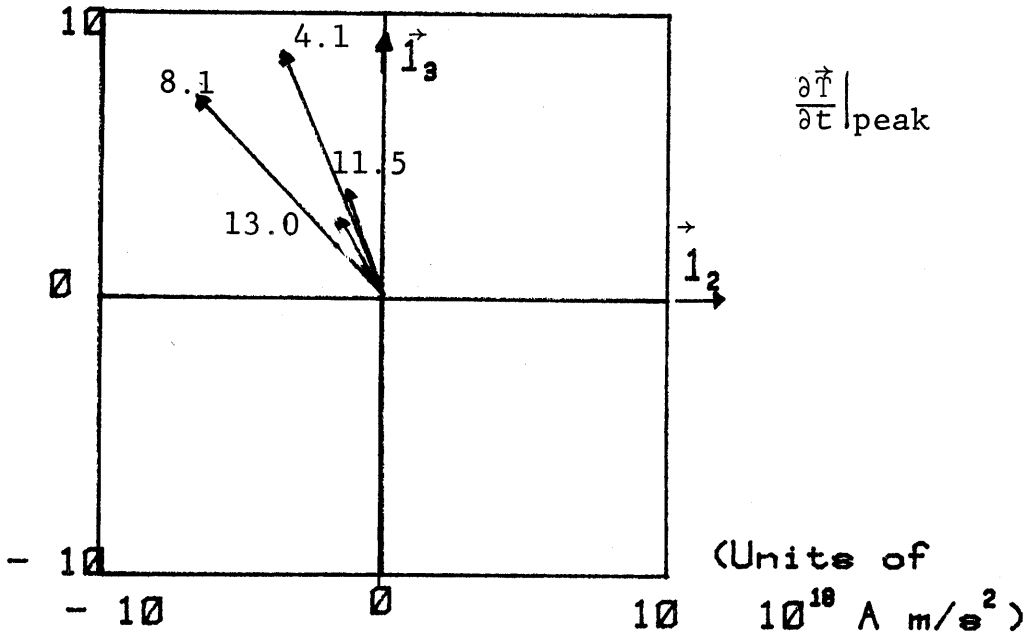

Peaks of $\partial\vec{T}/\partial t$

$\phi = 298^{\circ}$, $\theta = 32^{\circ}$, $r = 3350$ m

Date : 79219 M.S.T.: 1013.04

Figure 6.4.7A $\partial\vec{T}/\partial t$ for distant return-stroke

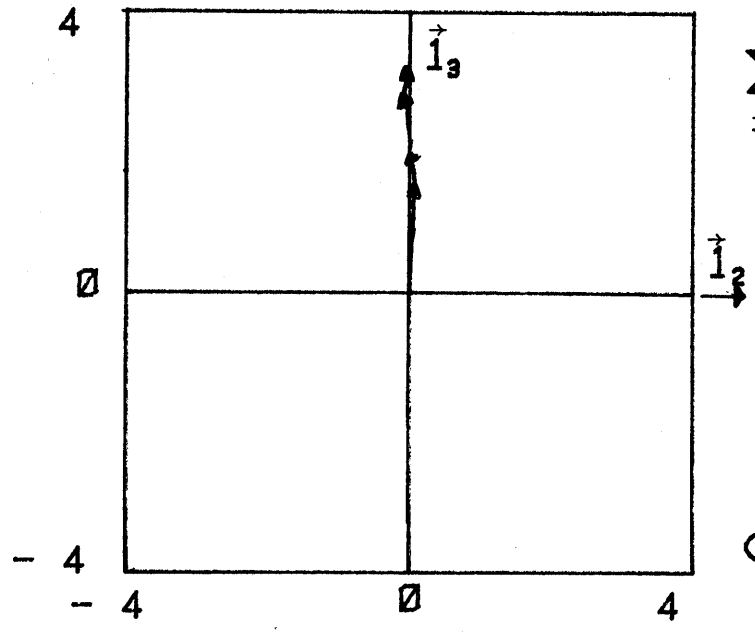

Effective reconstruction of positive streamer

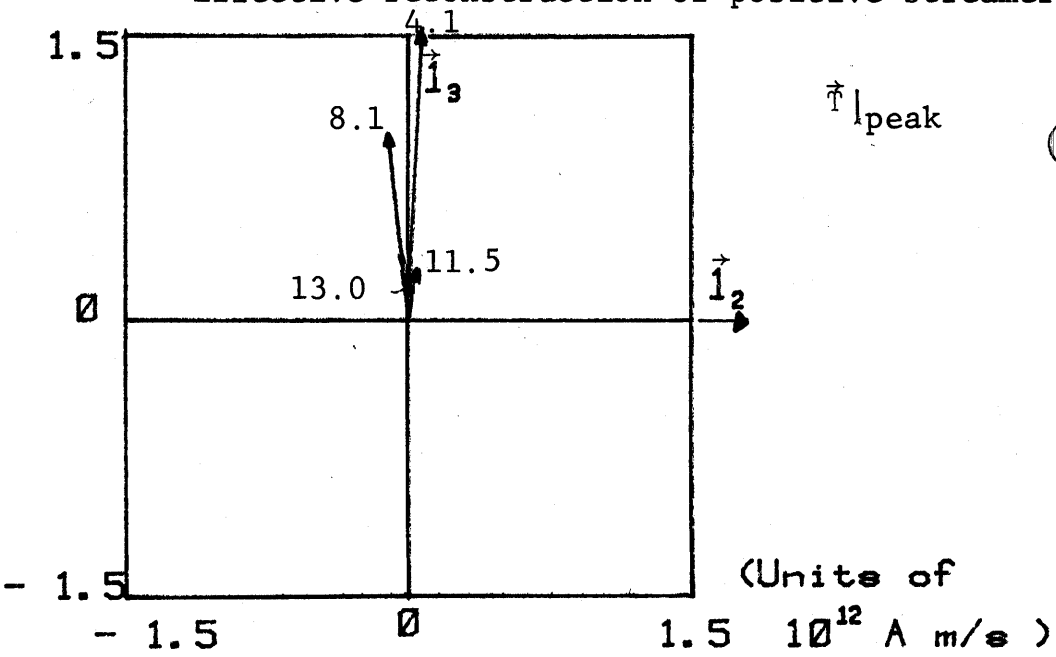

Peaks of $\vec{T}$

$\phi = 280^{o}$, $\theta = 23^{o}$, r = 4607 m

Date : 79219 M.S.T.: 1013.04

Figure 6.4.7B $\vec{T}$ for distant return-stroke

6.5 Midrange Leader(s)

Our fifth example is given in Figures 6.5.••• . This is labelled "midrange leader(s)". Figures 6.5.1A and 6.5.1B show the derivative fields and fields for the 20 μs record.

Figure 6.5.3 shows the slow electric field and thunder microphone records, from which a horizontal range of 672 m is estimated. Figure 6.5.4 gives the acoustic source reconstruction. This strike extends from about 3 km height. This can be compared to the videotape photographs showing the lightning arc reaching the ground east of the Kiva.

The θ, ϕ contours give two approximate sets of contour intersections estimated in Figures 6.5.5. Figures 6.5.7 are of significant help in noting the directions of the $\partial \vec{T} / \partial t$ pulses for each set.

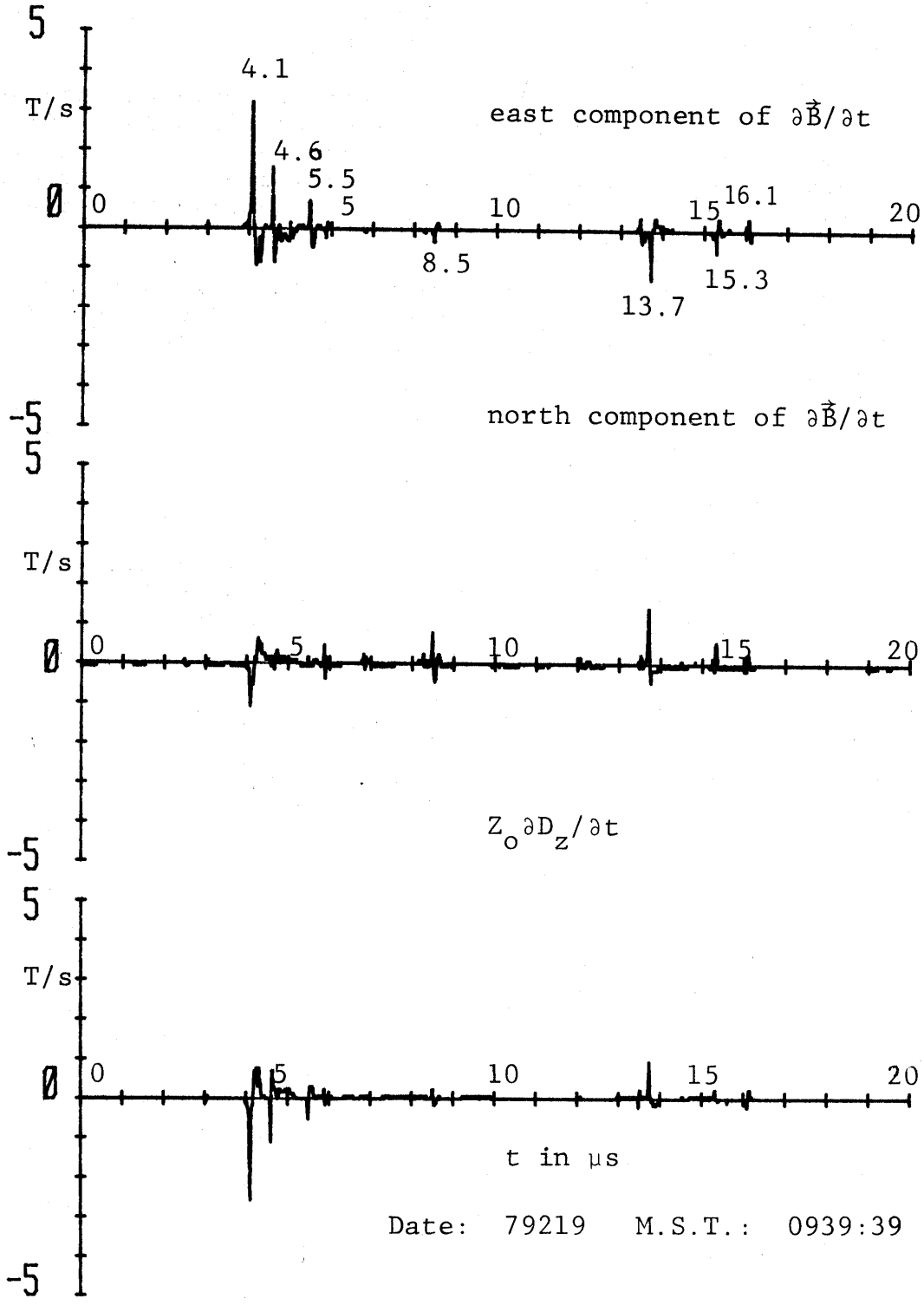

Figure 6.5.1A Derivative fields from midrange leader(s)

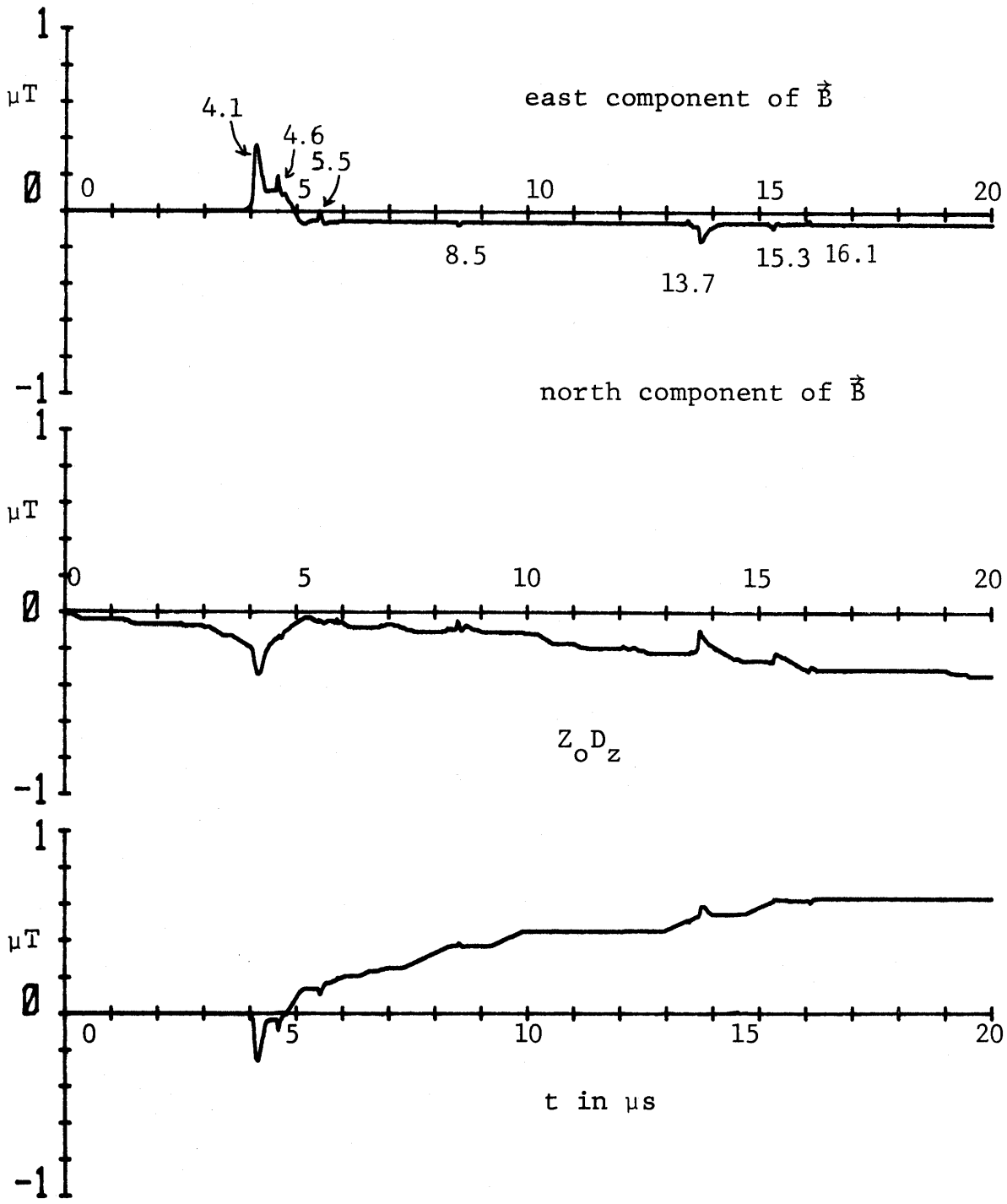

Date: 79219 M.S.T.: 0939:39

Figure 6.5.1B **Fields from midrange leader(s)**

Figure 6.5.2.1 Digital data for event 4.1

[ ] = baseline which is subtracted for peaks and numerical integrati

Yeardate: 79219 Time: 09:39:39 M.S.T.

Time (μs)	$\partial B_E/\partial t$ (T/s)	$\partial B_N/\partial t$ (T/s)	$Z_o \partial D_z/\partial t$ (T/s)	B_E (μT)	B_N (μT)	$Z_o D_z$ (μT)
3.95	0.000	0.000	0.000	0.000	0.000	0.000
3.96	0.000	0.000	0.000	0.000	0.000	0.000
3.97	0.078	0.000	-0.059	0.001	0.000	-0.001
3.98	0.078	0.000	-0.118	0.002	0.000	-0.002
3.99	0.156	0.000	-0.118	0.003	0.000	-0.003
4.00	0.234	0.000	-0.118	0.005	0.000	-0.004
4.01	0.313	0.000	-0.118	0.009	0.000	-0.005
4.02	0.313	0.000	-0.118	0.012	0.000	-0.006
4.03	0.547	-0.078	-0.236	0.017	-0.001	-0.009
4.04	1.172	-0.078	-0.236	0.029	-0.002	-0.011
4.05	2.422	-0.078	-0.295	0.053	-0.002	-0.014
4.06	3.125	-0.313	-0.353	0.084	-0.005	-0.018
4.07	3.125	-0.625	-0.648	0.116	-0.012	-0.024
4.08	2.422	-1.016	-1.355	0.140	-0.022	-0.038
4.09	1.250	-0.938	-2.297	0.152	-0.031	-0.061
4.10	0.547	-0.703	-2.592	0.158	-0.038	-0.087
4.11	0.000	-0.391	-1.885	0.158	-0.042	-0.105
4.12	0.000	-0.313	-1.355	0.158	-0.045	-0.119
4.13	-0.313	-0.391	-0.471	0.155	-0.049	-0.124
4.14	-0.391	-0.391	-0.236	0.151	-0.053	-0.126
4.15	-0.703	-0.469	-0.177	0.144	-0.058	-0.128
4.16	-1.016	-0.313	-0.177	0.134	-0.061	-0.130
4.17	-1.016	-0.078	0.000	0.123	-0.062	-0.130
4.18	-0.938	0.000	0.236	0.114	-0.062	-0.127
4.19	-0.859	0.234	0.471	0.105	-0.060	-0.122
4.20	-0.859	0.234	0.707	0.097	-0.057	-0.115
4.21	-0.859	0.234	0.707	0.088	-0.055	-0.108
4.22	-0.938	0.156	0.589	0.079	-0.053	-0.102
4.23	-0.938	0.156	0.648	0.069	-0.052	-0.096
4.24	-0.625	0.313	0.707	0.063	-0.049	-0.089
4.25	-0.313	0.547	0.766	0.060	-0.043	-0.081
4.26	-0.625	0.625	0.766	0.054	-0.037	-0.073
4.27	-0.938	0.703	0.707	0.044	-0.030	-0.066
4.28	-0.781	0.625	0.295	0.037	-0.024	-0.063
4.29	-0.703	0.625	0.471	0.030	-0.017	-0.059
4.30	-0.625	0.625	0.766	0.023	-0.011	-0.051
4.31	-0.391	0.547	0.766	0.019	-0.006	-0.043
4.32	-0.313	0.391	0.707	0.016	-0.002	-0.036
4.33	-0.078	0.469	0.471	0.016	0.003	-0.032
4.34	-0.078	0.547	0.412	0.015	0.008	-0.027
4.35	-0.078	0.547	0.353	0.014	0.014	-0.024
4.36	-0.078	0.313	0.236	0.013	0.017	-0.022
4.37	-0.078	0.313	0.059	0.012	0.020	-0.021
4.38	0.000	0.313	0.059	0.012	0.023	-0.020
4.39	0.000	0.313	0.059	0.012	0.026	-0.020
4.40	-0.078	0.313	0.059	0.012	0.029	-0.019

Figure 6.5.2.1 Digital data for event 4.1 (continued)

Time (μs)	$\partial B_E/\partial t$ (T/s)	$\partial B_N/\partial t$ (T/s)	$Z_o \partial D_z/\partial t$ (T/s)	B_E (μT)	B_N (μT)	$Z_o D_z$ (μT)
4.41	-0.078	0.313	0.059	0.011	0.032	-0.018
4.42	-0.078	0.313	0.059	0.010	0.035	-0.018
4.43	-0.078	0.313	0.059	0.010	0.038	-0.017
4.44	-0.078	0.234	0.059	0.009	0.041	-0.017
4.45	-0.078	0.234	0.059	0.008	0.043	-0.016
4.46	-0.078	0.156	0.000	0.007	0.045	-0.016
4.47	-0.078	0.156	0.000	0.007	0.046	-0.016
4.48	-0.078	0.234	0.000	0.006	0.049	-0.016
4.49	-0.078	0.234	0.000	0.005	0.051	-0.016
4.50	-0.078	0.234	0.000	0.004	0.053	-0.016
4.51	-0.078	0.234	0.000	0.003	0.056	-0.016
4.52	-0.078	0.234	0.000	0.003	0.058	-0.016

Figure 6.5.2.2 Digital data for event 4.6

[ ] = baseline which is subtracted for peaks and numerical integration

Yeardate: 79219 Time: 09:39:39 M.S.T.

Time (μs)	$\partial B_E/\partial t$ (T/s)	$\partial B_N/\partial t$ (T/s)	$Z_o \partial D_z/\partial t$ (T/s)	B_E (μT)	B_N (μT)	$Z_o D_z$ (μT)
4.52	-0.078	0.234	0.000	-0.000	0.000	0.000
4.53	[-0.078]	0.234	0.000	-0.000	0.000	0.000
4.54	0.000	0.234	0.000	0.001	0.000	0.000
4.55	1.172	[0.234]	0.000	0.013	0.000	0.000
4.56	1.484	0.156	0.000	0.029	-0.001	0.000
4.57	0.625	0.078	[0.000]	0.036	-0.002	0.000
4.58	0.234	0.000	-0.412	0.039	-0.005	-0.004
4.59	-0.703	0.156	-0.943	0.033	-0.005	-0.014
4.60	-0.938	0.234	-1.119	0.024	-0.005	-0.025
4.61	-0.938	0.234	-0.412	0.016	-0.005	-0.029
4.62	-0.703	0.234	0.471	0.009	-0.005	-0.024
4.63	-0.703	0.234	0.707	0.003	-0.005	-0.017
4.64	-0.625	0.000	0.707	-0.002	-0.008	-0.010
4.65	-0.391	0.000	0.471	-0.005	-0.010	-0.005
4.66	-0.391	-0.078	0.295	-0.009	-0.013	-0.002
4.67	-0.313	-0.078	0.295	-0.011	-0.016	0.001
4.68	-0.078	0.000	0.236	-0.011	-0.019	0.003
4.69	-0.078	0.234	0.236	-0.011	-0.019	0.005
4.70	-0.078	0.313	0.236	-0.011	-0.018	0.007
4.71	0.000	0.313	0.236	-0.010	-0.017	0.010
4.72	0.000	0.391	0.177	-0.009	-0.016	0.011
4.73	0.000	0.391	0.118	-0.009	-0.014	0.013
4.74	-0.078	0.313	0.059	-0.009	-0.014	0.013
4.75	-0.313	0.313	0.000	-0.011	-0.013	0.013
4.76	-0.391	0.234	0.000	-0.014	-0.013	0.013

Figure 6.5.2.3 Digital data for event 5.5

[ ] = baseline which is subtracted for peaks and numerical integration

Yeardate: 79219 Time: 09:39:39 M.S.T.

Time (μs)	$\partial B_E/\partial t$ (T/s)	$\partial B_N/\partial t$ (T/s)	$Z_o \partial D_z/\partial t$ (T/s)	B_E (μT)	B_N (μT)	$Z_o D_z$ (μT)
5.41	-0.078	0.000	0.000	-0.000	0.000	0.000
5.42	-0.078	0.000	0.000	-0.000	0.000	0.000
5.43	0.000	0.000	0.000	0.001	0.000	0.000
5.44	0.234	0.000	0.000	0.004	0.000	0.000
5.45	0.547	0.000	0.000	0.010	0.000	0.000
5.46	0.625	0.000	0.000	0.017	0.000	0.000
5.47	0.547	0.234	0.000	0.023	0.002	0.000
5.48	0.000	0.234	-0.236	0.024	0.005	-0.002
5.49	-0.078	0.234	-0.471	0.024	0.007	-0.007
5.50	-0.391	0.000	-0.530	0.021	0.007	-0.012
5.51	-0.547	0.000	-0.236	0.016	0.007	-0.015
5.52	-0.547	0.000	0.000	0.012	0.007	-0.015
5.53	-0.547	0.000	0.236	0.007	0.007	-0.012
5.54	-0.547	0.000	0.295	0.002	0.007	-0.009
5.55	-0.469	0.000	0.295	-0.002	0.007	-0.006
5.56	-0.469	0.000	0.295	-0.005	0.007	-0.004
5.57	-0.313	0.000	0.295	-0.008	0.007	-0.001
5.58	-0.313	0.000	0.295	-0.010	0.007	0.002
5.59	-0.078	0.000	0.295	-0.010	0.007	0.005
5.60	-0.078	0.000	0.295	-0.010	0.007	0.008
5.61	-0.078	0.156	0.236	-0.010	0.009	0.010
5.62	-0.078	0.156	0.236	-0.010	0.010	0.013
5.63	0.000	0.156	0.118	-0.009	0.012	0.014
5.64	0.000	0.156	0.059	-0.008	0.013	0.014
5.65	0.000	0.156	0.059	-0.008	0.015	0.015
5.66	0.000	0.156	0.059	-0.007	0.016	0.016
5.67	0.000	0.156	0.059	-0.006	0.018	0.016
5.68	0.000	0.156	0.000	-0.005	0.020	0.016
5.69	0.000	0.156	0.000	-0.005	0.021	0.016
5.70	0.000	0.078	0.000	-0.004	0.022	0.016
5.71	-0.078	0.078	0.000	-0.004	0.023	0.016

Figure 6.5.2.4 Digital data for event 8.5

[ ] = baseline which is subtracted for peaks and numerical integration

Yeardate: 79219 Time: 09:39:39 M.S.T.

Time (μs)	$\partial B_E/\partial t$ (T/s)	$\partial B_N/\partial t$ (T/s)	$Z_o \partial D_z/\partial t$ (T/s)	B_E (μT)	B_N (μT)	$Z_o D_z$ (μT)
8.39	-0.078	0.000	0.000	-0.000	0.000	0.000
8.40	-0.078	0.000	0.000	-0.000	0.000	0.000
8.41	-0.078	0.078	0.000	-0.000	0.001	0.000
8.42	-0.078	0.156	0.000	-0.000	0.002	0.000
8.43	-0.078	0.156	0.000	-0.000	0.004	0.000
8.44	-0.078	0.156	0.000	-0.000	0.005	0.000
8.45	-0.078	0.156	0.000	-0.000	0.007	0.000
8.46	-0.313	0.313	0.000	-0.002	0.010	0.000
8.47	-0.391	0.547	0.000	-0.005	0.016	0.000
8.48	-0.391	0.859	0.059	-0.009	0.024	0.001
8.49	-0.078	0.625	0.059	-0.009	0.030	0.001
8.50	-0.078	0.000	0.236	-0.009	0.030	0.004
8.51	0.000	-0.078	0.236	-0.008	0.030	0.006
8.52	0.000	-0.313	0.059	-0.007	0.027	0.006
8.53	0.000	-0.313	0.000	-0.006	0.023	0.006
8.54	0.078	-0.391	-0.177	-0.005	0.020	0.005
8.55	0.078	-0.313	-0.177	-0.003	0.016	0.003
8.56	0.078	-0.313	-0.118	-0.002	0.013	0.002
8.57	0.000	-0.078	-0.118	-0.001	0.013	0.001
8.58	0.000	0.000	-0.118	-0.000	0.013	-0.001

Figure 6.5.2.5 Digital data for event 13.7

[ ] = baseline which is subtracted for peaks and numerical integration

Yeardate: 79219 Time: 09:39:39 M.S.T.

Time (μs)	$\partial B_E/\partial t$ (T/s)	$\partial B_N/\partial t$ (T/s)	$Z_o \partial D_z/\partial t$ (T/s)	B_E (μT)	B_N (μT)	$Z_o D_z$ (μT)
13.57	-0.078	0.000	0.059	-0.000	0.000	-0.000
13.58	-0.078	0.000	0.059	-0.000	0.000	-0.000
13.59	-0.078	0.078	0.059	-0.000	0.001	-0.000
13.60	-0.078	0.156	0.059	-0.000	0.002	-0.000
13.61	-0.078	0.156	0.059	-0.000	0.004	-0.000
13.62	-0.078	0.156	0.059	-0.000	0.005	-0.000
13.63	-0.078	0.156	0.059	-0.000	0.007	-0.000
13.64	-0.078	0.156	0.059	-0.000	0.009	-0.000
13.65	-0.078	0.234	0.059	-0.000	0.011	-0.000
13.66	-0.156	0.234	0.059	-0.001	0.013	-0.000
13.67	-0.234	0.313	0.059	-0.002	0.016	-0.000
13.68	-0.391	0.547	0.059	-0.005	0.022	-0.000
13.69	-0.625	1.172	0.059	-0.011	0.034	-0.000
13.70	-1.250	1.484	0.059	-0.023	0.048	-0.000
13.71	-1.328	1.484	0.177	-0.035	0.063	0.001
13.72	-0.703	0.625	0.295	-0.041	0.070	0.004
13.73	-0.078	0.234	0.530	-0.041	0.072	0.008
13.74	-0.078	0.000	0.943	-0.041	0.072	0.017
13.75	0.000	-0.313	0.530	-0.041	0.069	0.022
13.76	0.000	-0.391	0.059	-0.040	0.065	0.022
13.77	0.000	-0.313	0.059	-0.039	0.062	0.022
13.78	0.000	-0.078	0.000	-0.038	0.061	0.021
13.79	0.234	-0.078	-0.059	-0.035	0.060	0.020
13.80	0.234	-0.078	0.000	-0.032	0.060	0.020
13.81	0.234	-0.078	0.000	-0.029	0.059	0.019
13.82	0.234	-0.078	0.000	-0.026	0.058	0.018
13.83	0.234	-0.078	-0.118	-0.023	0.057	0.017
13.84	0.078	-0.078	-0.118	-0.021	0.056	0.015
13.85	0.078	-0.078	-0.177	-0.020	0.056	0.013
13.86	0.078	-0.078	-0.177	-0.018	0.055	0.010
13.87	0.078	-0.078	-0.177	-0.017	0.054	0.008
13.88	0.078	-0.078	-0.177	-0.015	0.053	0.005
13.89	0.078	-0.078	-0.177	-0.013	0.053	0.003
13.90	0.078	-0.078	-0.177	-0.012	0.052	0.001
13.91	0.078	-0.078	-0.177	-0.010	0.051	-0.002
13.92	0.078	-0.078	-0.118	-0.009	0.050	-0.003
13.93	0.078	0.000	-0.118	-0.007	0.050	-0.005
13.94	0.000	0.000	-0.118	-0.006	0.050	-0.007
13.95	0.000	0.000	-0.118	-0.006	0.050	-0.009
13.96	0.000	0.000	-0.118	-0.005	0.050	-0.010
13.97	0.000	0.000	-0.059	-0.004	0.050	-0.012
13.98	0.000	0.000	-0.059	-0.003	0.050	-0.013
13.99	0.000	0.000	0.000	-0.003	0.050	-0.013
14.00	0.000	0.000	0.000	-0.002	0.050	-0.014
14.01	0.000	0.000	0.000	-0.001	0.050	-0.015
14.02	0.000	0.000	0.000	-0.000	0.050	-0.015

Figure 6.5.2.6 Digital data for event 15.3

[ ] = baseline which is subtracted for peaks and numerical integration

Yeardate: 79219 Time: 09:39:39 M.S.T.

Time (μs)	$\partial B_E/\partial t$ (T/s)	$\partial B_N/\partial t$ (T/s)	$Z_o \partial D_z/\partial t$ (T/s)	B_E (μT)	B_N (μT)	$Z_o D_z$ (μT)
15.21	-0.156	0.000	0.059	-0.000	0.000	-0.000
15.22	-0.156	0.000	0.059	-0.000	0.000	-0.000
15.23	-0.156	0.000	0.059	-0.000	0.000	-0.000
15.24	-0.156	0.234	0.059	-0.000	0.002	-0.000
15.25	-0.078	0.234	0.059	0.001	0.005	-0.000
15.26	-0.078	0.234	0.059	0.002	0.007	-0.000
15.27	-0.313	0.000	0.059	-0.000	0.007	-0.000
15.28	-0.625	-0.078	0.059	-0.005	0.006	-0.000
15.29	-0.078	-0.078	0.059	-0.004	0.005	-0.000
15.30	-0.078	0.234	0.059	-0.003	0.008	-0.000
15.31	0.000	0.547	0.236	-0.002	0.013	0.002
15.32	0.234	0.625	0.236	0.002	0.020	0.004
15.33	0.234	0.625	0.059	0.006	0.026	0.004
15.34	0.234	0.547	0.000	0.010	0.031	0.003
15.35	0.234	0.313	0.000	0.014	0.034	0.002
15.36	0.000	0.234	0.000	0.016	0.037	0.002
15.37	0.000	0.000	0.000	0.017	0.037	0.001
15.38	0.000	0.000	-0.059	0.019	0.037	-0.000

Figure 6.5.2.7 Digital data for event 16.1

[ ] = baseline which is subtracted for peaks and numerical integration

Yeardate: 79219 Time: 09:39:39 M.S.T.

Time (μs)	$\partial B_E/\partial t$ (T/s)	$\partial B_N/\partial t$ (T/s)	$Z_o \partial D_z/\partial t$ (T/s)	B_E (μT)	B_N (μT)	$Z_o D_z$ (μT)
16.02	-0.078	0.000	0.000	-0.000	0.000	0.000
16.03	-0.078	0.000	0.000	-0.000	0.000	0.000
16.04	0.000	-0.078	0.000	0.001	-0.001	0.000
16.05	0.234	-0.078	0.000	0.004	-0.002	0.000
16.06	0.234	-0.078	0.000	0.007	-0.002	0.000
16.07	0.000	0.234	0.000	0.008	0.000	0.000
16.08	-0.078	0.313	-0.177	0.008	0.003	-0.002
16.09	-0.313	0.313	-0.236	0.005	0.006	-0.004
16.10	-0.313	0.313	-0.177	0.003	0.009	-0.006
16.11	-0.313	0.313	0.000	0.001	0.013	-0.006
16.12	-0.313	0.234	0.059	-0.002	0.015	-0.005
16 13	-0.078	0.156	0.236	-0.002	0.016	-0.003
16.14	-0.078	0.078	0.236	-0.002	0.017	-0.001
16.15	-0.078	0.000	0.236	-0.002	0.017	0.002

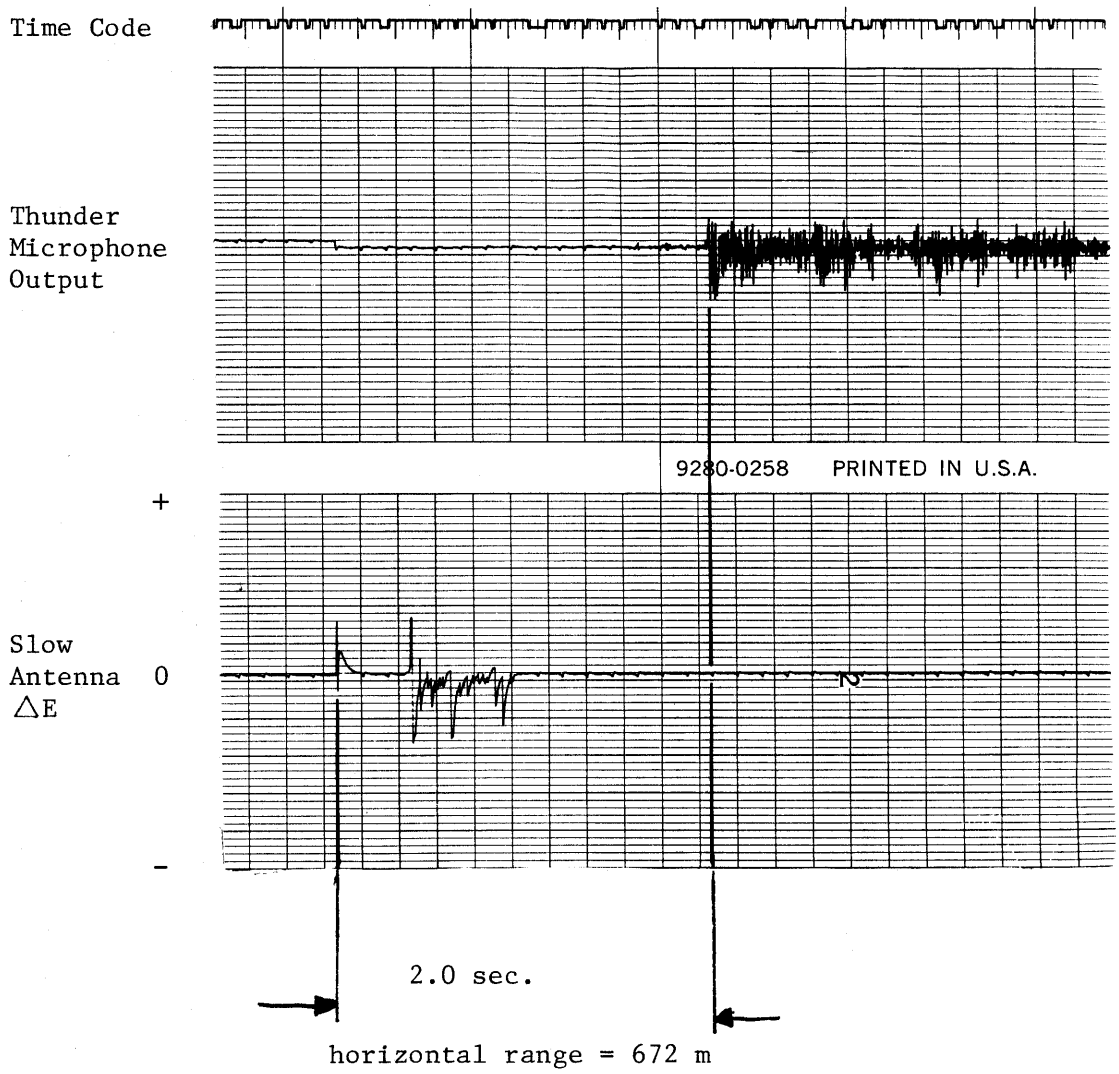

Figure 6.5.3 Slow E field change and thunder microphone record of midrange leader

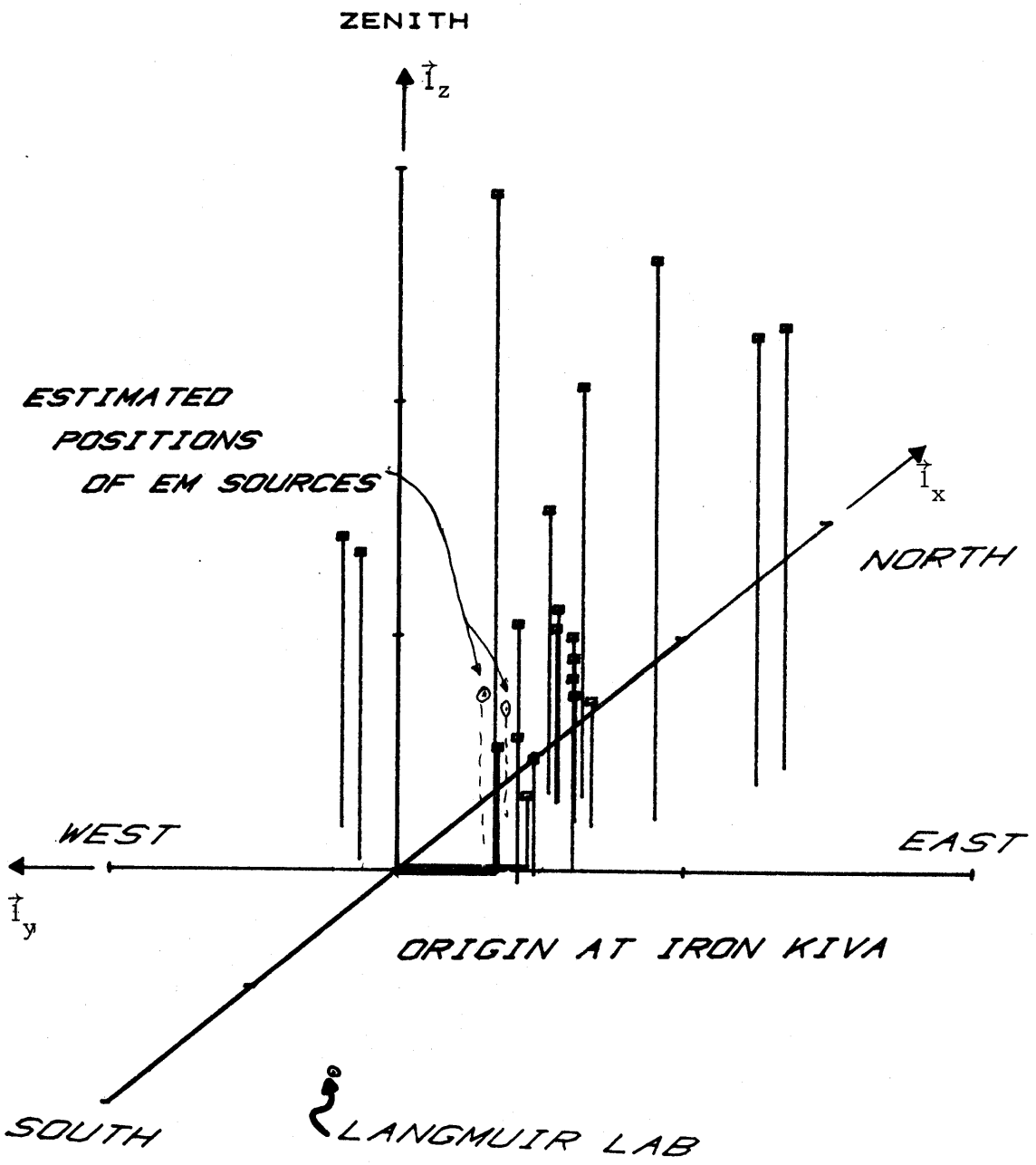

ticks on axes at 1 km intervals

Date : 79219 Time : 09:39:39

Figure 6.5.4 Acoustic location of midrange leader(s)

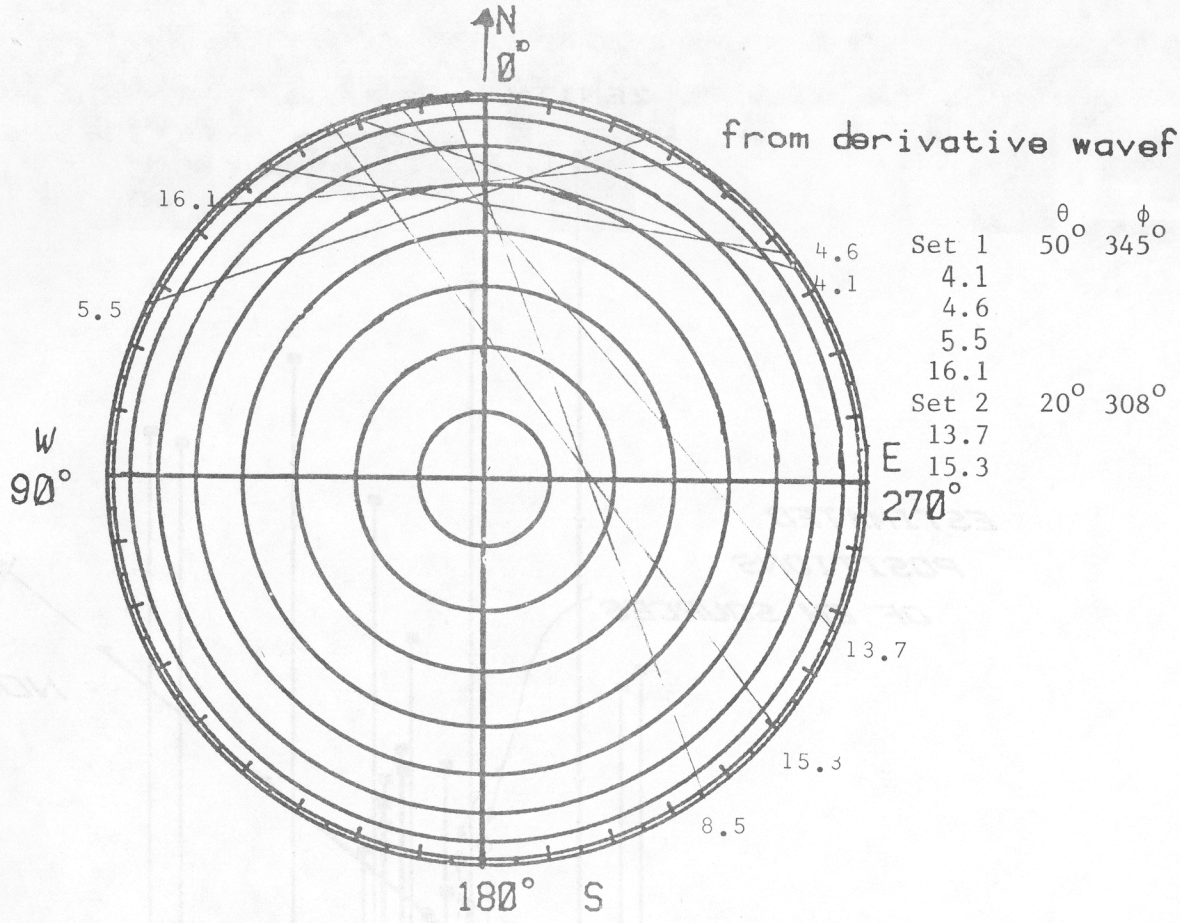

sin(θ),φ contour plot

N

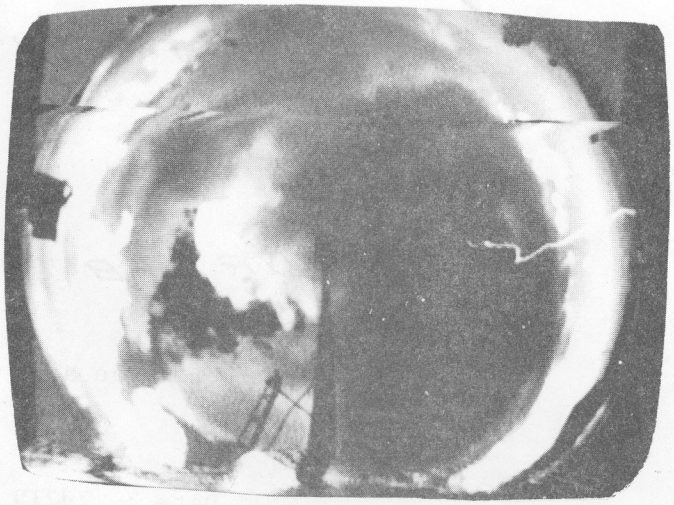

Whole-sky photograph from Kiva

Date: 79219 M.S.T.: 09:39:39

Figure 6.5.5A sin(θ),φ contours for midrange leader derivative waveform and whole-sky videotape photograph

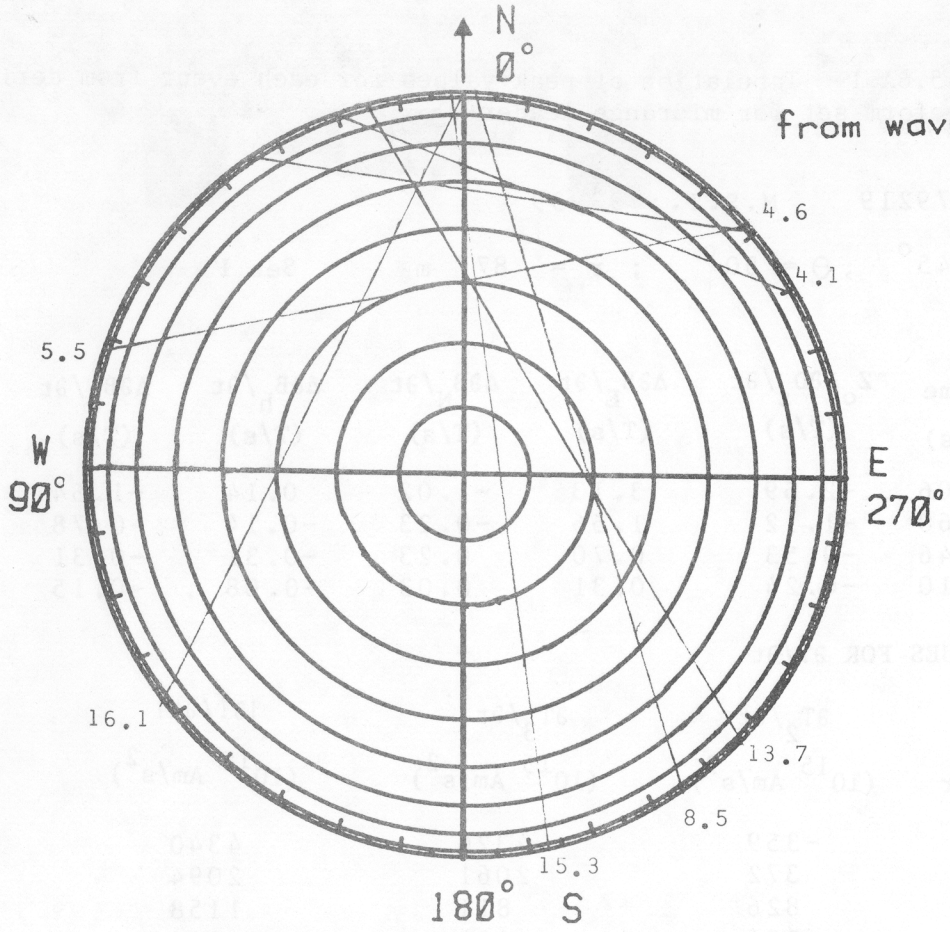

sin(θ),φ contour plot

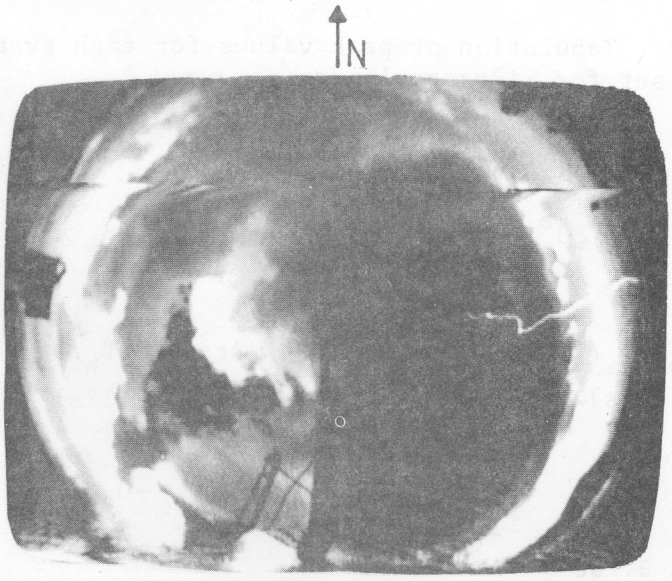

Whole-sky photograph from Kiva

Date: 79219 M.S.T.: 09:39:39

Figure 6.5.5B sin(θ),φ contours for midrange leader waveform and whole-sky videotape photograph

Figure 6.5.6A.1 Tabulation of peak values for each event from derivative waveform set for midrange leader(s)

Yeardate: 79219 M.S.T.: 93939

$\phi = 345^\circ$; $\theta = 50^\circ$; r = 877 m Set 1

Event Number	Time (μs)	$Z_o \Delta\partial D_z/\partial t$ (T/s)	$\Delta\partial B_E/\partial t$ (T/s)	$\Delta\partial B_N/\partial t$ (T/s)	$\Delta\partial B_h/\partial t$ (T/s)	$\Delta\partial B_e/\partial t$ (T/s)	$\lvert\Delta\partial\vec{B}/\partial t\rvert$ (T/s)
4.1	4.06	-2.59	3.13	-1.02	0.14	-1.64	1.65
4.6	4.60	-1.12	1.56	-0.23	-0.14	-0.78	0.80
5.5	5.46	-0.53	0.70	0.23	-0.31	-0.31	0.44
16.1	16.10	-0.24	0.31	0.03	-0.08	-0.15	0.17

CALCULATED VALUES FOR $\partial\vec{T}/\partial t$

Event Number	$\partial T_2/\partial t$ (10^{15} Am/s^2)	$\partial T_3/\partial t$ (10^{15} Am/s^2)	$\lvert\partial\vec{T}/\partial t\rvert$ (10^{15} Am/s^2)	α (deg)
4.1	-359	4326	4340	5
4.6	372	2061	2094	350
5.5	826	811	1158	314
16.1	224	384	444	330

Figure 6.5.6A.2 Tabulation of peak values for each event from derivative waveform set for midrange leader(s)

Yeardate: 79219 M.S.T.: 93939

$\phi = 308^\circ$; $\theta = 20^\circ$; r = 1965 m Set 2

Event Number	Time (μs)	$Z_o \Delta\partial D_z/\partial t$ (T/s)	$\Delta\partial B_E/\partial t$ (T/s)	$\Delta\partial B_N/\partial t$ (T/s)	$\Delta\partial B_h/\partial t$ (T/s)	$\Delta\partial B_e/\partial t$ (T/s)	$\lvert\Delta\partial\vec{B}/\partial t\rvert$ (T/s)
13.7	13.70	0.88	-1.25	1.48	0.04	0.97	0.97
15.3	15.32	0.18	-0.47	0.63	-0.01	0.39	0.39

CALCULATED VALUES FOR $\partial\vec{T}/\partial t$

Event Number	$\partial T_2/\partial t$ (10^{15} Am/s^2)	$\partial T_3/\partial t$ (10^{15} Am/s^2)	$\lvert\partial\vec{T}/\partial t\rvert$ (10^{15} Am/s^2)	α (deg)
13.7	-232	-5705	5710	178
15.3	55	-2316	2317	181

Figure 6.5.6B.1 Tabulation of peak values for each event from waveform set for midrange leader(s)

Yeardate: 79219 M.S.T.: 93939

$\phi = 338^\circ$; $\theta = 50^\circ$; r = 877 m Set 1

Event Number	Time (μs)	$Z_o \Delta D_z$ (μT)	ΔB_E (μT)	ΔB_N (μT)	ΔB_h (μT)	ΔB_e (μT)	$\lvert\Delta\vec{B}\rvert$ (μT)
4.1	4.07	-0.13	0.16	-0.06	-0.00	-0.09	0.09
4.6	4.58	-0.03	0.04	-0.01	-0.00	-0.02	0.02
5.5	5.48	-0.01	0.02	0.01	-0.01	-0.01	0.01
16.1	16.10	-0.01	0.01	0.02	-0.02	-0.00	0.02

CALCULATED VALUES FOR $\vec{I}_t . \hat{T}$

Event Number	T_2 (10^9 Am/s)	T_3 (10^9 Am/s)	$\lvert\vec{T}\rvert$ (10^9 Am/s)	α (deg)
4.1	9	225	225	358
4.6	12	54	55	348
5.5	34	19	39	300
16.1	46	2	46	273

Figure 6.5.6B.2 Tabulation of peak values for each event from waveform set for midrange leader(s)

Yeardate: 79219 M.S.T.: 93939

$\phi = 358^\circ$; $\theta = 30^\circ$; r =1344 m Set 2

Event Number	Time (μs)	$Z_o \Delta D_z$ (μT)	ΔB_E (μT)	ΔB_N (μT)	ΔB_h (μT)	ΔB_e (μT)	$\lvert\Delta\vec{B}\rvert$ (μT)
13.7	13.73	0.02	-0.04	0.07	-0.04	0.02	0.04
15.3	15.32	0.00	-0.01	0.04	-0.02	0.01	0.02

CALCULATED VALUES FOR $\vec{I}_t . \hat{T}$

Event Number	T_2 (10^9 Am/s)	T_3 (10^9 Am/s)	$\lvert\vec{T}\rvert$ (10^9 Am/s)	α (deg)
13.7	160	-86	181	242
15.3	92	-23	95	256

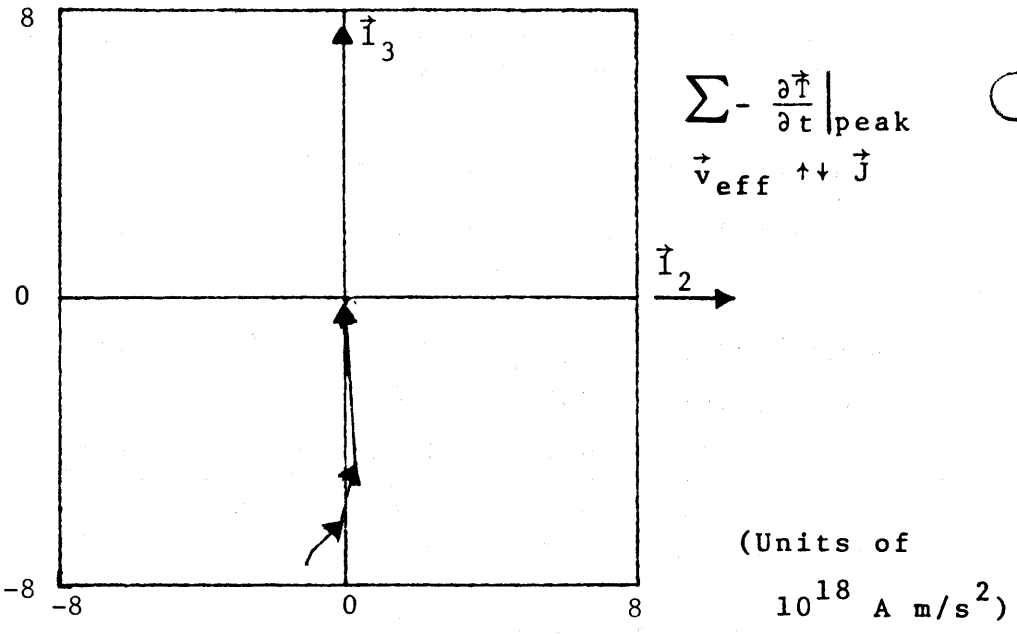

Effective reconstruction of negative streamer

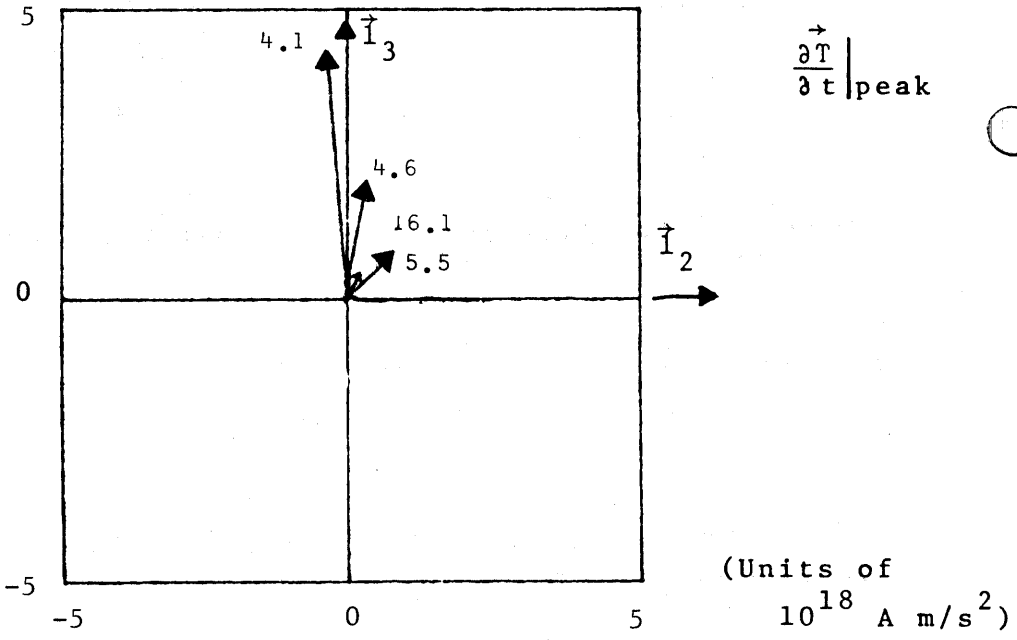

Peaks of $\partial\vec{T}/\partial t$

$\phi = 345^o$ $\theta = 50^o$ r = 877 m Set 1

Date: 79219 M.S.T.: 09:39:39

Figure 6.5.7A.1 $\partial\vec{T}/\partial t$ for midrange leader

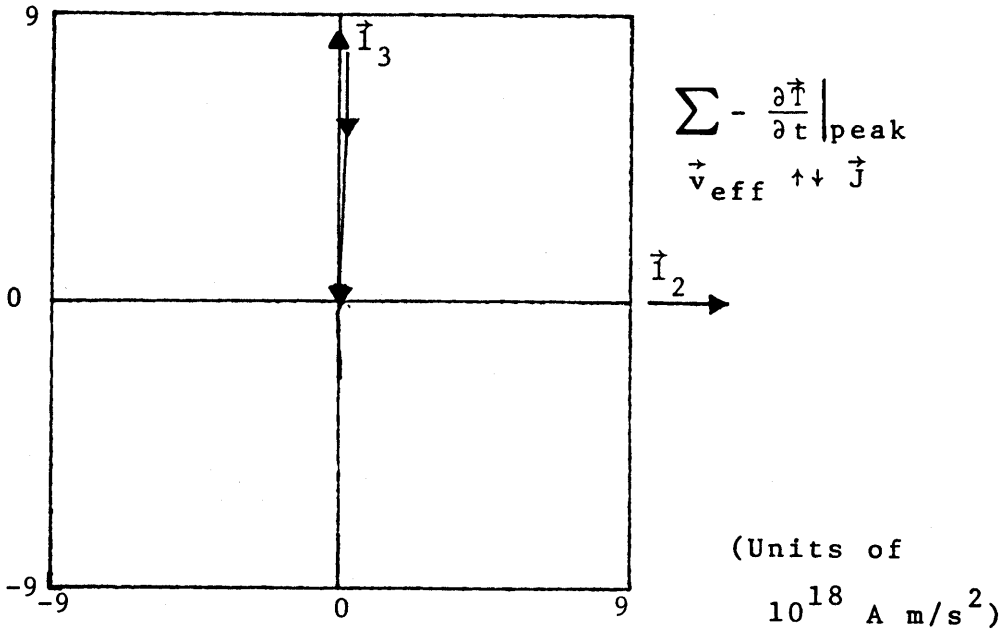

Effective reconstruction of negative streamer

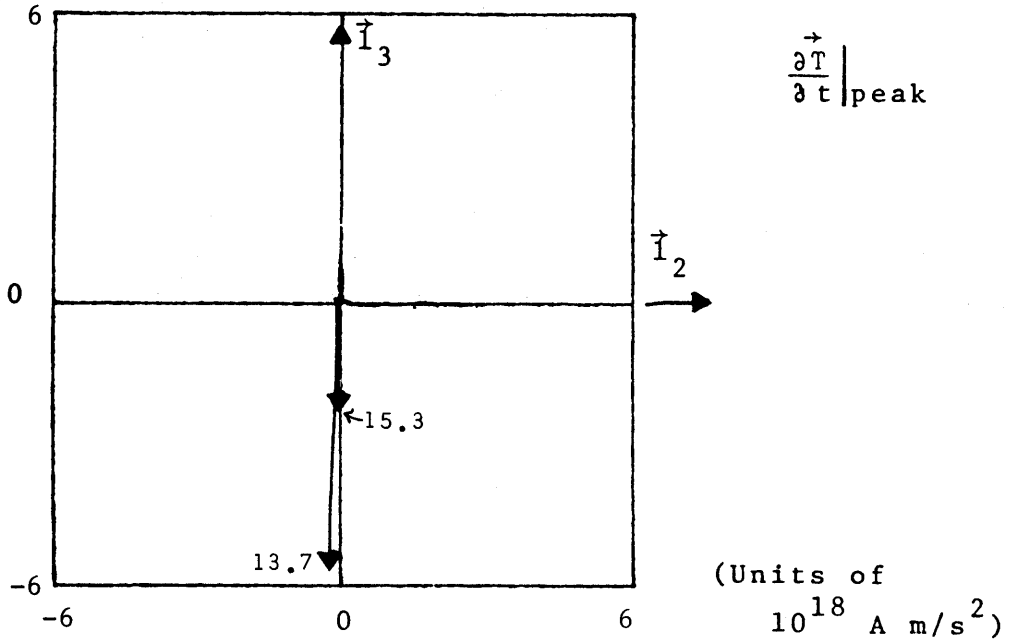

Peaks of $\partial\vec{T}/\partial t$

$\phi = 308^o$ $\theta = 20^o$ r = 1964 m Set 2

Date: 79219 M.S.T.: 09:39:39

Figure 6.5.7A.2 $\partial\vec{T}/\partial t$ for midrange leader

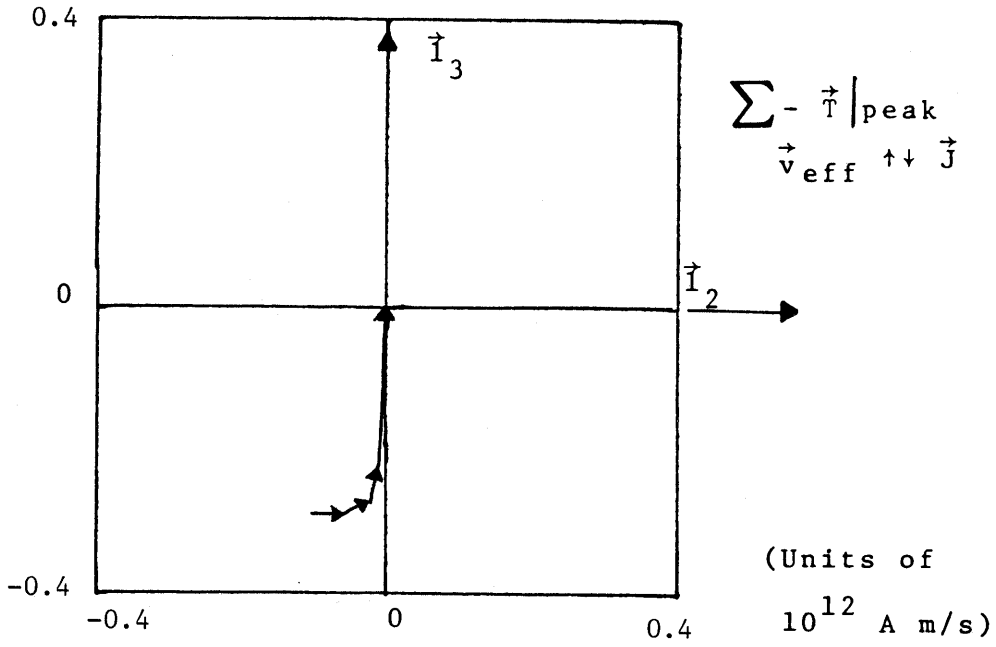

Effective reconstruction of negative streamer

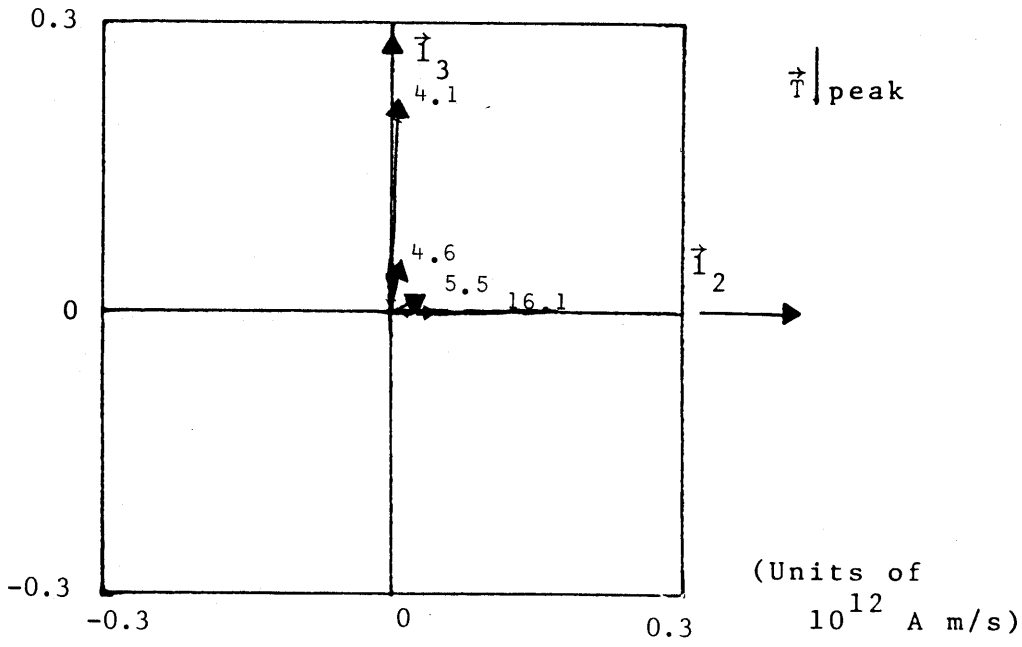

Peaks of $\vec{T}$

ϕ = 338° θ = 50° r = 877 m Set 1

Date: 79219 M.S.T.: 09:39:39

Figure 6.5.7B.1 $\vec{T}$ for midrange leader

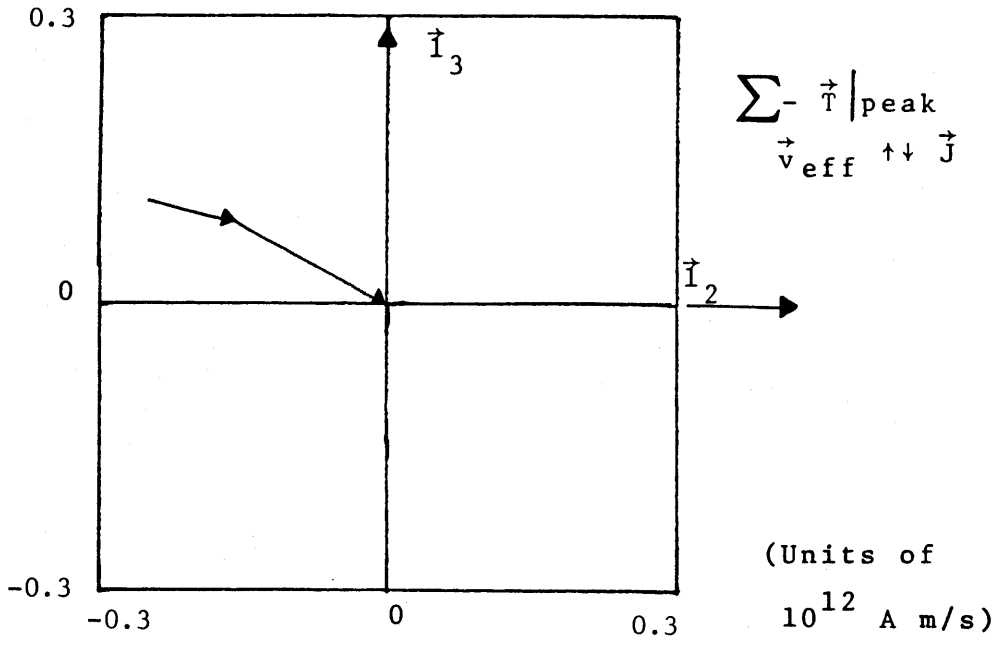

Effective reconstruction of negative streamer

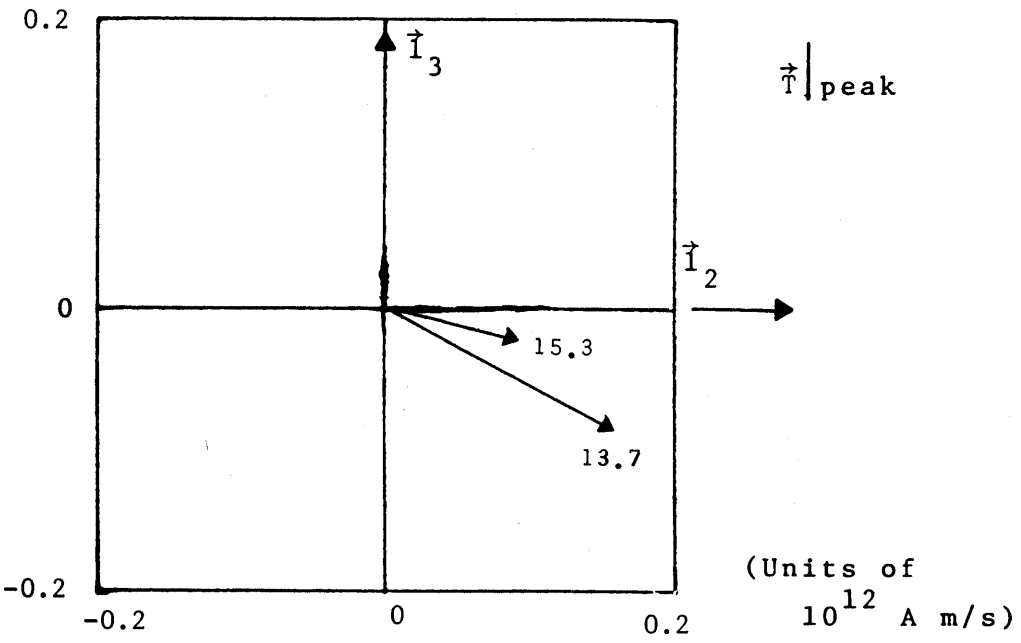

Peaks of $\vec{T}$

ϕ = 358° θ = 30° r = 1344 m Set 2

Date: 79219 M.S.T.: 09:39:39

Figure 6.5.7B.2 $\vec{T}$ for midrange leader

6.6 Midrange Return Stroke

Our sixth example is given in Figures 6.6.••• . This is labelled "midrange return stroke". Figures 6.6.1A and 6.6.1B show the derivative fields and fields for the 20 μs record.

Figure 6.6.3 shows the slow electric field and thunder microphone records, from which a horizontal range of 356 m is estimated. Figure 6.6.4 gives the acoustic source reconstruction showing a stroke extending from about 4 km height in the northeast. It strikes the ground north of the Kiva as also seen in the videotape photographs.

The θ , ϕ contours give two approximate sets of contour intersections estimated in Figures 6.6.5.

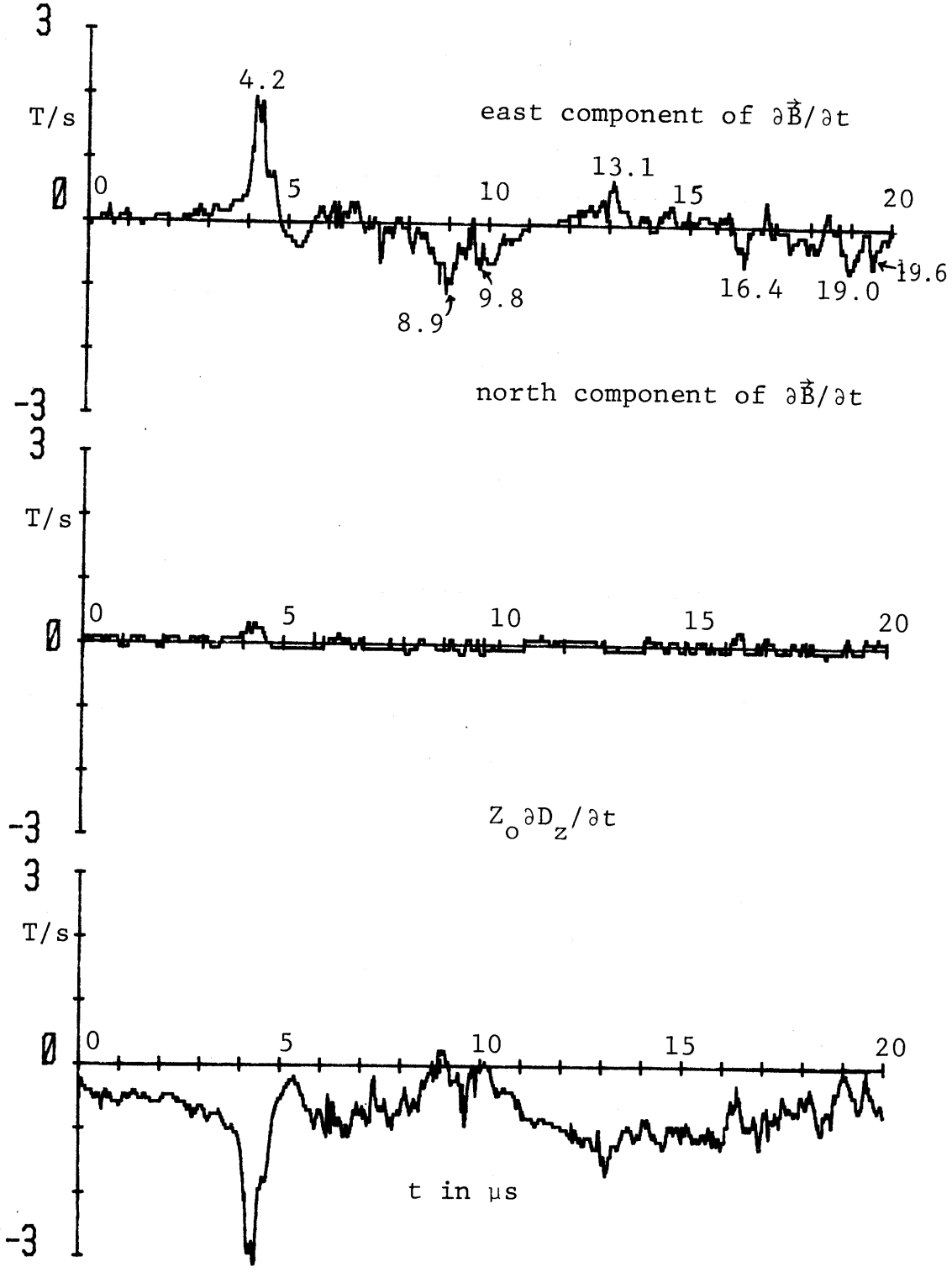

Date: 79219 M.S.T.: 0941:31

6.6.1A Derivative fields from midrange return stroke

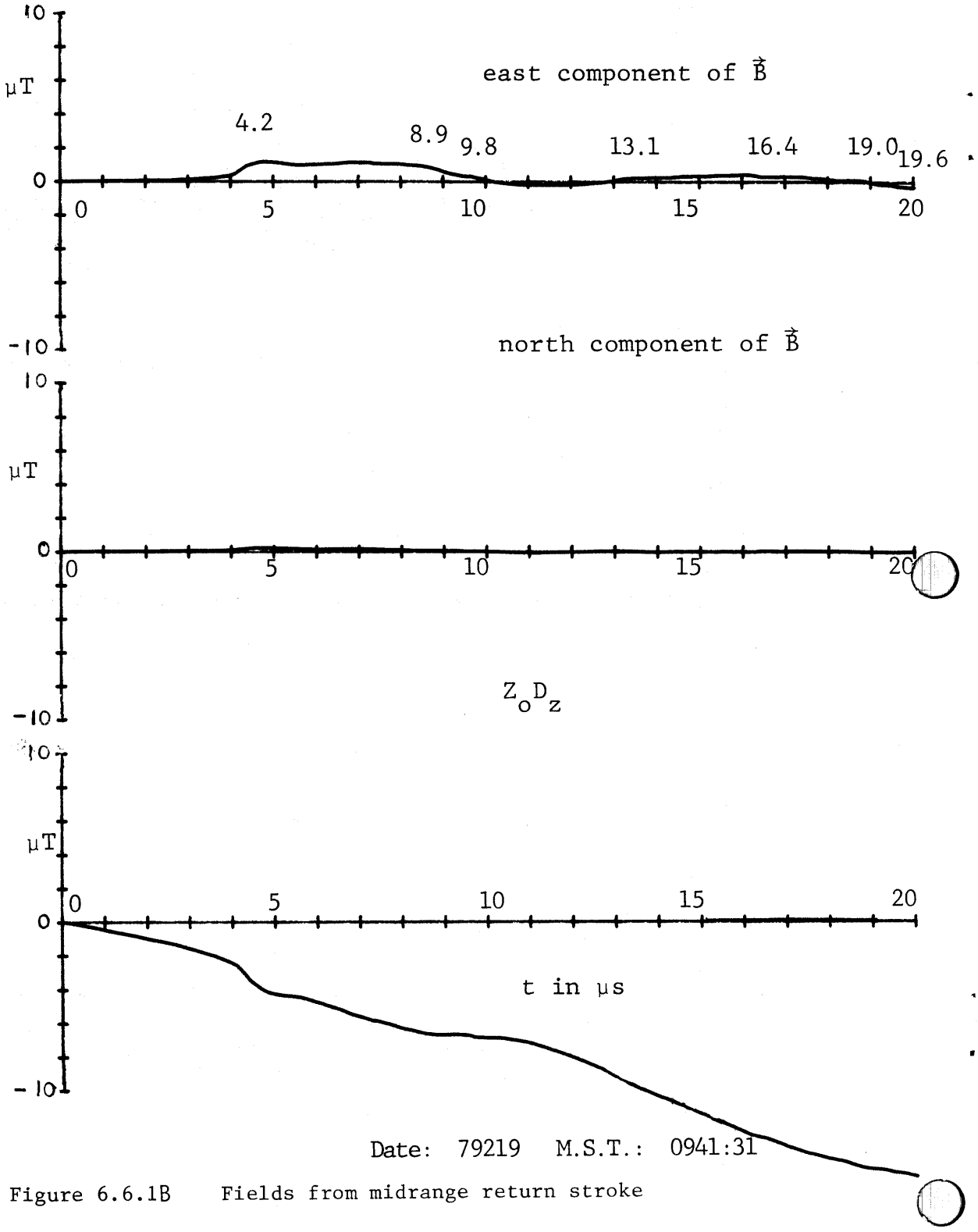

Figure 6.6.1B Fields from midrange return stroke

Figure 6.6.2.1 Digital data for event 4.2

[ ] = baseline which is subtracted for peaks and numerical integration

Yeardate: 79219 Time: 09:41:31 M.S.T.

Time (μs)	$\partial B_E/\partial t$ (T/s)	$\partial B_N/\partial t$ (T/s)	$Z_o \partial D_z/\partial t$ (T/s)	B_E (μT)	B_N (μT)	$Z_o D_z$ (μT)
3.93	0.391	0.234	-1.001	-0.000	0.000	-0.000
3.94	0.391	0.234	-1.001	-0.000	0.000	-0.000
3.95	0.469	0.234	-1.060	0.001	0.000	-0.001
3.96	0.469	0.234	-1.060	0.002	0.000	-0.001
3.97	0.469	0.234	-1.060	0.002	0.000	-0.002
3.98	0.547	0.234	-1.119	0.004	0.000	-0.003
3.99	0.547	0.234	-1.119	0.005	0.000	-0.004
4.00	0.625	0.234	-1.178	0.008	0.000	-0.006
4.01	0.625	0.234	-1.178	0.010	0.000	-0.008
4.02	0.703	0.234	-1.237	0.013	0.000	-0.010
4.03	0.781	0.234	-1.296	0.017	0.000	-0.013
4.04	0.859	0.234	-1.296	0.022	0.000	-0.016
4.05	0.938	0.234	-1.414	0.027	0.000	-0.020
4.06	0.938	0.234	-1.414	0.033	0.000	-0.024
4.07	1.094	0.234	-1.590	0.040	0.000	-0.030
4.08	1.172	0.234	-1.649	0.048	0.000	-0.037
4.09	1.172	0.313	-1.649	0.055	0.001	-0.043
4.10	1.094	0.313	-1.767	0.062	0.002	-0.051
4.11	1.094	0.391	-1.885	0.069	0.003	-0.060
4.12	1.484	0.391	-2.062	0.080	0.005	-0.070
4.13	1.563	0.391	-2.062	0.092	0.006	-0.081
4.14	1.875	0.391	-1.944	0.107	0.008	-0.090
4.15	1.875	0.391	-2.003	0.122	0.009	-0.100
4.16	1.953	0.313	-2.297	0.137	0.010	-0.113
4.17	1.953	0.313	-2.533	0.153	0.011	-0.129
4.18	1.875	0.234	-2.769	0.168	0.011	-0.146
4.19	1.797	0.234	-2.828	0.182	0.011	-0.164
4.20	1.797	0.234	-2.886	0.196	0.011	-0.183
4.21	1.797	0.234	-2.828	0.210	0.011	-0.202
4.22	1.797	0.234	-2.769	0.224	0.011	-0.219
4.23	1.797	0.313	-2.769	0.238	0.012	-0.237
4.24	1.719	0.313	-2.769	0.251	0.013	-0.255
4.25	1.641	0.313	-2.828	0.264	0.013	-0.273
4.26	1.563	0.391	-2.886	0.276	0.015	-0.292
4.27	1.563	0.391	-2.886	0.287	0.017	-0.311
4.28	1.641	0.391	-2.886	0.300	0.018	-0.329
4.29	1.797	0.391	-2.769	0.314	0.020	-0.347
4.30	1.797	0.391	-2.769	0.328	0.021	-0.365
4.31	1.875	0.391	-2.710	0.343	0.023	-0.382
4.32	1.875	0.313	-2.769	0.358	0.024	-0.400
4.33	1.875	0.313	-2.828	0.373	0.024	-0.418
4.34	1.875	0.313	-3.004	0.387	0.025	-0.438
4.35	1.797	0.313	-3.063	0.401	0.026	-0.458

Figure 6.6.2.1 Digital data for event 4.2 (continued)

Time (μs)	$\partial B_E/\partial t$ (T/s)	$\partial B_N/\partial t$ (T/s)	$Z_o \partial D_z/\partial t$ (T/s)	B_E (μT)	B_N (μT)	$Z_o D_z$ (μT)
4.36	1.563	0.313	-3.063	0.413	0.027	-0.479
4.37	1.484	0.313	-3.063	0.424	0.028	-0.500
4.38	1.250	0.313	-3.004	0.433	0.028	-0.520
4.39	1.172	0.313	-3.004	0.440	0.029	-0.540
4.40	0.938	0.313	-2.828	0.446	0.030	-0.558
4.41	0.859	0.313	-2.592	0.451	0.031	-0.574
4.42	0.781	0.313	-2.533	0.455	0.031	-0.589
4.43	0.781	0.313	-2.356	0.458	0.032	-0.603
4.44	0.703	0.313	-2.297	0.462	0.033	-0.616
4.45	0.703	0.313	-2.121	0.465	0.034	-0.627
4.46	0.703	0.313	-2.062	0.468	0.035	-0.638
4.47	0.781	0.313	-1.885	0.472	0.035	-0.646
4.48	0.781	0.313	-1.885	0.476	0.036	-0.655
4.49	0.781	0.234	-1.885	0.479	0.036	-0.664
4.50	0.703	0.234	-1.885	0.483	0.036	-0.673
4.51	0.703	0.234	-1.885	0.486	0.036	-0.682
4.52	0.703	0.234	-1.885	0.489	0.036	-0.691
4.53	0.703	0.156	-1.826	0.492	0.035	-0.699
4.54	0.703	0.156	-1.826	0.495	0.035	-0.707
4.55	0.703	0.156	-1.767	0.498	0.034	-0.715
4.56	0.703	0.156	-1.708	0.501	0.033	-0.722
4.57	0.703	0.078	-1.708	0.504	0.031	-0.729
4.58	0.703	0.078	-1.708	0.508	0.030	-0.736
4.59	0.703	0.078	-1.708	0.511	0.028	-0.743
4.60	0.781	0.078	-1.767	0.515	0.027	-0.751
4.61	0.781	0.078	-1.767	0.518	0.025	-0.758
4.62	0.781	0.078	-1.767	0.522	0.024	-0.766
4.63	0.703	0.078	-1.767	0.526	0.022	-0.774
4.64	0.703	0.078	-1.767	0.529	0.021	-0.781
4.65	0.625	0.078	-1.767	0.531	0.019	-0.789
4.66	0.547	0.078	-1.708	0.533	0.017	-0.796
4.67	0.547	0.078	-1.708	0.534	0.016	-0.803
4.68	0.469	0.078	-1.649	0.535	0.014	-0.810
4.69	0.391	0.078	-1.590	0.535	0.013	-0.816
4.70	0.313	0.000	-1.532	0.534	0.010	-0.821
4.71	0.313	0.000	-1.473	0.533	0.008	-0.826
4.72	0.234	0.000	-1.473	0.532	0.006	-0.830
4.73	0.234	0.000	-1.355	0.530	0.003	-0.834
4.74	0.234	0.000	-1.296	0.529	0.001	-0.837
4.75	0.156	0.000	-1.237	0.526	-0.001	-0.839
4.76	0.078	0.000	-1.178	0.523	-0.004	-0.841
4.77	0.078	0.000	-1.119	0.520	-0.006	-0.842
4.78	0.000	0.000	-1.060	0.516	-0.008	-0.843
4.79	0.000	0.000	-1.001	0.512	-0.010	-0.843
4.80	0.000	0.000	-1.001	0.508	-0.012	-0.843
4.81	-0.078	0.000	-0.884	0.503	-0.015	-0.842
4.82	-0.078	0.000	-0.884	0.499	-0.017	-0.841
4.83	-0.078	0.000	-0.766	0.494	-0.019	-0.838
4.84	-0.078	0.000	-0.766	0.489	-0.022	-0.836

Figure 6.6.2.1 Digital data for event 4.2 (continued)

Time (μs)	$\partial B_E/\partial t$ (T/s)	$\partial B_N/\partial t$ (T/s)	$Z_o \partial D_z/\partial t$ (T/s)	B_E (μT)	B_N (μT)	$Z_o D_z$ (μT)
4.85	-0.156	0.000	-0.707	0.484	-0.024	-0.833
4.86	-0.156	0.000	-0.707	0.478	-0.026	-0.830
4.87	-0.156	0.000	-0.648	0.473	-0.029	-0.827
4.88	-0.156	0.000	-0.648	0.467	-0.031	-0.823
4.89	-0.156	0.000	-0.648	0.462	-0.033	-0.819
4.90	-0.156	0.000	-0.589	0.456	-0.036	-0.815
4.91	-0.156	0.000	-0.589	0.451	-0.038	-0.811
4.92	-0.234	0.000	-0.589	0.445	-0.040	-0.807
4.93	-0.234	0.000	-0.530	0.439	-0.043	-0.802
4.94	-0.234	0.000	-0.530	0.432	-0.045	-0.798
4.95	-0.234	0.000	-0.530	0.426	-0.047	-0.793
4.96	-0.234	0.000	-0.530	0.420	-0.050	-0.788
4.97	-0.234	0.000	-0.471	0.413	-0.052	-0.783
4.98	-0.234	0.000	-0.471	0.407	-0.054	-0.778
4.99	-0.234	0.000	-0.471	0.401	-0.057	-0.772
5.00	-0.234	0.000	-0.471	0.395	-0.059	-0.767
5.01	-0.234	0.000	-0.471	0.388	-0.061	-0.762
5.02	-0.234	0.000	-0.471	0.382	-0.064	-0.757
5.03	-0.234	0.000	-0.471	0.376	-0.066	-0.751
5.04	-0.234	0.000	-0.412	0.370	-0.069	-0.745
5.05	-0.234	0.000	-0.412	0.363	-0.071	-0.739
5.06	-0.234	0.000	-0.412	0.357	-0.073	-0.734
5.07	-0.234	0.000	-0.412	0.351	-0.076	-0.728
5.08	-0.313	0.000	-0.412	0.344	-0.078	-0.722
5.09	-0.313	0.000	-0.412	0.337	-0.080	-0.716
5.10	-0.313	0.000	-0.353	0.330	-0.083	-0.709
5.11	-0.313	0.000	-0.353	0.323	-0.085	-0.703
5.12	-0.313	0.000	-0.295	0.316	-0.087	-0.696
5.13	-0.313	0.000	-0.295	0.309	-0.090	-0.689
5.14	-0.313	0.000	-0.295	0.302	-0.092	-0.682
5.15	-0.313	0.000	-0.295	0.295	-0.094	-0.675
5.16	-0.313	0.000	-0.295	0.288	-0.097	-0.668
5.17	-0.313	0.000	-0.295	0.281	-0.099	-0.661
5.18	-0.391	0.000	-0.236	0.273	-0.101	-0.653
5.19	-0.391	0.000	-0.236	0.265	-0.104	-0.645
5.20	-0.391	0.000	-0.236	0.257	-0.106	-0.638
5.21	-0.391	0.000	-0.236	0.249	-0.108	-0.630
5.22	-0.391	0.000	-0.236	0.242	-0.111	-0.622
5.23	-0.391	0.000	-0.236	0.234	-0.113	-0.615
5.24	-0.391	0.000	-0.177	0.226	-0.115	-0.606
5.25	-0.391	0.000	-0.177	0.218	-0.118	-0.598
5.26	-0.391	0.000	-0.177	0.210	-0.120	-0.590
5.27	-0.391	0.000	-0.177	0.202	-0.122	-0.582
5.28	-0.391	0.000	-0.177	0.195	-0.125	-0.573
5.29	-0.391	0.000	-0.177	0.187	-0.127	-0.565
5.30	-0.391	0.000	-0.177	0.179	-0.129	-0.557
5.31	-0.391	0.000	-0.177	0.171	-0.132	-0.549
5.32	-0.391	0.000	-0.177	0.163	-0.134	-0.540
5.33	-0.391	0.000	-0.177	0.156	-0.136	-0.532

Figure 6.6.2.1 Digital data for event 4.2 (continued)

Time (μs)	$\partial B_E/\partial t$ (T/s)	$\partial B_N/\partial t$ (T/s)	$Z_o \partial D_z/\partial t$ (T/s)	B_E (μT)	B_N (μT)	$Z_o D_z$ (μT)
5.34	-0.391	0.000	-0.177	0.148	-0.139	-0.524
5.35	-0.313	0.000	-0.118	0.141	-0.141	-0.515
5.36	-0.313	0.000	-0.118	0.134	-0.143	-0.506
5.37	-0.313	0.000	-0.177	0.127	-0.146	-0.498
5.38	-0.313	0.000	-0.177	0.120	-0.148	-0.490
5.39	-0.313	0.000	-0.236	0.113	-0.150	-0.482
5.40	-0.313	0.000	-0.236	0.106	-0.153	-0.474
5.41	-0.313	0.000	-0.236	0.098	-0.155	-0.467
5.42	-0.313	0.000	-0.236	0.091	-0.157	-0.459
5.43	-0.234	0.000	-0.236	0.085	-0.160	-0.452
5.44	-0.234	0.000	-0.236	0.079	-0.162	-0.444
5.45	-0.234	0.000	-0.236	0.073	-0.164	-0.436
5.46	-0.234	0.000	-0.236	0.066	-0.167	-0.429
5.47	-0.156	0.000	-0.236	0.061	-0.169	-0.421
5.48	-0.156	0.000	-0.295	0.055	-0.171	-0.414
5.49	-0.156	0.000	-0.295	0.050	-0.174	-0.407
5.50	-0.156	0.000	-0.353	0.045	-0.176	-0.400
5.51	-0.156	0.000	-0.353	0.039	-0.178	-0.394
5.52	-0.156	0.000	-0.353	0.034	-0.181	-0.387
5.53	-0.156	0.000	-0.412	0.028	-0.183	-0.381
5.54	-0.078	0.000	-0.412	0.023	-0.186	-0.376
5.55	-0.078	0.000	-0.412	0.019	-0.188	-0.370
5.56	-0.078	0.000	-0.412	0.014	-0.190	-0.364
5.57	0.000	0.000	-0.412	0.010	-0.193	-0.358
5.58	0.000	0.000	-0.412	0.006	-0.195	-0.352
5.59	0.000	0.000	-0.471	0.002	-0.197	-0.347
5.60	0.000	0.000	-0.471	-0.002	-0.200	-0.341

Figure 6.6.2.2 Digital data for event 8.9

[ ] = baseline which is subtracted for peaks and numerical integration

Yeardate: 79219 Time: 09:41:31 M.S.T.

Time (μs)	$\partial B_E/\partial t$ (T/s)	$\partial B_N/\partial t$ (T/s)	$Z_o \partial D_z/\partial t$ (T/s)	B_E (μT)	B_N (μT)	$Z_o D_z$ (μT)
8.42	-0.156	0.156	-0.530	-0.000	0.000	-0.000
8.43	[-0.156]	0.156	[-0.530]	-0.000	0.000	-0.000
8.44	-0.234	0.156	-0.589	-0.001	0.000	-0.001
8.45	-0.313	0.156	-0.589	-0.002	0.000	-0.001
8.46	-0.313	0.156	-0.648	-0.004	0.000	-0.002
8.47	-0.391	0.156	-0.648	-0.006	0.000	-0.004
8.48	-0.391	0.156	-0.471	-0.009	0.000	-0.003
8.49	-0.469	0.156	-0.412	-0.012	0.000	-0.002
8.50	-0.469	[0.156]	-0.412	-0.015	0.000	-0.001
8.51	-0.469	0.078	-0.412	-0.018	-0.001	0.001
8.52	-0.469	0.078	-0.295	-0.021	-0.002	0.003
8.53	-0.469	0.078	-0.295	-0.024	-0.002	0.005
8.54	-0.391	0.078	-0.236	-0.027	-0.003	0.008
8.55	-0.391	0.078	-0.177	-0.029	-0.004	0.012
8.56	-0.391	0.078	-0.236	-0.031	-0.005	0.015
8.57	-0.391	0.078	-0.236	-0.034	-0.005	0.018
8.58	-0.391	0.078	-0.236	-0.036	-0.006	0.021
8.59	-0.391	0.078	-0.236	-0.038	-0.007	0.024
8.60	-0.469	0.078	-0.295	-0.041	-0.008	0.026
8.61	-0.469	0.078	-0.295	-0.045	-0.009	0.028
8.62	-0.547	0.078	-0.295	-0.048	-0.009	0.031
8.63	-0.547	0.078	-0.236	-0.052	-0.010	0.034
8.64	-0.625	0.078	-0.177	-0.057	-0.011	0.037
8.65	-0.625	0.078	-0.177	-0.062	-0.012	0.041
8.66	-0.625	0.078	-0.177	-0.066	-0.012	0.044
8.67	-0.625	0.078	-0.177	-0.071	-0.013	0.048
8.68	-0.625	0.078	-0.118	-0.076	-0.014	0.052
8.69	-0.625	0.078	-0.118	-0.081	-0.015	0.056
8.70	-0.625	0.078	-0.118	-0.085	-0.016	0.060
8.71	-0.625	0.078	-0.059	-0.090	-0.016	0.065
8.72	-0.625	0.078	-0.059	-0.095	-0.017	0.069
8.73	-0.625	0.078	-0.059	-0.099	-0.018	0.074
8.74	-0.625	0.078	-0.059	-0.104	-0.019	0.079
8.75	-0.703	0.078	-0.059	-0.109	-0.019	0.084
8.76	-0.938	0.078	-0.059	-0.117	-0.020	0.088
8.77	-0.781	0.078	-0.059	-0.124	-0.021	0.093
8.78	-0.625	0.078	0.000	-0.128	-0.022	0.098
8.79	-0.625	0.078	0.000	-0.133	-0.023	0.104
8.80	-0.625	0.000	0.059	-0.138	-0.024	0.110
8.81	-0.625	0.000	0.118	-0.142	-0.026	0.116
8.82	-0.625	0.000	0.000	-0.147	-0.027	0.121
8.83	-0.625	0.000	-0.177	-0.152	-0.029	0.125
8.84	-0.625	0.000	-0.118	-0.156	-0.030	0.129

Figure 6.6.2.2 Digital data for event 8.9 (continued)

Time (μs)	$\partial B_E/\partial t$ (T/s)	$\partial B_N/\partial t$ (T/s)	$Z_o \partial D_z/\partial t$ (T/s)	B_E (μT)	B_N (μT)	$Z_o D_z$ (μT)
8.85	-0.625	0.000	0.000	-0.161	-0.032	0.134
8.86	-0.625	0.000	0.000	-0.166	-0.033	0.140
8.87	-0.625	0.000	-0.059	-0.170	-0.035	0.144
8.88	-0.625	0.000	0.000	-0.175	-0.037	0.150
8.89	-0.703	0.000	0.000	-0.181	-0.038	0.155
8.90	-0.938	0.000	0.000	-0.188	-0.040	0.160
8.91	-0.938	0.000	-0.059	-0.196	-0.041	0.165
8.92	-1.016	0.000	-0.118	-0.205	-0.043	0.169
8.93	-1.094	0.000	-0.059	-0.214	-0.044	0.174
8.94	-0.938	0.000	0.059	-0.222	-0.046	0.180
8.95	-0.938	0.000	0.236	-0.230	-0.048	0.187
8.96	-0.859	0.000	0.295	-0.237	-0.049	0.195
8.97	-0.859	0.000	0.295	-0.244	-0.051	0.204
8.98	-0.859	0.000	0.295	-0.251	-0.052	0.212
8.99	-0.938	0.000	0.236	-0.259	-0.054	0.220
9.00	-0.938	0.000	0.236	-0.267	-0.055	0.227
9.01	-0.938	0.000	0.236	-0.274	-0.057	0.235
9.02	-0.938	0.000	0.236	-0.282	-0.058	0.243
9.03	-0.938	0.000	0.295	-0.290	-0.060	0.251
9.04	-0.938	0.000	0.295	-0.298	-0.062	0.259
9.05	-0.938	0.000	0.295	-0.306	-0.063	0.267
9.06	-0.938	0.000	0.295	-0.313	-0.065	0.276
9.07	-0.859	0.000	0.295	-0.320	-0.066	0.284
9.08	-0.781	0.000	0.295	-0.327	-0.068	0.292
9.09	-0.781	0.000	0.295	-0.333	-0.069	0.300
9.10	-0.703	0.000	0.295	-0.338	-0.071	0.309
9.11	-0.625	0.000	0.236	-0.343	-0.072	0.316
9.12	-0.625	0.000	0.236	-0.348	-0.074	0.324
9.13	-0.703	0.000	0.177	-0.353	-0.076	0.331
9.14	-0.703	0.156	0.118	-0.359	-0.076	0.337
9.15	-0.703	0.156	0.059	-0.364	-0.076	0.343
9.16	-0.703	0.156	0.059	-0.370	-0.076	0.349
9.17	-0.625	0.156	0.059	-0.374	-0.076	0.355
9.18	-0.625	0.156	0.059	-0.379	-0.076	0.361
9.19	-0.547	0.156	0.059	-0.383	-0.076	0.367
9.20	-0.469	0.156	0.118	-0.386	-0.076	0.373
9.21	-0.391	0.156	0.059	-0.388	-0.076	0.379
9.22	-0.313	0.156	0.000	-0.390	-0.076	0.385
9.23	-0.313	0.078	0.000	-0.392	-0.076	0.390
9.24	-0.391	0.000	-0.177	-0.394	-0.078	0.393
9.25	-0.391	0.000	-0.236	-0.396	-0.079	0.396
9.26	-0.391	0.000	-0.236	-0.399	-0.081	0.399
9.27	-0.391	0.000	-0.236	-0.401	-0.083	0.402
9.28	-0.391	0.000	-0.236	-0.403	-0.084	0.405
9.29	-0.469	0.000	-0.177	-0.406	-0.086	0.409
9.30	-0.469	0.000	-0.177	-0.410	-0.087	0.412
9.31	-0.469	0.000	-0.177	-0.413	-0.089	0.416
9.32	-0.469	0.000	-0.177	-0.416	-0.090	0.419
9.33	-0.469	0.000	-0.177	-0.419	-0.092	0.423

Figure 6.6.2.2 Digital data for event 8.9 (continued)

Time (us)	$\partial B_E/\partial t$ (T/s)	$\partial B_N/\partial t$ (T/s)	$Z_o \partial D_z/\partial t$ (T/s)	B_E (μT)	B_N (μT)	$Z_o D_z$ (μT)
9.34	-0.469	0.000	-0.177	-0.422	-0.094	0.426
9.35	-0.391	0.000	-0.177	-0.424	-0.095	0.430
9.36	-0.469	0.000	-0.177	-0.428	-0.097	0.433
9.37	-0.469	0.000	-0.177	-0.431	-0.098	0.437
9.38	-0.469	-0.078	-0.177	-0.434	-0.101	0.440
9.39	-0.469	-0.078	-0.177	-0.437	-0.103	0.444
9.40	-0.547	-0.078	-0.177	-0.441	-0.105	0.448
9.41	-0.547	-0.078	-0.177	-0.445	-0.108	0.451
9.42	-0.469	-0.078	-0.118	-0.448	-0.110	0.455
9.43	-0.391	-0.078	-0.118	-0.450	-0.112	0.459
9.44	-0.391	-0.078	-0.059	-0.453	-0.115	0.464
9.45	-0.391	-0.078	-0.059	-0.455	-0.117	0.469
9.46	-0.391	-0.078	-0.118	-0.457	-0.119	0.473
9.47	-0.313	-0.078	-0.236	-0.459	-0.122	0.476
9.48	-0.078	-0.078	-0.236	-0.458	-0.124	0.479
9.49	-0.078	-0.078	-0.236	-0.457	-0.126	0.482
9.50	-0.078	-0.078	-0.236	-0.457	-0.129	0.485
9.51	-0.391	-0.078	-0.236	-0.459	-0.131	0.488
9.52	-0.313	0.000	-0.412	-0.460	-0.133	0.489
9.53	-0.313	0.000	-0.648	-0.462	-0.134	0.488
9.54	-0.234	0.078	-0.471	-0.463	-0.135	0.489
9.55	-0.078	0.078	-0.236	-0.462	-0.136	0.492
9.56	0.000	0.156	-0.236	-0.460	-0.136	0.494
9.57	0.078	0.156	-0.412	-0.458	-0.136	0.496
9.58	0.078	0.156	-0.412	-0.456	-0.136	0.497
9.59	0.078	0.156	-0.648	-0.453	-0.136	0.496
9.60	0.078	0.156	-0.884	-0.451	-0.136	0.492
9.61	0.000	0.156	-0.884	-0.450	-0.136	0.489
9.62	-0.078	0.156	-0.884	-0.449	-0.136	0.485
9.63	-0.313	0.156	-0.766	-0.450	-0.136	0.483
9.64	-0.313	0.156	-0.766	-0.452	-0.136	0.480
9.65	-0.391	0.156	-0.648	-0.454	-0.136	0.479
9.66	-0.469	0.156	-0.648	-0.457	-0.136	0.478

Figure 6.6.2.3 Digital data for event 9.8

[ ] = baseline which is subtracted for peaks and numerical integration

Yeardate: 79219 Time: 09:41:31 M.S.T.

Time (μs)	$\partial B_E/\partial t$ (T/s)	$\partial B_N/\partial t$ (T/s)	$Z_o \partial D_z/\partial t$ (T/s)	B_E (μT)	B_N (μT)	$Z_o D_z$ (μT)
9.56	[0.000]	0.156	[-0.236]	0.000	0.000	0.000
9.57	0.078	0.156	-0.412	0.001	0.000	-0.002
9.58	0.078	0.156	-0.412	0.002	0.000	-0.004
9.59	0.078	0.156	-0.648	0.002	0.000	-0.008
9.60	0.078	0.156	-0.884	0.003	0.000	-0.014
9.61	0.000	0.156	-0.884	0.003	0.000	-0.021
9.62	-0.078	0.156	-0.884	0.002	0.000	-0.027
9.63	-0.313	0.156	-0.766	-0.001	0.000	-0.032
9.64	-0.313	0.156	-0.766	-0.004	0.000	-0.038
9.65	-0.391	0.156	-0.648	-0.008	0.000	-0.042
9.66	-0.469	[0.156]	-0.648	-0.013	0.000	-0.046
9.67	-0.625	0.078	-0.471	-0.019	-0.001	-0.048
9.68	-0.625	0.000	-0.412	-0.025	-0.002	-0.050
9.69	-0.625	0.000	-0.295	-0.031	-0.004	-0.051
9.70	-0.547	0.000	-0.236	-0.037	-0.005	-0.051
9.71	-0.547	0.000	-0.177	-0.042	-0.007	-0.050
9.72	-0.547	0.000	-0.177	-0.048	-0.009	-0.049
9.73	-0.547	0.000	-0.059	-0.053	-0.010	-0.048
9.74	-0.625	0.000	-0.059	-0.059	-0.012	-0.046
9.75	-0.703	0.000	-0.118	-0.066	-0.013	-0.045
9.76	-0.703	0.000	-0.118	-0.073	-0.015	-0.044
9.77	-0.703	0.000	-0.059	-0.080	-0.016	-0.042
9.78	-0.703	0.000	0.000	-0.088	-0.018	-0.039
9.79	-0.625	0.000	0.059	-0.094	-0.019	-0.036
9.80	-0.625	0.000	0.059	-0.100	-0.021	-0.033
9.81	-0.625	0.000	0.059	-0.106	-0.023	-0.031
9.82	-0.469	0.078	0.059	-0.111	-0.023	-0.028
9.83	-0.313	0.156	0.059	-0.114	-0.023	-0.025
9.84	-0.313	0.156	0.000	-0.117	-0.023	-0.022
9.85	-0.391	0.156	0.000	-0.121	-0.023	-0.020
9.86	-0.391	0.078	-0.118	-0.125	-0.024	-0.019
9.87	-0.547	0.000	-0.236	-0.130	-0.026	-0.019
9.88	-0.547	0.000	-0.412	-0.136	-0.027	-0.020
9.89	-0.547	0.000	-0.295	-0.141	-0.029	-0.021
9.90	-0.547	-0.078	-0.177	-0.147	-0.031	-0.020
9.91	-0.547	-0.078	0.000	-0.152	-0.034	-0.018
9.92	-0.547	-0.078	0.000	-0.158	-0.036	-0.016
9.93	-0.547	-0.078	0.000	-0.163	-0.038	-0.013
9.94	-0.547	-0.078	0.000	-0.169	-0.041	-0.011
9.95	-0.625	-0.078	0.000	-0.175	-0.043	-0.009
9.96	-0.625	-0.078	0.000	-0.181	-0.045	-0.006
9.97	-0.625	-0.078	0.000	-0.188	-0.048	-0.004
9.98	-0.625	-0.078	0.000	-0.194	-0.050	-0.002

Figure 6.6.2.3 Digital data for event 9.8 (continued)

Time (μs)	$\partial B_E/\partial t$ (T/s)	$\partial B_N/\partial t$ (T/s)	$Z_o \partial D_z/\partial t$ (T/s)	B_E (μT)	B_N (μT)	$Z_o D_z$ (μT)
9.99	-0.625	-0.078	0.000	-0.200	-0.052	0.001
10.00	-0.625	-0.078	0.000	-0.206	-0.055	0.003
10.01	-0.625	-0.078	0.000	-0.213	-0.057	0.005
10.02	-0.625	0.000	0.000	-0.219	-0.058	0.008
10.03	-0.625	0.000	0.059	-0.225	-0.060	0.011
10.04	-0.625	0.000	0.059	-0.231	-0.062	0.014
10.05	-0.625	0.000	0.059	-0.238	-0.063	0.017
10.06	-0.625	0.000	0.059	-0.244	-0.065	0.020
10.07	-0.625	0.000	0.059	-0.250	-0.066	0.023
10.08	-0.625	0.000	0.059	-0.256	-0.068	0.026
10.09	-0.625	0.000	0.059	-0.263	-0.069	0.028
10.10	-0.625	0.000	0.059	-0.269	-0.071	0.031
10.11	-0.625	0.000	0.118	-0.275	-0.073	0.035
10.12	-0.625	0.000	0.059	-0.281	-0.074	0.038
10.13	-0.625	0.000	0.059	-0.288	-0.076	0.041
10.14	-0.625	0.000	0.059	-0.294	-0.077	0.044
10.15	-0.547	0.000	0.059	-0.299	-0.079	0.047
10.16	-0.547	0.000	0.059	-0.305	-0.080	0.050
10.17	-0.547	0.000	0.059	-0.310	-0.082	0.053
10.18	-0.547	0.000	0.059	-0.316	-0.083	0.056
10.19	-0.547	0.000	0.059	-0.321	-0.085	0.059
10.20	-0.469	0.078	0.059	-0.326	-0.086	0.062
10.21	-0.469	0.078	0.000	-0.330	-0.087	0.064
10.22	-0.469	0.078	0.000	-0.335	-0.087	0.066
10.23	-0.469	0.078	0.000	-0.340	-0.088	0.069
10.24	-0.391	0.078	0.000	-0.344	-0.089	0.071
10.25	-0.313	0.000	0.000	-0.347	-0.090	0.073
10.26	-0.313	0.000	-0.059	-0.350	-0.092	0.075
10.27	-0.313	0.000	-0.118	-0.353	-0.094	0.076
10.28	-0.313	0.000	-0.118	-0.356	-0.095	0.077
10.29	-0.313	0.000	-0.177	-0.359	-0.097	0.078
10.30	-0.313	0.000	-0.177	-0.363	-0.098	0.079
10.31	-0.313	0.000	-0.236	-0.366	-0.100	0.079
10.32	-0.234	0.000	-0.236	-0.368	-0.101	0.079
10.33	-0.234	0.000	-0.236	-0.370	-0.103	0.079
10.34	-0.234	0.000	-0.236	-0.373	-0.104	0.079
10.35	-0.156	0.000	-0.295	-0.374	-0.106	0.078
10.36	-0.156	0.000	-0.295	-0.376	-0.108	0.077
10.37	-0.234	0.000	-0.353	-0.378	-0.109	0.076
10.38	-0.313	0.156	-0.353	-0.381	-0.109	0.075
10.39	-0.313	0.078	-0.353	-0.384	-0.110	0.074
10.40	-0.313	0.000	-0.412	-0.388	-0.112	0.072
10.41	-0.234	0.000	-0.295	-0.390	-0.113	0.072
10.42	-0.234	0.000	-0.295	-0.392	-0.115	0.071
10.43	-0.234	0.000	-0.353	-0.395	-0.116	0.070
10.44	-0.234	0.000	-0.353	-0.397	-0.118	0.069
10.45	-0.234	0.000	-0.412	-0.399	-0.119	0.067
10.46	-0.234	0.000	-0.412	-0.402	-0.121	0.065
10.47	-0.234	0.000	-0.412	-0.404	-0.122	0.063

Figure 6.6.2.3 Digital data for event 9.8 (continued)

Time (μs)	$\partial B_E/\partial t$ (T/s)	$\partial B_N/\partial t$ (T/s)	$Z_o \partial D_z/\partial t$ (T/s)	B_E (μT)	B_N (μT)	$Z_o D_z$ (μT)
10.48	-0.234	0.000	-0.353	-0.406	-0.124	0.062
10.49	-0.234	0.000	-0.353	-0.409	-0.126	0.061
10.50	-0.234	0.000	-0.353	-0.411	-0.127	0.060
10.51	-0.234	0.000	-0.353	-0.413	-0.129	0.059
10.52	-0.313	0.000	-0.353	-0.416	-0.130	0.058
10.53	-0.313	0.000	-0.353	-0.420	-0.132	0.056
10.54	-0.313	0.000	-0.353	-0.423	-0.133	0.055
10.55	-0.313	0.000	-0.353	-0.426	-0.135	0.054
10.56	-0.313	0.000	-0.295	-0.429	-0.136	0.053
10.57	-0.313	0.000	-0.295	-0.432	-0.138	0.053
10.58	-0.234	0.000	-0.295	-0.434	-0.140	0.052
10.59	-0.234	0.000	-0.295	-0.437	-0.141	0.052
10.60	-0.234	0.000	-0.295	-0.439	-0.143	0.051
10.61	-0.234	0.000	-0.295	-0.441	-0.144	0.050
10.62	-0.234	0.000	-0.295	-0.444	-0.146	0.050
10.63	-0.234	0.000	-0.353	-0.446	-0.147	0.049
10.64	-0.234	0.000	-0.353	-0.448	-0.149	0.048
10.65	-0.234	0.000	-0.353	-0.451	-0.151	0.046
10.66	-0.234	0.000	-0.353	-0.453	-0.152	0.045
10.67	-0.234	0.000	-0.353	-0.455	-0.154	0.044
10.68	-0.234	0.000	-0.353	-0.458	-0.155	0.043
10.69	-0.234	0.000	-0.353	-0.460	-0.157	0.042
10.70	-0.234	0.000	-0.353	-0.463	-0.158	0.040
10.71	-0.234	0.000	-0.353	-0.465	-0.160	0.039
10.72	-0.234	0.000	-0.353	-0.467	-0.161	0.038
10.73	-0.234	0.000	-0.353	-0.470	-0.163	0.037
10.74	-0.234	0.000	-0.353	-0.472	-0.165	0.036
10.75	-0.234	0.000	-0.353	-0.474	-0.166	0.035
10.76	-0.156	0.000	-0.353	-0.476	-0.168	0.033
10.77	-0.156	0.000	-0.353	-0.477	-0.169	0.032
10.78	-0.156	0.000	-0.353	-0.479	-0.171	0.031
10.79	-0.156	0.000	-0.353	-0.480	-0.172	0.030
10.80	-0.156	0.000	-0.353	-0.482	-0.174	0.029
10.81	-0.156	0.000	-0.353	-0.484	-0.175	0.028
10.82	-0.078	0.000	-0.412	-0.484	-0.177	0.026
10.83	-0.078	0.000	-0.412	-0.485	-0.179	0.024
10.84	-0.078	0.000	-0.412	-0.486	-0.180	0.022
10.85	-0.078	0.000	-0.412	-0.487	-0.182	0.021
10.86	-0.078	0.000	-0.412	-0.488	-0.183	0.019
10.87	-0.078	0.000	-0.471	-0.488	-0.185	0.016
10.88	-0.078	0.000	-0.471	-0.489	-0.186	0.014
10.89	-0.078	0.000	-0.530	-0.490	-0.188	0.011
10.90	-0.078	0.000	-0.589	-0.491	-0.190	0.008
10.91	-0.078	0.000	-0.589	-0.491	-0.191	0.004
10.92	-0.078	0.000	-0.530	-0.492	-0.193	0.001
10.93	-0.078	0.000	-0.530	-0.493	-0.194	-0.002
10.94	-0.078	0.000	-0.530	-0.494	-0.196	-0.005
10.95	-0.078	0.000	-0.471	-0.495	-0.197	-0.007
10.96	-0.078	0.000	-0.471	-0.495	-0.199	-0.009
10.97	-0.078	0.000	-0.471	-0.496	-0.200	-0.012
10.98	0.000	0.000	-0.530	-0.496	-0.202	-0.015

Figure 6.6.2.4 Digital data for event 13.1

[ ] = baseline which is subtracted for peaks and numerical integration

Yeardate: 79219 Time: 09:41:31 M.S.T.

Time (μs)	$\partial B_E/\partial t$ (T/s)	$\partial B_N/\partial t$ (T/s)	$Z_o \partial D_z/\partial t$ (T/s)	B_E (μT)	B_N (μT)	$Z_o D_z$ (μT)
12.91	[0.078]	0.078	[-1.237]	0.000	0.000	-0.000
12.92	0.156	[0.078]	-1.119	0.001	0.000	0.001
12.93	0.156	0.156	-1.001	0.002	0.000	0.004
12.94	0.156	0.156	-0.943	0.002	0.001	0.006
12.95	0.313	0.156	-0.943	0.005	0.002	0.009
12.96	0.391	0.156	-0.943	0.008	0.002	0.012
12.97	0.469	0.156	-1.119	0.012	0.003	0.014
12.98	0.547	0.156	-1.119	0.016	0.004	0.015
12.99	0.547	0.156	-1.178	0.021	0.005	0.015
13.00	0.547	0.156	-1.355	0.026	0.005	0.014
13.01	0.547	0.078	-1.355	0.030	0.005	0.013
13.02	0.547	0.078	-1.473	0.035	0.005	0.011
13.03	0.547	0.000	-1.473	0.040	0.005	0.008
13.04	0.547	0.000	-1.414	0.045	0.004	0.006
13.05	0.547	0.000	-1.414	0.049	0.003	0.005
13.06	0.625	0.000	-1.355	0.055	0.002	0.004
13.07	0.625	0.000	-1.355	0.060	0.002	0.002
13.08	0.703	0.000	-1.414	0.066	0.001	0.001
13.09	0.625	0.000	-1.414	0.072	0.000	-0.001
13.10	0.625	0.000	-1.590	0.077	-0.001	-0.005
13.11	0.625	0.000	-1.649	0.083	-0.002	-0.009
13.12	0.625	0.000	-1.649	0.088	-0.002	-0.013
13.13	0.625	0.000	-1.590	0.094	-0.003	-0.017
13.14	0.547	0.000	-1.532	0.098	-0.004	-0.019
13.15	0.547	0.000	-1.532	0.103	-0.005	-0.022
13.16	0.469	0.000	-1.590	0.107	-0.005	-0.026
13.17	0.391	0.000	-1.532	0.110	-0.006	-0.029
13.18	0.391	0.000	-1.532	0.113	-0.007	-0.032
13.19	0.391	0.000	-1.473	0.116	-0.008	-0.034
13.20	0.391	0.000	-1.355	0.120	-0.009	-0.035
13.21	0.313	0.000	-1.355	0.122	-0.009	-0.037
13.22	0.313	0.000	-1.355	0.124	-0.010	-0.038
13.23	0.234	0.000	-1.355	0.126	-0.011	-0.039
13.24	0.234	0.000	-1.355	0.127	-0.012	-0.040
13.25	0.234	0.000	-1.355	0.129	-0.012	-0.041
13.26	0.234	0.000	-1.237	0.131	-0.013	-0.041

Figure 6.6.2.5 Digital data for event 16.4

[ ] = baseline which is subtracted for peaks and numerical integration

Yeardate: 79219 Time: 09:41:31 M.S.T.

Time (μs)	$\partial B_E/\partial t$ (T/s)	$\partial B_N/\partial t$ (T/s)	$Z_o \partial D_z/\partial t$ (T/s)	B_E (μT)	B_N (μT)	$Z_o D_z$ (μT)
16.05	0.000	0.000	-1.119	0.000	0.000	-0.000
16.06	0.000	0.000	-1.119	0.000	0.000	-0.000
16.07	-0.078	0.000	-1.119	-0.001	0.000	-0.000
16.08	-0.078	0.000	-0.884	-0.002	0.000	0.002
16.09	-0.078	0.000	-0.884	-0.002	0.000	0.005
16.10	-0.078	0.000	-0.884	-0.003	0.000	0.007
16.11	-0.234	0.000	-0.884	-0.005	0.000	0.009
16.12	-0.313	0.156	-0.884	-0.009	0.002	0.012
16.13	-0.313	0.156	-0.884	-0.012	0.003	0.014
16.14	-0.313	0.156	-0.884	-0.015	0.005	0.016
16.15	-0.313	0.156	-0.707	-0.018	0.006	0.021
16.16	-0.313	0.156	-0.648	-0.021	0.008	0.025
16.17	-0.391	0.234	-0.648	-0.025	0.010	0.030
16.18	-0.391	0.234	-0.648	-0.029	0.013	0.035
16.19	-0.391	0.156	-0.648	-0.033	0.014	0.039
16.20	-0.391	0.234	-0.648	-0.037	0.016	0.044
16.21	-0.391	0.234	-0.530	-0.041	0.019	0.050
16.22	-0.391	0.156	-0.471	-0.045	0.020	0.057
16.23	-0.313	0.156	-0.530	-0.048	0.022	0.062
16.24	-0.313	0.156	-0.530	-0.051	0.023	0.068
16.25	-0.313	0.156	-0.530	-0.054	0.025	0.074
16.26	-0.313	0.234	-0.530	-0.057	0.027	0.080
16.27	-0.313	0.234	-0.589	-0.060	0.030	0.085
16.28	-0.313	0.313	-0.648	-0.063	0.033	0.090
16.29	-0.391	0.313	-0.648	-0.067	0.036	0.095
16.30	-0.391	0.313	-0.589	-0.071	0.039	0.100
16.31	-0.391	0.313	-0.589	-0.075	0.042	0.105
16.32	-0.625	0.313	-0.589	-0.081	0.045	0.111
16.33	-0.625	0.313	-0.589	-0.088	0.048	0.116
16.34	-0.625	0.313	-0.530	-0.094	0.052	0.122
16.35	-0.547	0.313	-0.530	-0.099	0.055	0.128
16.36	-0.469	0.313	-0.530	-0.104	0.058	0.134
16.37	-0.469	0.313	-0.236	-0.109	0.061	0.142
16.38	-0.469	0.234	-0.412	-0.113	0.063	0.150
16.39	-0.469	0.234	-0.412	-0.118	0.066	0.157
16.40	-0.391	0.234	-0.412	-0.122	0.068	0.164
16.41	-0.391	0.234	-0.412	-0.126	0.070	0.171
16.42	-0.313	0.313	-0.412	-0.129	0.073	0.178
16.43	-0.078	0.234	-0.471	-0.130	0.076	0.184
16.44	-0.078	0.234	-0.530	-0.130	0.078	0.190
16.45	-0.156	0.156	-0.471	-0.132	0.080	0.197
16.46	-0.156	0.078	-0.589	-0.134	0.080	0.202
16.47	-0.156	0.000	-0.648	-0.135	0.080	0.207

Figure 6.6.2.5 Digital data for event 16.4 (continued)

Time (μs)	$\partial B_E/\partial t$ (T/s)	$\partial B_N/\partial t$ (T/s)	$Z_o \partial D_z/\partial t$ (T/s)	B_E (μT)	B_N (μT)	$Z_o D_z$ (μT)
16.48	-0.156	0.000	-0.707	-0.137	0.080	0.211
16.49	-0.078	0.000	-0.766	-0.138	0.080	0.214
16.50	-0.078	0.000	-0.707	-0.138	0.080	0.218
16.51	-0.078	0.000	-0.707	-0.139	0.080	0.223
16.52	-0.078	0.000	-0.825	-0.140	0.080	0.226
16.53	-0.078	0.000	-0.825	-0.141	0.080	0.228
16.54	-0.078	0.000	-0.943	-0.141	0.080	0.230
16.55	0.000	0.000	-0.884	-0.141	0.080	0.233
16.56	0.000	0.000	-0.884	-0.141	0.080	0.235
16.57	0.000	0.000	-0.884	-0.141	0.080	0.237
16.58	0.000	0.000	-0.884	-0.141	0.080	0.240
16.59	0.000	0.000	-0.943	-0.141	0.080	0.241
16.60	0.000	0.000	-0.943	-0.141	0.080	0.243
16.61	0.000	0.000	-0.884	-0.141	0.080	0.246
16.62	0.000	0.000	-0.884	-0.141	0.080	0.248
16.63	0.000	0.000	-0.884	-0.141	0.080	0.250
16.64	0.000	0.000	-0.884	-0.141	0.080	0.253
16.65	0.000	0.000	-0.884	-0.141	0.080	0.255
16.66	0.000	0.000	-0.943	-0.141	0.080	0.257
16.67	0.000	0.000	-0.943	-0.141	0.080	0.258
16.68	0.000	0.000	-0.943	-0.141	0.080	0.260
16.69	0.000	0.000	-0.943	-0.141	0.080	0.262
16.70	0.000	0.000	-0.943	-0.141	0.080	0.264
16.71	0.000	0.000	-0.943	-0.141	0.080	0.266
16.72	0.000	0.000	-0.884	-0.141	0.080	0.268
16.73	0.000	0.000	-0.884	-0.141	0.080	0.270
16.74	-0.078	0.000	-0.884	-0.142	0.080	0.273
16.75	-0.078	0.000	-0.884	-0.143	0.080	0.275
16.76	-0.078	0.000	-0.884	-0.144	0.080	0.277
16.77	-0.078	0.078	-0.884	-0.145	0.081	0.280
16.78	-0.078	0.156	-0.766	-0.145	0.083	0.283
16.79	-0.078	0.156	-0.766	-0.146	0.084	0.287
16.80	-0.078	0.156	-0.707	-0.147	0.086	0.291
16.81	0.000	0.156	-0.766	-0.147	0.088	0.294
16.82	0.078	0.078	-0.766	-0.146	0.088	0.298
16.83	0.156	0.000	-0.825	-0.145	0.088	0.301
16.84	0.156	0.000	-0.825	-0.143	0.088	0.304
16.85	0.313	0.000	-0.825	-0.140	0.088	0.307
16.86	0.313	0.000	-0.943	-0.137	0.088	0.308
16.87	0.391	0.000	-1.001	-0.133	0.088	0.310
16.88	0.391	0.000	-1.060	-0.129	0.088	0.310
16.89	0.391	0.000	-1.119	-0.125	0.088	0.310
16.90	0.313	0.078	-1.178	-0.122	0.089	0.309
16.91	0.234	0.078	-1.237	-0.120	0.090	0.308
16.92	0.234	0.156	-1.237	-0.117	0.091	0.307
16.93	0.156	0.156	-1.237	-0.116	0.093	0.306
16.94	0.078	0.156	-1.237	-0.115	0.094	0.305
16.95	0.078	0.156	-1.119	-0.114	0.096	0.305
16.96	0.000	0.156	-1.060	-0.114	0.097	0.305

Figure 6.6.2.6 Digital data for event 19.0

[ ] = baseline which is subtracted for peaks and numerical integration

Yeardate: 79219 Time: 09:41:31 M.S.T.

Time (μs)	$\partial B_E/\partial t$ (T/s)	$\partial B_N/\partial t$ (T/s)	$Z_o \partial D_z/\partial t$ (T/s)	B_E (μT)	B_N (μT)	$Z_o D_z$ (μT)
18.63	-0.078	0.000	-0.648	-0.000	0.000	0.000
18.64	-0.078	0.000	-0.648	-0.000	0.000	0.000
18.65	0.000	0.000	-0.648	0.001	0.000	0.000
18.66	0.000	0.000	-0.707	0.002	0.000	-0.001
18.67	0.078	0.000	-0.707	0.003	0.000	-0.001
18.68	0.078	0.000	-0.707	0.005	0.000	-0.002
18.69	0.078	0.000	-0.707	0.006	0.000	-0.002
18.70	0.000	0.000	-0.884	0.007	0.000	-0.005
18.71	-0.156	0.000	-0.884	0.006	0.000	-0.007
18.72	-0.234	0.000	-0.884	0.005	0.000	-0.009
18.73	-0.391	0.000	-0.707	0.002	0.000	-0.010
18.74	-0.391	0.000	-0.648	-0.002	0.000	-0.010
18.75	-0.391	0.000	-0.471	-0.005	0.000	-0.008
18.76	-0.313	0.000	-0.471	-0.007	0.000	-0.006
18.77	-0.313	0.000	-0.412	-0.009	0.000	-0.004
18.78	-0.391	0.000	-0.353	-0.013	0.000	-0.001
18.79	-0.391	0.000	-0.353	-0.016	0.000	0.002
18.80	-0.391	0.000	-0.412	-0.019	0.000	0.004
18.81	-0.391	0.000	-0.471	-0.022	0.000	0.006
18.82	-0.391	0.000	-0.412	-0.025	0.000	0.008
18.83	-0.391	0.000	-0.353	-0.028	0.000	0.011
18.84	-0.391	0.000	-0.353	-0.031	0.000	0.014
18.85	-0.391	0.000	-0.353	-0.034	0.000	0.017
18.86	-0.547	0.000	-0.353	-0.039	0.000	0.020
18.87	-0.547	0.000	-0.353	-0.044	0.000	0.023
18.88	-0.625	0.000	-0.353	-0.049	0.000	0.026
18.89	-0.625	0.000	-0.353	-0.055	0.000	0.029
18.90	-0.625	0.000	-0.295	-0.060	0.000	0.032
18.91	-0.625	0.078	-0.236	-0.066	0.001	0.037
18.92	-0.703	0.078	-0.177	-0.072	0.002	0.041
18.93	-0.703	0.078	-0.177	-0.078	0.002	0.046
18.94	-0.703	0.078	-0.177	-0.084	0.003	0.051
18.95	-0.703	0.078	-0.118	-0.091	0.004	0.056
18.96	-0.703	0.156	-0.118	-0.097	0.005	0.061
18.97	-0.703	0.156	-0.118	-0.103	0.007	0.067
18.98	-0.625	0.156	-0.118	-0.109	0.009	0.072
18.99	-0.625	0.156	-0.059	-0.114	0.010	0.078
19.00	-0.625	0.156	-0.059	-0.120	0.012	0.084
19.01	-0.625	0.234	-0.059	-0.125	0.014	0.090
19.02	-0.625	0.234	-0.059	-0.131	0.016	0.095
19.03	-0.625	0.234	-0.059	-0.136	0.019	0.101
19.04	-0.625	0.234	-0.118	-0.141	0.021	0.107
19.05	-0.547	0.156	-0.059	-0.146	0.023	0.113

Figure 6.6.2.6 Digital data for event 19.0 (continued)

Time (μs)	$\partial B_E/\partial t$ (T/s)	$\partial B_N/\partial t$ (T/s)	$Z_o \partial D_z/\partial t$ (T/s)	B_E (μT)	B_N (μT)	$Z_o D_z$ (μT)
19.06	-0.469	0.156	-0.059	-0.150	0.024	0.118
19.07	-0.469	0.156	-0.059	-0.154	0.026	0.124
19.08	-0.469	0.156	-0.059	-0.158	0.027	0.130
19.09	-0.547	0.078	-0.118	-0.163	0.028	0.135
19.10	-0.469	0.078	-0.118	-0.166	0.029	0.141
19.11	-0.469	0.078	-0.177	-0.170	0.030	0.146
19.12	-0.469	0.078	-0.177	-0.174	0.030	0.150
19.13	-0.391	0.078	-0.177	-0.177	0.031	0.155
19.14	-0.391	0.078	-0.177	-0.181	0.032	0.160
19.15	-0.391	0.000	-0.236	-0.184	0.032	0.164
19.16	-0.469	0.000	-0.236	-0.188	0.032	0.168
19.17	-0.391	0.000	-0.236	-0.191	0.032	0.172
19.18	-0.313	0.000	-0.353	-0.193	0.032	0.175
19.19	-0.313	0.000	-0.295	-0.195	0.032	0.179
19.20	-0.313	0.000	-0.295	-0.198	0.032	0.182
19.21	-0.313	0.000	-0.295	-0.200	0.032	0.186
19.22	-0.313	0.000	-0.353	-0.202	0.032	0.189
19.23	-0.313	0.000	-0.412	-0.205	0.032	0.191
19.24	-0.313	0.000	-0.412	-0.207	0.032	0.193
19.25	-0.313	0.000	-0.412	-0.209	0.032	0.196
19.26	-0.313	0.000	-0.412	-0.212	0.032	0.198
19.27	-0.234	0.000	-0.412	-0.213	0.032	0.200
19.28	-0.078	0.000	-0.412	-0.213	0.032	0.203
19.29	-0.078	0.000	-0.412	-0.213	0.032	0.205
19.30	-0.078	0.000	-0.412	-0.213	0.032	0.207
19.31	-0.078	0.000	-0.412	-0.213	0.032	0.210
19.32	-0.078	0.000	-0.471	-0.213	0.032	0.211
19.33	-0.078	0.000	-0.589	-0.213	0.032	0.212
19.34	-0.078	0.000	-0.589	-0.213	0.032	0.213
19.35	-0.078	0.000	-0.648	-0.213	0.032	0.213

Figure 6.6.2.7 Digital data for event 19.6

[ ] = baseline which is subtracted for peaks and numerical integration

Yeardate: 79219 Time: 09:41:31 M.S.T.

Time (μs)	$\partial B_E/\partial t$ (T/s)	$\partial B_N/\partial t$ (T/s)	$Z_o \partial D_z/\partial t$ (T/s)	B_E (μT)	B_N (μT)	$Z_o D_z$ (μT)
19.40	-0.078	0.000	-0.648	-0.000	0.000	0.000
19.41	-0.078	0.000	[-0.648]	-0.000	0.000	0.000
19.42	-0.078	[0.000]	-0.589	-0.000	0.000	0.001
19.43	[-0.078]	0.156	-0.589	-0.000	0.002	0.001
19.44	-0.313	0.156	-0.589	-0.002	0.003	0.002
19.45	-0.313	0.156	-0.589	-0.005	0.005	0.002
19.46	-0.391	0.156	-0.530	-0.008	0.006	0.004
19.47	-0.391	0.234	-0.530	-0.011	0.009	0.005
19.48	-0.391	0.234	-0.412	-0.014	0.011	0.007
19.49	-0.625	0.234	-0.412	-0.020	0.013	0.009
19.50	-0.625	0.234	-0.353	-0.025	0.016	0.012
19.51	-0.547	0.156	-0.295	-0.030	0.017	0.016
19.52	-0.547	0.156	-0.295	-0.034	0.019	0.019
19.53	-0.547	0.156	-0.118	-0.039	0.020	0.025
19.54	-0.625	0.156	-0.177	-0.045	0.022	0.029
19.55	-0.625	0.156	-0.177	-0.050	0.023	0.034
19.56	-0.391	0.156	-0.177	-0.053	0.025	0.039
19.57	-0.469	0.156	-0.177	-0.057	0.027	0.044
19.58	-0.469	0.156	0.000	-0.061	0.028	0.050
19.59	-0.469	0.156	-0.177	-0.065	0.030	0.055
19.60	-0.391	0.156	-0.236	-0.068	0.031	0.059
19.61	-0.313	0.156	-0.295	-0.070	0.033	0.062
19.62	-0.313	0.156	-0.236	-0.073	0.034	0.067
19.63	-0.313	0.156	-0.236	-0.075	0.036	0.071
19.64	-0.313	0.156	-0.236	-0.077	0.038	0.075
19.65	-0.313	0.156	-0.353	-0.080	0.039	0.078
19.66	-0.313	0.156	-0.353	-0.082	0.041	0.081
19.67	-0.313	0.156	-0.412	-0.084	0.042	0.083
19.68	-0.313	0.078	-0.412	-0.087	0.043	0.085
19.69	-0.313	0.156	-0.353	-0.089	0.045	0.088
19.70	-0.313	0.078	-0.412	-0.091	0.045	0.091
19.71	-0.313	0.078	-0.412	-0.094	0.046	0.093
19.72	-0.234	0.078	-0.412	-0.095	0.047	0.095
19.73	-0.234	0.156	-0.412	-0.097	0.048	0.098
19.74	-0.234	0.156	-0.412	-0.098	0.050	0.100
19.75	-0.156	0.156	-0.471	-0.099	0.052	0.102
19.76	-0.156	0.156	-0.530	-0.100	0.053	0.103
19.77	-0.156	0.156	-0.530	-0.101	0.055	0.104
19.78	-0.156	0.234	-0.530	-0.102	0.057	0.105
19.79	-0.156	0.234	-0.589	-0.102	0.059	0.106
19.80	-0.156	0.234	-0.589	-0.103	0.062	0.107
19.81	-0.156	0.156	-0.589	-0.104	0.063	0.107
19.82	-0.156	0.156	-0.589	-0.105	0.065	0.108

Figure 6.6.2.7 Digital data for event 19.6 (continued)

Time (μs)	$\partial B_E/\partial t$ (T/s)	$\partial B_N/\partial t$ (T/s)	$Z_o \partial D_z/\partial t$ (T/s)	B_E (μT)	B_N (μT)	$Z_o D_z$ (μT)
19.83	-0.156	0.156	-0.589	-0.106	0.066	0.108
19.84	-0.156	0.156	-0.648	-0.106	0.068	0.108
19.85	-0.156	0.156	-0.648	-0.107	0.070	0.108
19.86	-0.156	0.156	-0.589	-0.108	0.071	0.109
19.87	-0.234	0.156	-0.589	-0.109	0.073	0.110
19.88	-0.234	0.156	-0.589	-0.111	0.074	0.110
19.89	-0.234	0.156	-0.589	-0.113	0.076	0.111
19.90	-0.234	0.156	-0.589	-0.114	0.077	0.111
19.91	-0.156	0.156	-0.530	-0.115	0.079	0.113
19.92	-0.156	0.156	-0.530	-0.116	0.080	0.114
19.93	-0.156	0.156	-0.530	-0.116	0.082	0.115
19.94	-0.078	0.156	-0.530	-0.116	0.084	0.116
19.95	-0.078	0.156	-0.589	-0.116	0.085	0.117
19.96	-0.078	0.156	-0.589	-0.116	0.087	0.117
19.97	-0.078	0.156	-0.648	-0.116	0.088	0.117
19.98	-0.078	0.156	-0.707	-0.116	0.090	0.117
19.99	-0.078	0.156	-0.707	-0.116	0.091	0.116
20.00	-0.078	0.078	-0.707	-0.116	0.092	0.115
20.01	0.000	0.000	-0.707	-0.116	0.092	0.115

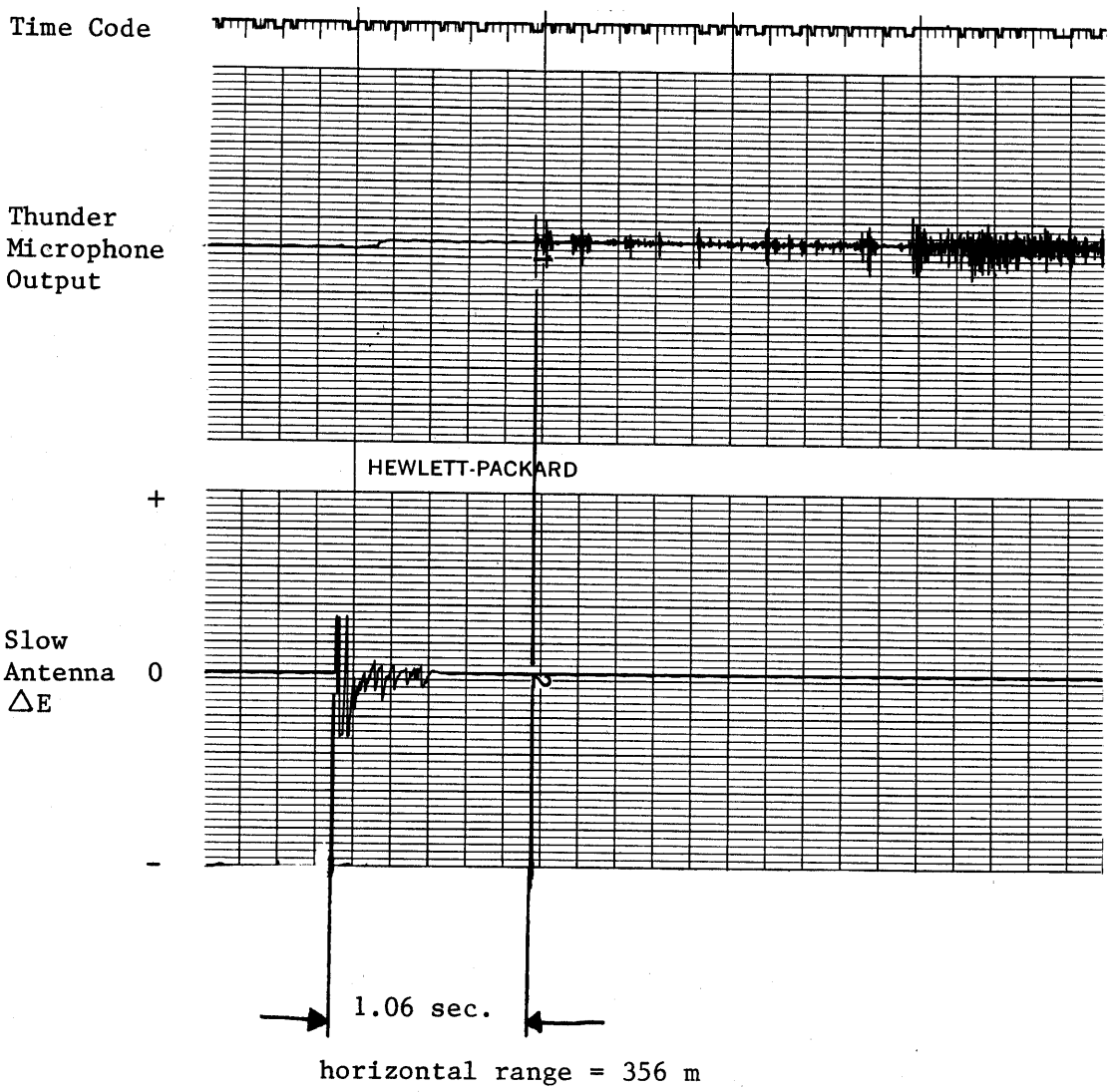

Figure 6.6.3 Slow E field change and thunder microphone record of midrange return stroke

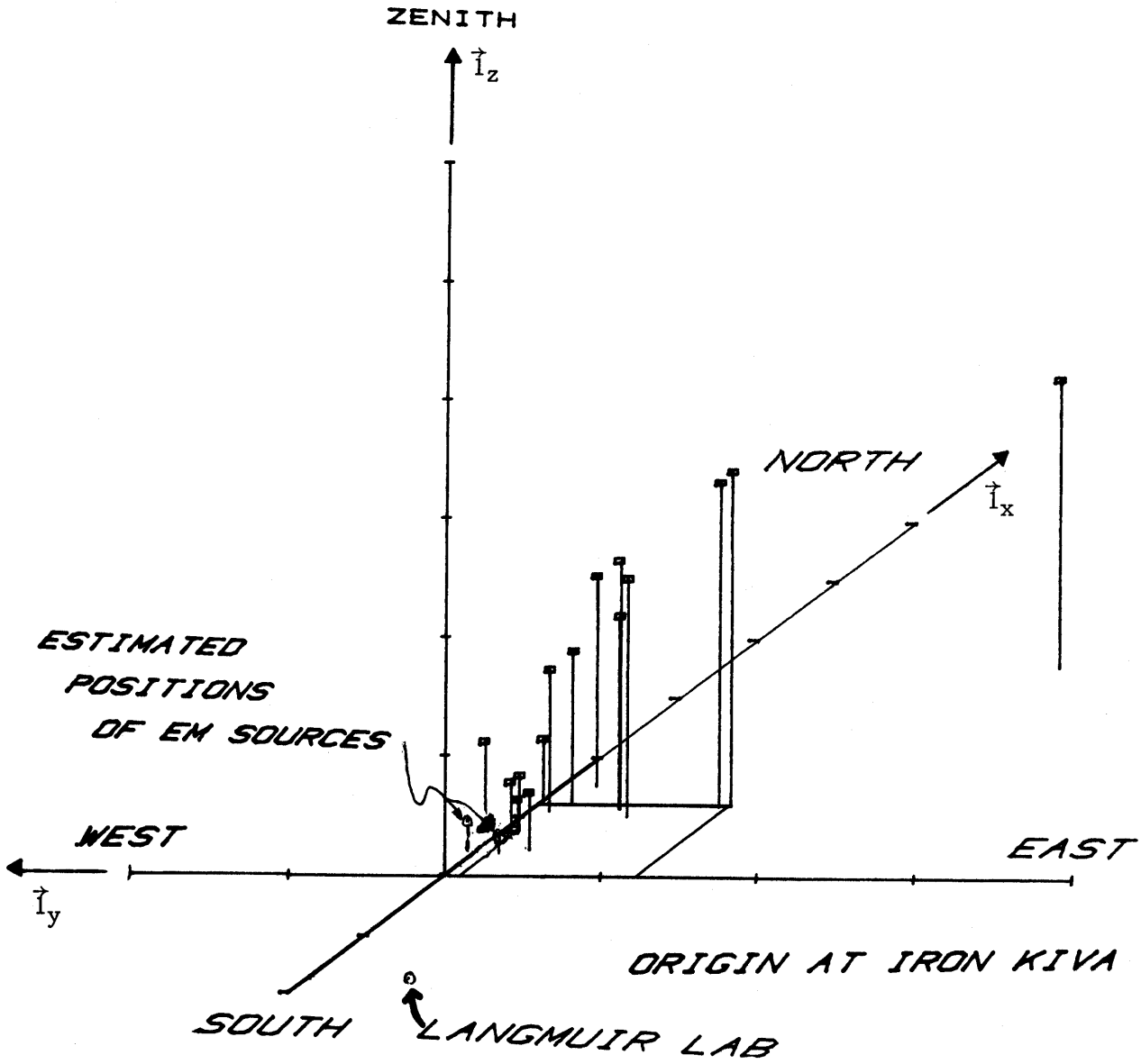

ticks on axes at 1 km intervals

Date : 79219 Time : 9:41:31

Figure 6.6.4 Acoustic location of midrange return stroke

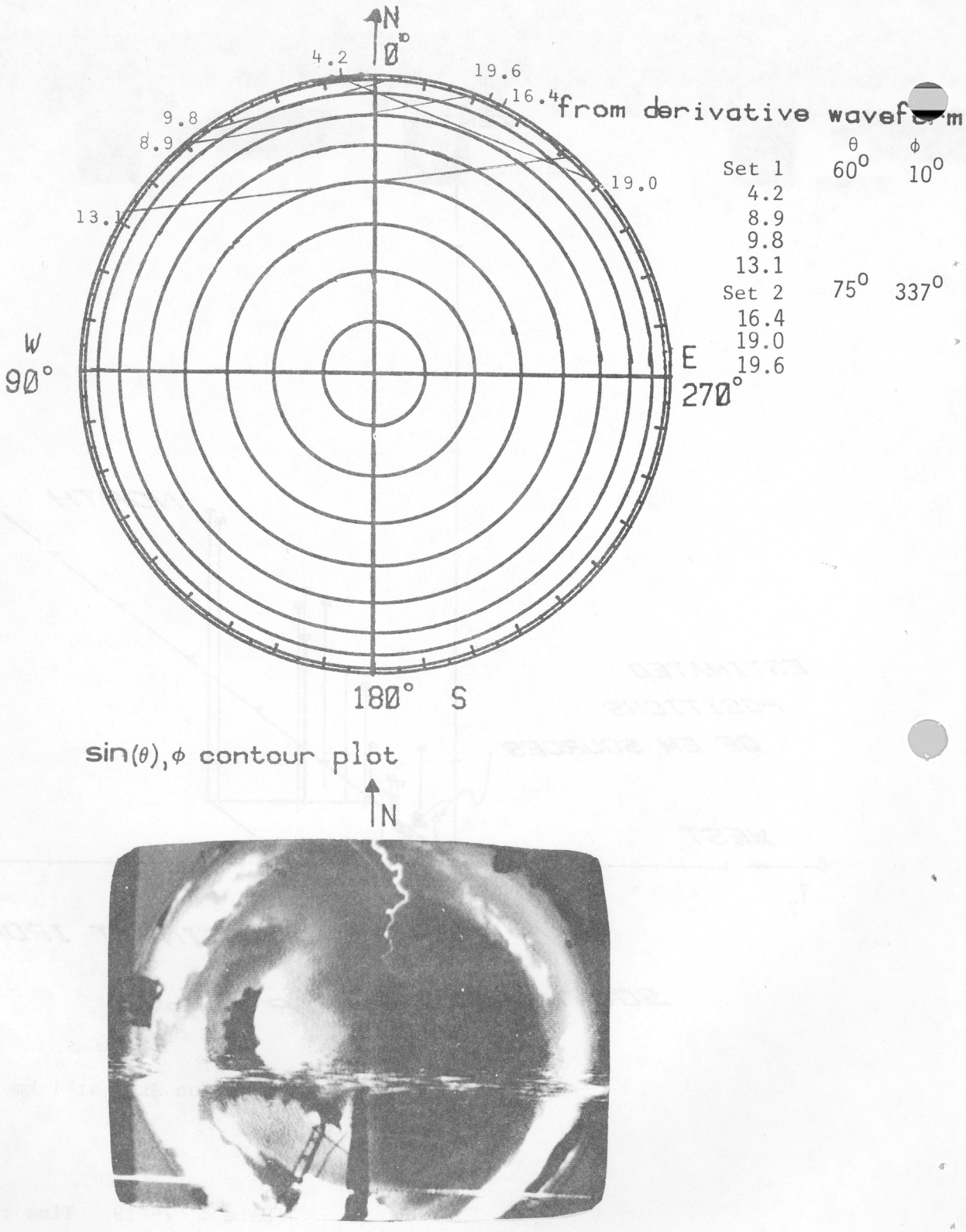

Figure 6.6.5A sin(θ),φ contours for midrange return stroke derivative waveform and whole-sky videotape photograph

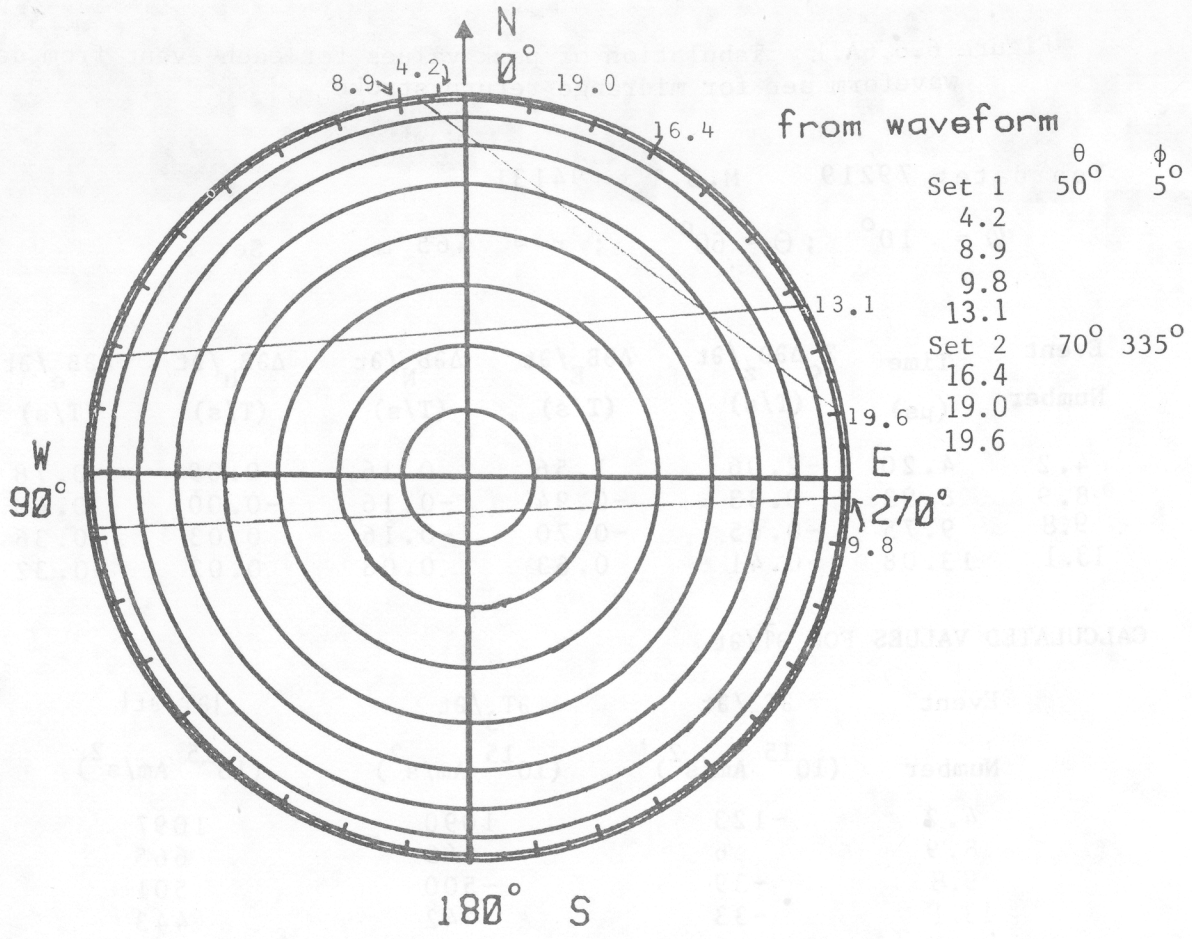

Figure 6.6.5B sin(θ),φ contours for midrange return stroke waveform and whole-sky videotape photograph

Figure 6.6.6A.1 Tabulation of peak values for each event from derivative waveform set for midrange return stroke

Yeardate: 79219 M.S.T.: 94131

$\phi = 10^{o}$; $\theta = 60^{o}$; r = 465 m Set 1

Event Number	Time (μs)	$Z_o \Delta\partial D_z/\partial t$ (T/s)	$\Delta\partial B_E/\partial t$ (T/s)	$\Delta\partial B_N/\partial t$ (T/s)	$\Delta\partial B_h/\partial t$ (T/s)	$\Delta\partial B_e/\partial t$ (T/s)	$\lvert\Delta\partial\vec{B}/\partial t\rvert$ (T/s)
4.2	4.20	-2.06	1.56	0.16	0.09	-0.78	0.79
8.9	8.93	0.83	-0.94	-0.16	-0.00	0.48	0.48
9.8	9.75	-0.65	-0.70	-0.16	0.03	0.36	0.36
13.1	13.08	-0.41	0.63	0.08	0.02	-0.32	0.32

CALCULATED VALUES FOR $\partial\vec{T}/\partial t$

Event Number	$\partial T_2/\partial t$ (10^{15} Am/s^2)	$\partial T_3/\partial t$ (10^{15} Am/s^2)	$\lvert\partial\vec{T}/\partial t\rvert$ (10^{15} Am/s^2)	α (deg)
4.2	-123	1090	1097	6
8.9	6	-665	665	181
9.8	-39	-500	501	176
13.1	-33	442	443	4

Figure 6.6.6A.2 Tabulation of peak values for each event from derivative waveform set for midrange return stroke

Yeardate: 79219 M.S.T.: 94131

$\phi = 337^{o}$; $\theta = 75^{o}$; r = 379 m Set 2

Event Number	Time (μs)	$Z_o \Delta\partial D_z/\partial t$ (T/s)	$\Delta\partial B_E/\partial t$ (T/s)	$\Delta\partial B_N/\partial t$ (T/s)	$\Delta\partial B_h/\partial t$ (T/s)	$\Delta\partial B_e/\partial t$ (T/s)	$\lvert\Delta\partial\vec{B}/\partial t\rvert$ (T/s)
16.4	16.37	0.88	-0.63	0.31	-0.06	0.35	0.36
19.0	18.97	0.59	-0.63	0.23	0.05	0.33	0.34
19.6	19.58	0.65	-0.55	0.23	0.00	0.30	0.30

CALCULATED VALUES FOR $\partial\vec{T}/\partial t$

Event Number	$\partial T_2/\partial t$ (10^{15} Am/s^2)	$\partial T_3/\partial t$ (10^{15} Am/s^2)	$\lvert\partial\vec{T}/\partial t\rvert$ (10^{15} Am/s^2)	α (deg)
16.4	65	-398	404	189
19.0	-57	-381	385	171
19.6	-5	-339	339	179

Figure 6.6.6B.1 Tabulation of peak values for each event from waveform set for midrange return stroke

Yeardate: 79219 M.S.T.: 94131

ϕ = 5° ; θ = 50° ; r = 465 m Set 1

Event Number	Time (μs)	$Z_o \Delta D_z$ (μT)	ΔB_E (μT)	ΔB_N (μT)	ΔB_h (μT)	ΔB_e (μT)	$\lvert\Delta\vec{B}\rvert$ (μT)
4.2	4.20	-0.84	0.53	0.04	0.00	-0.27	0.27
8.9	8.93	0.50	-0.46	-0.08	0.03	0.23	0.23
9.8	9.75	-0.05	-0.50	-0.02	-0.02	0.25	0.25
13.1	13.09	-0.05	0.13	0.01	0.00	-0.07	0.07

CALCULATED VALUES FOR $\vec{1}_t \cdot \vec{T}$

Event Number	T_2 (10^9 Am/s)	T_3 (10^9 Am/s)	$\lvert\vec{T}\rvert$ (10^9 Am/s)	α (deg)
4.2	-7	370	371	1
8.9	-43	-324	327	172
9.8	26	-348	349	184
13.1	-1	91	91	1

Figure 6.6.6B.2 Tabulation of peak values for each event from waveform set for midrange return stroke

Yeardate: 79219 M.S.T.: 94131

ϕ = 335° ; θ = 70° ; r = 379 m Set 2

Event Number	Time (μs)	$Z_o \Delta D_z$ (μT)	ΔB_E (μT)	ΔB_N (μT)	ΔB_h (μT)	ΔB_e (μT)	$\lvert\Delta\vec{B}\rvert$ (μT)
16.4	16.37	0.31	-0.14	0.08	-0.02	0.08	0.08
19.0	19.00	0.21	-0.21	0.03	0.09	0.10	0.14
19.6	19.55	0.11	-0.12	0.09	-0.05	0.07	0.09

CALCULATED VALUES FOR $\vec{1}_t \cdot \vec{T}$

Event Number	T_2 (10^9 Am/s)	T_3 (10^9 Am/s)	$\lvert\vec{T}\rvert$ (10^9 Am/s)	α (deg)
16.4	22	-91	94	194
19.0	-102	-115	154	138
19.6	51	-83		

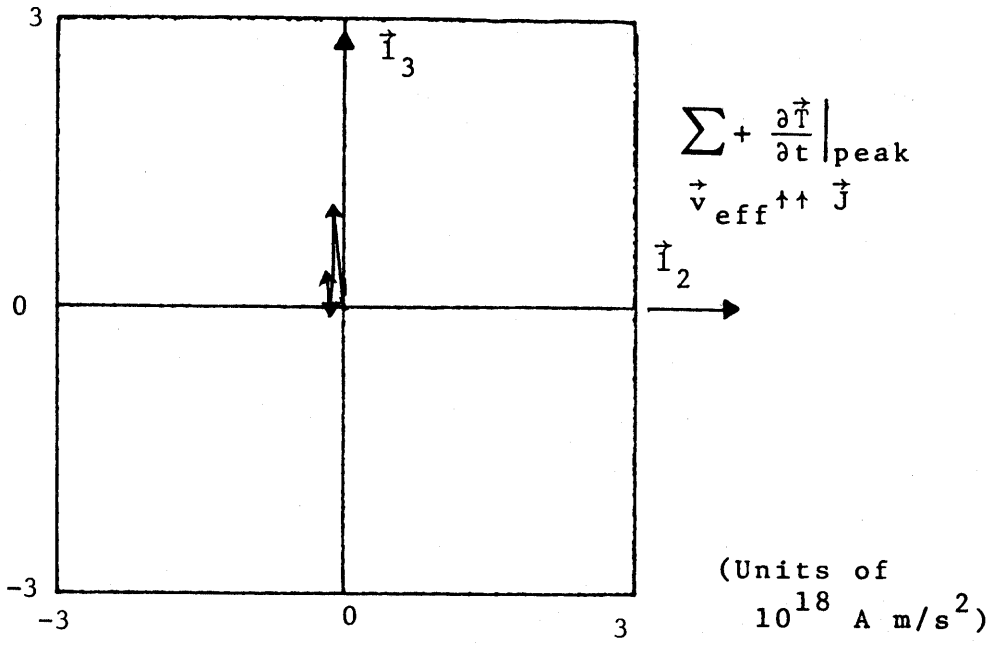

Effective reconstruction of positive streamer

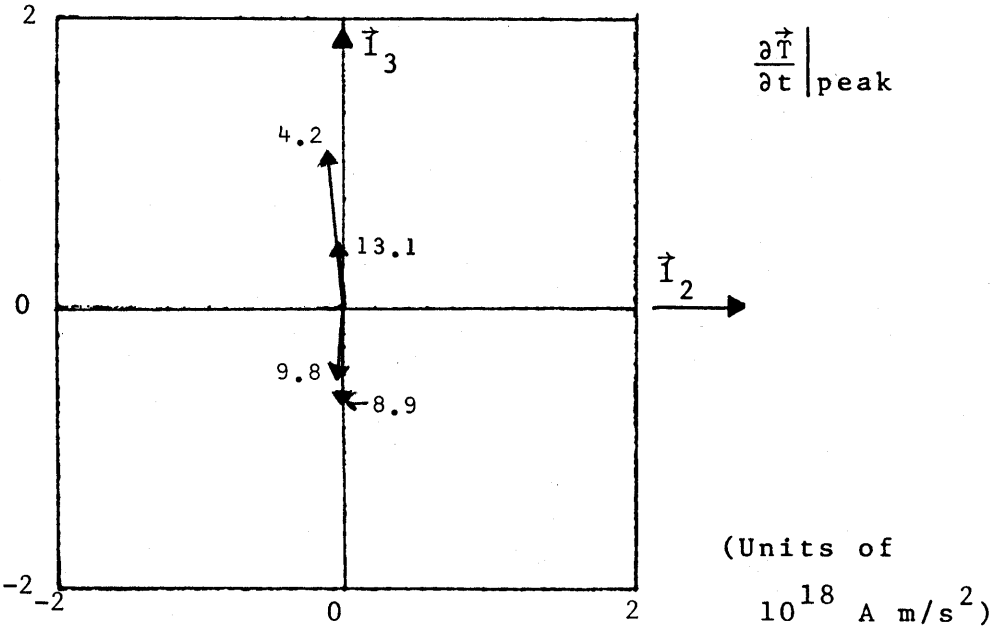

Peaks of $\partial\vec{T}/\partial t$

ϕ = 10^o θ = 60^o r = 411 m Set 1

Date: 79219 M.S.T.: 09:41:31

Figure 6.6.7A.1 $\partial\vec{T}/\partial t$ for midrange return stroke

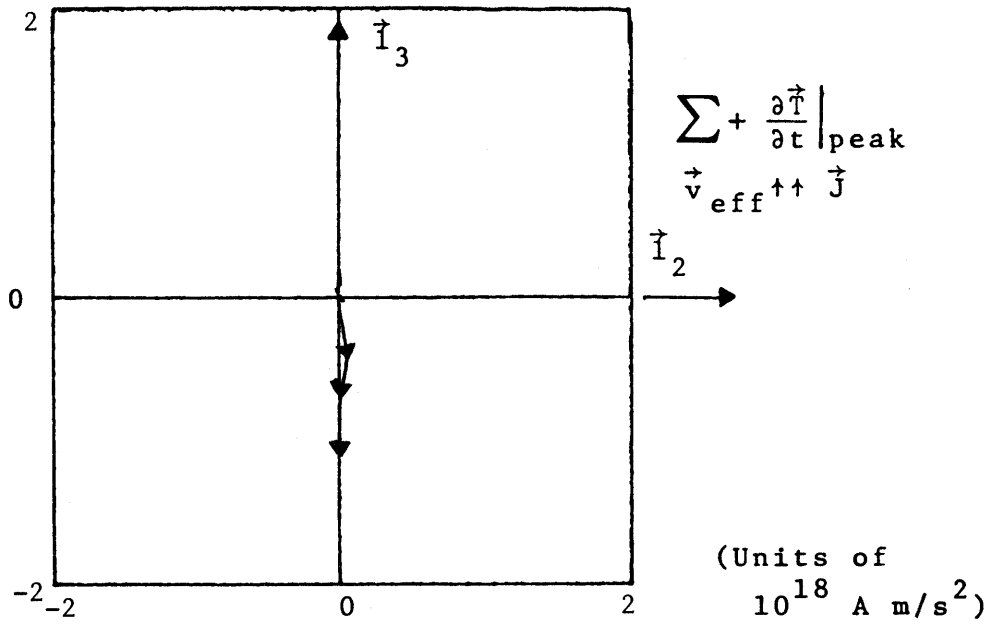

Effective reconstruction of positive streamer

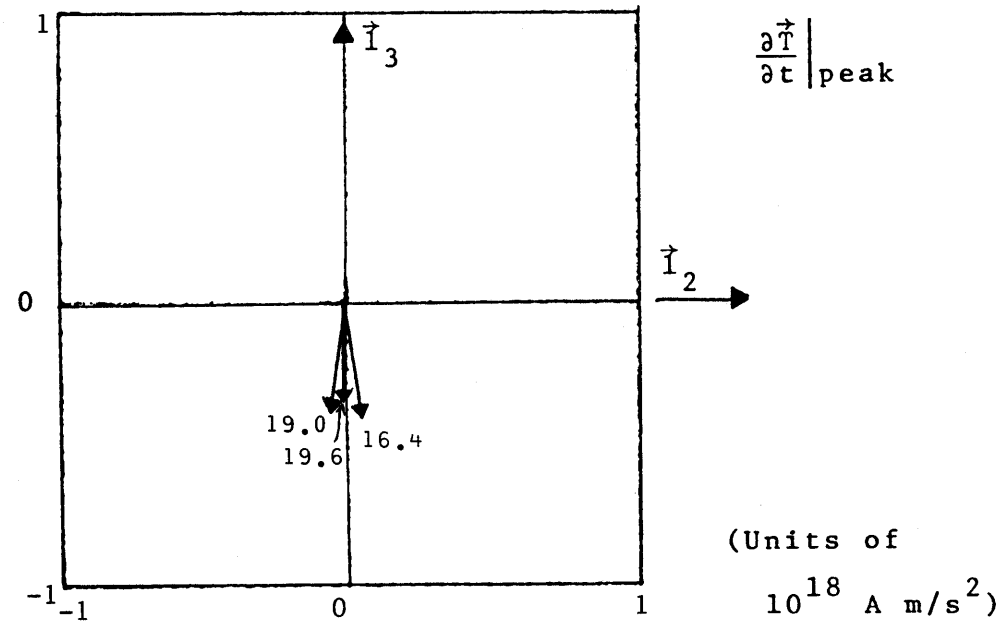

Peaks of $\partial\vec{T}/\partial t$

ϕ = 337° θ = 75° r = 369 m Set 2

Date: 79219 M.S.T.:

Figure 6.6.7A.2 $\partial\vec{T}/\partial t$ for midrange return stroke

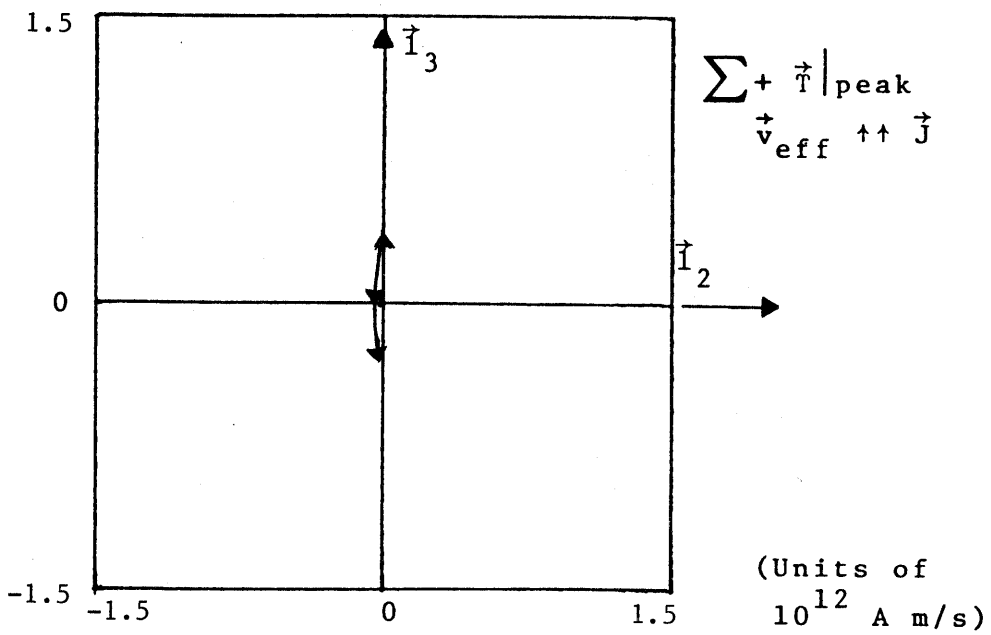

Effective reconstruction of positive streamer

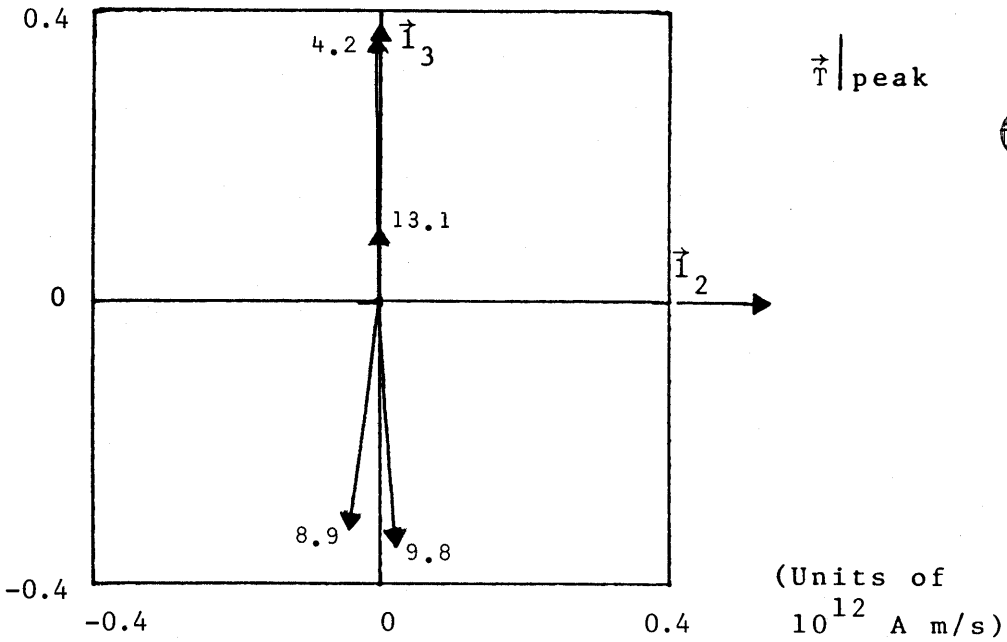

Peaks of $\vec{T}$

$\phi = 5^{o}$ $\theta = 50^{o}$ r = 465 m Set 1

Date: 79219 M.S.T.: 09:41:31

Figure 6.6.7B.1 $\vec{T}$ for midrange return stroke

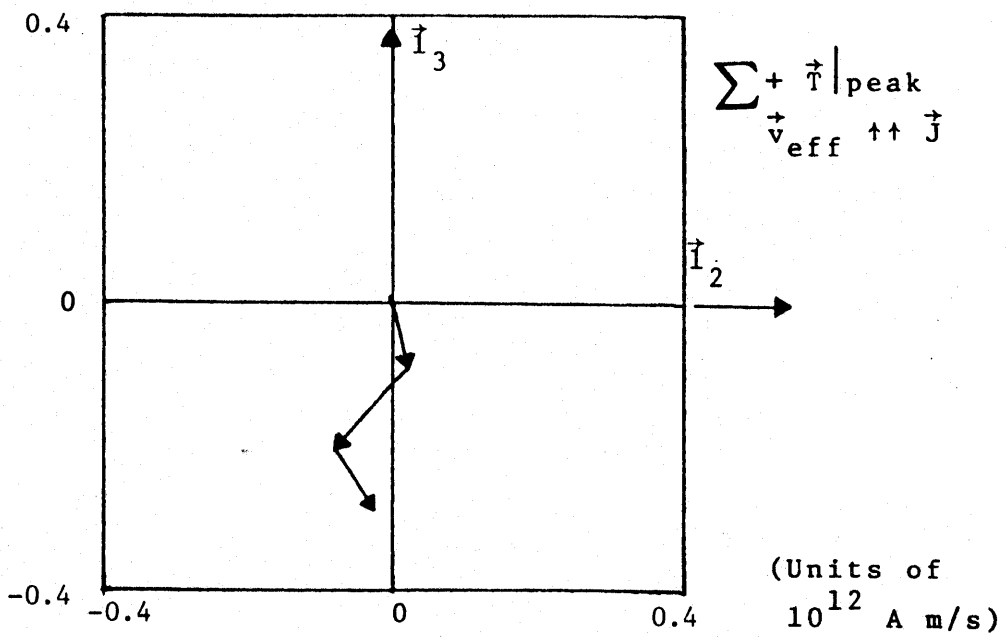

Effective reconstruction of positive streamer

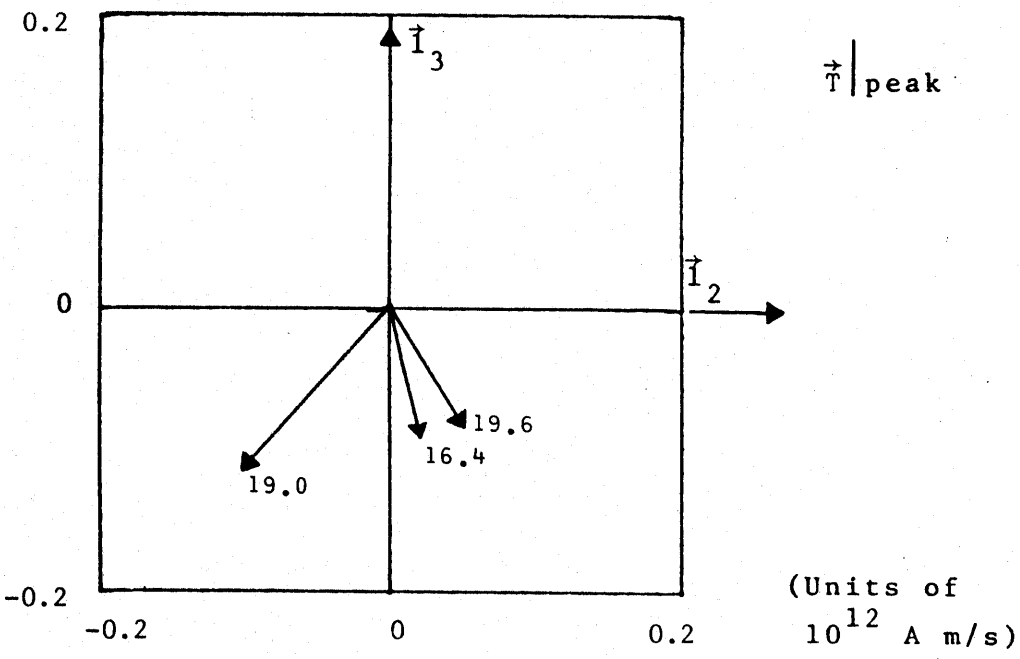

Peaks of $\vec{T}$

$\phi = 335^{o}$ $\theta = 70^{o}$ r = 379 m Set 2

Date: 79219 M.S.T.: 09:41:31

Figure 6.6.7B.2 $\vec{T}$ for midrange return stroke

6.7 Midrange Return Stroke

Our seventh example is given in Figures 6.7.•••. This is labelled "midrange return stroke". Figures 6.7.1A and 6.7.1B show the derivative fields and fields for the 20 μs record.

Figure 6.7.3 shows the slow electric field and thunder microphone records, from which a horizontal range of 1115 m is estimated. The acoustic source reconstruction in Figure 6.7.4 shows a complex strike extending to 4 km height with significant components extending 4 km to the northeast and 2.5 km to the south; the strike reaches the ground approximately north of the Kiva.

The θ , ϕ contours give four approximate sets of contour intersections, all generally north as seen in figures 6.7.5 aided by figures 6.7.7. These would appear to correspond to signals from different locations along the arc channel.

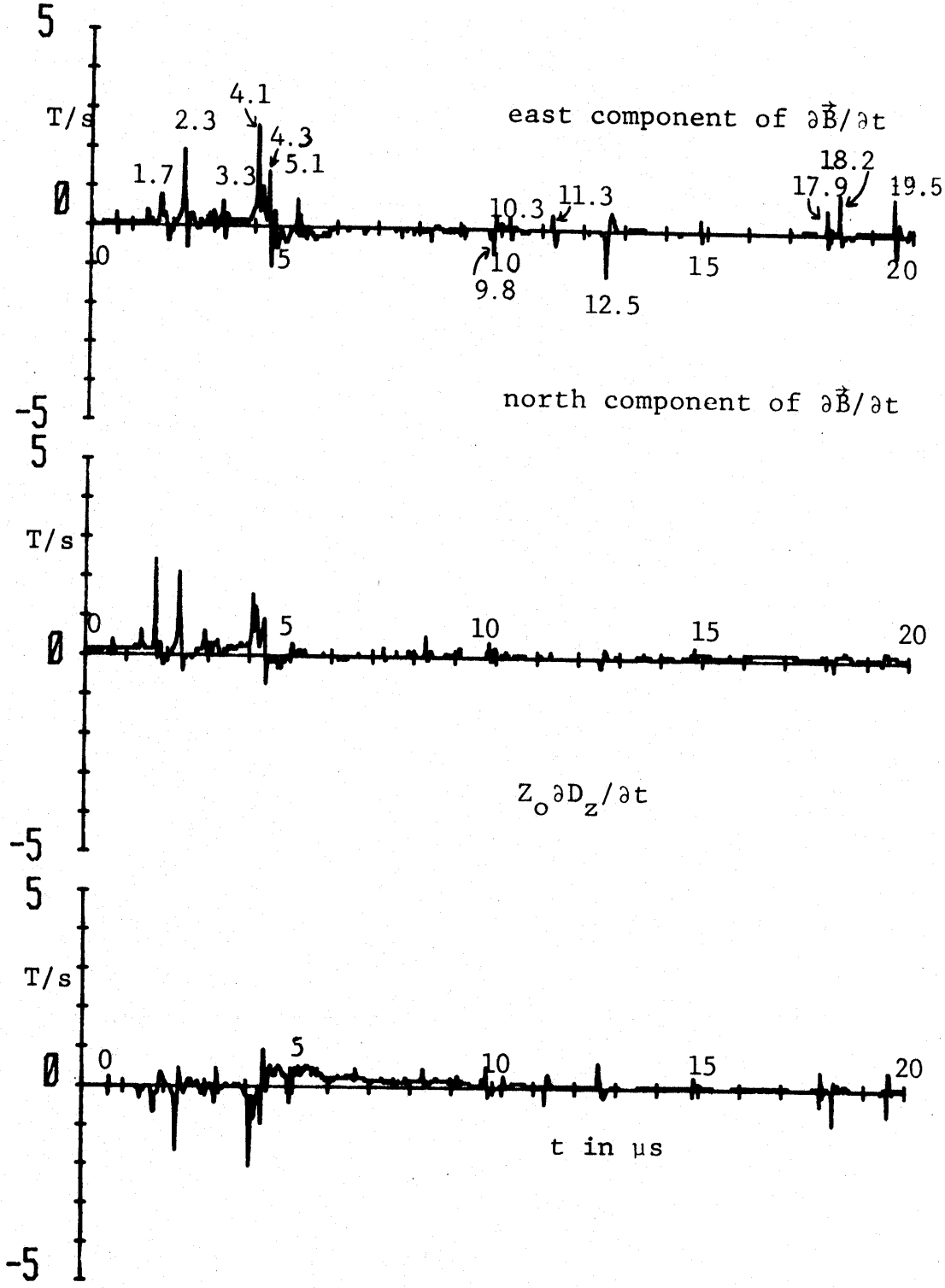

Date: 79219 M.S.T.: 0953:39

Figure 6.7.1A Derivative fields from midrange return stroke

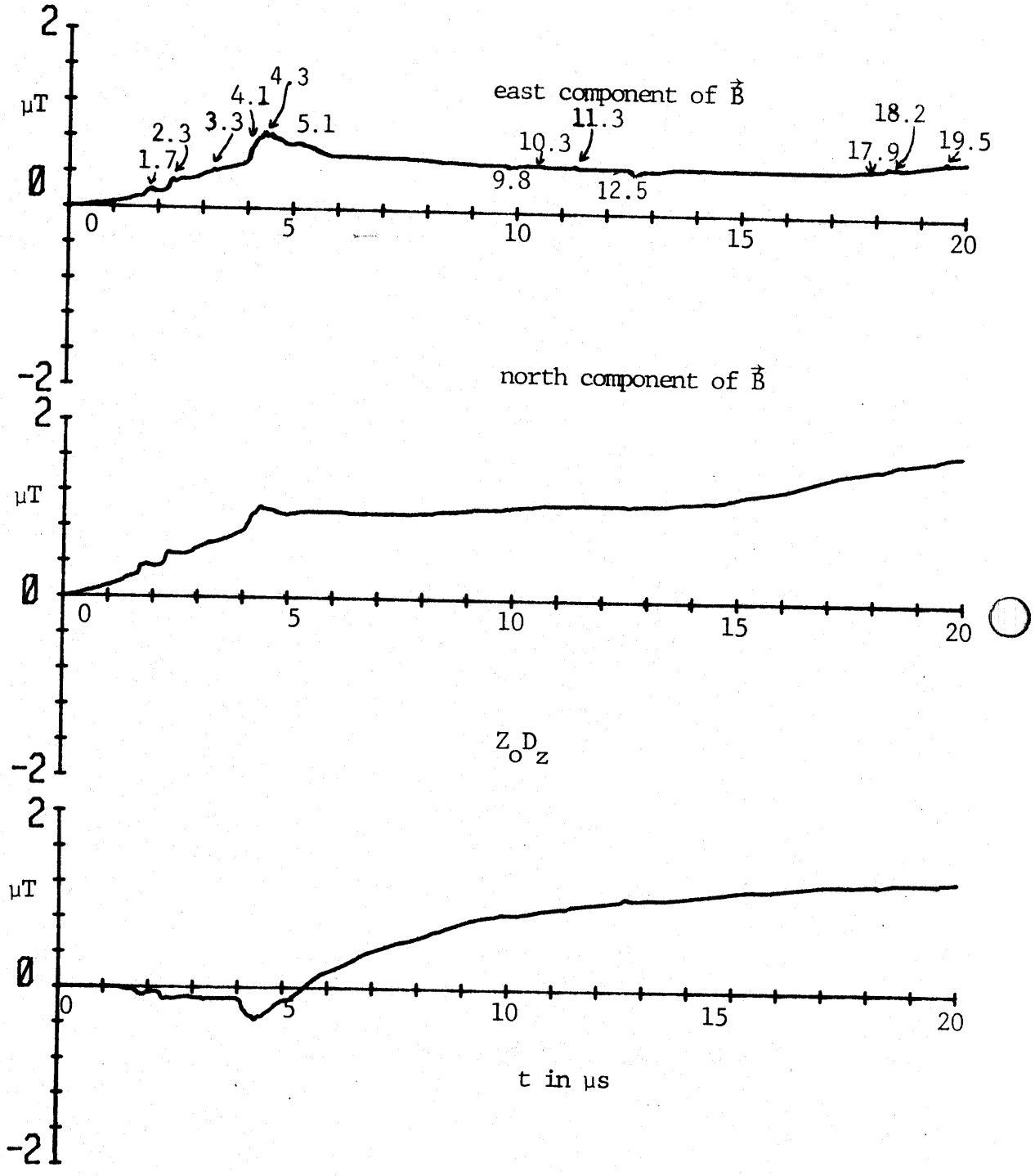

Date: 79219 M.S.T.: 0953:39

Figure 6.7.1B Fields from midrange return stroke

Figure 6.7.2.1 Digital data for event 1.7

[ ] = baseline which is subtracted for peaks and numerical integration

Yeardate: 79219 Time: 09:53:39 M.S.T.

Time (μs)	$\partial B_E/\partial t$ (T/s)	$\partial B_N/\partial t$ (T/s)	$Z_o \partial D_z/\partial t$ (T/s)	B_E (μT)	B_N (μT)	$Z_o D_z$ (μT)
1.63	0.000	0.156	0.000	0.000	0.000	0.000
1.64	0.000	0.156	0.000	0.000	0.000	0.000
1.65	0.078	0.313	0.000	0.001	0.002	0.000
1.66	0.156	0.313	0.000	0.002	0.003	0.000
1.67	0.313	0.547	-0.059	0.005	0.007	-0.001
1.68	0.547	0.859	-0.118	0.011	0.014	-0.002
1.69	0.625	1.797	-0.177	0.017	0.030	-0.004
1.70	0.703	2.422	-0.412	0.024	0.053	-0.008
1.71	0.703	2.109	-0.471	0.031	0.073	-0.012
1.72	0.703	1.172	-0.589	0.038	0.083	-0.018
1.73	0.703	0.234	-0.648	0.045	0.084	-0.025
1.74	0.469	0.000	-0.648	0.050	0.082	-0.031
1.75	0.234	-0.078	-0.648	0.052	0.080	-0.038
1.76	0.234	-0.078	-0.648	0.055	0.077	-0.044
1.77	0.156	0.000	-0.412	0.056	0.076	-0.048
1.78	0.156	0.234	-0.177	0.058	0.077	-0.050
1.79	0.156	0.313	-0.177	0.059	0.078	-0.052
1.80	0.234	0.313	-0.177	0.062	0.080	-0.054
1.81	0.234	0.313	-0.177	0.064	0.081	-0.055
1.82	0.156	0.313	-0.177	0.066	0.083	-0.057
1.83	0.078	0.234	-0.177	0.066	0.084	-0.059
1.84	0.000	0.234	-0.177	0.066	0.084	-0.061
1.85	-0.078	0.000	-0.118	0.066	0.083	-0.062
1.86	-0.313	-0.078	-0.059	0.063	0.081	-0.062
1.87	-0.391	-0.078	0.000	0.059	0.078	-0.062
1.88	-0.469	-0.234	0.059	0.054	0.074	-0.061
1.89	-0.469	-0.234	0.236	0.050	0.070	-0.059
1.90	-0.469	-0.234	0.295	0.045	0.066	-0.056
1.91	-0.469	-0.234	0.295	0.040	0.062	-0.053
1.92	-0.391	-0.156	0.353	0.036	0.059	-0.050
1.93	-0.313	-0.156	0.353	0.033	0.056	-0.046
1.94	-0.313	-0.156	0.353	0.030	0.053	-0.043
1.95	-0.234	-0.078	0.295	0.028	0.051	-0.040
1.96	-0.156	-0.078	0.295	0.026	0.048	-0.037
1.97	-0.078	-0.078	0.236	0.025	0.046	-0.034
1.98	-0.078	-0.078	0.236	0.025	0.044	-0.032
1.99	-0.078	-0.078	0.177	0.024	0.041	-0.030
2.00	-0.078	-0.078	0.118	0.023	0.039	-0.029
2.01	-0.078	-0.078	0.118	0.022	0.037	-0.028
2.02	-0.078	0.000	0.118	0.022	0.035	-0.027
2.03	0.000	0.000	0.118	0.022	0.034	-0.025
2.04	0.000	0.000	0.059	0.022	0.032	-0.025
2.05	0.000	0.000	0.059	0.022	0.030	-0.024
2.06	0.000	0.000	0.059	0.022	0.029	-0.024
2.07	0.000	0.000	0.000	0.022	0.027	-0.024
2.08	0.000	0.000	0.000	0.022	0.026	-0.024
2.09	0.000	0.000	0.000	0.022	0.024	-0.024
2.10	0.078	0.078	0.000	0.022	0.023	-0.024
2.11	0.078	0.078	0.000	0.023	0.023	-0.024

Figure 6.7.2.2 Digital data for event 2.3

[ ] = baseline which is subtracted for peaks and numerical integrati

Yeardate: 79219 Time: 09:53:39 M.S.T.

Time (μs)	$\partial B_E/\partial t$ (T/s)	$\partial B_N/\partial t$ (T/s)	$Z_o \partial D_z/\partial t$ (T/s)	B_E (μT)	B_N (μT)	$Z_o D_z$ (μT)
2.08	0.000	0.000	0.000	0.000	0.000	0.000
2.09	0.000	0.000	0.000	0.000	0.000	0.000
2.10	0.078	0.078	0.000	0.001	0.001	0.000
2.11	0.078	0.078	0.000	0.002	0.002	0.000
2.12	0.078	0.156	0.000	0.002	0.003	0.000
2.13	0.078	0.156	0.000	0.003	0.005	0.000
2.14	0.156	0.156	0.000	0.005	0.006	0.000
2.15	0.156	0.156	0.000	0.006	0.008	0.000
2.16	0.156	0.234	0.000	0.008	0.010	0.000
2.17	0.234	0.234	-0.118	0.010	0.013	-0.001
2.18	0.234	0.234	-0.118	0.013	0.015	-0.002
2.19	0.234	0.313	-0.118	0.015	0.018	-0.004
2.20	0.313	0.313	-0.177	0.018	0.021	-0.005
2.21	0.313	0.313	-0.177	0.021	0.024	-0.007
2.22	0.547	0.391	-0.177	0.027	0.028	-0.009
2.23	0.547	0.469	-0.236	0.032	0.033	-0.011
2.24	0.938	0.547	-0.236	0.041	0.038	-0.014
2.25	1.797	0.859	-0.412	0.059	0.047	-0.018
2.26	1.875	1.250	-0.471	0.078	0.059	-0.022
2.27	1.797	1.875	-0.884	0.096	0.078	-0.031
2.28	0.938	2.109	-1.414	0.105	0.099	-0.045
2.29	0.625	1.875	-1.649	0.112	0.118	-0.062
2.30	0.547	1.250	-0.943	0.117	0.130	-0.071
2.31	0.234	0.938	-0.648	0.120	0.140	-0.078
2.32	0.000	0.859	-0.471	0.120	0.148	-0.082
2.33	-0.625	0.625	-0.412	0.113	0.155	-0.087
2.34	-0.625	0.313	-0.177	0.107	0.158	-0.088
2.35	-0.625	0.000	0.059	0.101	0.158	-0.088
2.36	-0.625	-0.078	0.295	0.095	0.157	-0.085
2.37	-0.391	-0.313	0.471	0.091	0.154	-0.080
2.38	-0.078	-0.391	0.353	0.090	0.150	-0.077
2.39	-0.078	-0.313	0.295	0.089	0.147	-0.074
2.40	0.000	-0.313	0.236	0.089	0.144	-0.072
2.41	0.234	-0.078	0.059	0.092	0.143	-0.071
2.42	0.234	-0.078	0.059	0.094	0.142	-0.070
2.43	0.234	-0.078	0.000	0.096	0.142	-0.070
2.44	0.234	-0.078	-0.059	0.099	0.141	-0.071
2.45	0.234	-0.078	-0.059	0.101	0.140	-0.072
2.46	0.234	0.000	-0.118	0.103	0.140	-0.073
2.47	0.234	0.000	-0.118	0.106	0.140	-0.074
2.48	0.234	0.000	-0.118	0.108	0.140	-0.075
2.49	0.156	0.000	-0.177	0.110	0.140	-0.077
2.50	0.078	0.000	-0.118	0.110	0.140	-0.078
2.51	0.078	0.000	-0.118	0.111	0.140	-0.079
2.52	0.000	0.000	-0.059	0.111	0.140	-0.080

Figure 6.7.2.2 Digital data for event 2.3 (continued)

Time (μs)	$\partial B_E/\partial t$ (T/s)	$\partial B_N/\partial t$ (T/s)	$Z_o \partial D_z/\partial t$ (T/s)	B_E (μT)	B_N (μT)	$Z_o D_z$ (μT)
2.53	0.000	0.000	-0.059	0.111	0.140	-0.080
2.54	-0.078	0.000	-0.059	0.110	0.140	-0.081
2.55	-0.078	0.000	0.059	0.110	0.140	-0.080
2.56	-0.078	0.000	0.059	0.109	0.140	-0.080
2.57	-0.156	0.000	0.059	0.107	0.140	-0.079
2.58	-0.156	0.000	0.118	0.106	0.140	-0.078
2.59	-0.078	-0.078	0.177	0.105	0.139	-0.076
2.60	-0.156	-0.078	0.177	0.103	0.138	-0.074
2.61	-0.078	-0.078	0.118	0.103	0.138	-0.073
2.62	-0.078	0.000	0.177	0.102	0.138	-0.072
2.63	-0.078	0.000	0.177	0.101	0.138	-0.070
2.64	-0.078	0.000	0.118	0.100	0.138	-0.069
2.65	0.078	0.000	0.118	0.101	0.138	-0.067
2.66	-0.156	0.000	0.177	0.099	0.138	-0.066
2.67	-0.078	0.000	0.177	0.099	0.138	-0.064
2.68	0.078	0.000	0.059	0.099	0.138	-0.063
2.69	0.078	0.000	0.059	0.100	0.138	-0.063

Figure 6.7.2.3 Digital data for event 3.3

[ ] = baseline which is subtracted for peaks and numerical integration

Yeardate: 79219 Time: 09:53:39 M.S.T.

Time (μs)	$\partial B_E/\partial t$ (T/s)	$\partial B_N/\partial t$ (T/s)	$Z_o \partial D_z/\partial t$ (T/s)	B_E (μT)	B_N (μT)	$Z_o D_z$ (μT)
3.12	0.000	0.234	0.059	0.000	0.000	-0.000
3.13	[0.000]	[0.234]	0.059	0.000	0.000	-0.000
3.14	0.078	0.313	0.059	0.001	0.001	-0.000
3.15	0.156	0.313	0.059	0.002	0.002	-0.000
3.16	0.156	0.313	[0.059]	0.004	0.002	-0.000
3.17	0.156	0.313	0.000	0.005	0.003	-0.001
3.18	0.156	0.313	-0.118	0.007	0.004	-0.002
3.19	0.234	0.313	-0.059	0.009	0.005	-0.004
3.20	0.547	0.313	-0.059	0.015	0.006	-0.005
3.21	0.547	0.313	-0.118	0.020	0.006	-0.006
3.22	0.547	0.391	-0.236	0.026	0.008	-0.009
3.23	0.000	0.234	-0.412	0.026	0.008	-0.014
3.24	0.000	0.234	-0.412	0.026	0.008	-0.019
3.25	-0.313	0.156	-0.412	0.023	0.007	-0.024
3.26	-0.391	0.156	0.000	0.019	0.006	-0.024
3.27	-0.313	0.000	0.059	0.016	0.004	-0.024
3.28	-0.391	0.000	0.471	0.012	0.002	-0.020
3.29	-0.313	0.000	0.295	0.009	-0.001	-0.018
3.30	-0.078	0.000	0.236	0.008	-0.003	-0.016
3.31	0.234	0.000	0.295	0.011	-0.005	-0.013
3.32	0.234	0.000	0.059	0.013	-0.008	-0.013

Figure 6.7.2.4 Digital data for event 4.1

[ ] = baseline which is subtracted for peaks and numerical integrati

Yeardate: 79219 Time: 09:53:39 M.S.T.

Time (μs)	$\partial B_E/\partial t$ (T/s)	$\partial B_N/\partial t$ (T/s)	$Z_o \partial D_z/\partial t$ (T/s)	B_E (μT)	B_N (μT)	$Z_o D_z$ (μT)
3.90	0.156	0.234	0.000	0.000	0.000	0.000
3.91	0.156	0.234	0.000	0.000	0.000	0.000
3.92	0.156	0.234	-0.059	0.000	0.000	-0.001
3.93	0.234	0.234	-0.059	0.001	0.000	-0.001
3.94	0.234	0.234	-0.059	0.002	0.000	-0.002
3.95	0.313	0.313	-0.118	0.003	0.001	-0.003
3.96	0.313	0.313	-0.118	0.005	0.002	-0.004
3.97	0.391	0.234	-0.118	0.007	0.002	-0.005
3.98	0.391	0.234	-0.236	0.009	0.002	-0.008
3.99	0.391	0.234	-0.236	0.012	0.002	-0.010
4.00	0.391	0.313	-0.236	0.014	0.002	-0.012
4.01	0.469	0.313	-0.236	0.017	0.003	-0.015
4.02	0.625	0.391	-0.236	0.022	0.005	-0.017
4.03	0.625	0.469	-0.236	0.027	0.007	-0.019
4.04	1.250	0.547	-0.412	0.038	0.010	-0.024
4.05	2.422	0.625	-0.471	0.060	0.014	-0.028
4.06	2.500	0.938	-0.707	0.084	0.021	-0.035
4.07	2.422	1.250	-1.355	0.106	0.031	-0.049
4.08	2.188	1.563	-2.062	0.127	0.045	-0.070
4.09	1.250	1.250	-1.885	0.138	0.055	-0.088
4.10	0.625	0.625	-1.649	0.142	0.059	-0.105
4.11	0.313	0.625	-1.414	0.144	0.063	-0.119
4.12	0.313	0.859	-0.943	0.145	0.069	-0.128
4.13	0.625	0.938	-0.412	0.150	0.076	-0.133
4.14	0.859	1.250	-0.236	0.157	0.086	-0.135
4.15	0.938	1.250	-0.412	0.165	0.096	-0.139
4.16	0.938	1.172	-0.648	0.173	0.106	-0.145
4.17	0.938	1.172	-0.707	0.181	0.115	-0.153
4.18	0.938	1.016	-0.825	0.188	0.123	-0.161
4.19	0.859	0.859	-0.766	0.195	0.129	-0.168
4.20	0.781	0.625	-0.766	0.202	0.133	-0.176
4.21	0.625	0.547	-0.648	0.206	0.136	-0.183
4.22	0.313	0.313	-0.530	0.208	0.137	-0.188
4.23	0.313	0.313	-0.471	0.209	0.138	-0.193
4.24	0.234	0.234	-0.412	0.210	0.138	-0.197
4.25	0.234	0.313	-0.236	0.211	0.138	-0.199
4.26	0.156	0.313	-0.236	0.211	0.139	-0.201
4.27	0.078	0.391	-0.177	0.210	0.141	-0.203
4.28	0.078	0.469	-0.177	0.209	0.143	-0.205
4.29	0.156	0.547	-0.059	0.209	0.146	-0.206
4.30	0.234	0.625	0.000	0.210	0.150	-0.206

Figure 6.7.2.5 Digital data for event 4.3

[ ] = baseline which is subtracted for peaks and numerical integration

Yeardate: 79219 Time: 09:53:39 M.S.T.

Time (μs)	$\partial B_E/\partial t$ (T/s)	$\partial B_N/\partial t$ (T/s)	$Z_o \partial D_z/\partial t$ (T/s)	B_E (μT)	B_N (μT)	$Z_o D_z$ (μT)
4.27	0.078	[0.391]	-0.177	0.000	-0.000	0.000
4.28	[0.078]	0.469	[-0.177]	0.000	0.001	0.000
4.29	0.156	0.547	-0.059	0.001	0.002	0.001
4.30	0.234	0.625	0.000	0.002	0.005	0.003
4.31	0.547	0.625	-0.059	0.007	0.007	0.004
4.32	0.625	0.625	-0.059	0.013	0.009	0.005
4.33	1.250	0.703	-0.236	0.024	0.012	0.005
4.34	1.328	0.781	-0.412	0.037	0.016	0.002
4.35	0.625	0.938	-0.707	0.042	0.022	-0.003
4.36	0.000	0.938	-0.943	0.041	0.027	-0.011
4.37	-0.078	0.625	-0.943	0.040	0.030	-0.018
4.38	-0.703	0.234	-0.471	0.032	0.028	-0.021
4.39	-1.016	-0.078	0.000	0.021	0.023	-0.019
4.40	-1.094	-0.625	0.471	0.009	0.013	-0.013
4.41	-0.703	-0.703	0.766	0.001	0.002	-0.003
4.42	-0.625	-0.391	0.943	-0.006	-0.006	0.008

Figure 6.7.2.6 Digital data for event 5.1

[ ] = baseline which is subtracted for peaks and numerical integration

Yeardate: 79219 Time: 09:53:39 M.S.T.

Time (μs)	$\partial B_E/\partial t$ (T/s)	$\partial B_N/\partial t$ (T/s)	$Z_o \partial D_z/\partial t$ (T/s)	B_E (μT)	B_N (μT)	$Z_o D_z$ (μT)
5.00	0.000	0.000	0.236	0.000	0.000	-0.000
5.01	0.000	0.000	0.236	0.000	0.000	-0.000
5.02	0.547	0.234	0.177	0.005	0.002	-0.001
5.03	0.625	0.313	0.059	0.012	0.005	-0.002
5.04	0.000	0.313	0.059	0.012	0.009	-0.004
5.05	0.000	0.313	-0.412	0.012	0.012	-0.011
5.06	-0.313	0.234	-0.412	0.009	0.014	-0.017
5.07	-0.313	0.156	0.000	0.005	0.016	-0.019
5.08	0.000	0.000	0.471	0.005	0.016	-0.017
5.09	0.000	0.000	0.471	0.005	0.016	-0.015
5.10	0.234	0.000	0.059	0.007	0.016	-0.016
5.11	0.000	0.000	0.059	0.007	0.016	-0.018
5.12	0.000	0.000	0.000	0.007	0.016	-0.021
5.13	-0.313	0.000	-0.177	0.004	0.016	-0.025
5.14	-0.313	0.000	0.059	0.001	0.016	-0.026
5.15	-0.313	0.000	0.295	-0.002	0.016	-0.026
5.16	-0.313	0.000	0.471	-0.005	0.016	-0.024
5.17	-0.078	0.000	0.471	-0.006	0.016	-0.021
5.18	-0.313	0.156	0.412	-0.009	0.018	-0.019
5.19	-0.313	0.156	0.353	-0.012	0.019	-0.018
5.20	-0.313	0.156	0.295	-0.015	0.021	-0.018
5.21	-0.313	0.156	0.471	-0.018	0.022	-0.015
5.22	-0.234	0.156	0.471	-0.021	0.024	-0.013
5.23	-0.234	0.156	0.412	-0.023	0.025	-0.011
5.24	-0.234	0.156	0.412	-0.025	0.027	-0.009
5.25	-0.391	0.156	0.412	-0.029	0.029	-0.008
5.26	-0.391	0.078	0.412	-0.033	0.029	-0.006
5.27	-0.313	0.078	0.412	-0.036	0.030	-0.004
5.28	-0.078	0.078	0.530	-0.037	0.031	-0.001
5.29	-0.078	0.000	0.471	-0.038	0.031	0.001
5.30	-0.078	0.000	0.295	-0.039	0.031	0.002

Figure 6.7.2.7 Digital data for event 9.8

[ ] = baseline which is subtracted for peaks and numerical integration

Yeardate: 79219 Time: 09:53:39 M.S.T.

Time (μs)	$\partial B_E/\partial t$ (T/s)	$\partial B_N/\partial t$ (T/s)	$Z_o \partial D_z/\partial t$ (T/s)	B_E (μT)	B_N (μT)	$Z_o D_z$ (μT)
9.75	-0.078	0.000	0.059	-0.000	0.000	-0.000
9.76	-0.078	0.156	0.059	-0.000	0.002	-0.000
9.77	-0.078	0.156	0.059	-0.000	0.003	-0.000
9.78	-0.156	0.078	0.059	-0.001	0.004	-0.000
9.79	-0.234	0.156	0.059	-0.002	0.005	-0.000
9.80	-0.625	0.156	0.059	-0.008	0.007	-0.000
9.81	-0.703	0.313	0.118	-0.014	0.010	0.001
9.82	-0.703	0.391	0.177	-0.020	0.014	0.002
9.83	-0.313	0.313	0.471	-0.023	0.017	0.006
9.84	-0.078	0.000	0.530	-0.023	0.017	0.011
9.85	0.234	0.000	0.295	-0.020	0.017	0.013
9.86	0.234	-0.078	0.059	-0.016	0.016	0.013
9.87	0.234	-0.078	0.000	-0.013	0.015	0.012
9.88	0.000	-0.078	-0.177	-0.012	0.014	0.010
9.89	0.000	-0.078	-0.236	-0.011	0.014	0.007
9.90	0.000	-0.078	-0.177	-0.011	0.013	0.005
9.91	-0.078	-0.078	0.000	-0.011	0.012	0.004
9.92	-0.078	-0.078	0.000	-0.011	0.011	0.004
9.93	-0.078	0.000	0.000	-0.011	0.011	0.003
9.94	-0.078	0.234	0.000	-0.011	0.014	0.002
9.95	-0.078	0.156	0.000	-0.011	0.015	0.002
9.96	0.000	0.234	0.000	-0.010	0.018	0.001
9.97	0.078	0.234	0.000	-0.008	0.020	0.001
9.98	0.078	0.234	0.000	-0.007	0.022	0.000
9.99	0.078	0.156	0.000	-0.005	0.024	-0.001
10.00	0.078	0.156	0.000	-0.004	0.025	-0.001
10.01	0.078	0.000	-0.059	-0.002	0.025	-0.002
10.02	0.000	0.000	-0.059	-0.001	0.025	-0.004
10.03	0.000	0.000	-0.059	-0.000	0.025	-0.005
10.04	0.000	0.000	0.000	0.000	0.025	-0.005

Figure 6.7.2.8 Digital data for event 10.3

[ ] = baseline which is subtracted for peaks and numerical integration

Yeardate: 79219 Time: 09:53:39 M.S.T.

Time (μs)	$\partial B_E/\partial t$ (T/s)	$\partial B_N/\partial t$ (T/s)	$Z_o \partial D_z/\partial t$ (T/s)	B_E (μT)	B_N (μT)	$Z_o D_z$ (μT)
10.18	[-0.078]	0.000	0.059	-0.000	0.000	-0.000
10.19	0.234	0.000	0.059	0.003	0.000	-0.000
10.20	0.234	0.000	[0.059]	0.006	0.000	-0.000
10.21	0.000	[0.000]	0.000	0.007	0.000	-0.001
10.22	-0.078	0.156	-0.177	0.007	0.002	-0.003
10.23	-0.313	0.156	-0.177	0.005	0.003	-0.005
10.24	-0.313	0.156	0.000	0.002	0.005	-0.006
10.25	-0.313	0.078	0.236	-0.000	0.005	-0.004
10.26	-0.313	0.078	0.295	-0.002	0.006	-0.002
10.27	-0.156	0.078	0.236	-0.003	0.007	-0.000
10.28	-0.078	0.078	0.236	-0.003	0.008	0.002
10.29	-0.078	0.078	0.177	-0.003	0.009	0.003
10.30	0.000	0.078	0.118	-0.002	0.009	0.004
10.31	0.000	0.000	0.059	-0.002	0.009	0.004
10.32	0.000	0.000	0.059	-0.001	0.009	0.004
10.33	0.000	0.000	0.059	-0.000	0.009	0.004
10.34	0.000	0.000	0.059	0.001	0.009	0.004
10.35	0.000	0.000	0.000	0.002	0.009	0.003
10.36	0.000	0.000	0.000	0.003	0.009	0.002
10.37	-0.078	0.000	0.000	0.003	0.009	0.002
10.38	-0.078	0.000	0.059	0.003	0.009	0.002

Figure 6.7.2.9 Digital data for event 11.3

[ ] = baseline which is subtracted for peaks and numerical integration

Yeardate: 79219 Time: 09:53:39 M.S.T.

Time (μs)	$\partial B_E/\partial t$ (T/s)	$\partial B_N/\partial t$ (T/s)	$Z_o \partial D_z/\partial t$ (T/s)	B_E (μT)	B_N (μT)	$Z_o D_z$ (μT)
11.20	[-0.078]	0.000	0.059	-0.000	0.000	-0.000
11.21	0.000	0.000	0.059	0.001	0.000	-0.000
11.22	0.234	0.000	0.059	0.004	0.000	-0.000
11.23	0.313	0.000	0.059	0.008	0.000	-0.000
11.24	0.313	0.000	[0.059]	0.012	0.000	-0.000
11.25	0.234	0.000	-0.177	0.015	0.000	-0.002
11.26	0.000	0.000	-0.412	0.016	0.000	-0.007
11.27	-0.078	0.000	-0.236	0.016	0.000	-0.010
11.28	-0.313	0.000	0.000	0.013	0.000	-0.011
11.29	-0.313	[0.000]	0.059	0.011	0.000	-0.011
11.30	-0.391	0.078	0.059	0.008	0.001	-0.011
11.31	-0.469	0.078	0.236	0.004	0.002	-0.009
11.32	-0.469	0.156	0.295	-0.000	0.003	-0.006
11.33	-0.391	0.078	0.295	-0.003	0.004	-0.004
11.34	-0.313	0.078	0.353	-0.005	0.005	-0.001
11.35	-0.313	0.000	0.353	-0.008	0.005	0.002

Figure 6.7.2.10 Digital data for event 12.5

[ ] = baseline which is subtracted for peaks and numerical integration

Yeardate: 79219 Time: 09:53:39 M.S.T.

Time (μs)	$\partial B_E/\partial t$ (T/s)	$\partial B_N/\partial t$ (T/s)	$Z_o \partial D_z/\partial t$ (T/s)	B_E (μT)	B_N (μT)	$Z_o D_z$ (μT)
12.40	-0.078	0.000	0.059	-0.000	0.000	-0.000
12.41	[-0.078]	0.000	0.059	-0.000	0.000	-0.000
12.42	-0.156	0.000	0.059	-0.001	0.000	-0.000
12.43	-0.156	0.000	0.059	-0.002	0.000	-0.000
12.44	-0.156	0.000	0.059	-0.002	0.000	-0.000
12.45	-0.156	0.000	0.059	-0.003	0.000	-0.000
12.46	-0.156	0.000	0.059	-0.004	0.000	-0.000
12.47	-0.156	0.000	0.059	-0.005	0.000	-0.000
12.48	-0.156	0.000	0.059	-0.005	0.000	-0.000
12.49	-0.234	[0.000]	0.059	-0.007	0.000	-0.000
12.50	-0.234	-0.078	0.059	-0.009	-0.001	-0.000
12.51	-0.391	-0.078	0.059	-0.012	-0.002	-0.000
12.52	-0.625	-0.234	0.059	-0.017	-0.004	-0.000
12.53	-1.016	-0.234	[0.059]	-0.027	-0.006	-0.000
12.54	-1.250	-0.156	0.236	-0.038	-0.008	0.002
12.55	-1.250	-0.234	0.471	-0.050	-0.010	0.006
12.56	-0.938	-0.234	0.530	-0.059	-0.013	0.011
12.57	-0.625	-0.156	0.648	-0.064	-0.014	0.016
12.58	-0.391	-0.078	0.589	-0.067	-0.015	0.022
12.59	-0.313	0.000	0.295	-0.070	-0.015	0.024
12.60	-0.078	0.000	0.236	-0.070	-0.015	0.026
12.61	0.000	0.156	0.236	-0.069	-0.013	0.028
12.62	0.234	0.156	0.177	-0.066	-0.012	0.029
12.63	0.234	0.234	0.059	-0.063	-0.009	0.029
12.64	0.234	0.234	0.000	-0.060	-0.007	0.028
12.65	0.313	0.234	-0.177	-0.056	-0.004	0.026
12.66	0.313	0.156	-0.118	-0.052	-0.003	0.024
12.67	0.391	0.156	-0.118	-0.047	-0.001	0.023
12.68	0.313	0.156	-0.118	-0.043	0.000	0.021
12.69	0.313	0.078	-0.236	-0.040	0.001	0.018
12.70	0.234	0.078	-0.236	-0.036	0.002	0.015
12.71	0.234	0.000	-0.236	-0.033	0.002	0.012
12.72	0.234	0.000	-0.177	-0.030	0.002	0.010
12.73	0.156	0.000	-0.177	-0.028	0.002	0.007
12.74	0.078	0.000	-0.177	-0.026	0.002	0.005
12.75	0.078	0.000	-0.118	-0.025	0.002	0.003
12.76	0.000	0.000	-0.118	-0.024	0.002	0.001
12.77	0.000	0.000	-0.059	-0.023	0.002	0.000
12.78	0.000	0.000	-0.059	-0.022	0.002	-0.001
12.79	0.000	0.000	0.000	-0.022	0.002	-0.002

Figure 6.7.2.11 Digital data for event 17.9

[ ] = baseline which is subtracted for peaks and numerical integration

Yeardate: 79219 Time: 09:53:39 M.S.T.

Time (μs)	$\partial B_E/\partial t$ (T/s)	$\partial B_N/\partial t$ (T/s)	$Z_o \partial D_z/\partial t$ (T/s)	B_E (μT)	B_N (μT)	$Z_o D_z$ (μT)
17.87	[-0.078]	0.078	0.000	-0.000	0.000	0.000
17.88	0.000	[0.078]	0.000	0.001	0.000	0.000
17.89	0.234	0.156	0.000	0.004	0.001	0.000
17.90	0.547	0.156	0.000	0.010	0.002	0.000
17.91	0.234	0.156	[0.000]	0.013	0.002	0.000
17.92	-0.391	0.156	-0.236	0.010	0.003	-0.002
17.93	-0.391	0.078	-0.412	0.007	0.003	-0.006
17.94	-0.313	0.078	0.000	0.005	0.003	-0.006
17.95	-0.078	0.078	0.471	0.005	0.003	-0.002
17.96	-0.078	0.078	0.295	0.005	0.003	0.001
17.97	0.000	0.078	0.236	0.006	0.003	0.003
17.98	0.000	0.078	0.059	0.007	0.003	0.004
17.99	0.078	0.078	0.000	0.008	0.003	0.004
18.00	0.078	0.078	-0.059	0.010	0.003	0.003
18.01	0.078	0.078	-0.059	0.011	0.003	0.003
18.02	0.000	0.078	-0.059	0.012	0.003	0.002
18.03	0.000	0.078	-0.059	0.013	0.003	0.002
18.04	-0.078	0.078	-0.059	0.013	0.003	0.001
18.05	-0.078	0.078	0.059	0.013	0.003	0.002
18.06	-0.078	0.078	0.059	0.013	0.003	0.002
18.07	-0.078	0.078	0.059	0.013	0.003	0.003
18.08	-0.078	0.078	0.059	0.013	0.003	0.003
18.09	-0.078	0.078	0.059	0.013	0.003	0.004
18.10	-0.078	0.078	0.059	0.013	0.003	0.004
18.11	0.000	0.078	0.059	0.014	0.003	0.005
18.12	0.000	0.078	0.059	0.014	0.003	0.006
18.13	0.000	0.078	0.000	0.015	0.003	0.006
18.14	0.000	0.078	0.000	0.016	0.003	0.006
18.15	0.000	0.000	0.000	0.017	0.002	0.006
18.16	0.000	0.000	0.000	0.017	0.001	0.006
18.17	0.000	-0.078	0.000	0.018	-0.000	0.006

Figure 6.7.2.12 Digital data for event 18.2

[ ] = baseline which is subtracted for peaks and numerical integratio

Yeardate: 79219 Time: 09:53:39 M.S.T.

Time (μs)	$\partial B_E/\partial t$ (T/s)	$\partial B_N/\partial t$ (T/s)	$Z_o \partial D_z/\partial t$ (T/s)	B_E (μT)	B_N (μT)	$Z_o D_z$ (μT)
18.15	0.000	0.000	0.000	0.000	0.000	0.000
18.16	0.000	0.000	0.000	0.000	0.000	0.000
18.17	0.000	-0.078	0.000	0.000	-0.001	0.000
18.18	0.000	-0.234	0.000	0.000	-0.003	0.000
18.19	0.547	-0.078	0.000	0.005	-0.004	0.000
18.20	0.938	0.000	0.000	0.015	-0.004	0.000
18.21	0.859	0.078	-0.177	0.023	-0.003	-0.002
18.22	0.000	0.078	-0.471	0.023	-0.002	-0.006
18.23	0.000	0.078	-0.884	0.023	-0.002	-0.015
18.24	-0.078	0.156	-0.471	0.023	0.000	-0.020
18.25	-0.313	0.156	0.000	0.020	0.002	-0.020
18.26	-0.313	0.156	0.059	0.017	0.004	-0.019
18.27	-0.313	0.156	0.236	0.014	0.005	-0.017
18.28	-0.234	0.156	0.177	0.011	0.007	-0.015
18.29	-0.156	0.156	0.177	0.010	0.008	-0.014
18.30	-0.156	0.156	0.177	0.008	0.010	-0.012
18.31	-0.156	0.156	0.118	0.007	0.011	-0.011
18.32	-0.156	0.156	0.118	0.005	0.013	-0.009
18.33	-0.156	0.156	0.118	0.004	0.015	-0.008
18.34	-0.156	0.156	0.118	0.002	0.016	-0.007
18.35	-0.156	0.156	0.118	0.000	0.018	-0.006
18.36	-0.078	0.156	0.177	-0.000	0.019	-0.004
18.37	-0.078	0.156	0.177	-0.001	0.021	-0.002
18.38	-0.078	0.156	0.118	-0.002	0.022	-0.001
18.39	-0.078	0.156	0.059	-0.003	0.024	-0.001
18.40	-0.078	0.156	0.059	-0.003	0.025	0.000

Figure 6.7.2.13 Digital data for event 19.5

[ ] = baseline which is subtracted for peaks and numerical integration

Yeardate: 79219 Time: 09:53:39 M.S.T.

Time (μs)	$\partial B_E/\partial t$ (T/s)	$\partial B_N/\partial t$ (T/s)	$Z_o \partial D_z/\partial t$ (T/s)	B_E (μT)	B_N (μT)	$Z_o D_z$ (μT)
19.51	[0.000]	0.000	[0.059]	0.000	0.000	-0.000
19.52	0.547	0.000	0.000	0.005	0.000	-0.001
19.53	0.859	[0.000]	0.000	0.014	0.000	-0.001
19.54	0.547	0.156	0.000	0.020	0.002	-0.002
19.55	0.000	0.156	-0.412	0.020	0.003	-0.006
19.56	-0.391	0.156	-0.648	0.016	0.005	-0.014
19.57	-0.625	0.156	-0.412	0.009	0.006	-0.018
19.58	-0.625	0.156	0.059	0.003	0.008	-0.018
19.59	-0.625	0.156	0.471	-0.003	0.009	-0.014
19.60	-0.625	0.156	0.471	-0.009	0.011	-0.010
19.61	-0.391	0.156	0.471	-0.013	0.013	-0.006
19.62	-0.078	0.156	0.471	-0.014	0.014	-0.002
19.63	-0.078	0.156	0.412	-0.015	0.016	0.002
19.64	0.000	0.156	0.236	-0.015	0.017	0.004
19.65	0.234	0.156	0.059	-0.013	0.019	0.004
19.66	0.156	0.156	0.059	-0.011	0.020	0.004
19.67	0.156	0.156	0.000	-0.009	0.022	0.003
19.68	0.078	0.156	-0.059	-0.009	0.023	0.002
19.69	0.000	0.156	-0.059	-0.009	0.025	0.001
19.70	0.000	0.156	0.000	-0.009	0.027	-0.000
19.71	-0.078	0.156	0.000	-0.009	0.028	-0.001
19.72	-0.078	0.078	0.000	-0.010	0.029	-0.001
19.73	-0.078	0.078	0.000	-0.011	0.030	-0.002
19.74	-0.078	0.078	0.000	-0.012	0.030	-0.002
19.75	-0.078	0.078	0.059	-0.013	0.031	-0.002
19.76	-0.078	0.078	0.059	-0.013	0.032	-0.002
19.77	-0.078	0.078	0.059	-0.014	0.033	-0.002
19.78	-0.078	0.078	0.059	-0.015	0.034	-0.002
19.79	-0.078	0.078	0.059	-0.016	0.034	-0.002
19.80	-0.078	0.078	0.059	-0.016	0.035	-0.002
19.81	-0.078	0.078	0.059	-0.017	0.036	-0.002
19.82	-0.078	0.078	0.059	-0.018	0.037	-0.002
19.83	-0.078	0.078	0.059	-0.019	0.038	-0.002
19.84	-0.078	0.078	0.059	-0.020	0.038	-0.002
19.85	-0.156	0.078	0.059	-0.021	0.039	-0.002
19.86	-0.156	0.000	0.059	-0.023	0.039	-0.002

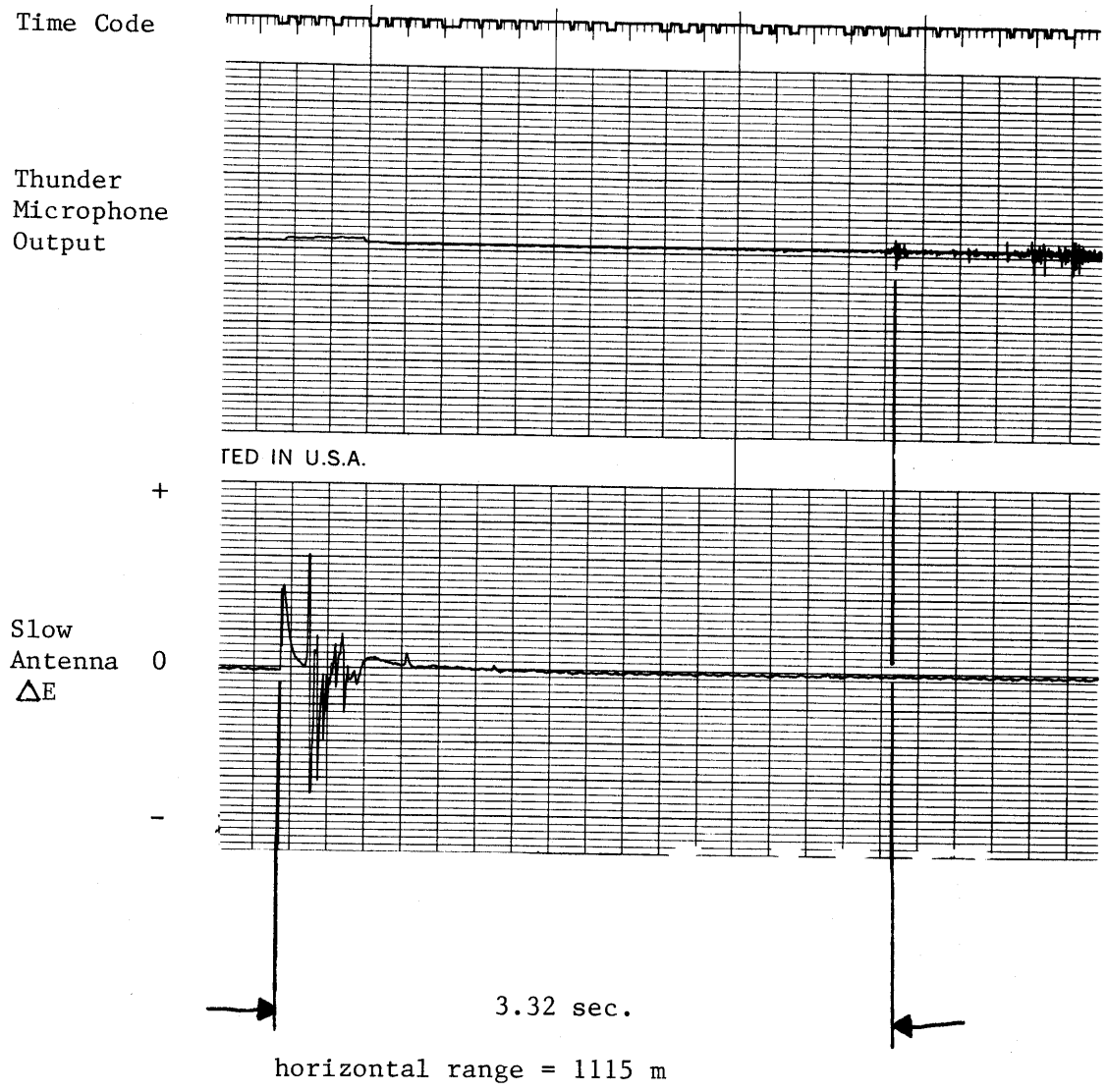

Figure 6.7.3 Slow E field change and thunder microphone record of midrange return stroke

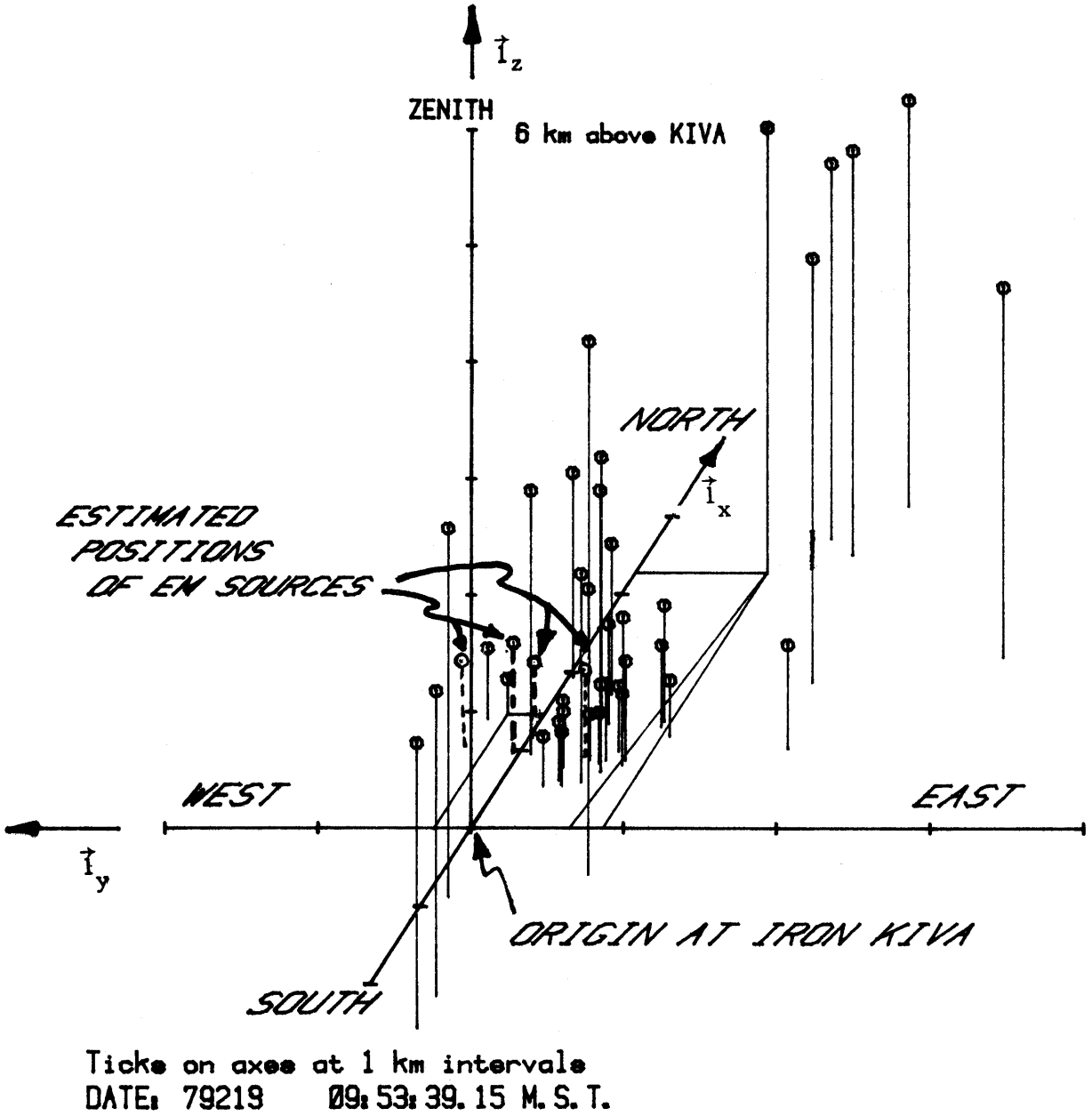

Figure 6.7.4 Acoustic location of midrange return stroke

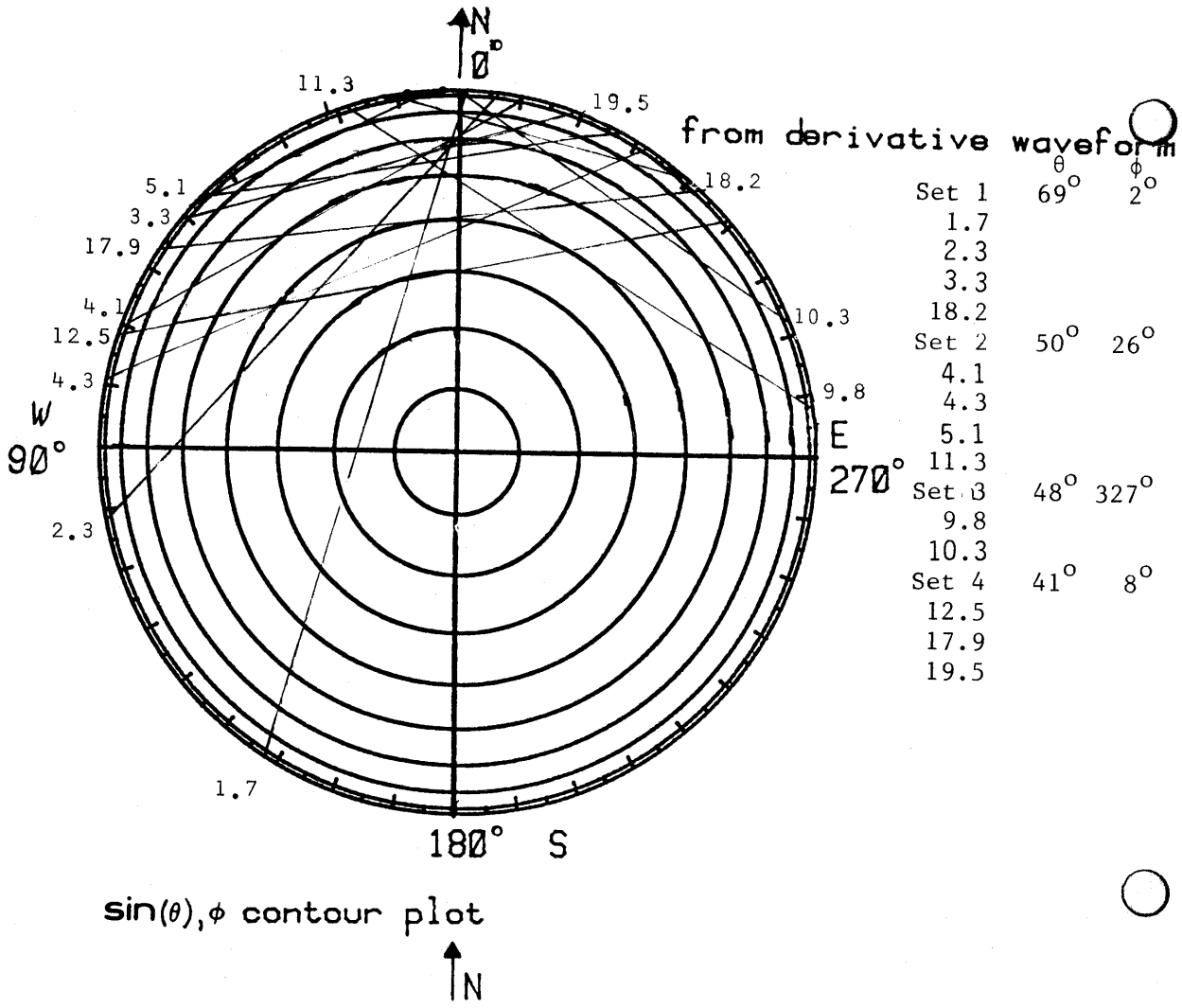

No photograph available

Whole-sky photograph from Kiva

Date: 79219 M.S.T.: 09:53:39

Figure 6.7.5A sin(θ),φ contours for midrange return stroke derivative waveform and whole-sky videotape photograph

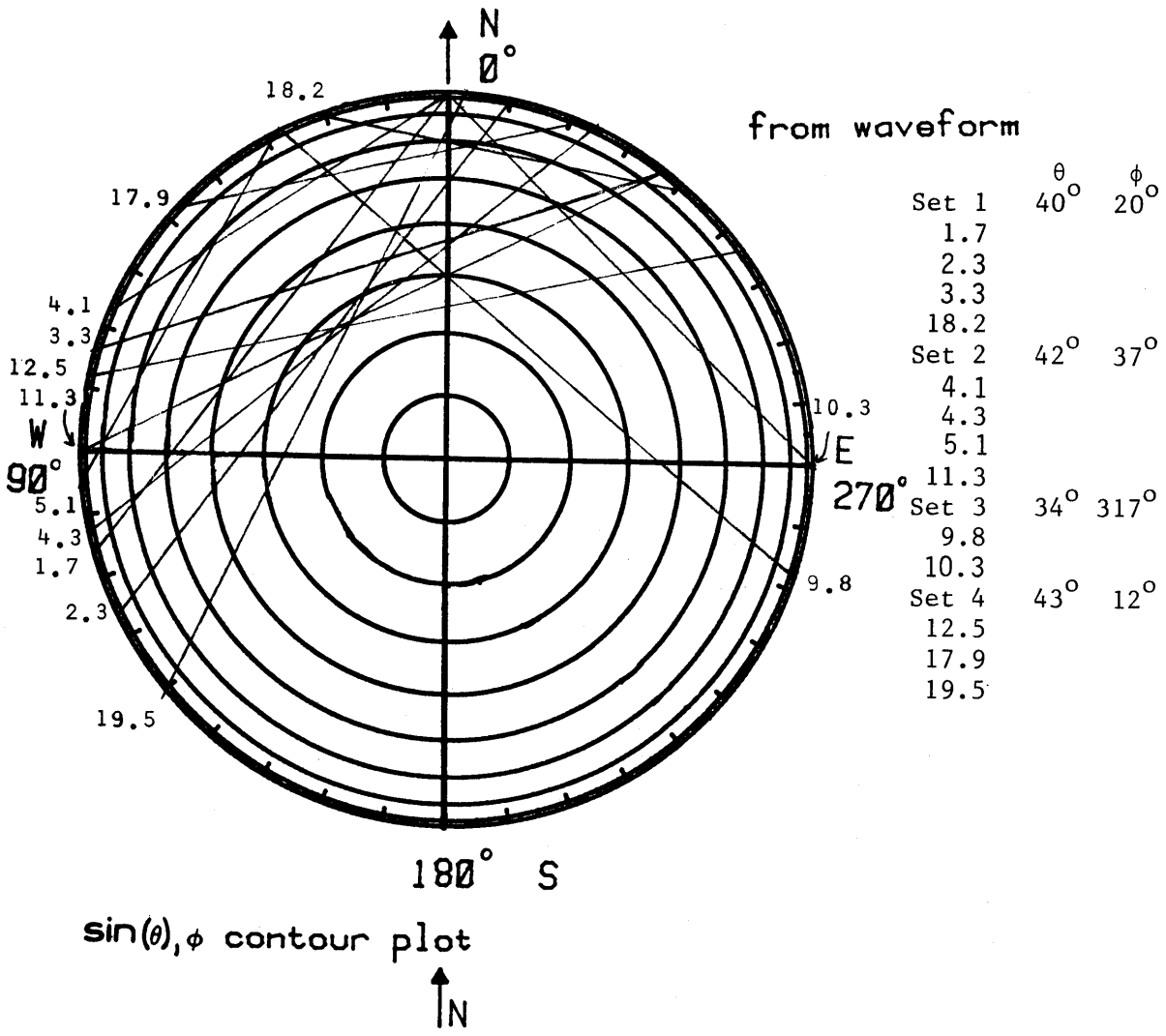

No photograph available

Whole-sky photograph from Kiva

Date: 79219 M.S.T.: 09:53:39

Figure 6.7.5B sin(θ),φ contours for midrange return stroke waveform and whole-sky videotape photograph

Figure 6.7.6A.1 Tabulation of peak values for each event from derivative waveform set for midrange return stroke

Yeardate: 79219 M.S.T.: 95339

ϕ = 2° ; θ = 69° ; r = 1194 m Set 1

Event Number	Time (μs)	$Z_o \Delta\partial D_z/\partial t$ (T/s)	$\Delta\partial B_E/\partial t$ (T/s)	$\Delta\partial B_N/\partial t$ (T/s)	$\Delta\partial B_h/\partial t$ (T/s)	$\Delta\partial B_e/\partial t$ (T/s)	$\lvert\Delta\partial\vec{B}/\partial t\rvert$ (T/s)
1.7	1.70	-0.65	0.70	2.27	-3.13	-0.39	3.16
2.3	2.28	-1.65	1.88	2.11	-2.85	-0.98	3.01
3.3	3.26	-0.47	0.55	0.16	-0.20	-0.28	0.34
18.2	18.23	-0.88	0.94	-0.23	0.37	-0.47	0.59

CALCULATED VALUES FOR $\partial\vec{T}/\partial t$

Event Number	$\partial T_2/\partial t$ (10^{15} Am/s^2)	$\partial T_3/\partial t$ (10^{15} Am/s^2)	$\lvert\partial\vec{T}/\partial t\rvert$ (10^{15} Am/s^2)	α (deg)
1.7	11219	1395	11305	277
2.3	10214	3498	10796	289
3.3	703	995	1218	325
18.2	-1313	1669	2123	38

Figure 6.7.6A.2 Tabulation of peak values for each event from derivative waveform set for midrange return stroke

Yeardate: 79219 M.S.T.: 95339

ϕ = 26° ; θ = 50° ; r = 1456 m Set 2

Event Number	Time (μs)	$Z_o \Delta\partial D_z/\partial t$ (T/s)	$\Delta\partial B_E/\partial t$ (T/s)	$\Delta\partial B_N/\partial t$ (T/s)	$\Delta\partial B_h/\partial t$ (T/s)	$\Delta\partial B_e/\partial t$ (T/s)	$\lvert\Delta\partial\vec{B}/\partial t\rvert$ (T/s)
4.1	4.06	-2.06	2.34	1.33	-0.13	-1.34	1.35
4.3	4.34	-0.77	1.25	0.55	0.04	-0.68	0.68
5.1	5.05	-0.65	0.63	0.31	-0.00	-0.35	0.35
11.3	11.34	-0.47	0.39	0.16	0.02	-0.21	0.21

CALCULATED VALUES FOR $\partial\vec{T}/\partial t$

Event Number	$\partial T_2/\partial t$ (10^{15} Am/s^2)	$\partial T_3/\partial t$ (10^{15} Am/s^2)	$\lvert\partial\vec{T}/\partial t\rvert$ (10^{15} Am/s^2)	α (deg)
4.1	576	5865	5893	354
4.3	-182	2979	2985	3
5.1	8	1533	1533	360
11.3	-92	918	923	6

Figure 6.7.6A.3 Tabulation of peak values for each event from derivative waveform set for midrange return stroke

Yeardate: 79219 M.S.T.: 95339

$\phi = 327^\circ$; $\theta = 48^\circ$; r = 1500 m Set 3

Event Number	Time (μs)	$Z_o \Delta\partial D_z/\partial t$ (T/s)	$\Delta\partial B_E/\partial t$ (T/s)	$\Delta\partial B_N/\partial t$ (T/s)	$\Delta\partial B_h/\partial t$ (T/s)	$\Delta\partial B_e/\partial t$ (T/s)	$\lvert\Delta\partial\vec{B}/\partial t\rvert$ (T/s)
9.8	9.81	0.47	-0.63	0.39	0.01	0.37	0.37
10.3	10.26	0.24	-0.24	0.16	-0.00	0.14	0.14

CALCULATED VALUES FOR $\partial\vec{T}/\partial t$

Event Number	$\partial T_2/\partial t$ (10^{15} Am/s^2)	$\partial T_3/\partial t$ (10^{15} Am/s^2)	$\lvert\partial\vec{T}/\partial t\rvert$ (10^{15} Am/s^2)	α (deg)
9.8	-54	-1667	1668	178
10.3	12	-649	649	181

Figure 6.7.6A.4 Tabulation of peak values for each event from derivative waveform set for midrange return stroke

Yeardate: 79219 M.S.T.: 95339

$\phi = 8^\circ$; $\theta = 41^\circ$; r = 1700 m Set 4

Event Number	Time (μs)	$Z_o \Delta\partial D_z/\partial t$ (T/s)	$\Delta\partial B_E/\partial t$ (T/s)	$\Delta\partial B_N/\partial t$ (T/s)	$\Delta\partial B_h/\partial t$ (T/s)	$\Delta\partial B_e/\partial t$ (T/s)	$\lvert\Delta\partial\vec{B}/\partial t\rvert$ (T/s)
12.5	12.54	0.59	-1.17	-0.23	0.04	0.60	0.60
17.9	17.90	-0.41	0.63	0.08	0.01	-0.32	0.32
19.5	19.56	-0.71	0.86	0.16	-0.03	-0.44	0.44

CALCULATED VALUES FOR $\partial\vec{T}/\partial t$

Event Number	$\partial T_2/\partial t$ (10^{15} Am/s^2)	$\partial T_3/\partial t$ (10^{15} Am/s^2)	$\lvert\partial\vec{T}/\partial t\rvert$ (10^{15} Am/s^2)	α (deg)
12.5	-219	-3035	3043	176
17.9	-29	1619	1619	1
19.5	131	2228	2232	357

Figure 6.7.6B.1 Tabulation of peak values for each event from waveform set for midrange return stroke

Yeardate: 79219 M.S.T.: 95339

ϕ = 20° ; θ = 40° ; r = 1735 m Set 1

Event Number	Time (μs)	$Z_o \Delta D_z$ (μT)	ΔB_E (μT)	ΔB_N (μT)	ΔB_h (μT)	ΔB_e (μT)	$\lvert\Delta\vec{B}\rvert$ (μT)
1.7	1.70	-0.06	0.06	0.08	-0.04	-0.04	0.06
2.3	2.26	-0.09	0.12	0.16	-0.07	-0.08	0.11
3.3	3.25	-0.02	0.03	0.01	0.00	-0.02	0.02
18.2	18.23	-0.02	0.02	0.00	0.00	-0.01	0.01

CALCULATED VALUES FOR $\overrightarrow{1_t}.\vec{T}$

Event Number	T_2 (10^9 Am/s)	T_3 (10^9 Am/s)	$\lvert\vec{T}\rvert$ (10^9 Am/s)	α (deg)
1.7	186	218	286	320
2.3	371	436	573	320
3.3	-3	82	82	2
18.2	-23	49	54	25

Figure 6.7.6B.2 Tabulation of peak values for each event from waveform set for midrange return stroke

Yeardate: 79219 M.S.T.: 95339

ϕ = 37° ; θ = 42° ; r = 1666 m Set 2

Event Number	Time (μs)	$Z_o \Delta D_z$ (μT)	ΔB_E (μT)	ΔB_N (μT)	ΔB_h (μT)	ΔB_e (μT)	$\lvert\Delta\vec{B}\rvert$ (μT)
4.1	4.06	-0.21	0.21	0.14	0.01	-0.13	0.13
4.3	4.35	-0.02	0.04	0.03	0.00	-0.02	0.03
5.1	5.07	-0.02	0.01	0.02	-0.01	-0.01	0.01
11.3	11.34	-0.01	0.02	0.01	0.00	-0.01	0.01

CALCULATED VALUES FOR $\vec{I}_t . \vec{T}$

Event Number	T_2 (10^9 Am/s)	T_3 (10^9 Am/s)	$\lvert\vec{T}\rvert$ (10^9 Am/s)	α (deg)
4.1	-49	630	632	4
4.3	-0	125	125	0
5.1	33	50	60	326
11.3	-14	55	57	14

Figure 6.7.6B.3 Tabulation of peak values for each event from waveform set for midrange return stroke

Yeardate: 79219 M.S.T.: 95339

$\phi = 317^\circ$; $\theta = 34^\circ$; r =1994 m Set 3

Event Number	Time (μs)	$Z_o \Delta D_z$ (μT)	ΔB_E (μT)	ΔB_N (μT)	ΔB_h (μT)	ΔB_e (μT)	$\lvert\Delta\vec{B}\rvert$ (μT)
9.8	9.83	0.01	-0.02	0.02	-0.00	0.01	0.01
10.3	10.21	0.01	-0.01	0.01	-0.00	0.01	0.01

CALCULATED VALUES FOR $\vec{1}_t \cdot \vec{T}$

Event Number	T_2 (10^9 Am/s)	T_3 (10^9 Am/s)	$\lvert\vec{T}\rvert$ (10^9 Am/s)	α (deg)
9.8	4	-85	85	182
10.3	2	-42	42	182

Figure 6.7.6B.4 Tabulation of peak values for each event from waveform set for midrange return stroke

Yeardate: 79219 M.S.T.: 95339

$\phi = 12^\circ$; $\theta = 43^\circ$; r =1635 m Set 4

Event Number	Time (μs)	$Z_o \Delta D_z$ (μT)	ΔB_E (μT)	ΔB_N (μT)	ΔB_h (μT)	ΔB_e (μT)	$\lvert\Delta\vec{B}\rvert$ (μT)
12.5	12.59	0.03	-0.07	-0.02	0.00	0.04	0.04
17.9	17.91	-0.01	0.01	0.00	0.00	-0.00	0.01
19.5	19.54	-0.02	0.02	0.04	-0.02	-0.01	0.03

CALCULATED VALUES FOR $\vec{1}_t \cdot \vec{T}$

Event Number	T_2 (10^9 Am/s)	T_3 (10^9 Am/s)	$\lvert\vec{T}\rvert$ (10^9 Am/s)	α (deg)
12.5	-17	-178	179	175
17.9	-7	24	25	16
19.5	117	68	136	300

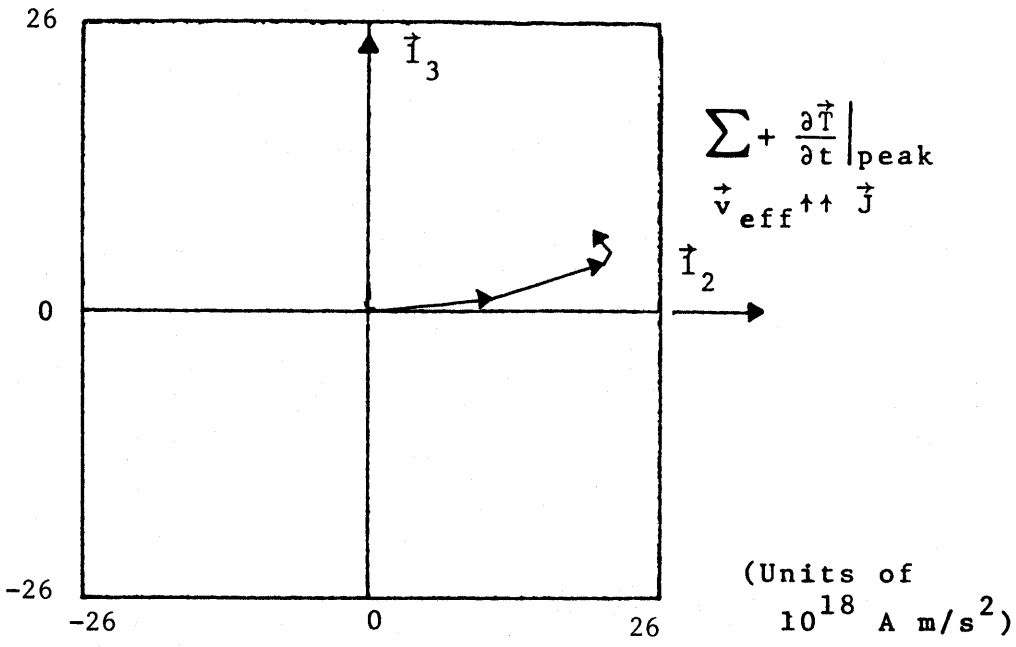

Effective reconstruction of positive streamer

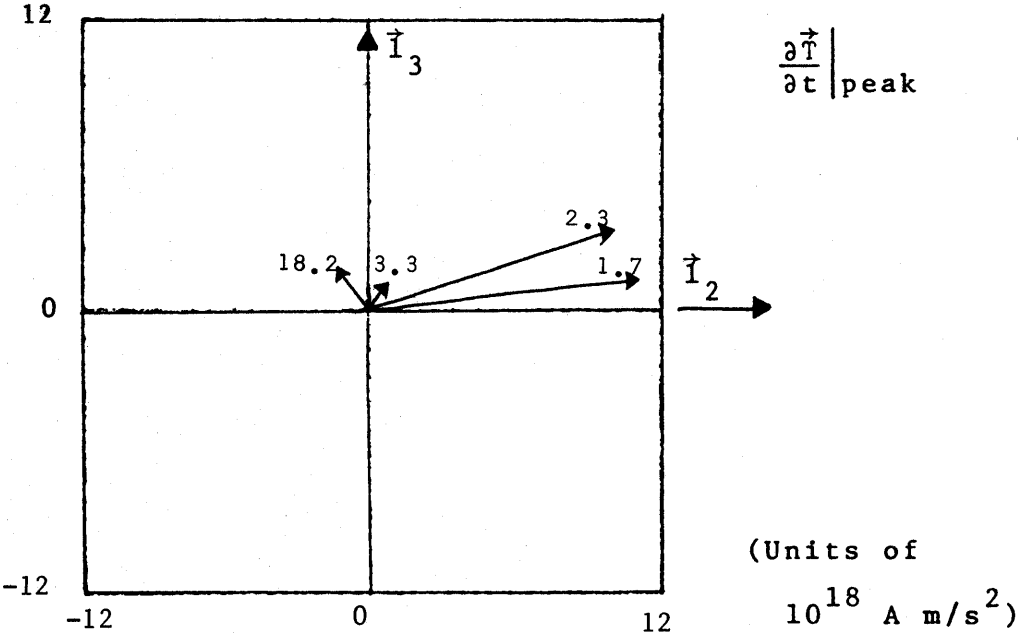

Peaks of $\partial\vec{I}/\partial t$

$\phi = 2^o$ $\theta = 69^o$ r = 1194 m Set 1

Date: 79219 M.S.T.: 09:53:39

Figure 6.7.7A.1 $\partial\vec{I}/\partial t$ for midrange return stroke

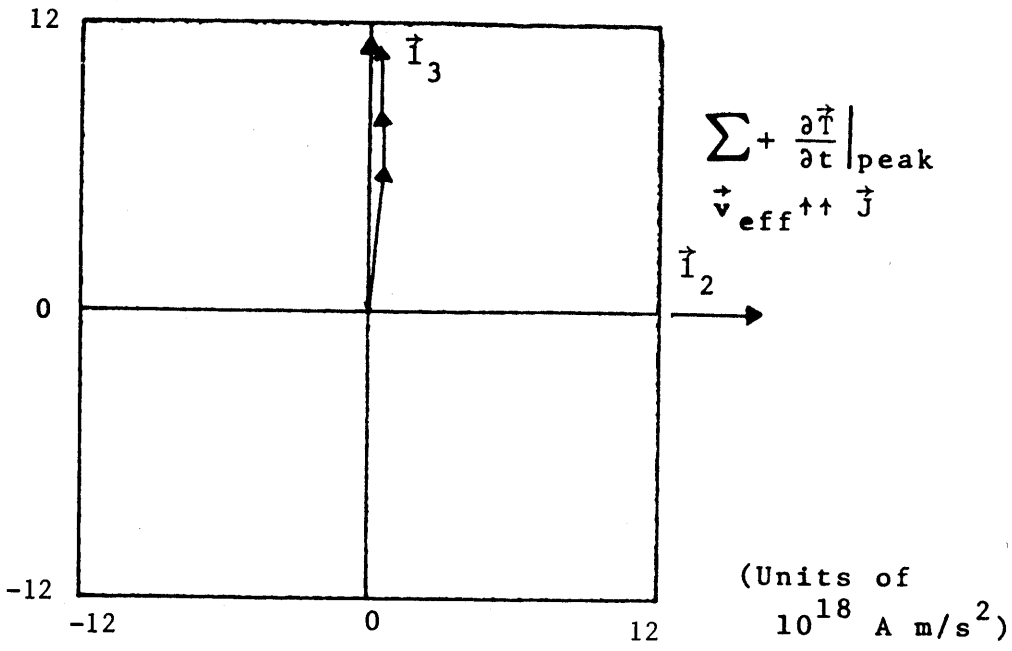

Effective reconstruction of positive streamer

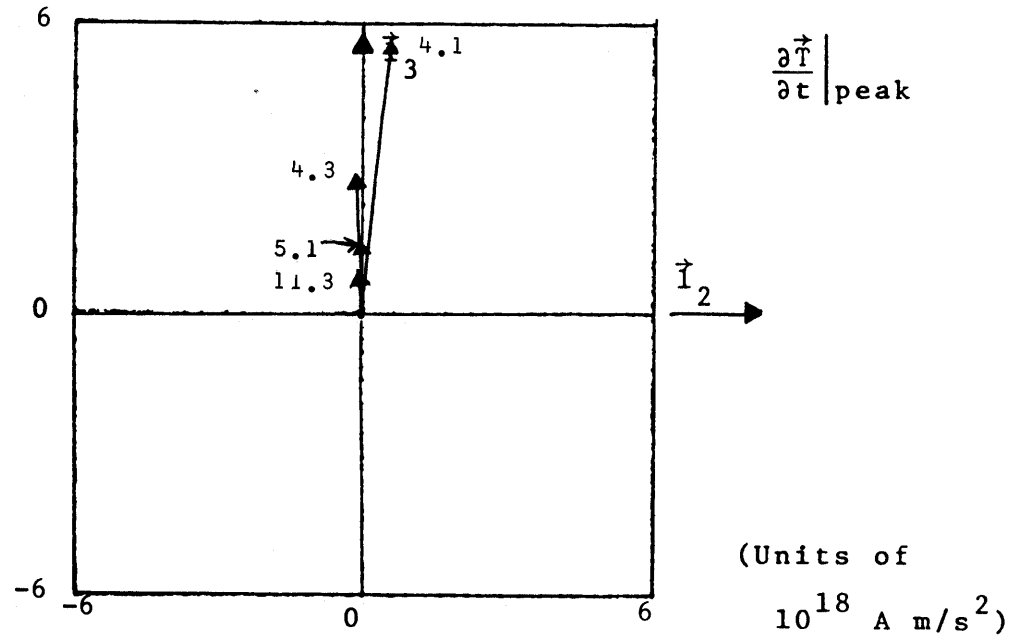

Peaks of $\partial\vec{I}/\partial t$

ϕ = 26° θ = 50° r = 1456 m Set 2

Date: 79219 M.S.T.: 09:53:39

Figure 6.7.7A.2 $\partial\vec{I}/\partial t$ for midrange return stroke

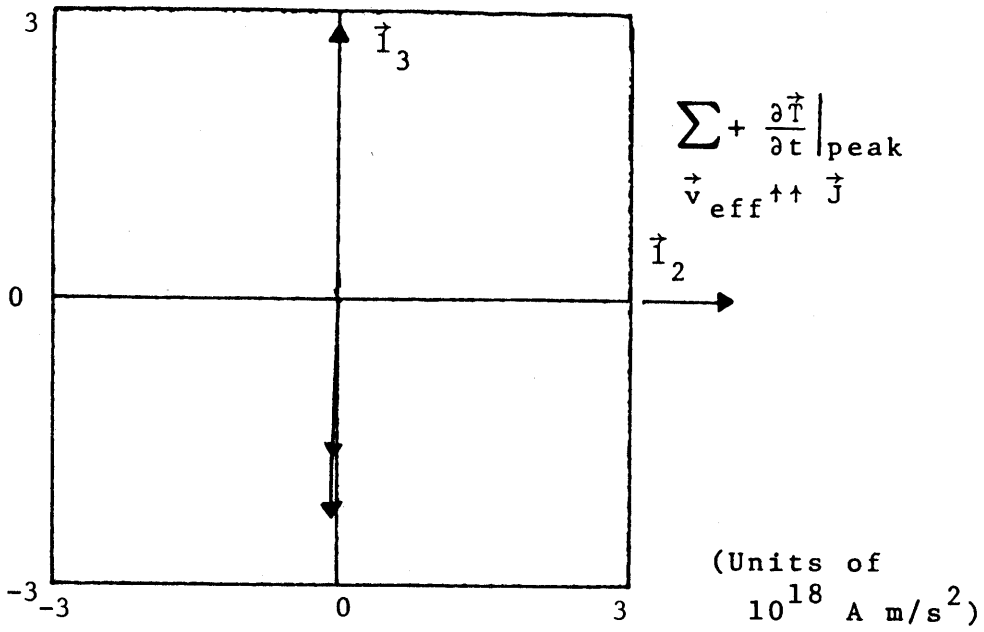

Effective reconstruction of positive streamer

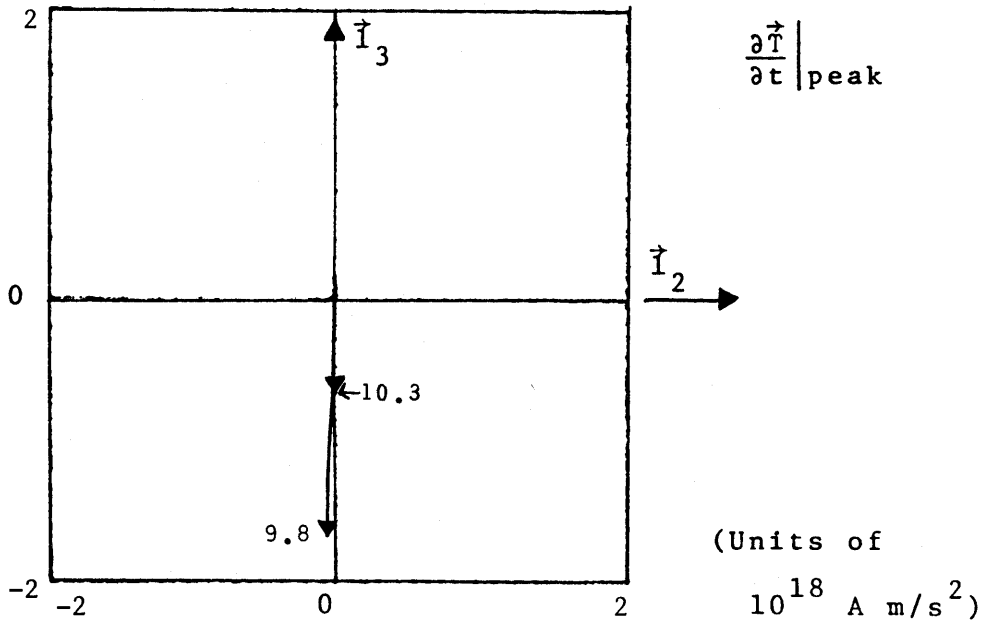

Peaks of $\partial\vec{I}/\partial t$

ϕ = 327° θ = 48° r = 1500 m Set 3

Date: 79219 M.S.T.: 09:53:39

Figure 6.7.7A.3 $\partial\vec{I}/\partial t$ for midrange return stroke

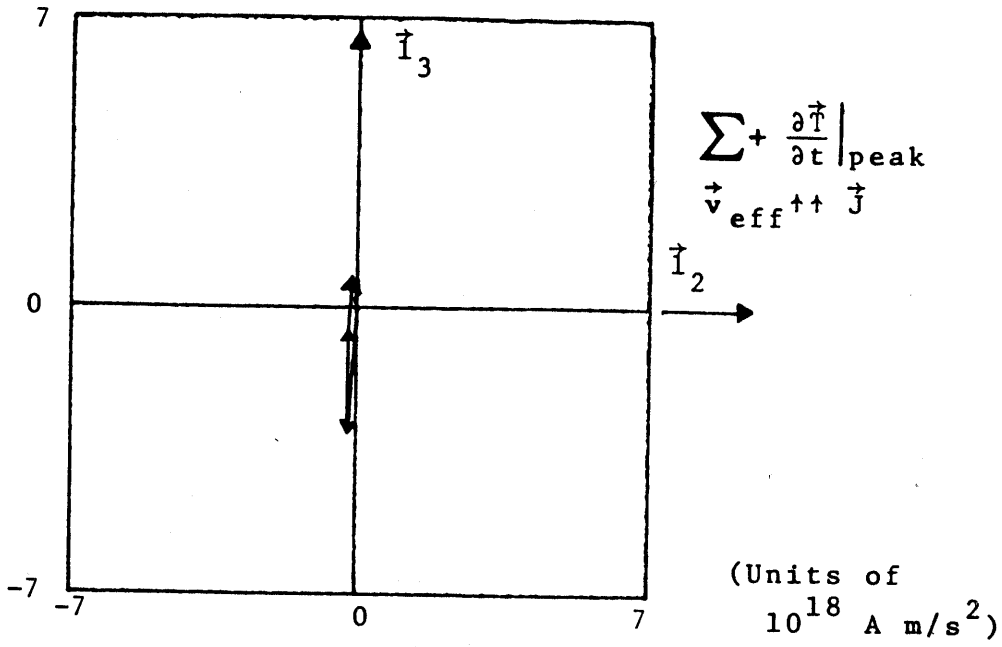

Effective reconstruction of positive streamer

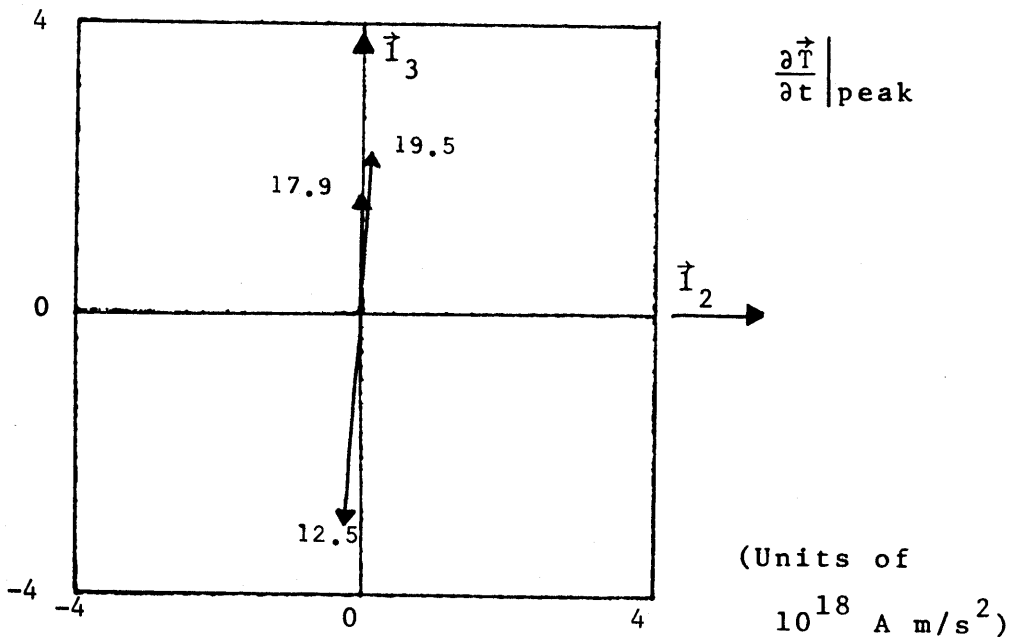

Peaks of $\partial\vec{I}/\partial t$

ϕ = 8° θ = 41° r = 1700 m Set 4

Date: 79219 M.S.T.: 09:53:39

Figure 6.7.7A.4 $\partial\vec{I}/\partial t$ for midrange return stroke

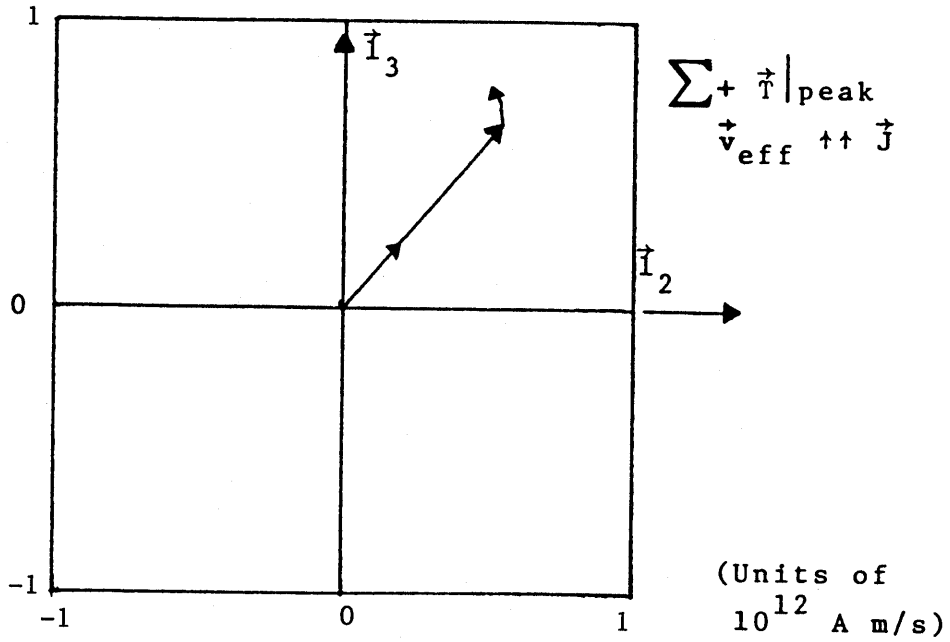

Effective reconstruction of positive streamer

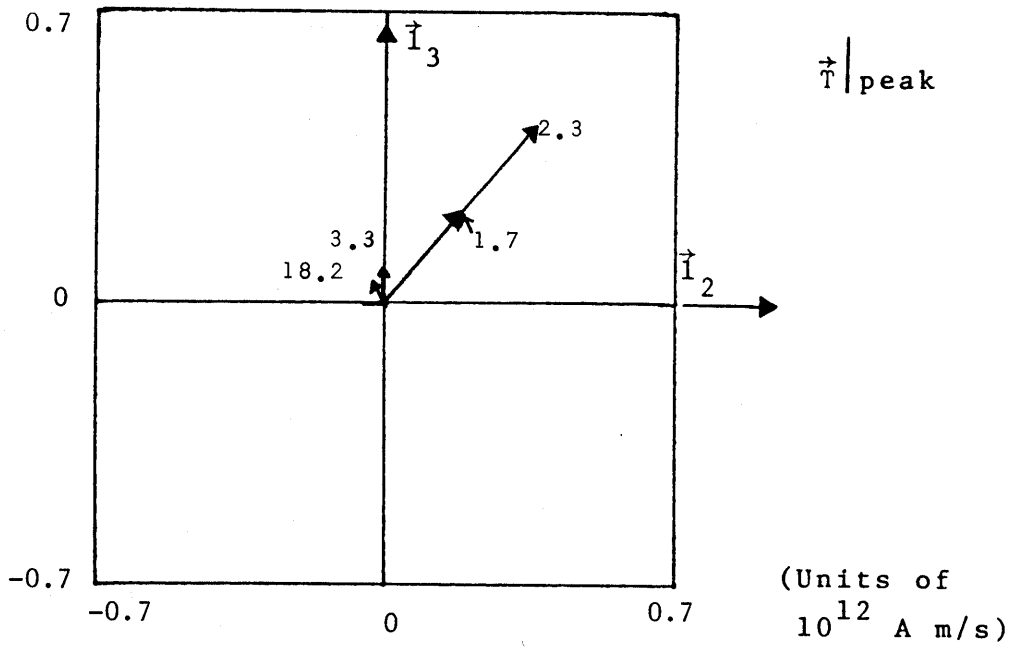

Peaks of $\vec{T}$

$\phi = 20^{\circ}$ $\theta = 40^{\circ}$ r = 1735 m Set 1

Date: 79219 M.S.T.: 09:53:39

Figure 6.7.7B.1 $\vec{T}$ for midrange return stroke

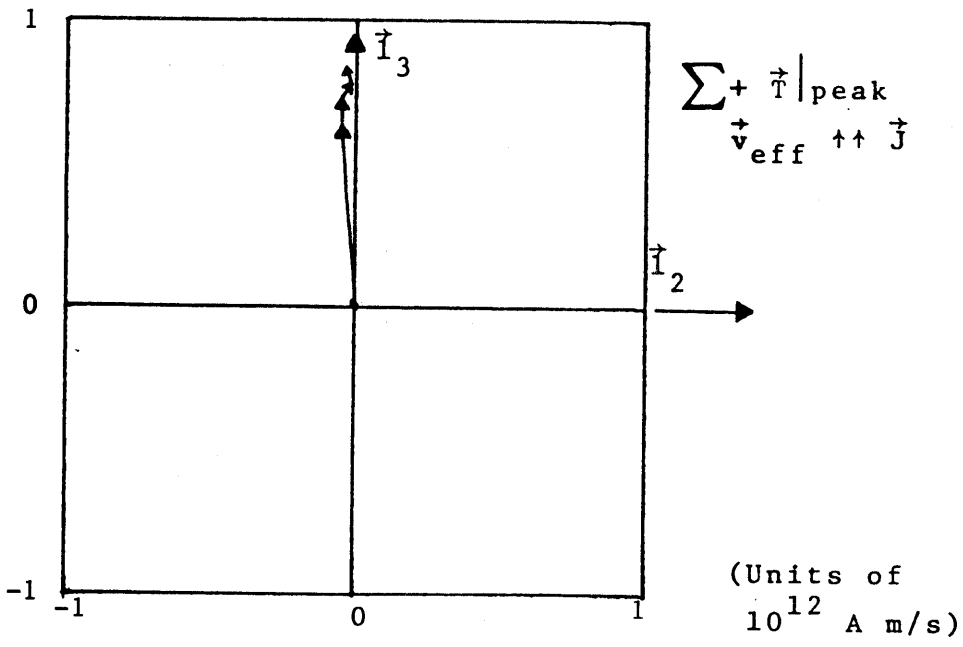

Effective reconstruction of positive streamer

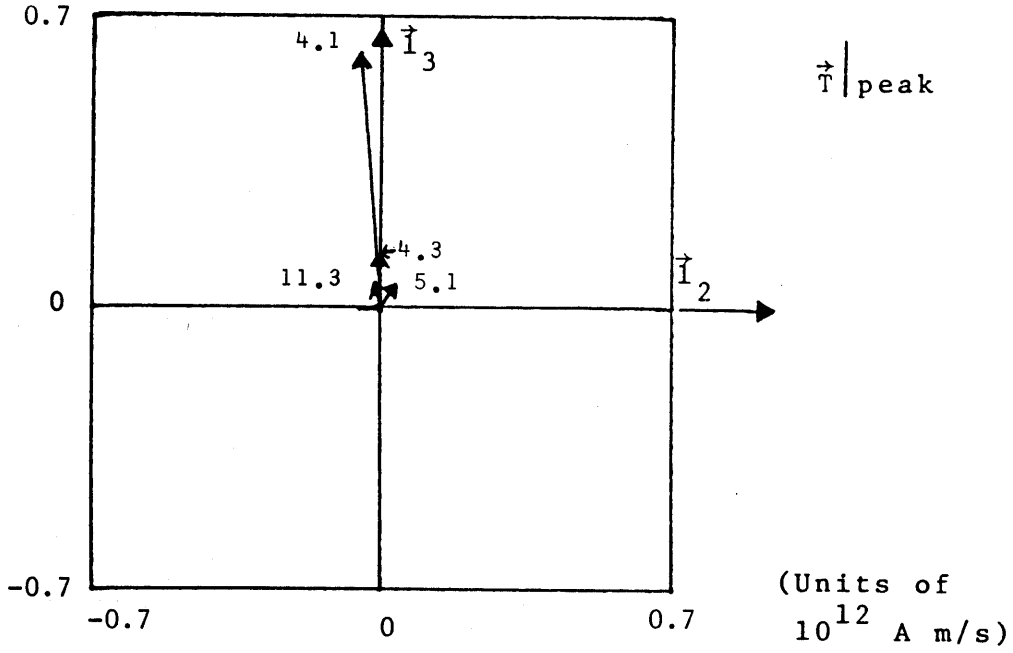

Peaks of $\vec{T}$

ϕ = 37° θ = 42° r = 1666 m Set 2

Date: 79219 M.S.T.: 09:53:39

Figure 6.7.7B.2 $\vec{T}$ for midrange return stroke

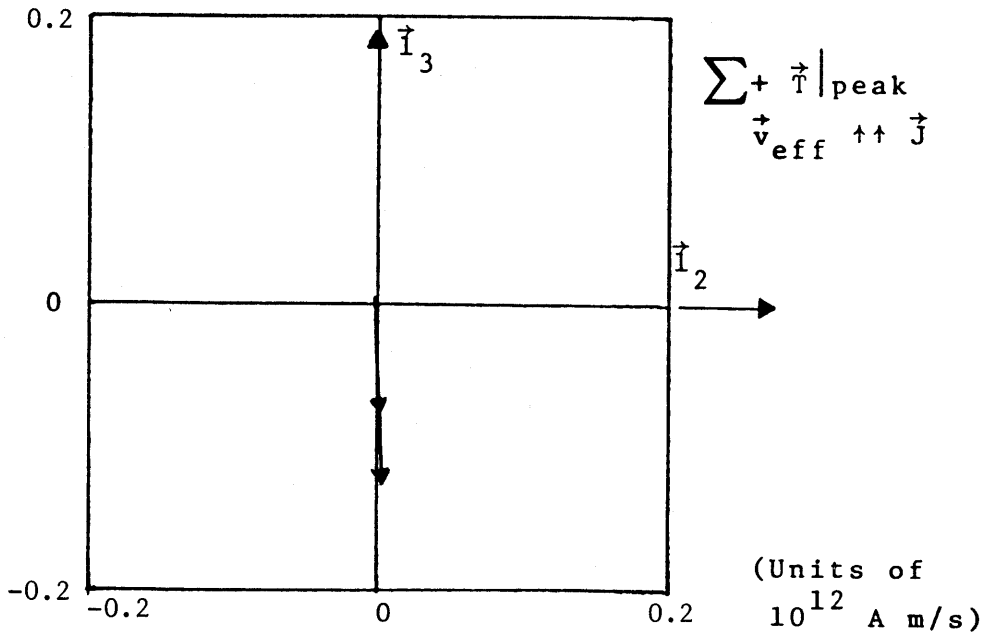

Effective reconstruction of positive streamer

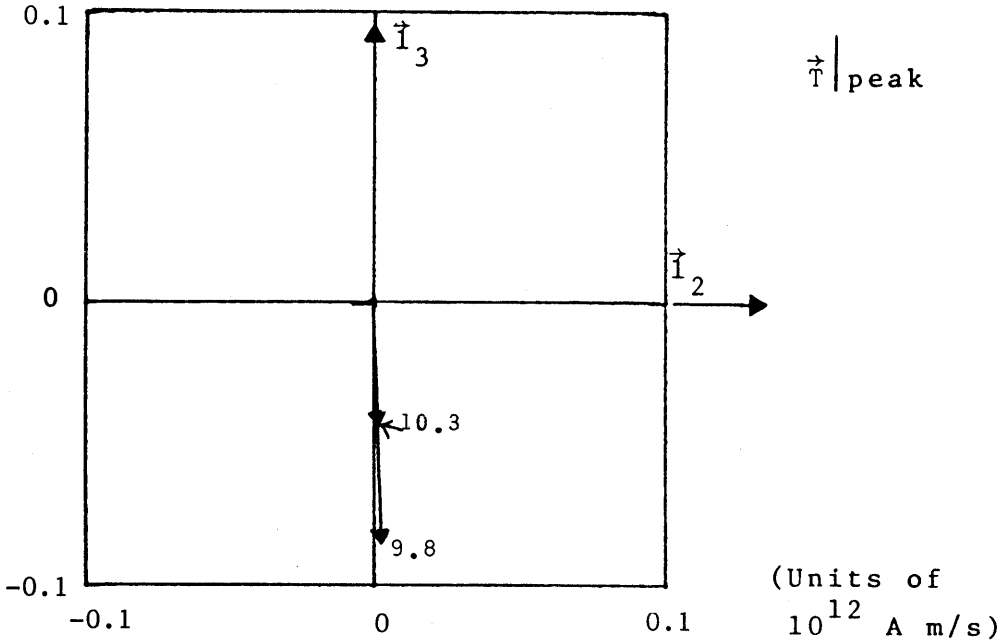

Peaks of $\vec{T}$

$\phi = 317^{o}$ $\theta = 34^{o}$ r = 1994 m Set 3

Date: 79219 M.S.T.: 09:53:39

Figure 6.7.7B.3 $\vec{T}$ for midrange return stroke

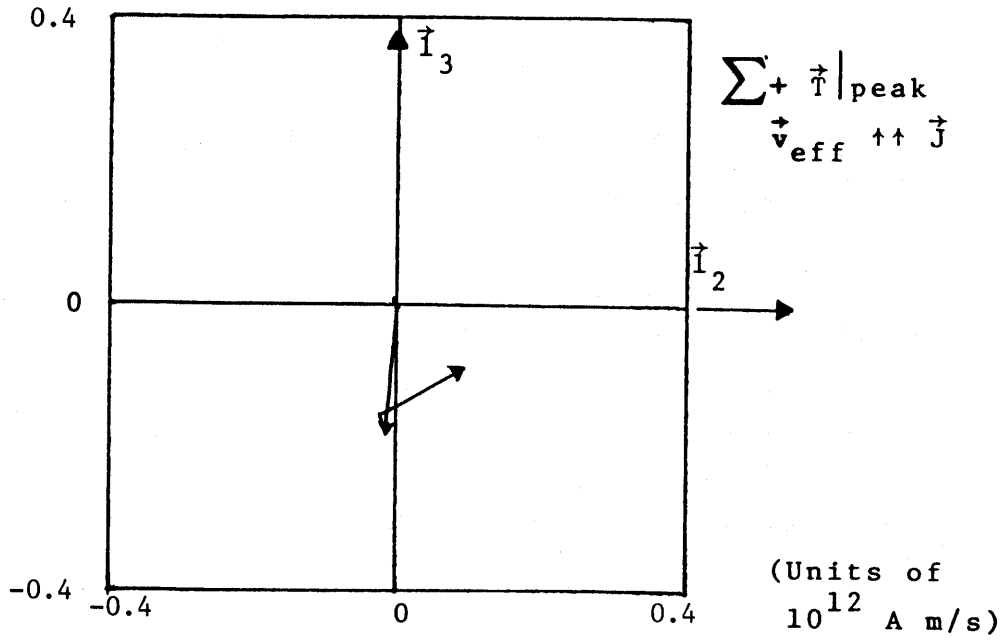

Effective reconstruction of positive streamer

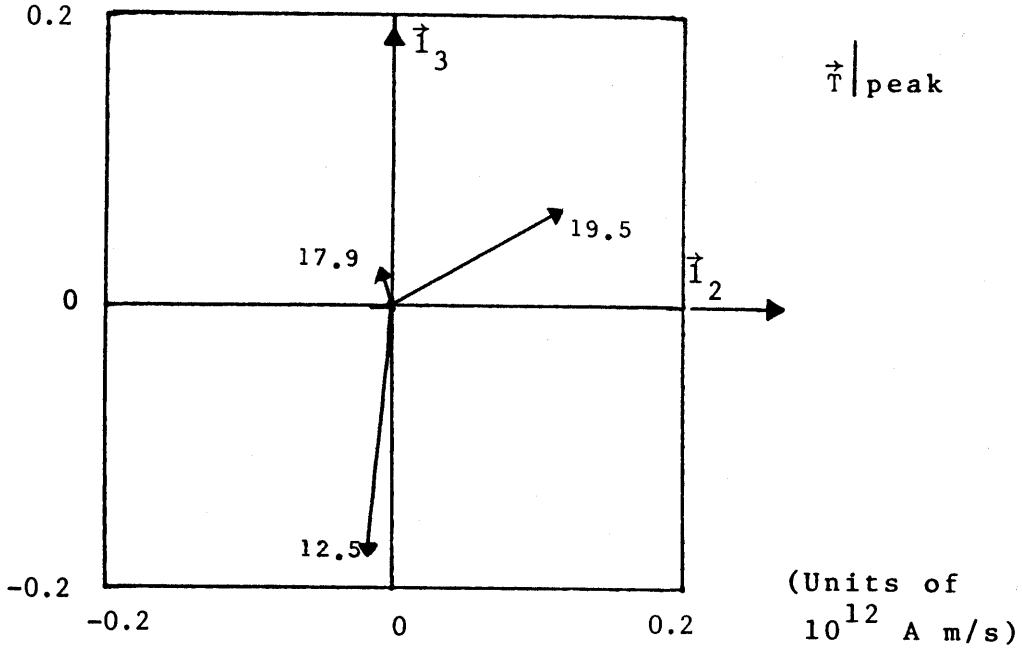

Peaks of $\vec{T}$

ϕ = 12° θ = 43° r = 1635 m Set 4

Date: 79219 M.S.T.: 09:53:39

Figure 6.7.7B.4 $\vec{T}$ for midrange return stroke

6.8 Midrange Return Stroke

Our eighth example is given in figures 6.8.•••. This is labelled "midrange return stroke". Figures 6.8.1A and 6.8.1B show the derivative fields and fields for the 20 μs record.

Figure 6.8.3 shows the slow electric field and thunder microphone records, from which a horizontal range of 833 m is estimated. The acoustic source reconstruction in Figure 6.8.4 shows a very extended strike of about 3.5 km height ranging about 3 km to the northeast and 5 km to the west of south; the strike reaches the ground southeast of the Kiva.

The θ, ϕ contours give two approximate sets of contour intersections. These agree with the videotape photographs and the acoustic reconstruction.

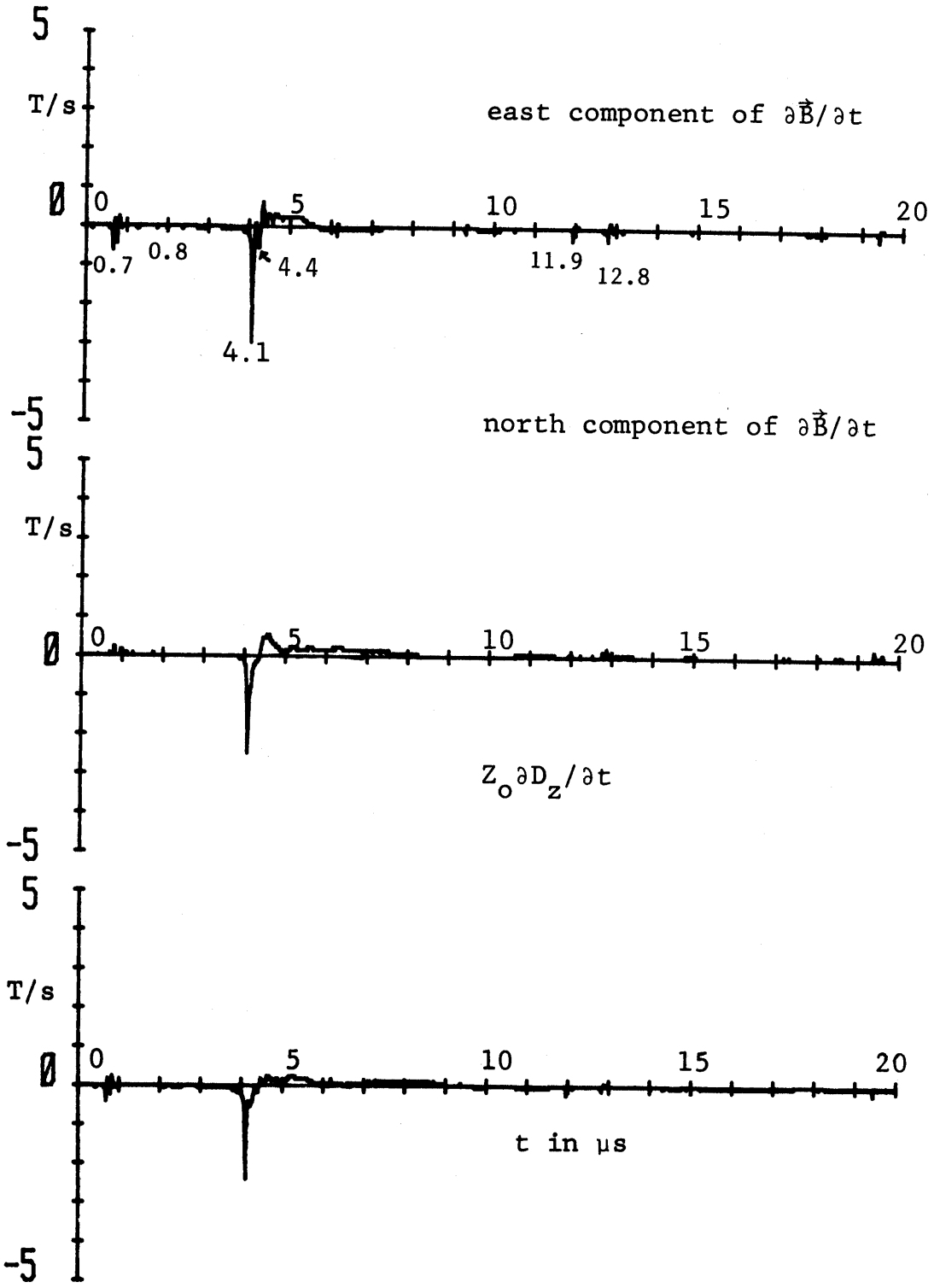

Figure 6.8.1 A **Derivative fields from midrange return stroke**

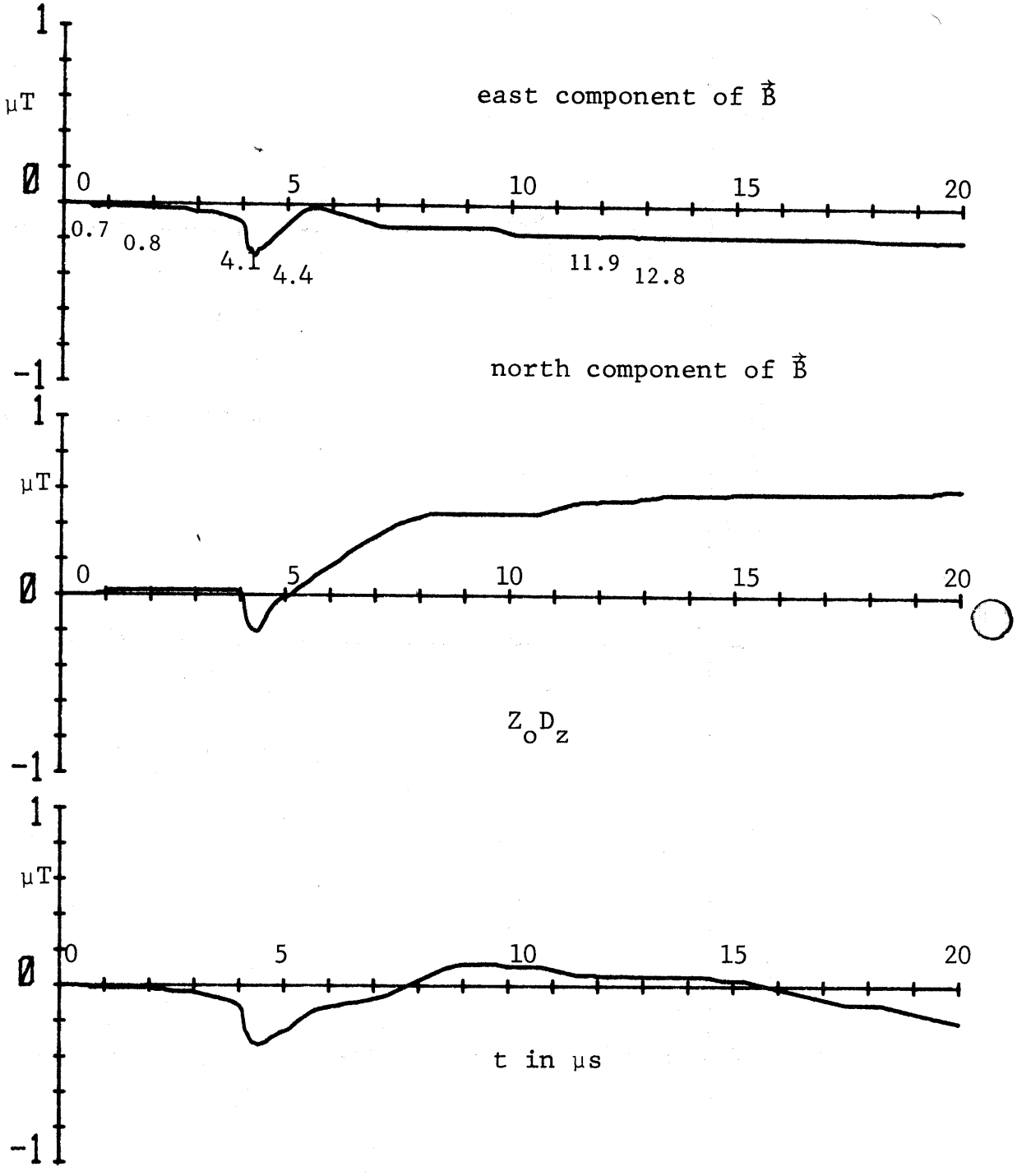

Figure 6.8.1B Fields from midrange return stroke

Figure 6.8.2.1 Digital data for event 0.7

[ ] = baseline which is subtracted for peaks and numerical integration

Yeardate: 79219 Time: 10:34:22 M.S.T.

Time (μs)	$\partial B_E/\partial t$ (T/s)	$\partial B_N/\partial t$ (T/s)	$Z_o \partial D_z/\partial t$ (T/s)	B_E (μT)	B_N (μT)	$Z_o D_z$ (μT)
0.63	[-0.234]	0.000	0.000	-0.000	0.000	0.000
0.64	-0.391	0.000	0.000	-0.002	0.000	0.000
0.65	-0.703	0.000	0.000	-0.006	0.000	0.000
0.66	-0.781	0.000	[0.000]	-0.012	0.000	0.000
0.67	-0.391	0.000	-0.236	-0.013	0.000	-0.002
0.68	-0.078	[0.000]	-0.353	-0.012	0.000	-0.006
0.69	-0.078	0.078	-0.177	-0.010	0.001	-0.008
0.70	0.000	0.000	0.000	-0.008	0.001	-0.008
0.71	0.000	0.000	0.059	-0.006	0.001	-0.007
0.72	0.000	0.000	0.236	-0.003	0.001	-0.005
0.73	0.000	0.000	0.177	-0.001	0.001	-0.003
0.74	-0.078	0.000	0.118	0.001	0.001	-0.002
0.75	-0.391	0.000	0.118	-0.001	0.001	-0.001
0.76	-0.625	0.000	0.059	-0.005	0.001	-0.000
0.77	-0.391	0.000	0.000	-0.006	0.001	-0.000

Figure 6.8.2.2 Digital data for event 0.8

[ ] = baseline which is subtracted for peaks and numerical integration

Yeardate: 79219 Time: 10:34:22 M.S.T.

Time (μs)	$\partial B_E/\partial t$ (T/s)	$\partial B_N/\partial t$ (T/s)	$Z_o \partial D_z/\partial t$ (T/s)	B_E (μT)	B_N (μT)	$Z_o D_z$ (μT)
0.73	[0.000]	0.000	[0.177]	0.000	0.000	-0.000
0.74	-0.078	0.000	0.118	-0.001	0.000	-0.001
0.75	-0.391	0.000	0.118	-0.005	0.000	-0.001
0.76	-0.625	0.000	0.059	-0.011	0.000	-0.002
0.77	-0.391	0.000	0.000	-0.015	0.000	-0.004
0.78	-0.078	[0.000]	-0.177	-0.016	0.000	-0.008
0.79	-0.078	0.234	-0.177	-0.016	0.002	-0.011
0.80	0.000	0.234	0.059	-0.016	0.005	-0.012
0.81	0.078	0.234	0.236	-0.016	0.007	-0.012
0.82	0.000	0.156	0.295	-0.016	0.009	-0.011
0.83	0.000	0.000	0.236	-0.016	0.009	-0.010
0.84	-0.156	0.000	0.236	-0.018	0.009	-0.009
0.85	-0.156	0.000	0.059	-0.019	0.009	-0.011

Figure 6.8.2.3 Digital data for event 4.1

[ ] = baseline which is subtracted for peaks and numerical integrati

Yeardate: 79219 Time: 10:34:22 M.S.T.

Time (μs)	$\partial B_E/\partial t$ (T/s)	$\partial B_N/\partial t$ (T/s)	$Z_o \partial D_z/\partial t$ (T/s)	B_E (μT)	B_N (μT)	$Z_o D_z$ (μT)
3.98	-0.391	-0.078	-0.118	0.000	-0.000	0.000
3.99	-0.391	[-0.078]	-0.118	0.000	-0.000	0.000
4.00	[-0.391]	-0.156	[-0.118]	0.000	-0.001	0.000
4.01	-0.469	-0.234	-0.177	-0.001	-0.002	-0.001
4.02	-0.547	-0.234	-0.236	-0.002	-0.004	-0.002
4.03	-0.547	-0.234	-0.236	-0.004	-0.005	-0.003
4.04	-0.703	-0.391	-0.236	-0.007	-0.009	-0.004
4.05	-0.938	-0.625	-0.295	-0.012	-0.014	-0.006
4.06	-1.328	-0.938	-0.353	-0.022	-0.023	-0.008
4.07	-2.578	-1.328	-0.471	-0.044	-0.035	-0.012
4.08	-3.125	-2.500	-0.884	-0.071	-0.059	-0.019
4.09	-2.578	-2.266	-1.826	-0.093	-0.081	-0.036
4.10	-1.328	-1.875	-2.356	-0.102	-0.099	-0.059
4.11	-1.250	-1.563	-2.356	-0.111	-0.114	-0.081
4.12	-0.938	-1.328	-1.414	-0.116	-0.127	-0.094
4.13	-0.391	-0.938	-0.943	-0.116	-0.135	-0.102
4.14	-0.078	-0.938	-0.943	-0.113	-0.144	-0.111
4.15	-0.078	-0.859	-0.471	-0.110	-0.152	-0.114
4.16	-0.078	-0.781	-0.412	-0.107	-0.159	-0.117
4.17	-0.078	-0.781	-0.353	-0.104	-0.166	-0.120
4.18	-0.313	-0.625	-0.412	-0.103	-0.171	-0.122
4.19	-0.391	-0.391	-0.412	-0.103	-0.174	-0.125
4.20	-0.625	-0.469	-0.471	-0.105	-0.178	-0.129
4.21	-0.703	-0.313	-0.471	-0.109	-0.180	-0.132
4.22	-0.703	-0.313	-0.471	-0.112	-0.183	-0.136
4.23	-0.703	-0.234	-0.471	-0.115	-0.184	-0.140
4.24	-0.703	-0.234	-0.412	-0.118	-0.186	-0.143
4.25	-0.703	-0.234	-0.353	-0.121	-0.188	-0.145
4.26	-0.391	-0.234	-0.353	-0.121	-0.189	-0.147
4.27	-0.313	-0.156	-0.353	-0.120	-0.190	-0.150
4.28	-0.078	-0.156	-0.295	-0.117	-0.191	-0.151
4.29	-0.078	-0.156	-0.177	-0.114	-0.191	-0.152
4.30	0.234	-0.156	-0.177	-0.108	-0.192	-0.153
4.31	0.313	-0.156	-0.118	-0.101	-0.193	-0.153
4.32	0.313	-0.156	0.000	-0.094	-0.194	-0.151
4.33	0.469	-0.078	0.000	-0.085	-0.194	-0.150
4.34	0.469	-0.078	0.000	-0.076	-0.194	-0.149
4.35	0.156	-0.078	0.000	-0.071	-0.194	-0.148
4.36	0.234	0.000	0.000	-0.065	-0.193	-0.146
4.37	0.000	0.000	0.000	-0.061	-0.192	-0.145
4.38	0.000	0.000	-0.118	-0.057	-0.192	-0.145
4.39	-0.078	0.156	-0.118	-0.054	-0.189	-0.145
4.40	-0.078	0.156	-0.118	-0.051	-0.187	-0.145
4.41	-0.156	0.234	-0.059	-0.048	-0.184	-0.145
4.42	-0.156	0.313	0.059	-0.046	-0.180	-0.143

Figure 6.8.2.3 Digital data for event 4.1 (continued)

Time (μs)	$\partial B_E/\partial t$ (T/s)	$\partial B_N/\partial t$ (T/s)	$Z_o \partial D_z/\partial t$ (T/s)	B_E (μT)	B_N (μT)	$Z_o D_z$ (μT)
4.43	-0.156	0.313	0.059	-0.044	-0.176	-0.141
4.44	0.078	0.391	0.059	-0.039	-0.171	-0.139
4.45	0.078	0.469	0.059	-0.034	-0.166	-0.138
4.46	0.078	0.469	0.177	-0.029	-0.160	-0.135
4.47	0.156	0.469	0.236	-0.024	-0.155	-0.131
4.48	0.156	0.469	0.177	-0.019	-0.149	-0.128
4.49	0.156	0.469	0.177	-0.013	-0.144	-0.125
4.50	0.156	0.469	0.177	-0.008	-0.139	-0.122
4.51	0.078	0.469	0.177	-0.003	-0.133	-0.119
4.52	0.078	0.469	0.177	0.002	-0.128	-0.116

Figure 6.8.2.4 Digital data for event 4.4

[ ] = baseline which is subtracted for peaks and numerical integratio

Yeardate: 79219 Time: 10:34:22 M.S.T.

Time (μs)	$\partial B_E/\partial t$ (T/s)	$\partial B_N/\partial t$ (T/s)	$Z_o \partial D_z/\partial t$ (T/s)	B_E (μT)	B_N (μT)	$Z_o D_z$ (μT)
4.37	0.000	0.000	0.000	0.000	0.000	0.000
4.38	0.000	0.000	-0.118	0.000	0.000	-0.001
4.39	-0.078	0.156	-0.118	-0.001	0.002	-0.002
4.40	-0.078	0.156	-0.118	-0.002	0.003	-0.004
4.41	-0.156	0.234	-0.059	-0.003	0.005	-0.004
4.42	-0.156	0.313	0.059	-0.005	0.009	-0.004
4.43	-0.156	0.313	0.059	-0.006	0.012	-0.003
4.44	0.078	0.391	0.059	-0.005	0.016	-0.002
4.45	0.078	0.469	0.059	-0.005	0.020	-0.002
4.46	0.078	0.469	0.177	-0.004	0.025	0.000
4.47	0.156	0.469	0.236	-0.002	0.030	0.002
4.48	0.156	0.469	0.177	-0.001	0.034	0.004
4.49	0.156	0.469	0.177	0.001	0.039	0.006
4.50	0.156	0.469	0.177	0.002	0.044	0.008
4.51	0.078	0.469	0.177	0.003	0.048	0.009
4.52	0.078	0.469	0.177	0.004	0.053	0.011
4.53	0.078	0.469	0.177	0.005	0.058	0.013
4.54	0.078	0.469	0.177	0.005	0.063	0.015
4.55	0.000	0.547	0.118	0.005	0.068	0.016
4.56	-0.078	0.547	0.118	0.005	0.073	0.017
4.57	-0.078	0.547	0.118	0.004	0.079	0.018
4.58	0.000	0.547	0.177	0.004	0.084	0.020
4.59	0.078	0.547	0.177	0.005	0.090	0.022
4.60	0.078	0.547	0.177	0.005	0.095	0.024
4.61	0.078	0.547	0.236	0.006	0.101	0.026
4.62	0.156	0.469	0.295	0.008	0.105	0.029
4.63	0.156	0.469	0.295	0.009	0.110	0.032
4.64	0.156	0.391	0.295	0.011	0.114	0.035
4.65	0.156	0.391	0.295	0.013	0.118	0.038
4.66	0.156	0.391	0.295	0.014	0.122	0.041
4.67	0.156	0.391	0.295	0.016	0.126	0.044
4.68	0.156	0.391	0.295	0.017	0.130	0.047
4.69	0.156	0.313	0.236	0.019	0.133	0.049
4.70	0.078	0.313	0.236	0.020	0.136	0.051
4.71	0.078	0.313	0.236	0.020	0.139	0.054
4.72	0.078	0.313	0.236	0.021	0.142	0.056
4.73	0.078	0.313	0.236	0.022	0.145	0.058
4.74	0.078	0.313	0.177	0.023	0.148	0.060
4.75	0.078	0.313	0.177	0.023	0.152	0.062
4.76	0.078	0.313	0.177	0.024	0.155	0.064
4.77	0.078	0.234	0.177	0.025	0.157	0.065
4.78	0.078	0.234	0.177	0.026	0.159	0.067
4.79	0.078	0.234	0.177	0.027	0.162	0.069
4.80	0.078	0.234	0.177	0.027	0.164	0.071

Figure 6.8.2.4 Digital data for event 4.4 (continued)

Time (μs)	$\partial B_E/\partial t$ (T/s)	$\partial B_N/\partial t$ (T/s)	$Z_o \partial D_z/\partial t$ (T/s)	B_E (μT)	B_N (μT)	$Z_o D_z$ (μT)
4.81	0.000	0.234	0.177	0.027	0.166	0.072
4.82	0.078	0.234	0.177	0.028	0.169	0.074
4.83	0.078	0.234	0.177	0.029	0.171	0.076
4.84	0.078	0.234	0.177	0.030	0.173	0.078
4.85	0.078	0.156	0.236	0.030	0.175	0.080
4.86	0.078	0.156	0.236	0.031	0.177	0.082
4.87	0.078	0.156	0.236	0.032	0.178	0.085
4.88	0.078	0.156	0.236	0.033	0.180	0.087
4.89	0.078	0.156	0.177	0.034	0.181	0.089
4.90	0.078	0.156	0.177	0.034	0.183	0.091
4.91	0.078	0.156	0.177	0.035	0.184	0.092
4.92	0.078	0.078	0.177	0.036	0.185	0.094
4.93	0.078	0.078	0.177	0.037	0.186	0.096
4.94	0.078	0.078	0.177	0.038	0.187	0.098
4.95	0.078	0.078	0.177	0.038	0.188	0.100
4.96	0.078	0.078	0.177	0.039	0.188	0.101
4.97	0.078	0.078	0.177	0.040	0.189	0.103
4.98	0.078	0.078	0.118	0.041	0.190	0.104
4.99	0.078	0.000	0.118	0.041	0.190	0.105

Figure 6.8.2.5 Digital data for event 11.9

[ ] = baseline which is subtracted for peaks and numerical integration

Yeardate: 79219 Time: 10:34:22 M.S.T.

Time (μs)	$\partial B_E/\partial t$ (T/s)	$\partial B_N/\partial t$ (T/s)	$Z_o \partial D_z/\partial t$ (T/s)	B_E (μT)	B_N (μT)	$Z_o D_z$ (μT)
11.90	-0.156	0.000	0.059	-0.000	0.000	-0.000
11.91	[-0.156]	0.000	0.059	-0.000	0.000	-0.000
11.92	-0.469	0.000	0.059	-0.003	0.000	-0.000
11.93	-0.391	0.000	[0.059]	-0.005	0.000	-0.000
11.94	-0.313	0.000	0.000	-0.007	0.000	-0.001
11.95	-0.078	[0.000]	-0.177	-0.006	0.000	-0.003
11.96	-0.078	0.078	-0.177	-0.005	0.001	-0.005
11.97	-0.078	0.078	0.059	-0.005	0.002	-0.005
11.98	-0.078	0.078	0.059	-0.004	0.002	-0.005
11.99	-0.078	0.078	0.118	-0.003	0.003	-0.005
12.00	-0.078	0.078	0.059	-0.002	0.004	-0.005
12.01	-0.078	0.078	0.059	-0.002	0.005	-0.005
12.02	-0.078	0.078	0.059	-0.001	0.005	-0.005
12.03	-0.078	0.078	0.059	-0.000	0.006	-0.005
12.04	-0.078	0.000	0.059	0.001	0.006	-0.005

Figure 6.8.2.6 Digital data for event 12.8

[ ] = baseline which is subtracted for peaks and numerical integratio

Yeardate: 79219 Time: 10:34:22 M.S.T.

Time (μs)	$\partial B_E/\partial t$ (T/s)	$\partial B_N/\partial t$ (T/s)	$Z_o \partial D_z/\partial t$ (T/s)	B_E (μT)	B_N (μT)	$Z_o D_z$ (μT)
12.72	-0.156	0.000	0.059	-0.000	0.000	-0.000
12.73	[-0.156]	0.000	0.059	-0.000	0.000	-0.000
12.74	-0.234	0.000	0.059	-0.001	0.000	-0.000
12.75	-0.234	[0.000]	0.059	-0.002	0.000	-0.000
12.76	-0.234	0.156	0.059	-0.002	0.002	-0.000
12.77	-0.234	0.156	0.059	-0.003	0.003	-0.000
12.78	-0.391	0.078	0.059	-0.005	0.004	-0.000
12.79	-0.469	0.000	[0.059]	-0.009	0.004	-0.000
12.80	-0.313	0.000	0.000	-0.010	0.004	-0.001
12.81	-0.078	0.000	0.000	-0.009	0.004	-0.001
12.82	-0.078	0.000	-0.059	-0.009	0.004	-0.002
12.83	-0.078	0.000	0.000	-0.008	0.004	-0.003
12.84	0.000	0.000	0.059	-0.006	0.004	-0.003
12.85	0.000	0.156	0.059	-0.004	0.006	-0.003
12.86	0.000	0.156	0.059	-0.003	0.007	-0.003
12.87	-0.078	0.234	0.118	-0.002	0.009	-0.002
12.88	-0.078	0.156	0.118	-0.001	0.011	-0.002
12.89	-0.078	0.156	0.118	-0.001	0.013	-0.001
12.90	-0.156	0.078	0.118	-0.001	0.013	-0.001
12.91	-0.234	0.078	0.059	-0.001	0.014	-0.001

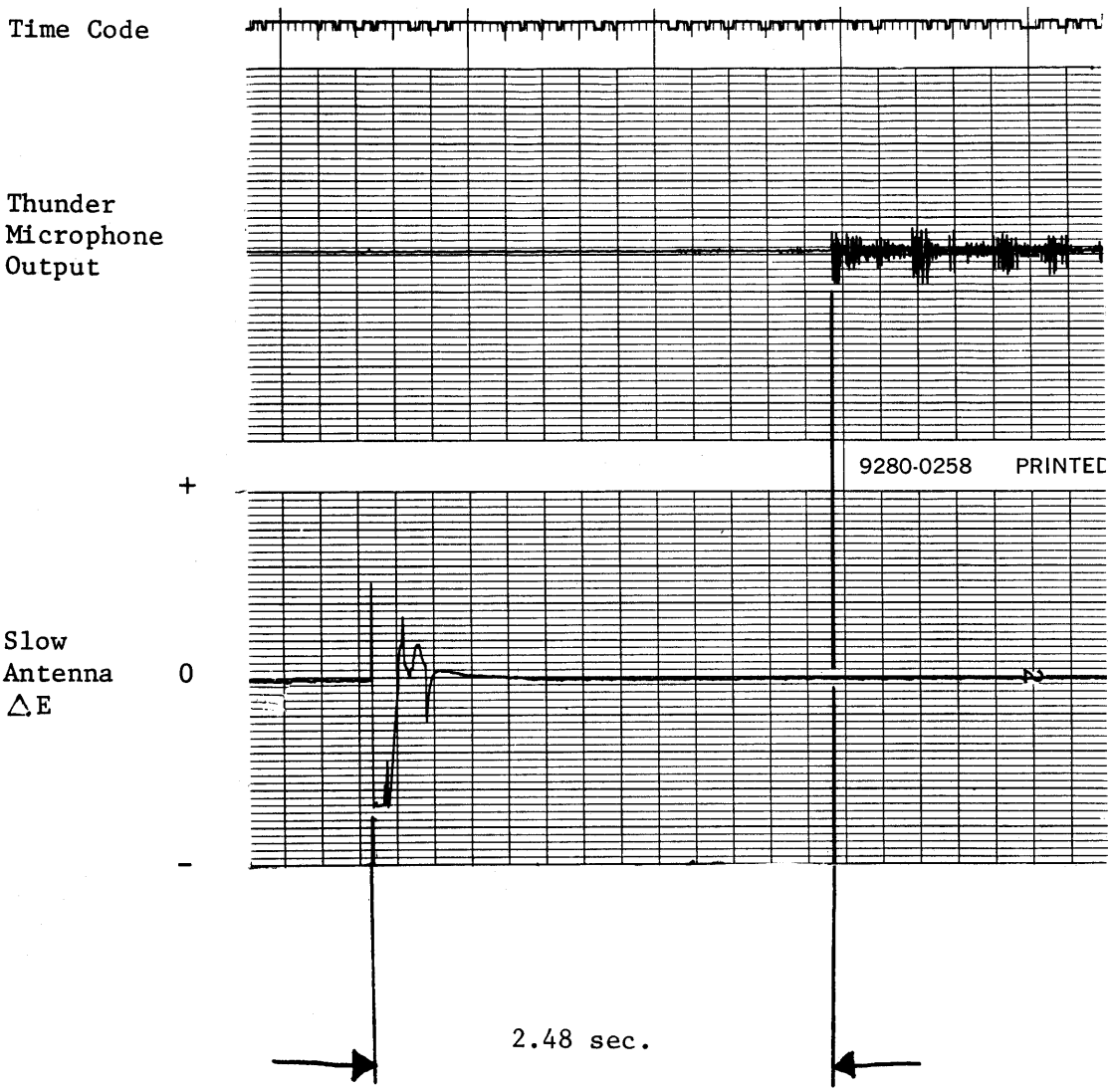

Figure 6.8.3 Slow E field change and thunder microphone record of midrange return stroke

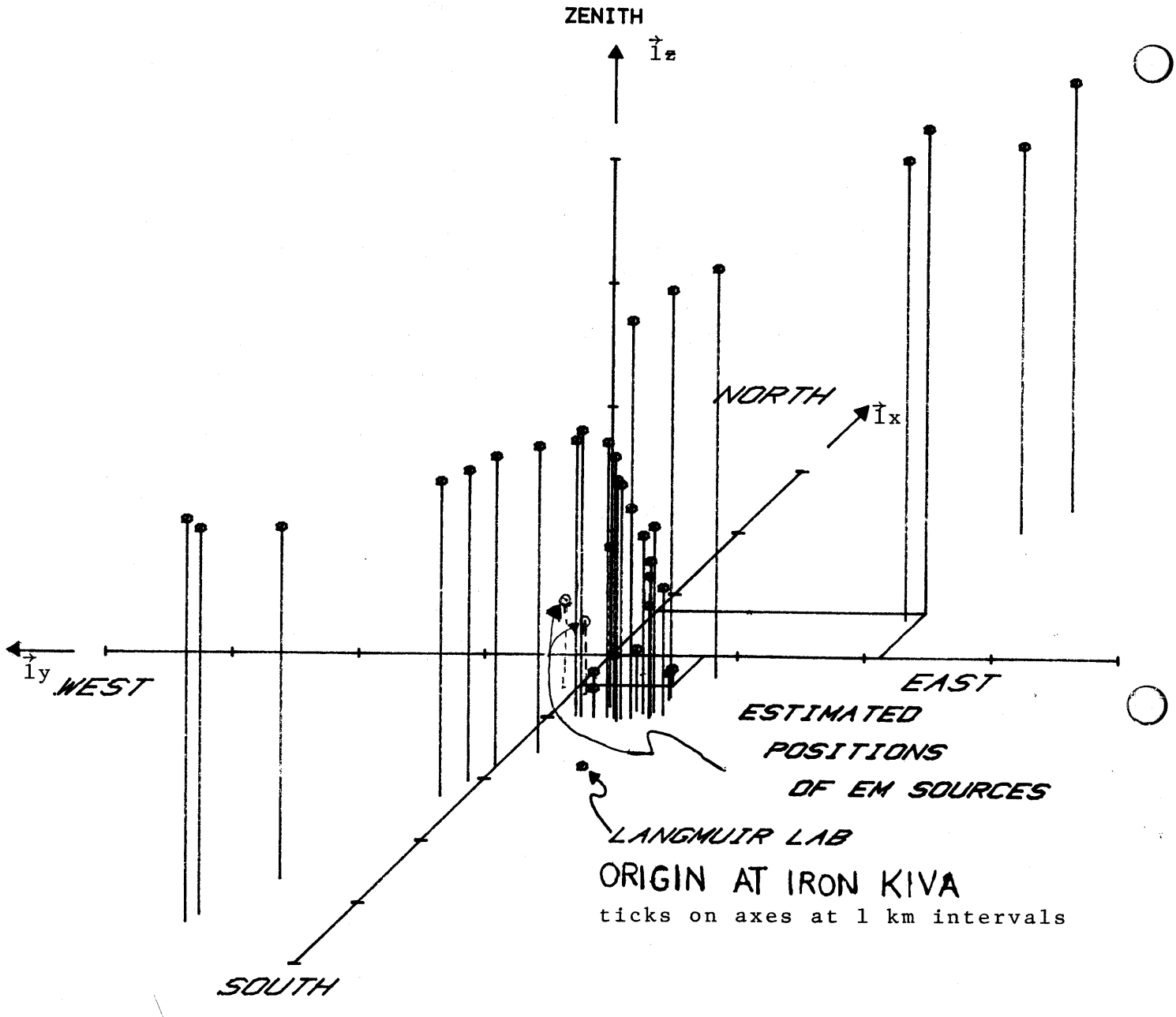

Date: 79219 M.S.T.: 1034:21.5

Figure 6.8.4 Acoustic location of midrange return stroke

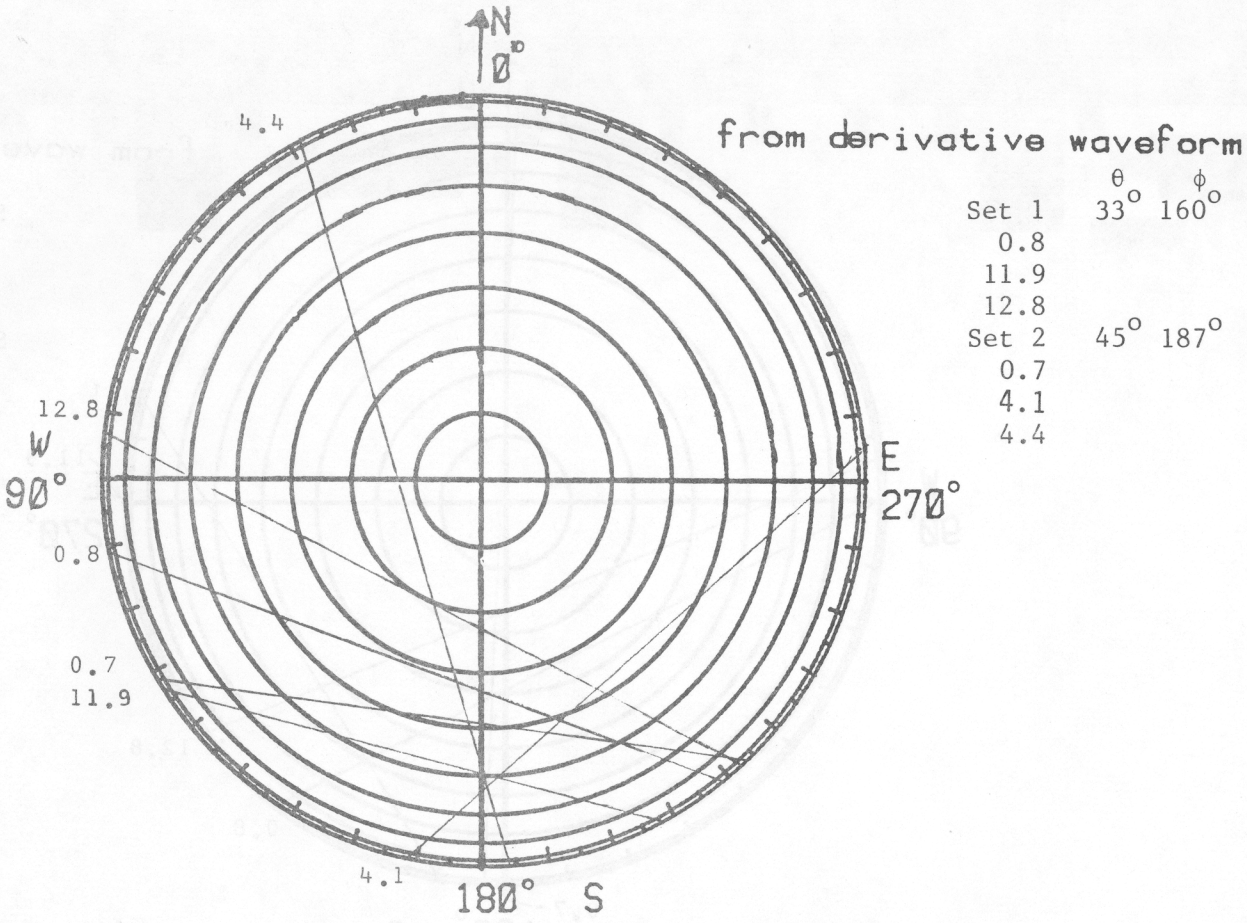

Whole-sky photograph from Kiva

Date: 79219 M.S.T.: 10:34:22

Figure 6.8.5A sin(θ),φ contours for midrange return stroke derivative waveform and whole-sky videotape photograph

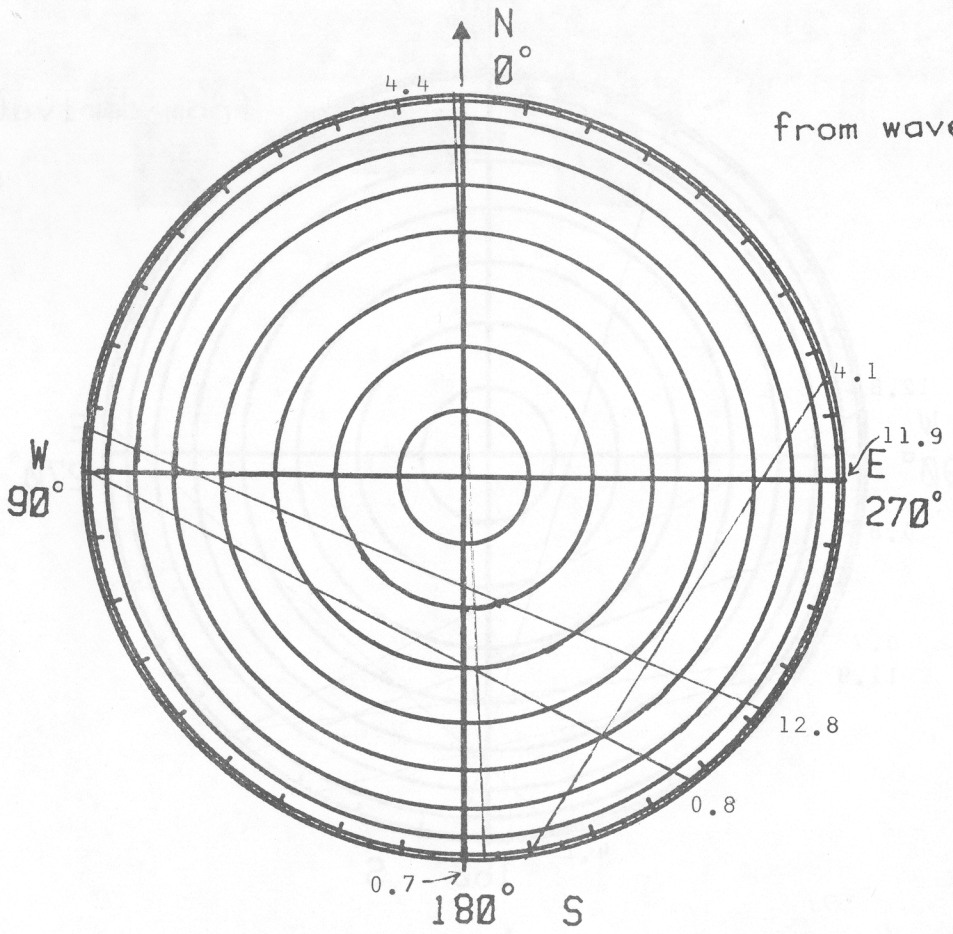

from waveform

	θ	ϕ
Set 1	21°	155°
0.8		
11.9		
12.8		
Set 2	87°	184°
0.7		
4.1		
4.4		

sin(θ),ϕ contour plot

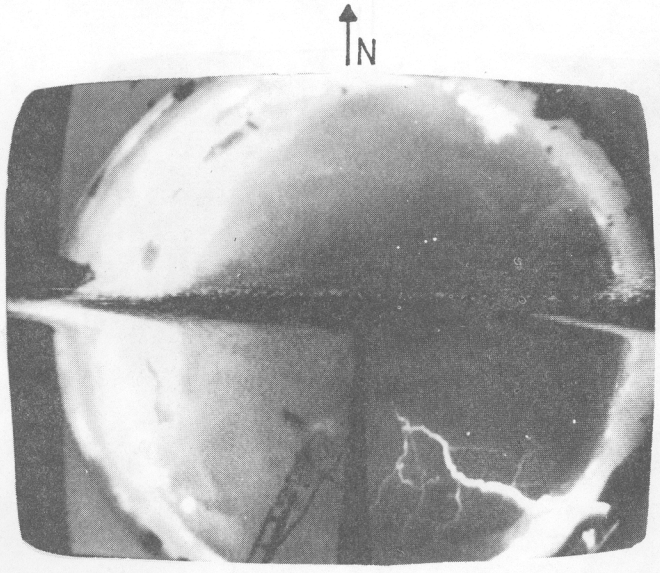

Whole-sky photograph from Kiva

Date: 79219 M.S.T.: 10:34:22

Figure 6.8.5B sin(θ),ϕ contours for midrange return stroke waveform and whole-sky videotape photograph

Figure 6.8.6A.1 Tabulation of peak values for each event from derivative waveform set for midrange return stroke

Yeardate: 79219 M.S.T.:103422

$\phi = 160^\circ$; $\theta = 33^\circ$; r = 1529 m Set 1

Event Number	Time (μs)	$Z_o \Delta\partial D_z/\partial t$ (T/s)	$\Delta\partial B_E/\partial t$ (T/s)	$\Delta\partial B_N/\partial t$ (T/s)	$\Delta\partial B_h/\partial t$ (T/s)	$\Delta\partial B_e/\partial t$ (T/s)	$\lvert\Delta\partial\vec{B}/\partial t\rvert$ (T/s)
0.8	0.80	-0.35	-0.63	0.23	0.00	-0.34	0.34
11.9	11.90	-0.24	-0.31	0.08	-0.02	-0.16	0.16
12.8	12.80	-0.12	-0.31	0.16	0.03	-0.17	0.18

CALCULATED VALUES FOR $\partial\vec{T}/\partial t$

Event Number	$\partial T_2/\partial t$ (10^{15} Am/s^2)	$\partial T_3/\partial t$ (10^{15} Am/s^2)	$\lvert\partial\vec{T}/\partial t\rvert$ (10^{15} Am/s^2)	α (deg)
0.8	-2	1539	1539	0
11.9	84	731	736	353
12.8	-121	794	803	9

Figure 6.8.6A.2 Tabulation of peak values for each event from derivative waveform set for midrange return stroke

Yeardate: 79219 M.S.T.:103422

$\phi = 187^\circ$; $\theta = 45^\circ$; r = 1178 m Set 2

Event Number	Time (μs)	$Z_o \Delta\partial D_z/\partial t$ (T/s)	$\Delta\partial B_E/\partial t$ (T/s)	$\Delta\partial B_N/\partial t$ (T/s)	$\Delta\partial B_h/\partial t$ (T/s)	$\Delta\partial B_e/\partial t$ (T/s)	$\lvert\Delta\partial\vec{B}/\partial t\rvert$ (T/s)
0.7	0.70	-0.35	-0.55	0.08	0.10	-0.27	0.29
4.1	4.08	-2.24	-2.73	-2.42	-1.46	-1.50	2.10
4.4	4.45	-0.12	-0.16	0.55	0.40	-0.05	0.40

CALCULATED VALUES FOR $\partial\vec{T}/\partial t$

Event Number	$\partial T_2/\partial t$ (10^{15} Am/s^2)	$\partial T_3/\partial t$ (10^{15} Am/s^2)	$\lvert\partial\vec{T}/\partial t\rvert$ (10^{15} Am/s^2)	α (deg)
0.7	-366	947	1016	21
4.1	5171	5309	7411	316
4.4	-1413	162	1422	83

Figure 6.8.6B.1 Tabulation of peak values for each event from waveform set for midrange return stroke

Yeardate: 79219 M.S.T.:103422

$\phi = 155^{\circ}$; $\theta = 21^{\circ}$; r =2324 m Set 1

Event Number	Time (μs)	$Z_o \Delta D_z$ (μT)	ΔB_E (μT)	ΔB_N (μT)	ΔB_h (μT)	ΔB_e (μT)	$\lvert\Delta\vec{B}\rvert$ (μT)
0.8	0.80	-0.01	-0.02	0.01	0.00	-0.01	0.01
11.9	11.90	-0.01	-0.01	0.01	0.00	-0.01	0.01
12.8	12.80	0.00	-0.01	0.00	-0.00	-0.00	0.01

CALCULATED VALUES FOR $\overleftarrow{I}_t . \vec{T}$

Event Number	T_2 (10^9 Am/s)	T_3 (10^9 Am/s)	$\lvert\vec{T}\rvert$ (10^9 Am/s)	α (deg)
0.8	-2	78	78	2
11.9	-18	46	50	21
12.8	16	32	35	333

Figure 6.8.6B.2 Tabulation of peak values for each event from waveform set for midrange return stroke

Yeardate: 79219 M.S.T.:103422

$\emptyset = 184^{\circ}$; $\Theta = 87^{\circ}$; r = 834 m Set 2

Event Number	Time (μs)	$Z_o \Delta D_z$ (μT)	ΔB_E (μT)	ΔB_N (μT)	ΔB_h (μT)	ΔB_e (μT)	$\lvert\Delta\vec{B}\rvert$ (μT)
0.7	0.70	-0.01	-0.01	0.00	0.00	-0.00	0.01
4.1	4.08	-0.15	-0.12	-0.19	-0.09	-0.07	0.11
4.4	4.42	0.00	-0.01	0.19	0.10	0.00	0.10

CALCULATED VALUES FOR $\overleftarrow{I}_t . \vec{T}$

Event Number	T_2 (10^9 Am/s)	T_3 (10^9 Am/s)	$\lvert\vec{T}\rvert$ (10^9 Am/s)	α (deg)
0.7	-1	12	13	4
4.1	227	166	281	306
4.4	-238	-4	238	91

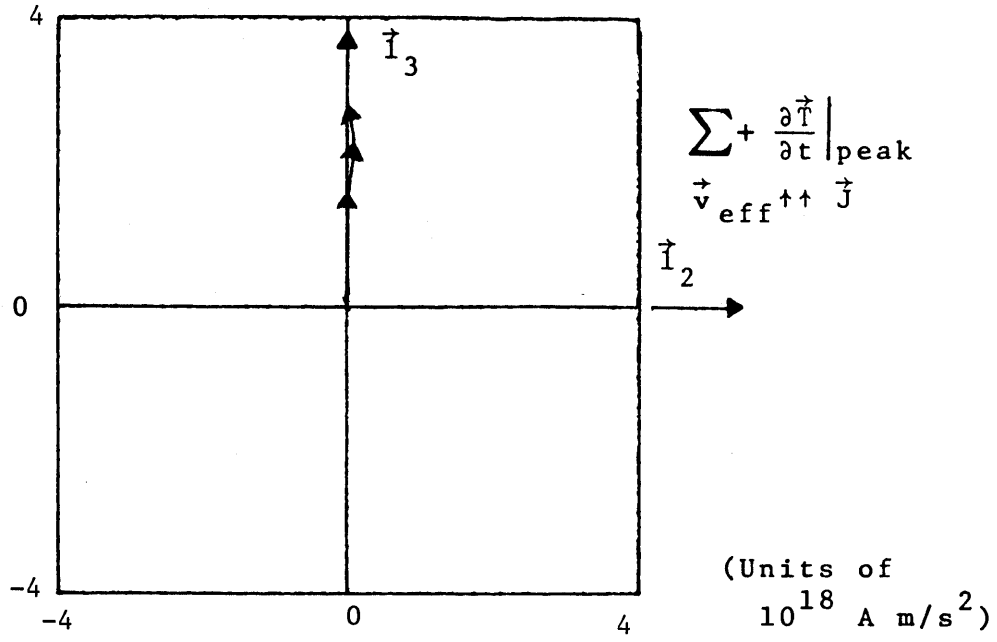

Effective reconstruction of positive streamer

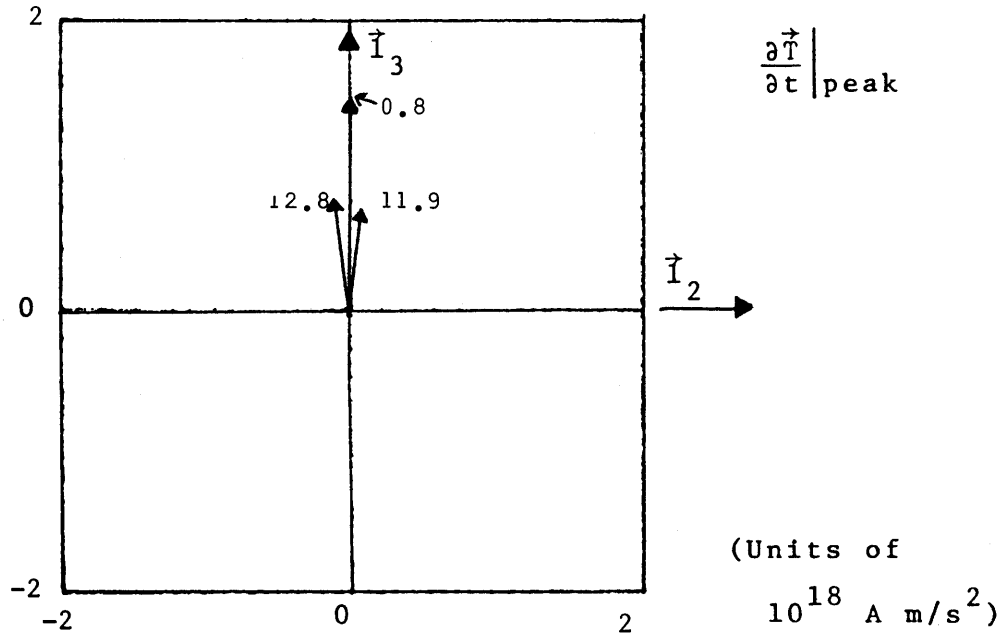

Peaks of $\partial\vec{I}/\partial t$

ϕ = 160° θ = 33° r = 1529 m Set 1

Date: 79219 M.S.T.: 10:34:22

Figure 6.8.7A.1 $\partial\vec{I}/\partial t$ for midrange return stroke

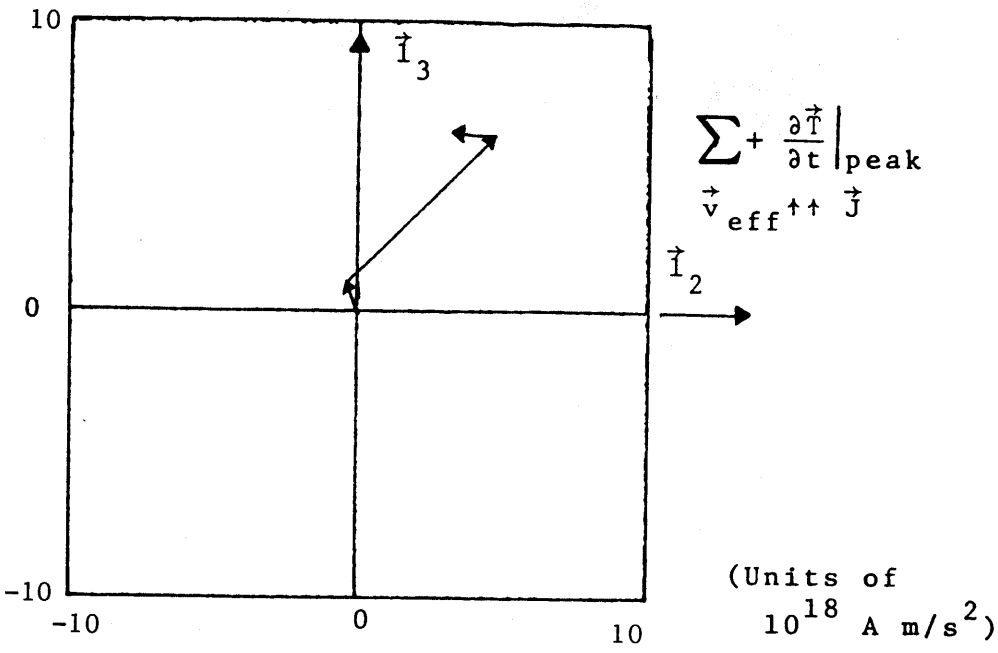

Effective reconstruction of positive streamer

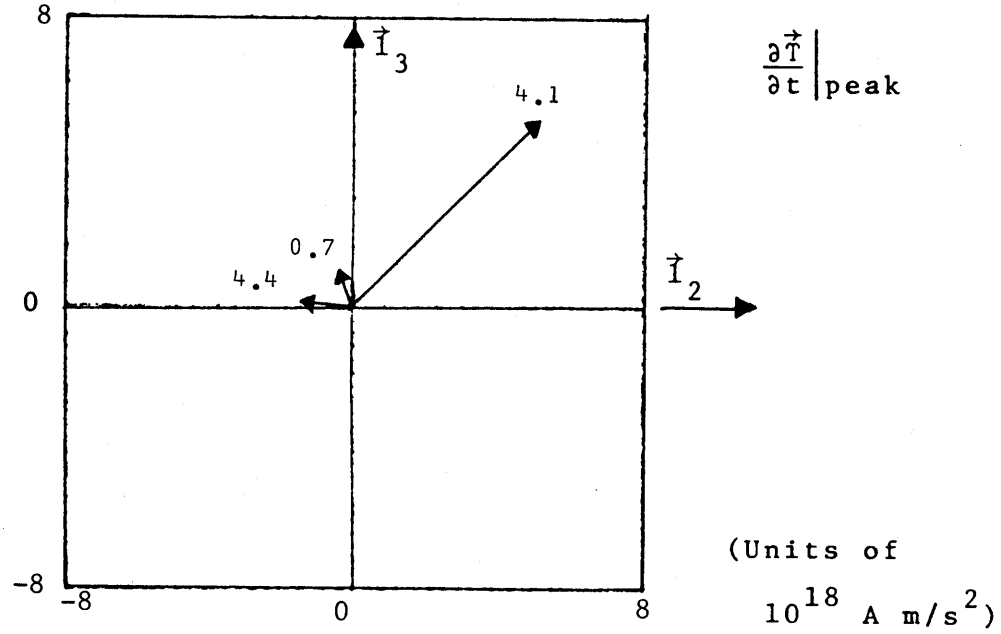

Peaks of $\partial\vec{I}/\partial t$

ϕ = 187° θ = 45° r = 1178 m Set 2

Date: 79219 M.S.T.: 10:34:22

Figure 6.8.7 A.2 $\partial\vec{I}/\partial t$ for midrange return stroke

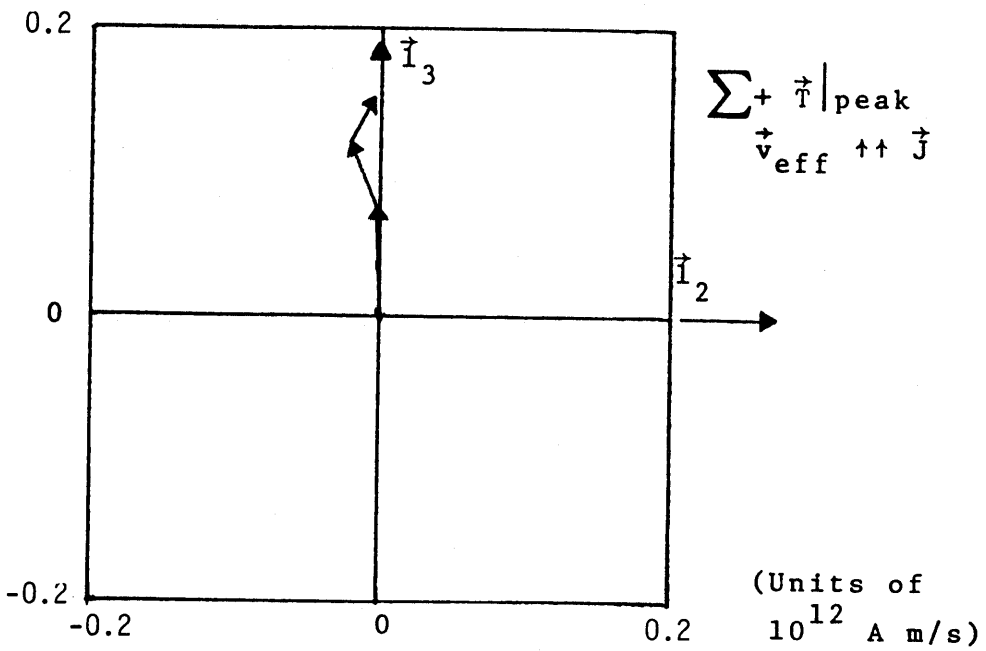

Effective reconstruction of positive streamer

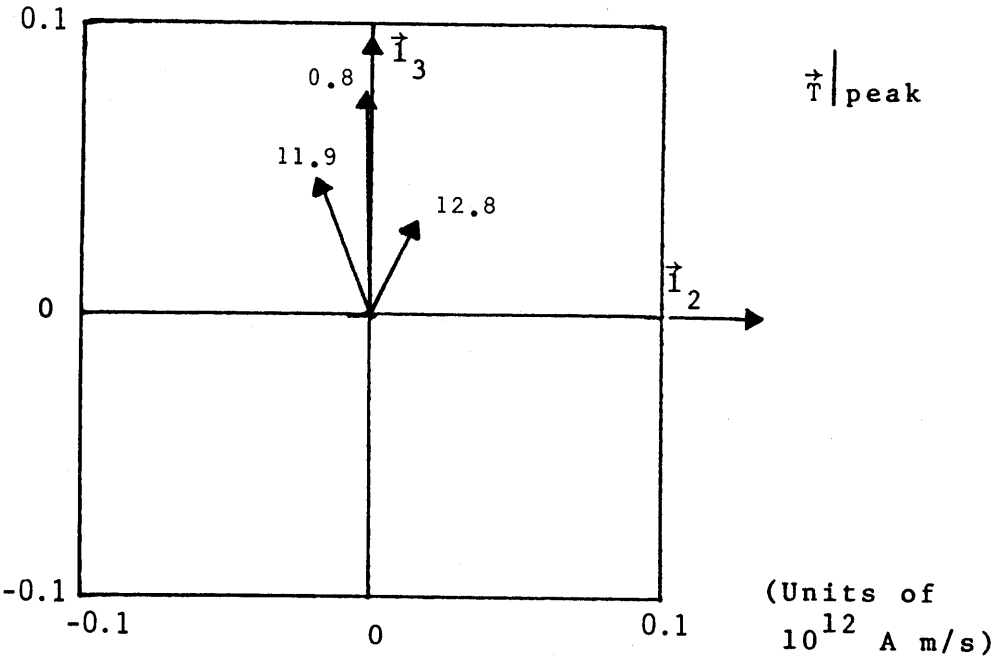

Peaks of $\vec{T}$

$\phi = 155^0$ $\theta = 21^0$ r = 2324 m Set 1

Date: 79219 M.S.T.: 10:34:22

Figure 6.8.7B.1 $\vec{T}$ for midrange return stroke

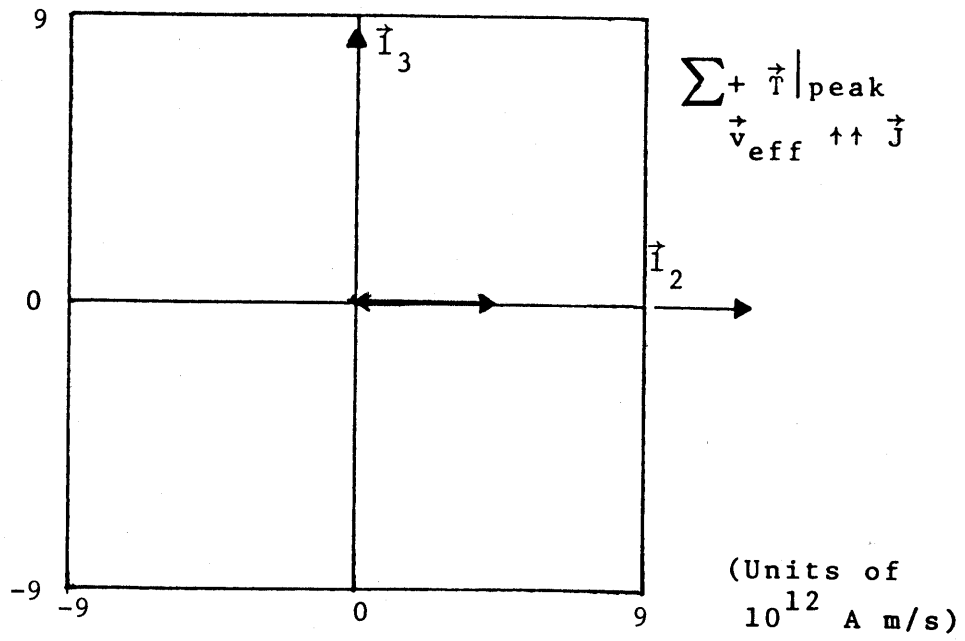

Effective reconstruction of positive streamer

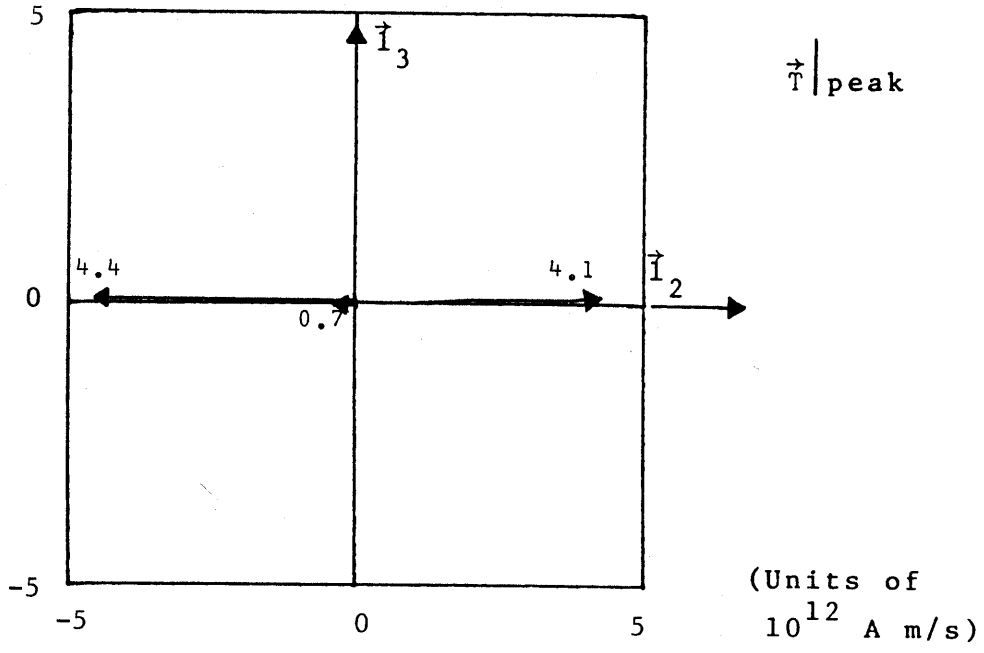

Peaks of $\vec{T}$

$\phi = 184^{o}$ $\theta = 87^{o}$ $r = 834$ m Set 2

Date: 79219 M.S.T.: 10:34:22

Figure 6.8.7B.2 $\vec{T}$ for midrange return stroke

6.9 Midrange Return Stroke

Our ninth example is given in Figures 6.9.•••. This is labelled "midrange return stroke". Figures 6.9.1A and 6.9.1B show the derivative fields and fields for the 20 μs record.

Figure 6.9.3 shows the slow electric field and thunder microphone records, from which a horizontal range of 759 m is estimated. The acoustic source reconstruction in Figure 6.9.4 shows a very extended strike of about 4 km height ranging about 3 km to the east and 5 km to the southwest; the strike reaches ground generally south or somewhat southeast of the Kiva.

The θ , ϕ contours give two approximate sets of contour intersections near the horizon to the southeast in agreement with the videotape photographs.

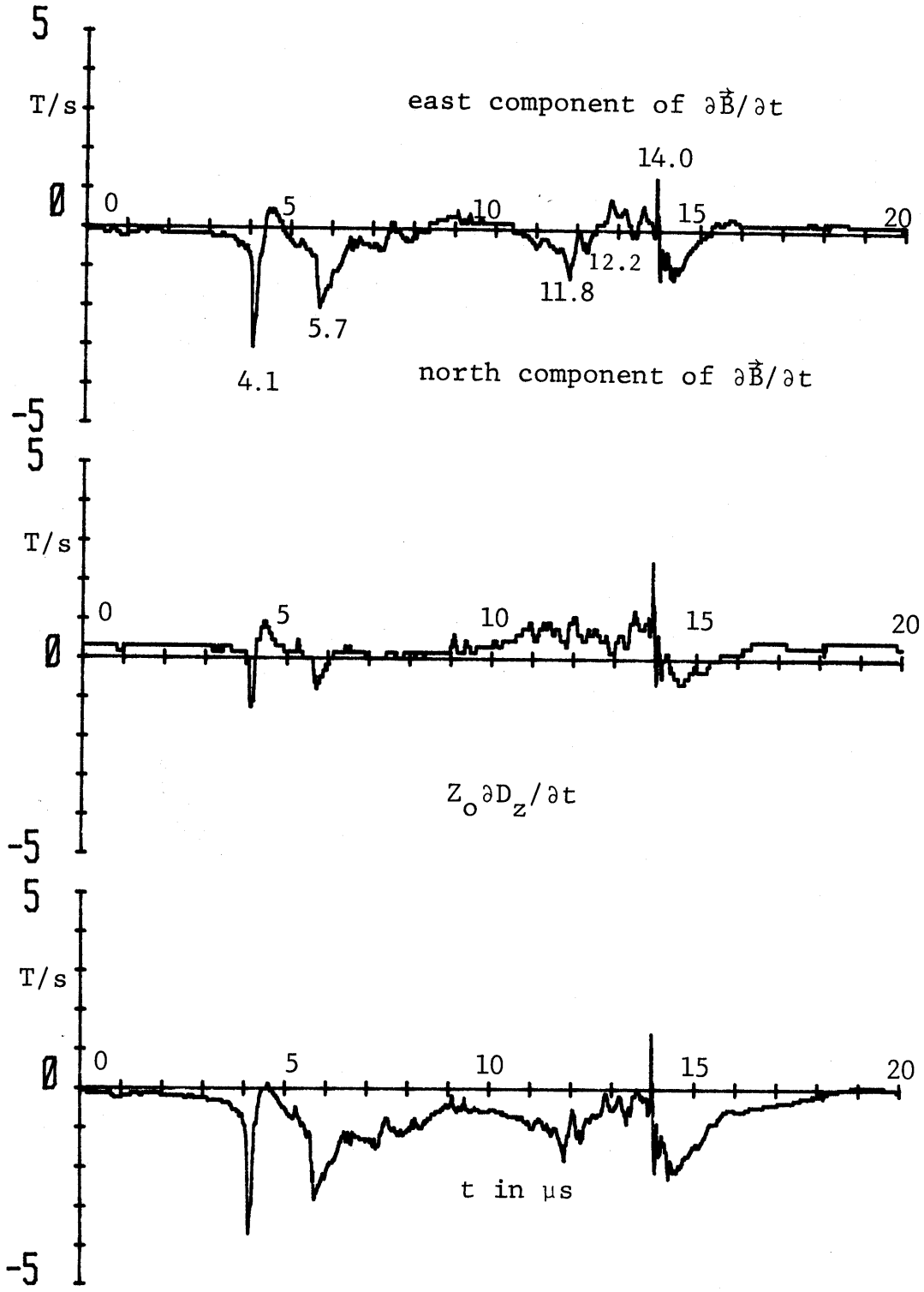

Date: 79230 M.S.T.: 1315:17

Figure 6.9.1 A Derivative fields from midrange return stroke

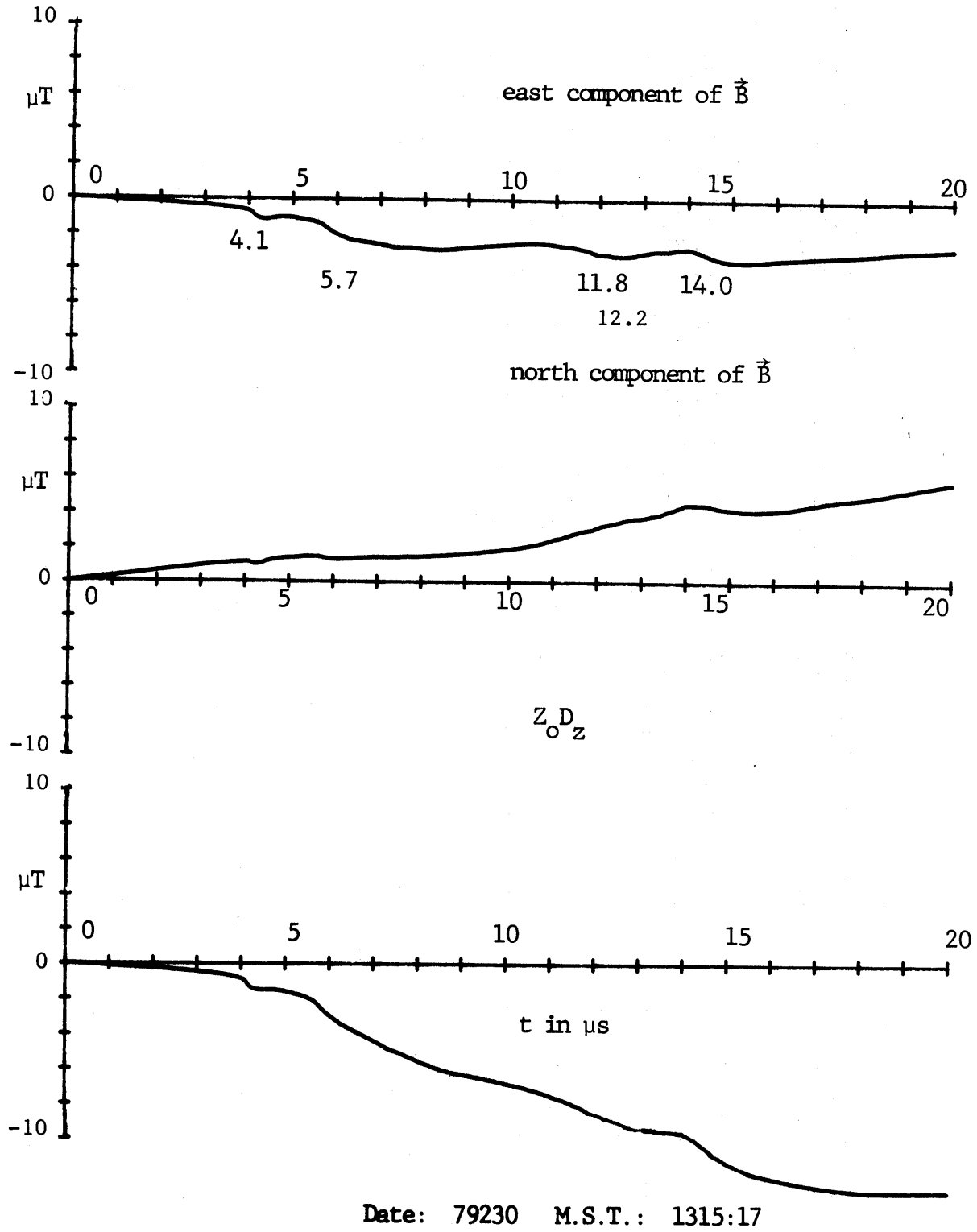

Figure 6.9.1B Fields from midrange return stroke

Figure 6.9.2.1 Digital data for event 4.1

[ ] = baseline which is subtracted for peaks and numerical integratio

Yeardate: 79230 Time: 13:15:17 M.S.T.

Time (μs)	$\partial B_E/\partial t$ (T/s)	$\partial B_N/\partial t$ (T/s)	$Z_o \partial D_z/\partial t$ (T/s)	B_E (μT)	B_N (μT)	$Z_o D_z$ (μT)
3.93	-0.547	0.000	-0.648	0.000	0.000	0.000
3.94	-0.547	0.000	-0.648	0.000	0.000	0.000
3.95	-0.625	0.000	-0.648	-0.001	0.000	0.000
3.96	-0.703	0.000	-0.648	-0.002	0.000	0.000
3.97	-0.703	0.000	-0.707	-0.004	0.000	-0.001
3.98	-0.703	0.000	-0.825	-0.005	0.000	-0.002
3.99	-0.703	0.000	-0.884	-0.007	0.000	-0.005
4.00	-0.781	0.000	-0.884	-0.009	0.000	-0.007
4.01	-0.859	-0.156	-0.943	-0.012	-0.002	-0.010
4.02	-0.859	-0.156	-0.943	-0.016	-0.003	-0.013
4.03	-0.938	-0.156	-0.943	-0.020	-0.005	-0.016
4.04	-1.016	-0.156	-1.060	-0.024	-0.006	-0.020
4.05	-1.250	-0.156	-1.119	-0.031	-0.008	-0.025
4.06	-1.328	-0.156	-1.178	-0.039	-0.009	-0.030
4.07	-2.500	-0.156	-1.355	-0.059	-0.011	-0.037
4.08	-3.125	-0.625	-1.649	-0.084	-0.017	-0.047
4.09	-3.125	-1.250	-2.297	-0.110	-0.030	-0.064
4.10	-2.891	-1.406	-3.240	-0.134	-0.044	-0.090
4.11	-2.813	-1.406	-3.711	-0.156	-0.058	-0.120
4.12	-2.578	-1.406	-3.534	-0.177	-0.072	-0.149
4.13	-2.500	-1.406	-3.299	-0.196	-0.086	-0.176
4.14	-2.422	-1.250	-3.240	-0.215	-0.098	-0.201
4.15	-2.344	-1.250	-3.063	-0.233	-0.111	-0.226
4.16	-2.344	-1.250	-3.004	-0.251	-0.123	-0.249
4.17	-2.188	-1.250	-3.004	-0.267	-0.136	-0.273
4.18	-1.953	-1.250	-2.945	-0.281	-0.148	-0.296
4.19	-1.641	-0.938	-2.886	-0.292	-0.158	-0.318
4.20	-1.563	-0.781	-2.533	-0.302	-0.166	-0.337
4.21	-1.328	-0.625	-2.297	-0.310	-0.172	-0.353
4.22	-1.016	-0.156	-1.885	-0.315	-0.173	-0.366
4.23	-0.938	-0.156	-1.649	-0.319	-0.175	-0.376
4.24	-0.859	0.000	-1.590	-0.322	-0.175	-0.385
4.25	-0.781	0.313	-1.178	-0.324	-0.172	-0.391
4.26	-0.781	0.313	-0.943	-0.327	-0.169	-0.393
4.27	-0.781	0.313	-0.943	-0.329	-0.166	-0.396
4.28	-0.703	0.313	-0.884	-0.330	-0.163	-0.399
4.29	-0.703	0.313	-0.884	-0.332	-0.159	-0.401
4.30	-0.625	0.313	-0.884	-0.333	-0.156	-0.403
4.31	-0.547	0.313	-0.884	-0.333	-0.153	-0.406
4.32	-0.469	0.313	-0.766	-0.332	-0.150	-0.407
4.33	-0.391	0.313	-0.648	-0.330	-0.147	-0.407
4.34	-0.313	0.313	-0.471	-0.328	-0.144	-0.405
4.35	-0.313	0.469	-0.471	-0.325	-0.139	-0.403
4.36	-0.078	0.625	-0.412	-0.321	-0.133	-0.401
4.37	-0.078	0.625	-0.353	-0.316	-0.127	-0.398

Figure 6.9.2.1 Digital data for event 4.1 (continued)

Time (μs)	$\partial B_E/\partial t$ (T/s)	$\partial B_N/\partial t$ (T/s)	$Z_o \partial D_z/\partial t$ (T/s)	B_E (μT)	B_N (μT)	$Z_o D_z$ (μT)
4.38	0.000	0.625	-0.236	-0.310	-0.120	-0.394
4.39	0.156	0.625	-0.177	-0.303	-0.114	-0.389
4.40	0.234	0.625	-0.177	-0.296	-0.108	-0.385
4.41	0.234	0.625	-0.118	-0.288	-0.102	-0.379
4.42	0.313	0.781	-0.059	-0.279	-0.094	-0.373
4.43	0.313	0.781	-0.059	-0.271	-0.086	-0.368
4.44	0.313	0.781	-0.059	-0.262	-0.078	-0.362
4.45	0.313	0.781	0.000	-0.253	-0.070	-0.355
4.46	0.391	0.781	0.000	-0.244	-0.063	-0.349
4.47	0.391	0.781	0.000	-0.235	-0.055	-0.342
4.48	0.391	0.781	0.000	-0.225	-0.047	-0.336
4.49	0.391	0.625	0.000	-0.216	-0.041	-0.329
4.50	0.391	0.625	0.000	-0.207	-0.035	-0.323
4.51	0.391	0.625	0.000	-0.197	-0.028	-0.316
4.52	0.391	0.625	0.000	-0.188	-0.022	-0.310
4.53	0.313	0.625	0.000	-0.179	-0.016	-0.303
4.54	0.313	0.625	0.000	-0.171	-0.010	-0.297
4.55	0.313	0.625	0.000	-0.162	-0.003	-0.290
4.56	0.391	0.469	0.059	-0.153	0.001	-0.283
4.57	0.391	0.469	0.059	-0.143	0.006	-0.276
4.58	0.391	0.469	0.118	-0.134	0.011	-0.269
4.59	0.391	0.469	0.118	-0.124	0.016	-0.261
4.60	0.391	0.469	0.118	-0.115	0.020	-0.253
4.61	0.313	0.469	0.118	-0.107	0.025	-0.246
4.62	0.313	0.313	0.059	-0.098	0.028	-0.239
4.63	0.313	0.313	0.000	-0.089	0.031	-0.232
4.64	0.234	0.313	-0.059	-0.082	0.034	-0.226
4.65	0.234	0.313	-0.059	-0.074	0.037	-0.220
4.66	0.234	0.313	-0.059	-0.066	0.041	-0.214
4.67	0.234	0.313	-0.059	-0.058	0.044	-0.208
4.68	0.234	0.313	-0.059	-0.050	0.047	-0.203
4.69	0.156	0.313	-0.059	-0.043	0.050	-0.197
4.70	0.156	0.313	-0.059	-0.036	0.053	-0.191
4.71	0.078	0.156	-0.118	-0.030	0.055	-0.186
4.72	0.078	0.156	-0.118	-0.024	0.056	-0.180
4.73	0.078	0.156	-0.118	-0.017	0.058	-0.175
4.74	0.078	0.156	-0.118	-0.011	0.059	-0.170
4.75	0.078	0.156	-0.177	-0.005	0.061	-0.165
4.76	0.078	0.156	-0.177	0.001	0.062	-0.160
4.77	0.078	0.156	-0.177	0.008	0.064	-0.155
4.78	0.078	0.156	-0.177	0.014	0.066	-0.151
4.79	-0.156	0.156	-0.177	0.018	0.067	-0.146
4.80	-0.156	0.156	-0.236	0.022	0.069	-0.142
4.81	-0.156	0.156	-0.236	0.026	0.070	-0.138
4.82	-0.156	0.156	-0.236	0.029	0.072	-0.134
4.83	-0.156	0.156	-0.236	0.033	0.073	-0.130
4.84	-0.156	0.156	-0.295	0.037	0.075	-0.126
4.85	-0.234	0.156	-0.295	0.040	0.076	-0.122
4.86	-0.234	0.156	-0.353	0.044	0.078	-0.120

Figure 6.9.2.1 Digital data for event 4.1 (continued)

Time (μs)	$\partial B_E/\partial t$ (T/s)	$\partial B_N/\partial t$ (T/s)	$Z_o \partial D_z/\partial t$ (T/s)	B_E (μT)	B_N (μT)	$Z_o D_z$ (μT)
4.87	-0.234	0.156	-0.353	0.047	0.080	-0.117
4.88	-0.234	0.156	-0.353	0.050	0.081	-0.114
4.89	-0.313	0.156	-0.412	0.052	0.083	-0.111
4.90	-0.313	0.156	-0.412	0.054	0.084	-0.109
4.91	-0.313	0.156	-0.412	0.056	0.086	-0.107
4.92	-0.313	0.000	-0.412	0.059	0.086	-0.104
4.93	-0.313	0.000	-0.471	0.061	0.086	-0.103
4.94	-0.313	0.000	-0.471	0.063	0.086	-0.101
4.95	-0.313	0.000	-0.471	0.066	0.086	-0.099
4.96	-0.313	0.000	-0.471	0.068	0.086	-0.097
4.97	-0.391	0.000	-0.471	0.070	0.086	-0.095
4.98	-0.391	0.000	-0.471	0.071	0.086	-0.094
4.99	-0.391	0.000	-0.471	0.073	0.086	-0.092
5.00	-0.391	0.000	-0.530	0.074	0.086	-0.091
5.01	-0.391	0.000	-0.530	0.076	0.086	-0.090
5.02	-0.391	0.000	-0.530	0.077	0.086	-0.088
5.03	-0.469	0.000	-0.589	0.078	0.086	-0.088
5.04	-0.469	0.000	-0.589	0.079	0.086	-0.087
5.05	-0.469	0.000	-0.589	0.080	0.086	-0.087

Figure 6.9.2.2 Digital data for event 5.7

[ ] = baseline which is subtracted for peaks and numerical integration

Yeardate: 79230 Time: 13:15:17 M.S.T.

Time (μs)	$\partial B_E/\partial t$ (T/s)	$\partial B_N/\partial t$ (T/s)	$Z_o \partial D_z/\partial t$ (T/s)	B_E (μT)	B_N (μT)	$Z_o D_z$ (μT)
5.59	-0.781	-0.156	-1.178	-0.000	-0.000	-0.000
5.60	-0.781	-0.156	-1.178	-0.000	-0.000	-0.000
5.61	-0.859	-0.156	-1.119	-0.001	-0.000	0.001
5.62	-1.016	-0.156	-1.178	-0.003	-0.000	0.001
5.63	-1.328	-0.156	-1.178	-0.009	-0.000	0.001
5.64	-1.328	-0.469	-1.355	-0.014	-0.003	-0.001
5.65	-1.563	-0.469	-1.826	-0.022	-0.006	-0.008
5.66	-1.641	-0.625	-1.885	-0.030	-0.011	-0.015
5.67	-1.641	-0.781	-1.885	-0.039	-0.017	-0.022
5.68	-1.875	-0.625	-2.356	-0.050	-0.022	-0.034
5.69	-1.953	-0.625	-2.121	-0.062	-0.027	-0.043
5.70	-2.109	-0.781	-2.121	-0.075	-0.033	-0.052
5.71	-2.109	-0.938	-2.769	-0.088	-0.041	-0.068
5.72	-2.031	-0.938	-2.828	-0.101	-0.048	-0.085
5.73	-1.953	-0.938	-2.769	-0.113	-0.056	-0.101
5.74	-1.953	-0.781	-2.769	-0.124	-0.063	-0.117
5.75	-1.953	-0.781	-2.592	-0.136	-0.069	-0.131
5.76	-1.953	-0.781	-2.592	-0.148	-0.075	-0.145
5.77	-1.953	-0.781	-2.592	-0.159	-0.081	-0.159
5.78	-1.875	-0.781	-2.651	-0.170	-0.088	-0.174
5.79	-1.875	-0.781	-2.592	-0.181	-0.094	-0.188
5.80	-1.797	-0.625	-2.592	-0.191	-0.098	-0.202
5.81	-1.797	-0.625	-2.533	-0.202	-0.103	-0.216
5.82	-1.797	-0.625	-2.474	-0.212	-0.108	-0.229
5.83	-1.719	-0.625	-2.474	-0.221	-0.113	-0.242
5.84	-1.719	-0.625	-2.474	-0.231	-0.117	-0.255
5.85	-1.641	-0.625	-2.474	-0.239	-0.122	-0.267
5.86	-1.641	-0.625	-2.415	-0.248	-0.127	-0.280
5.87	-1.641	-0.625	-2.356	-0.256	-0.131	-0.292
5.88	-1.641	-0.469	-2.356	-0.265	-0.134	-0.303
5.89	-1.641	-0.469	-2.356	-0.274	-0.138	-0.315
5.90	-1.563	-0.469	-2.297	-0.281	-0.141	-0.326
5.91	-1.563	-0.469	-2.297	-0.289	-0.144	-0.338
5.92	-1.563	-0.469	-2.238	-0.297	-0.147	-0.348
5.93	-1.563	-0.469	-2.180	-0.305	-0.150	-0.358
5.94	-1.563	-0.313	-2.180	-0.313	-0.152	-0.368
5.95	-1.563	-0.469	-2.238	-0.320	-0.155	-0.379
5.96	-1.563	-0.469	-2.238	-0.328	-0.158	-0.389
5.97	-1.563	-0.469	-2.238	-0.336	-0.161	-0.400
5.98	-1.406	-0.313	-2.297	-0.342	-0.163	-0.411
5.99	-1.328	-0.313	-2.238	-0.348	-0.164	-0.422
6.00	-1.250	-0.313	-2.180	-0.352	-0.166	-0.432
6.01	-1.250	-0.313	-2.121	-0.357	-0.167	-0.441

Figure 6.9.2.2 Digital data for event 5.7 (continued)

Time (μs)	$\partial B_E/\partial t$ (T/s)	$\partial B_N/\partial t$ (T/s)	$Z_o \partial D_z/\partial t$ (T/s)	B_E (μT)	B_N (μT)	$Z_o D_z$ (μT)
6.01	-1.250	-0.313	-2.121	-0.362	-0.169	-0.450
6.02	-1.172	-0.313	-2.062	-0.366	-0.170	-0.459
6.03	-1.172	-0.313	-2.062	-0.370	-0.172	-0.468
6.04	-1.172	-0.156	-2.003	-0.373	-0.172	-0.476
6.05	-1.172	-0.156	-2.003	-0.377	-0.172	-0.485
6.06	-1.172	-0.156	-1.944	-0.381	-0.172	-0.492
6.07	-1.172	-0.156	-1.944	-0.385	-0.172	-0.500
6.08	-1.172	-0.156	-1.944	-0.389	-0.172	-0.508
6.09	-1.172	-0.156	-1.944	-0.393	-0.172	-0.515
6.10	-1.172	-0.156	-1.885	-0.397	-0.172	-0.522
6.11	-1.172	-0.156	-1.885	-0.401	-0.172	-0.529
6.12	-1.172	-0.156	-1.885	-0.405	-0.172	-0.536
6.13	-1.172	0.000	-1.885	-0.409	-0.170	-0.544
6.14	-1.094	0.000	-1.885	-0.412	-0.169	-0.551
6.15	-1.094	0.000	-1.885	-0.415	-0.167	-0.558
6.16	-1.094	0.000	-1.885	-0.418	-0.165	-0.565
6.17	-1.094	0.000	-1.885	-0.421	-0.164	-0.572
6.18	-1.016	0.000	-1.826	-0.423	-0.162	-0.578
6.19	-1.016	0.000	-1.826	-0.426	-0.161	-0.585
6.20	-1.016	0.000	-1.826	-0.428	-0.159	-0.591
6.21	-1.016	0.000	-1.826	-0.430	-0.158	-0.598
6.22	-0.938	0.000	-1.826	-0.432	-0.156	-0.604
6.23	-0.938	0.000	-1.767	-0.434	-0.155	-0.610
6.24	-0.938	0.000	-1.767	-0.435	-0.153	-0.616
6.25	-0.859	0.000	-1.708	-0.436	-0.151	-0.621
6.26	-0.859	0.000	-1.708	-0.437	-0.150	-0.627
6.27	-0.781	0.000	-1.649	-0.437	-0.148	-0.631
6.28	-0.781	0.000	-1.649	-0.437	-0.147	-0.636
6.29	-0.781	0.000	-1.590	-0.437	-0.145	-0.640
6.30	-0.703	0.000	-1.590	-0.436	-0.144	-0.644
6.31	-0.703	0.000	-1.532	-0.435	-0.142	-0.648
6.32	-0.703	0.000	-1.473	-0.434	-0.141	-0.651
6.33	-0.625	0.000	-1.473	-0.433	-0.139	-0.654
6.34	-0.625	0.000	-1.414	-0.431	-0.137	-0.656
6.35	-0.625	0.000	-1.355	-0.430	-0.136	-0.658
6.36	-0.547	0.000	-1.355	-0.427	-0.134	-0.660
6.37	-0.547	0.000	-1.355	-0.425	-0.133	-0.661
6.38	-0.547	0.000	-1.296	-0.423	-0.131	-0.663
6.39	-0.547	0.000	-1.237	-0.420	-0.130	-0.663
6.40	-0.547	0.000	-1.237	-0.418	-0.128	-0.664
6.41	-0.469	0.156	-1.237	-0.415	-0.125	-0.664
6.42	-0.391	0.156	-1.237	-0.411	-0.122	-0.665
6.43	-0.391	0.156	-1.237	-0.407	-0.119	-0.665
6.44	-0.313	0.156	-1.178	-0.402	-0.116	-0.665
6.45	-0.313	0.000	-1.119	-0.397	-0.114	-0.664
6.46	-0.391	0.000	-1.119	-0.393	-0.113	-0.664
6.47	-0.625	0.000	-1.178	-0.392	-0.111	-0.664
6.48	-0.625	0.000	-1.178	-0.390	-0.110	-0.664

Figure 6.9.2.2 Digital data for event 5.7 (continued)

Time (μs)	$\partial B_E/\partial t$ (T/s)	$\partial B_N/\partial t$ (T/s)	$Z_o \partial D_z/\partial t$ (T/s)	B_E (μT)	B_N (μT)	$Z_o D_z$ (μT)
6.49	-0.625	0.000	-1.355	-0.389	-0.108	-0.666
6.50	-0.625	0.000	-1.355	-0.387	-0.107	-0.667
6.51	-0.469	0.000	-1.355	-0.384	-0.105	-0.669
6.52	-0.391	0.000	-1.355	-0.380	-0.104	-0.671
6.53	-0.391	0.156	-1.355	-0.376	-0.100	-0.673
6.54	-0.391	0.156	-1.119	-0.372	-0.097	-0.672
6.55	-0.391	0.000	-1.119	-0.368	-0.096	-0.671
6.56	-0.469	0.000	-1.178	-0.365	-0.094	-0.671
6.57	-0.469	0.000	-1.355	-0.362	-0.093	-0.673
6.58	-0.469	0.000	-1.237	-0.359	-0.091	-0.674
6.59	-0.547	0.000	-1.355	-0.357	-0.089	-0.676
6.60	-0.547	0.000	-1.355	-0.354	-0.088	-0.677
6.61	-0.469	0.000	-1.414	-0.351	-0.086	-0.680
6.62	-0.469	0.000	-1.355	-0.348	-0.085	-0.682
6.63	-0.391	0.000	-1.414	-0.344	-0.083	-0.684
6.64	-0.391	0.000	-1.355	-0.340	-0.082	-0.686
6.65	-0.391	0.000	-1.178	-0.336	-0.080	-0.686
6.66	-0.313	0.000	-1.119	-0.332	-0.079	-0.685
6.67	-0.313	0.000	-1.178	-0.327	-0.077	-0.685
6.68	-0.313	0.000	-1.178	-0.322	-0.075	-0.685
6.69	-0.391	0.000	-1.178	-0.318	-0.074	-0.685
6.70	-0.391	0.000	-1.178	-0.315	-0.072	-0.685
6.71	-0.391	0.000	-1.178	-0.311	-0.071	-0.685
6.72	-0.391	0.000	-1.237	-0.307	-0.069	-0.686
6.73	-0.469	0.000	-1.237	-0.304	-0.068	-0.686
6.74	-0.469	0.000	-1.237	-0.301	-0.066	-0.687
6.75	-0.469	0.000	-1.237	-0.297	-0.065	-0.687
6.76	-0.469	0.000	-1.237	-0.294	-0.063	-0.688
6.77	-0.469	0.000	-1.237	-0.291	-0.061	-0.689
6.78	-0.469	0.000	-1.237	-0.288	-0.060	-0.689
6.79	-0.469	0.000	-1.237	-0.285	-0.058	-0.690
6.80	-0.469	0.000	-1.237	-0.282	-0.057	-0.690
6.81	-0.469	0.000	-1.237	-0.279	-0.055	-0.691
6.82	-0.469	0.000	-1.237	-0.276	-0.054	-0.692
6.83	-0.469	0.000	-1.296	-0.272	-0.052	-0.693
6.84	-0.469	0.000	-1.296	-0.269	-0.050	-0.694
6.85	-0.469	0.000	-1.296	-0.266	-0.049	-0.695
6.86	-0.469	0.000	-1.296	-0.263	-0.047	-0.696
6.87	-0.469	0.000	-1.296	-0.260	-0.046	-0.697
6.88	-0.469	0.000	-1.296	-0.257	-0.044	-0.699
6.89	-0.469	0.000	-1.296	-0.254	-0.043	-0.700
6.90	-0.469	0.000	-1.296	-0.251	-0.041	-0.701
6.91	-0.547	-0.156	-1.296	-0.248	-0.041	-0.702

Figure 6.9.2.3 Digital data for event 11.8

[ ] = baseline which is subtracted for peaks and numerical integration

Yeardate: 79230 Time: 13:15:17 M.S.T.

Time (μs)	$\partial B_E/\partial t$ (T/s)	$\partial B_N/\partial t$ (T/s)	$Z_o \partial D_z/\partial t$ (T/s)	B_E (μT)	B_N (μT)	$Z_o D_z$ (μT)
11.63	-0.547	0.625	-1.001	0.000	0.000	-0.000
11.64	-0.547	0.625	-1.001	0.000	0.000	-0.000
11.65	-0.625	0.625	-1.001	-0.001	0.000	-0.000
11.66	-0.625	0.469	-1.060	-0.002	-0.002	-0.001
11.67	-0.703	0.469	-1.119	-0.003	-0.003	-0.002
11.68	-0.703	0.313	-1.178	-0.005	-0.006	-0.004
11.69	-0.703	0.313	-1.178	-0.006	-0.009	-0.005
11.70	-0.781	0.313	-1.237	-0.009	-0.013	-0.008
11.71	-0.859	0.313	-1.237	-0.012	-0.016	-0.010
11.72	-0.859	0.313	-1.296	-0.015	-0.019	-0.013
11.73	-0.859	0.313	-1.296	-0.018	-0.022	-0.016
11.74	-0.938	0.313	-1.355	-0.022	-0.025	-0.019
11.75	-1.016	0.313	-1.414	-0.027	-0.028	-0.024
11.76	-1.016	0.313	-1.414	-0.031	-0.031	-0.028
11.77	-1.094	0.313	-1.414	-0.037	-0.034	-0.032
11.78	-1.094	0.313	-1.532	-0.042	-0.038	-0.037
11.79	-1.172	0.313	-1.532	-0.048	-0.041	-0.042
11.80	-1.250	0.313	-1.590	-0.055	-0.044	-0.048
11.81	-1.250	0.156	-1.590	-0.062	-0.048	-0.054
11.82	-1.328	0.156	-1.649	-0.070	-0.053	-0.061
11.83	-1.250	0.156	-1.826	-0.077	-0.058	-0.069
11.84	-1.016	0.156	-1.826	-0.082	-0.063	-0.077
11.85	-0.938	0.313	-1.826	-0.086	-0.066	-0.086
11.86	-0.938	0.313	-1.590	-0.090	-0.069	-0.091
11.87	-0.938	0.625	-1.414	-0.094	-0.069	-0.096
11.88	-0.938	0.625	-1.414	-0.098	-0.069	-0.100
11.89	-0.859	0.781	-1.414	-0.101	-0.067	-0.104
11.90	-0.781	0.781	-1.355	-0.103	-0.066	-0.107
11.91	-0.781	0.781	-1.178	-0.105	-0.064	-0.109
11.92	-0.781	0.781	-1.178	-0.108	-0.063	-0.111
11.93	-0.703	0.781	-1.178	-0.109	-0.061	-0.113
11.94	-0.625	0.781	-1.178	-0.110	-0.059	-0.114
11.95	-0.625	0.781	-1.178	-0.111	-0.058	-0.116
11.96	-0.469	0.781	-1.119	-0.110	-0.056	-0.117
11.97	-0.391	0.781	-1.001	-0.109	-0.055	-0.117
11.98	-0.313	0.781	-0.943	-0.107	-0.053	-0.116
11.99	-0.313	0.938	-0.884	-0.104	-0.050	-0.115
12.00	-0.156	0.938	-0.825	-0.100	-0.047	-0.113
12.01	-0.156	0.938	-0.766	-0.096	-0.044	-0.111
12.02	-0.156	0.938	-0.648	-0.093	-0.041	-0.108
12.03	-0.156	0.938	-0.648	-0.089	-0.038	-0.104
12.04	-0.156	0.938	-0.530	-0.085	-0.035	-0.099
12.05	-0.156	0.938	-0.530	-0.081	-0.032	-0.095
12.06	-0.156	0.938	-0.589	-0.077	-0.028	-0.091
12.07	-0.156	0.781	-0.648	-0.073	-0.027	-0.087

Figure 6.9.2.3 Digital data for event 11.8 (continued)

Time (μs)	$\partial B_E/\partial t$ (T/s)	$\partial B_N/\partial t$ (T/s)	$Z_o \partial D_z/\partial t$ (T/s)	B_E (μT)	B_N (μT)	$Z_o D_z$ (μT)
12.08	-0.156	0.781	-0.648	-0.069	-0.025	-0.083
12.09	-0.234	0.625	-0.648	-0.066	-0.025	-0.080
12.10	-0.313	0.469	-0.707	-0.064	-0.027	-0.077
12.11	-0.391	0.469	-0.884	-0.062	-0.028	-0.076
12.12	-0.391	0.469	-0.943	-0.061	-0.030	-0.075
12.13	-0.469	0.469	-1.119	-0.060	-0.032	-0.076
12.14	-0.547	0.469	-1.178	-0.060	-0.033	-0.078
12.15	-0.469	0.469	-1.178	-0.059	-0.035	-0.080
12.16	-0.469	0.469	-1.237	-0.058	-0.036	-0.082
12.17	-0.469	0.469	-1.237	-0.057	-0.038	-0.085
12.18	-0.391	0.469	-1.178	-0.056	-0.039	-0.086
12.19	-0.391	0.469	-1.119	-0.054	-0.041	-0.088
12.20	-0.469	0.469	-1.119	-0.054	-0.043	-0.089
12.21	-0.625	0.313	-1.060	-0.054	-0.046	-0.089
12.22	-0.625	0.313	-1.060	-0.055	-0.049	-0.090
12.23	-0.625	0.313	-1.178	-0.056	-0.052	-0.092
12.24	-0.625	0.313	-1.355	-0.057	-0.055	-0.095
12.25	-0.625	0.313	-1.355	-0.057	-0.058	-0.099
12.26	-0.625	0.313	-1.355	-0.058	-0.061	-0.102
12.27	-0.547	0.313	-1.296	-0.058	-0.064	-0.105
12.28	-0.469	0.313	-1.237	-0.057	-0.068	-0.108
12.29	-0.391	0.313	-1.237	-0.056	-0.071	-0.110
12.30	-0.313	0.313	-1.237	-0.053	-0.074	-0.112
12.31	-0.313	0.313	-1.119	-0.051	-0.077	-0.114
12.32	-0.313	0.469	-0.943	-0.049	-0.078	-0.113
12.33	-0.234	0.469	-0.943	-0.046	-0.080	-0.112
12.34	-0.234	0.469	-0.884	-0.043	-0.082	-0.111
12.35	-0.234	0.625	-0.884	-0.039	-0.082	-0.110
12.36	-0.156	0.625	-0.825	-0.036	-0.082	-0.108
12.37	-0.156	0.625	-0.825	-0.032	-0.082	-0.107
12.38	-0.156	0.625	-0.766	-0.028	-0.082	-0.104
12.39	-0.156	0.469	-0.766	-0.024	-0.083	-0.102
12.40	-0.156	0.469	-0.766	-0.020	-0.085	-0.100
12.41	-0.156	0.469	-0.766	-0.016	-0.086	-0.097
12.42	-0.156	0.469	-0.766	-0.012	-0.088	-0.095
12.43	-0.156	0.469	-0.766	-0.008	-0.089	-0.092
12.44	-0.156	0.469	-0.766	-0.004	-0.091	-0.090
12.45	-0.156	0.469	-0.766	-0.000	-0.093	-0.088
12.46	-0.156	0.469	-0.825	0.004	-0.094	-0.086

Figure 6.9.2.4 Digital data for event 12.2

[ ] = baseline which is subtracted for peaks and numerical integration

Yeardate: 79230 Time: 13:15:17 M.S.T.

Time (μs)	$\partial B_E/\partial t$ (T/s)	$\partial B_N/\partial t$ (T/s)	$Z_o \partial D_z/\partial t$ (T/s)	B_E (μT)	B_N (μT)	$Z_o D_z$ (μT)
12.04	-0.156	0.938	-0.530	-0.000	-0.000	-0.000
12.05	-0.156	0.938	-0.530	-0.000	-0.000	-0.000
12.06	-0.156	0.938	-0.589	-0.000	-0.000	-0.001
12.07	-0.156	0.781	-0.648	-0.000	-0.002	-0.002
12.08	-0.156	0.781	-0.648	-0.000	-0.003	-0.003
12.09	-0.234	0.625	-0.648	-0.001	-0.006	-0.004
12.10	-0.313	0.469	-0.707	-0.002	-0.011	-0.006
12.11	-0.391	0.469	-0.884	-0.005	-0.016	-0.009
12.12	-0.391	0.469	-0.943	-0.007	-0.020	-0.014
12.13	-0.469	0.469	-1.119	-0.010	-0.025	-0.019
12.14	-0.547	0.469	-1.178	-0.014	-0.030	-0.026
12.15	-0.469	0.469	-1.178	-0.017	-0.034	-0.032
12.16	-0.469	0.469	-1.237	-0.020	-0.039	-0.039
12.17	-0.469	0.469	-1.237	-0.023	-0.044	-0.047
12.18	-0.391	0.469	-1.178	-0.026	-0.049	-0.053
12.19	-0.391	0.469	-1.119	-0.028	-0.053	-0.059
12.20	-0.469	0.469	-1.119	-0.031	-0.058	-0.065
12.21	-0.625	0.313	-1.060	-0.036	-0.064	-0.070
12.22	-0.625	0.313	-1.060	-0.041	-0.070	-0.075
12.23	-0.625	0.313	-1.178	-0.045	-0.077	-0.082
12.24	-0.625	0.313	-1.355	-0.050	-0.083	-0.090
12.25	-0.625	0.313	-1.355	-0.055	-0.089	-0.098
12.26	-0.625	0.313	-1.355	-0.059	-0.095	-0.107
12.27	-0.547	0.313	-1.296	-0.063	-0.102	-0.114
12.28	-0.469	0.313	-1.237	-0.066	-0.108	-0.121
12.29	-0.391	0.313	-1.237	-0.069	-0.114	-0.128
12.30	-0.313	0.313	-1.237	-0.070	-0.120	-0.136
12.31	-0.313	0.313	-1.119	-0.072	-0.127	-0.141
12.32	-0.313	0.469	-0.943	-0.074	-0.131	-0.146
12.33	-0.234	0.469	-0.943	-0.074	-0.136	-0.150
12.34	-0.234	0.469	-0.884	-0.075	-0.141	-0.153
12.35	-0.234	0.625	-0.884	-0.076	-0.144	-0.157
12.36	-0.156	0.625	-0.825	-0.076	-0.147	-0.160
12.37	-0.156	0.625	-0.825	-0.076	-0.150	-0.163
12.38	-0.156	0.625	-0.766	-0.076	-0.153	-0.165
12.39	-0.156	0.469	-0.766	-0.076	-0.158	-0.167
12.40	-0.156	0.469	-0.766	-0.076	-0.163	-0.170
12.41	-0.156	0.469	-0.766	0.076	-0.167	-0.172
12.42	-0.156	0.469	-0.766	-0.076	-0.172	-0.174
12.43	-0.156	0.469	-0.766	-0.076	-0.177	-0.177
12.44	-0.156	0.469	-0.766	-0.076	-0.181	-0.179
12.45	-0.156	0.469	-0.766	-0.076	-0.186	-0.181
12.46	-0.156	0.469	-0.825	-0.076	-0.191	-0.184

Figure 6.9.2.4 Digital data for event 12.2(continued)

Time (μs)	$\partial B_E/\partial t$ (T/s)	$\partial B_N/\partial t$ (T/s)	$Z_o \partial D_z/\partial t$ (T/s)	B_E (μT)	B_N (μT)	$Z_o D_z$ (μT)
12.47	0.078	0.469	-0.825	-0.074	-0.196	-0.187
12.48	0.078	0.469	-0.825	-0.071	-0.200	-0.190
12.49	0.078	0.625	-0.766	-0.069	-0.203	-0.193
12.50	0.078	0.625	-0.707	-0.067	-0.206	-0.194
12.51	0.078	0.625	-0.707	-0.064	-0.210	-0.196
12.52	0.078	0.625	-0.707	-0.062	-0.213	-0.198
12.53	0.078	0.625	-0.648	-0.060	-0.216	-0.199
12.54	0.078	0.625	-0.648	-0.057	-0.219	-0.200
12.55	0.078	0.625	-0.648	-0.055	-0.222	-0.202
12.56	0.078	0.625	-0.648	-0.052	-0.225	-0.203
12.57	0.078	0.625	-0.648	-0.050	-0.228	-0.204
12.58	0.078	0.469	-0.648	-0.048	-0.233	-0.205
12.59	0.078	0.469	-0.648	-0.045	-0.238	-0.206
12.60	0.078	0.469	-0.707	-0.043	-0.242	-0.208
12.61	0.078	0.469	-0.707	-0.041	-0.247	-0.210
12.62	0.078	0.469	-0.707	-0.038	-0.252	-0.212
12.63	0.078	0.469	-0.707	-0.036	-0.257	-0.213
12.64	0.078	0.469	-0.707	-0.034	-0.261	-0.215
12.65	0.078	0.313	-0.707	-0.031	-0.267	-0.217
12.66	0.156	0.313	-0.648	-0.028	-0.274	-0.218
12.67	0.156	0.313	-0.648	-0.025	-0.280	-0.219
12.68	0.156	0.313	-0.648	-0.022	-0.286	-0.220
12.69	0.156	0.313	-0.648	-0.019	-0.293	-0.222
12.70	0.156	0.313	-0.648	-0.016	-0.299	-0.223
12.71	0.156	0.313	-0.648	-0.013	-0.305	-0.224
12.72	0.156	0.313	-0.648	-0.010	-0.311	-0.225
12.73	0.234	0.313	-0.648	-0.006	-0.318	-0.226
12.74	0.313	0.313	-0.648	-0.001	-0.324	-0.227
12.75	0.313	0.313	-0.589	0.004	-0.330	-0.228
12.76	0.391	0.313	-0.530	0.009	-0.336	-0.228
12.77	0.469	0.313	-0.530	0.015	-0.342	-0.228
12.78	0.547	0.469	-0.471	0.022	-0.347	-0.227
12.79	0.625	0.469	-0.412	0.030	-0.352	-0.226
12.80	0.625	0.469	-0.295	0.038	-0.356	-0.224
12.81	0.703	0.469	-0.236	0.046	-0.361	-0.221
12.82	0.703	0.313	-0.177	0.055	-0.367	-0.217
12.83	0.703	0.313	-0.177	0.064	-0.374	-0.214
12.84	0.703	0.313	-0.118	0.072	-0.380	-0.210
12.85	0.703	0.156	-0.118	0.081	-0.388	-0.206
12.86	0.625	0.156	-0.118	0.089	-0.395	-0.202
12.87	0.547	0.000	-0.118	0.096	-0.405	-0.197
12.88	0.547	0.000	-0.177	0.103	-0.414	-0.194
12.89	0.547	0.000	-0.236	0.110	-0.424	-0.191
12.90	0.469	0.000	-0.236	0.116	-0.433	-0.188
12.91	0.469	0.000	-0.353	0.122	-0.442	-0.186
12.92	0.391	0.000	-0.412	0.128	-0.452	-0.185
12.93	0.391	0.000	-0.412	0.133	-0.461	-0.184
12.94	0.391	0.000	-0.412	0.139	-0.470	-0.183
12.95	0.391	0.000	-0.471	0.144	-0.480	-0.182
12.96	0.313	0.000	-0.530	0.149	-0.489	-0.182

Figure 6.9.2.4 Digital data for event 12.2 (continued)

Time (μs)	$\partial B_E/\partial t$ (T/s)	$\partial B_N/\partial t$ (T/s)	$Z_o \partial D_z/\partial t$ (T/s)	B_E (μT)	B_N (μT)	$Z_o D_z$ (μT)
12.97	0.313	0.000	-0.530	0.153	-0.499	-0.182
12.98	0.313	0.000	-0.530	0.158	-0.508	-0.182
12.99	0.313	0.000	-0.530	0.163	-0.517	-0.182
13.00	0.313	0.000	-0.530	0.168	-0.527	-0.182
13.01	0.313	0.000	-0.530	0.172	-0.536	-0.182
13.02	0.313	0.156	-0.530	0.177	-0.544	-0.182
13.03	0.313	0.313	-0.530	0.182	-0.550	-0.182
13.04	0.313	0.313	-0.530	0.186	-0.556	-0.182
13.05	0.313	0.313	-0.530	0.191	-0.563	-0.182
13.06	0.313	0.313	-0.471	0.196	-0.569	-0.182
13.07	0.313	0.313	-0.471	0.200	-0.575	-0.181
13.08	0.391	0.313	-0.471	0.206	-0.581	-0.180
13.09	0.391	0.313	-0.471	0.211	-0.588	-0.180
13.10	0.391	0.469	-0.412	0.217	-0.592	-0.179
13.11	0.391	0.469	-0.412	0.222	-0.597	-0.177
13.12	0.391	0.469	-0.412	0.228	-0.602	-0.176
13.13	0.391	0.469	-0.353	0.233	-0.606	-0.174
13.14	0.469	0.469	-0.295	0.239	-0.611	-0.172
13.15	0.469	0.469	-0.295	0.246	-0.616	-0.170
13.16	0.469	0.469	-0.236	0.252	-0.621	-0.167
13.17	0.469	0.469	-0.236	0.258	-0.625	-0.164
13.18	0.469	0.469	-0.177	0.264	-0.630	-0.160
13.19	0.391	0.469	-0.177	0.270	-0.635	-0.157
13.20	0.391	0.469	-0.177	0.275	-0.639	-0.153
13.21	0.313	0.469	-0.236	0.280	-0.644	-0.150
13.22	0.234	0.313	-0.236	0.284	-0.650	-0.147
13.23	0.234	0.313	-0.236	0.288	-0.657	-0.144
13.24	0.156	0.156	-0.353	0.291	-0.664	-0.143
13.25	0.078	0.156	-0.412	0.293	-0.672	-0.141
13.26	0.078	0.156	-0.471	0.296	-0.680	-0.141
13.27	0.078	0.156	-0.530	0.298	-0.688	-0.141
13.28	0.078	0.156	-0.530	0.300	-0.696	-0.141
13.29	0.078	0.156	-0.530	0.303	-0.703	-0.141
13.30	0.078	0.156	-0.589	0.305	-0.711	-0.141
13.31	-0.156	0.156	-0.648	0.305	-0.719	-0.143
13.32	-0.156	0.156	-0.589	0.305	-0.727	-0.143
13.33	-0.234	0.156	-0.648	0.304	-0.735	-0.144
13.34	-0.234	0.313	-0.707	0.303	-0.741	-0.146
13.35	-0.234	0.313	-0.825	0.303	-0.747	-0.149
13.36	-0.156	0.625	-0.884	0.303	-0.750	-0.153
13.37	-0.156	0.625	-0.884	0.303	-0.753	-0.156
13.38	-0.156	0.781	-0.648	0.303	-0.755	-0.157
13.39	-0.156	0.781	-0.589	0.303	-0.757	-0.158
13.40	-0.156	0.781	-0.530	0.303	-0.758	-0.158
13.41	-0.156	0.781	-0.471	0.303	-0.760	-0.157

Figure 6.9.2.5 Digital data for event 14.0

[ ] = baseline which is subtracted for peaks and numerical integration

Yeardate: 79230 Time: 13:15:17 M.S.T.

Time (μs)	$\partial B_E/\partial t$ (T/s)	$\partial B_N/\partial t$ (T/s)	$Z_o \partial D_z/\partial t$ (T/s)	B_E (μT)	B_N (μT)	$Z_o D_z$ (μT)
13.90	-0.156	0.625	-0.589	-0.000	0.000	-0.000
13.91	-0.156	0.625	-0.589	-0.000	0.000	-0.000
13.92	-0.156	1.250	-0.530	-0.000	0.006	0.001
13.93	1.250	2.344	-0.471	0.014	0.023	0.002
13.94	1.250	1.250	-0.471	0.028	0.030	0.003
13.95	0.625	1.250	-0.412	0.036	0.036	0.005
13.96	0.313	1.094	1.414	0.041	0.041	0.025
13.97	0.313	1.094	1.001	0.045	0.045	0.041
13.98	0.234	0.469	0.059	0.049	0.044	0.047
13.99	-0.391	0.000	0.059	0.047	0.038	0.054
14.00	-0.938	-0.156	0.059	0.039	0.030	0.060
14.01	-1.250	-0.625	-0.412	0.028	0.017	0.062
14.02	-1.328	-0.781	-1.355	0.016	0.003	0.054
14.03	-1.328	-0.625	-1.826	0.004	-0.010	0.042
14.04	-0.938	-0.156	-2.062	-0.004	-0.017	0.027
14.05	-0.703	-0.156	-2.121	-0.009	-0.025	0.012
14.06	-0.625	0.000	-1.885	-0.014	-0.031	-0.001

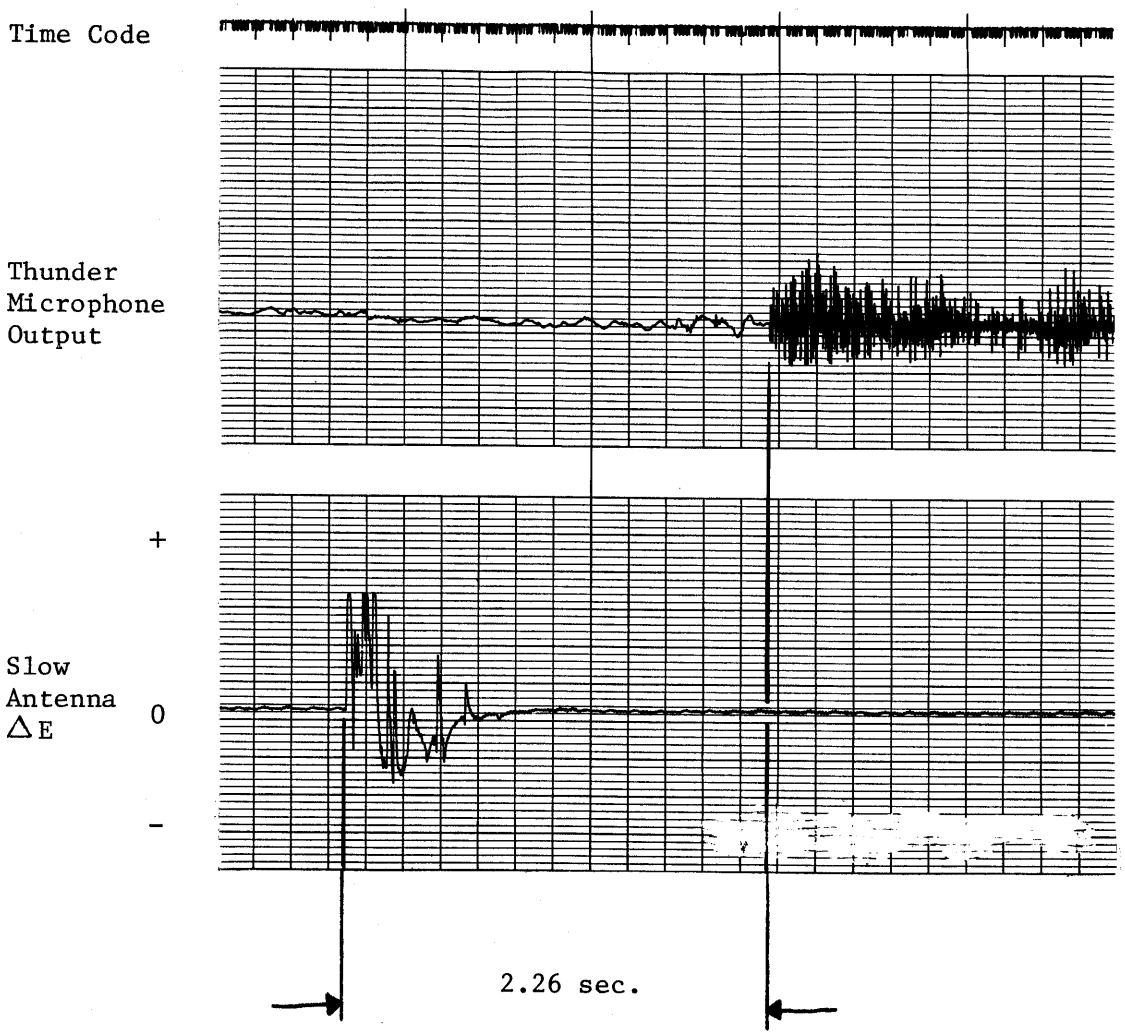

horizontal range = 759 m

Date : 79230 Time : 13:15:17

Figure 6.9.3 Slow E field change and thunder microphone record of midrange return stroke

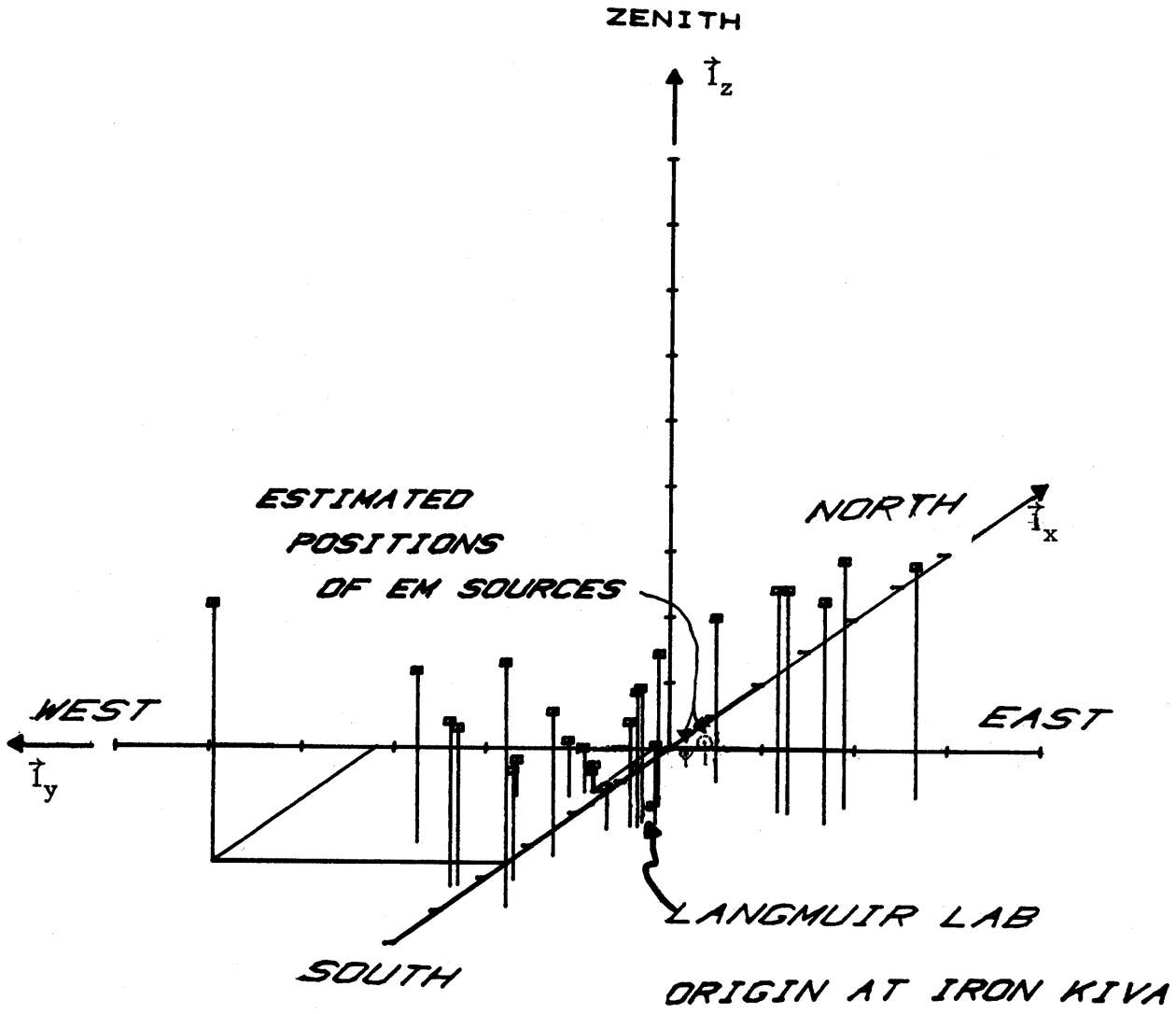

Date : 79230 Time : 13:15:17

Figure 6.9.4 Acoustic location of midrange return stroke

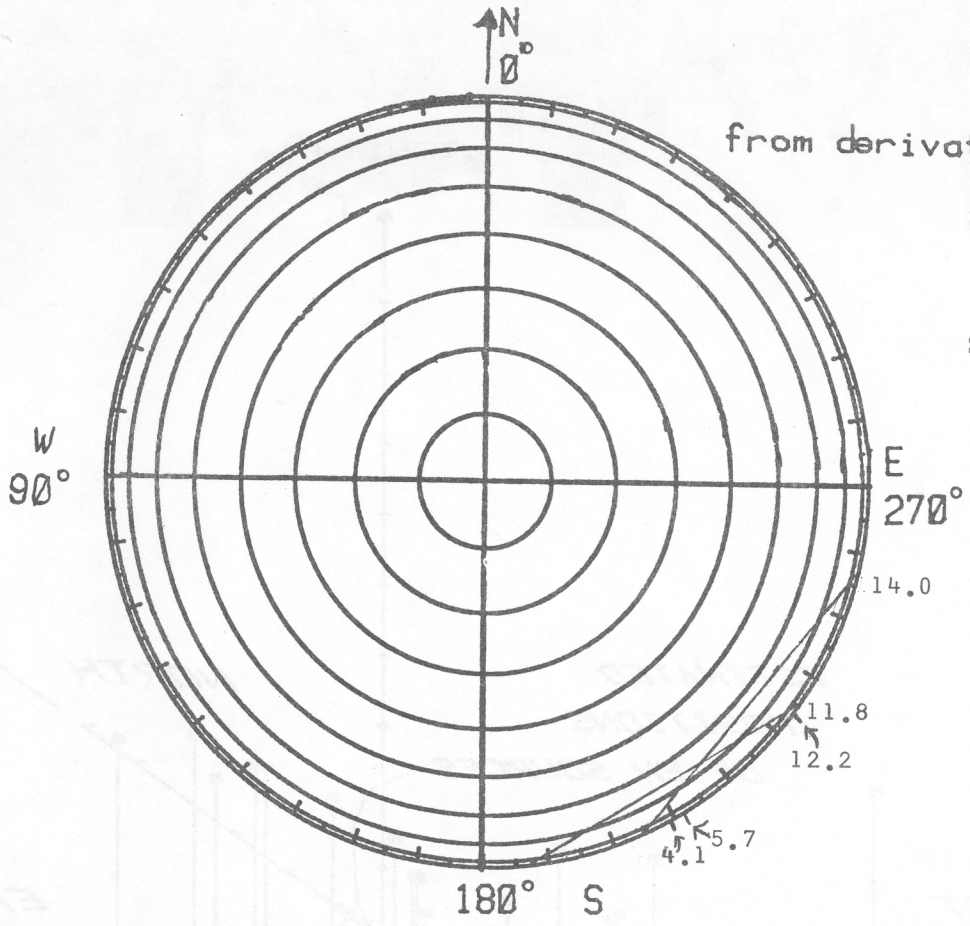

sin(θ),φ contour plot

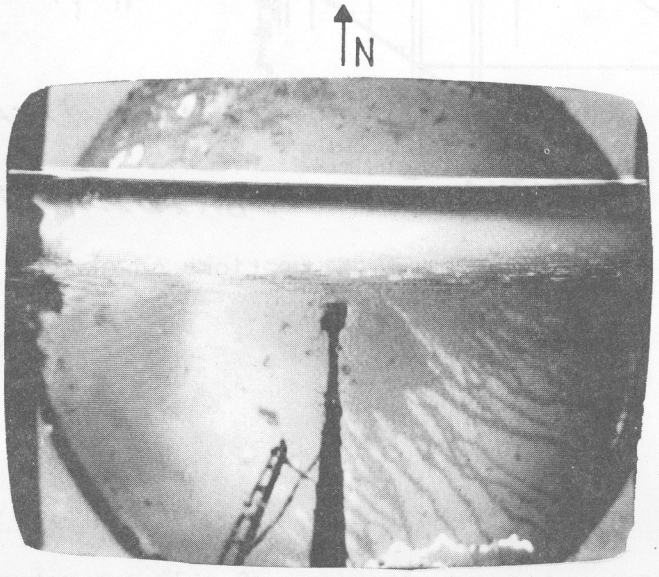

Whole-sky photograph from Kiva

Date: 79230 M.S.T.: 13:15:17

Figure 6.9.5A sin(θ),φ contours for midrange return stroke derivative waveform and whole-sky videotape photograph

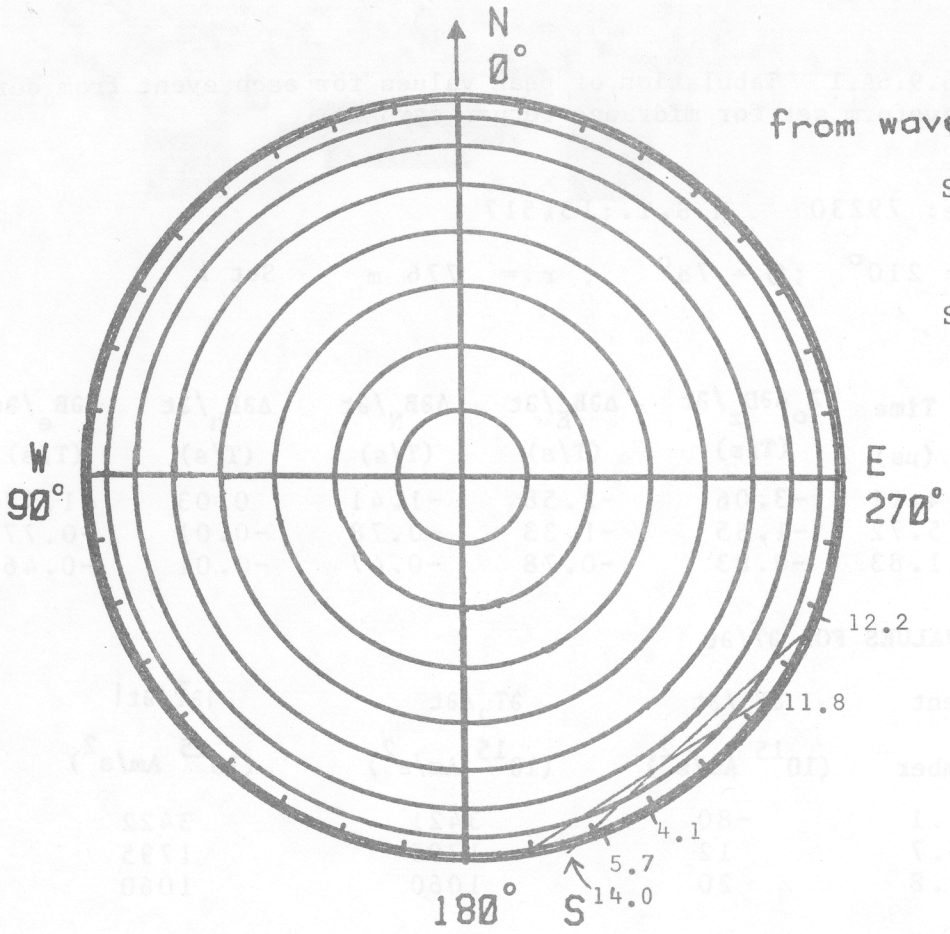

from waveform

	θ	ϕ
Set 1	75°	207°
4.1		
5.7		
11.8		
Set 2	75°	235°
12.2		
14.0		

sin(θ),ϕ contour plot

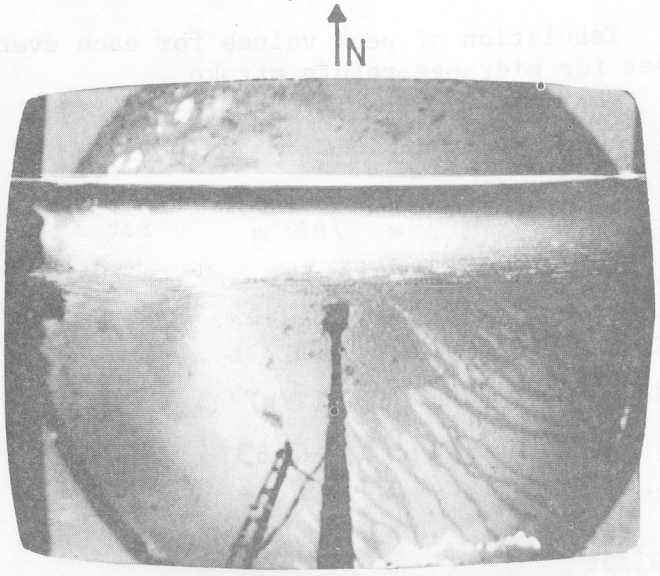

Whole-sky photograph from Kiva

Date: 79230 M.S.T.: 13:15:17

Figure 6.9.5B sin(θ),ϕ contours for midrange return stroke waveform and whole-sky videotape photograph

Figure 6.9.6A.1 Tabulation of peak values for each event from derivative waveform set for midrange return stroke

Yeardate: 79230 M.S.T.:131517

$\phi = 210^\circ$; $\theta = 78^\circ$; r = 776 m Set 1

Event Number	Time (μs)	$Z_o \Delta\partial D_z/\partial t$ (T/s)	$\Delta\partial B_E/\partial t$ (T/s)	$\Delta\partial B_N/\partial t$ (T/s)	$\Delta\partial B_h/\partial t$ (T/s)	$\Delta\partial B_e/\partial t$ (T/s)	$\lvert\Delta\partial\vec{B}/\partial t\rvert$ (T/s)
4.1	4.11	-3.06	-2.58	-1.41	0.03	-1.47	1.47
5.7	5.72	-1.65	-1.33	-0.78	-0.01	-0.77	0.77
11.8	11.83	-0.83	-0.78	-0.47	-0.01	-0.46	0.46

CALCULATED VALUES FOR $\partial\vec{T}/\partial t$

Event Number	$\partial T_2/\partial t$ (10^{15} Am/s^2)	$\partial T_3/\partial t$ (10^{15} Am/s^2)	$\lvert\partial\vec{T}/\partial t\rvert$ (10^{15} Am/s^2)	α (deg)
4.1	-80	3421	3422	1
5.7	12	1795	1795	360
11.8	20	1060	1060	359

Figure 6.9.6A.2 Tabulation of peak values for each event from derivative waveform set for midrange return stroke

Yeardate: 79230 M.S.T.:131517

$\phi = 232^\circ$; $\theta = 75^\circ$; r = 786 m Set 2

Event Number	Time (μs)	$Z_o \Delta\partial D_z/\partial t$ (T/s)	$\Delta\partial B_E/\partial t$ (T/s)	$\Delta\partial B_N/\partial t$ (T/s)	$\Delta\partial B_h/\partial t$ (T/s)	$\Delta\partial B_e/\partial t$ (T/s)	$\lvert\Delta\partial\vec{B}/\partial t\rvert$ (T/s)
12.2	12.20	-0.83	-0.47	-0.63	-0.03	-0.39	0.39
14.0	13.96	2.00	1.41	1.72	-0.10	1.11	1.12

CALCULATED VALUES FOR $\partial\vec{T}/\partial t$

Event Number	$\partial T_2/\partial t$ (10^{15} Am/s^2)	$\partial T_3/\partial t$ (10^{15} Am/s^2)	$\lvert\partial\vec{T}/\partial t\rvert$ (10^{15} Am/s^2)	α (deg)
12.2	80	926	930	355
14.0	238	-2621	2631	185

Figure 6.9.6B.1. Tabulation of peak values for each event from waveform set for midrange return stroke

Yeardate: 79230 M.S.T.:131517

$\phi = 207^\circ$; $\theta = 75^\circ$; r = 786 m Set 1

Event Number	Time (μs)	$Z_o \Delta D_s$ (μT)	ΔB_E (μT)	ΔB_N (μT)	ΔB_h (μT)	ΔB_e (μT)	$\lvert\Delta\vec{B}\rvert$ (μT)
4.1	4.11	-0.41	-0.33	-0.18	-0.02	-0.19	0.19
5.7	5.71	-0.67	-0.43	-0.17	0.08	-0.23	0.25
11.8	11.83	-0.12	-0.11	-0.07	-0.02	-0.06	0.07

CALCULATED VALUES FOR $\vec{I}_t \cdot \hat{T}$

Event Number	T_2 (10^9 Am/s)	T_3 (10^9 Am/s)	$\lvert\vec{T}\rvert$ (10^9 Am/s)	α (deg)
4.1	48	443	445	354
5.7	-199	543	578	20
11.8	57	153	163	340

Figure 6.9.6B.2 Tabulation of peak values for each event from waveform set for midrange return stroke

Yeardate: 79230 M.S.T.:131517

$\phi = 235^\circ$; $\theta = 75^\circ$; r = 786 m Set 2

Event Number	Time (μs)	$Z_o \Delta D_s$ (μT)	ΔB_E (μT)	ΔB_N (μT)	ΔB_h (μT)	ΔB_e (μT)	$\lvert\Delta\vec{B}\rvert$ (μT)
12.2	12.20	-0.23	-0.08	-0.20	-0.10	-0.10	0.14
14.0	13.99	0.06	0.05	0.05	-0.02	0.03	0.04

CALCULATED VALUES FOR $\vec{I}_t \cdot \hat{T}$

Event Number	T_2 (10^9 Am/s)	T_3 (10^9 Am/s)	$\lvert\vec{T}\rvert$ (10^9 Am/s)	α (deg)
12.2	224	247	334	318
14.0	56	-82	99	214

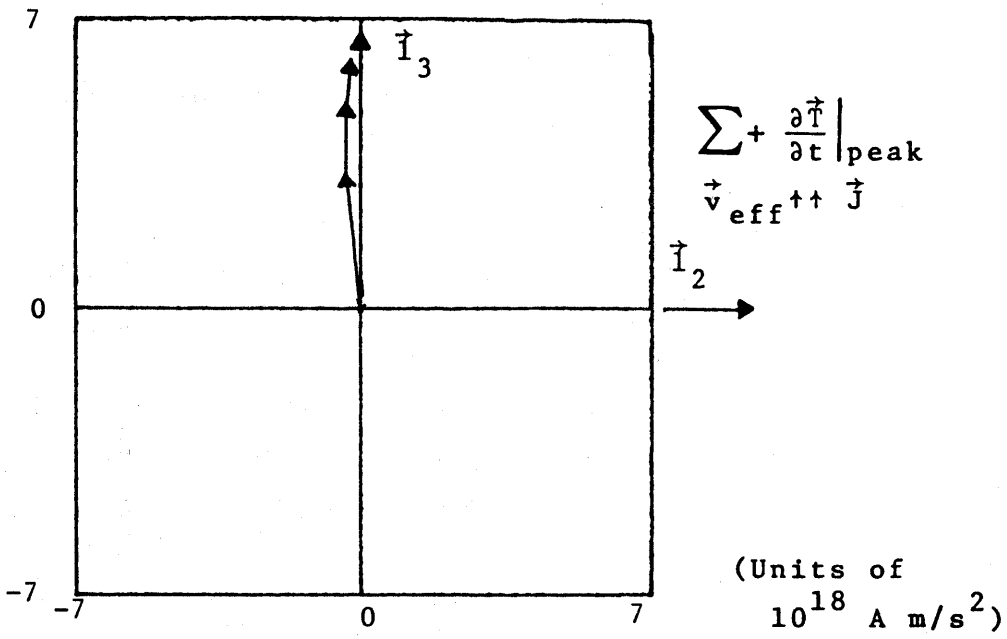

Effective reconstruction of positive streamer

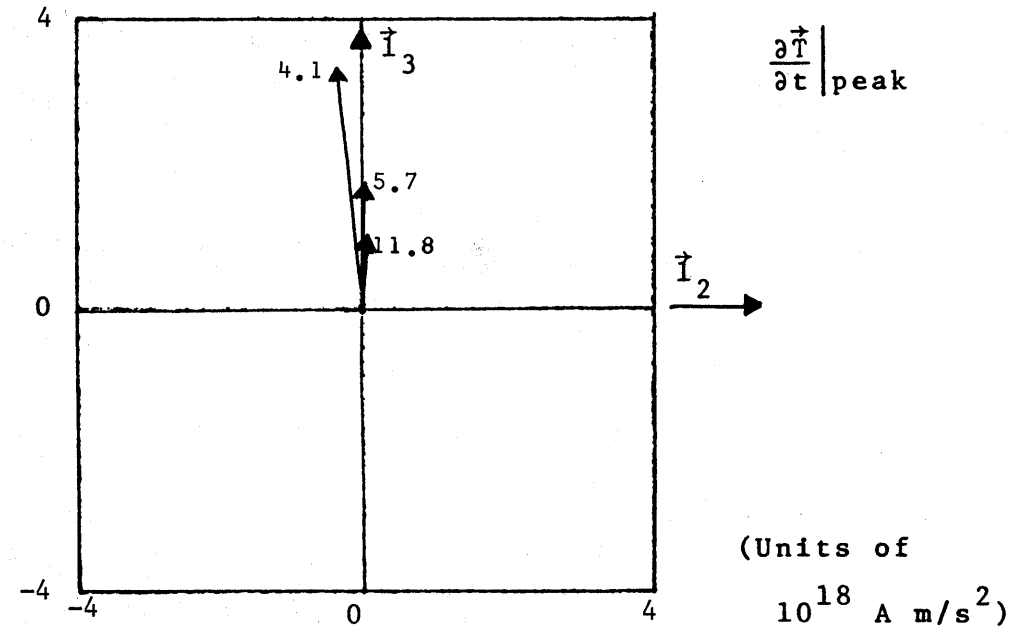

Peaks of $\partial\vec{T}/\partial t$

ϕ = 210° θ = 78° r = 776 m Set 1

Date: 79230 M.S.T.: 13:15:17

Figure 6.9.7A.1 $\partial\vec{T}/\partial t$ for midrange return stroke

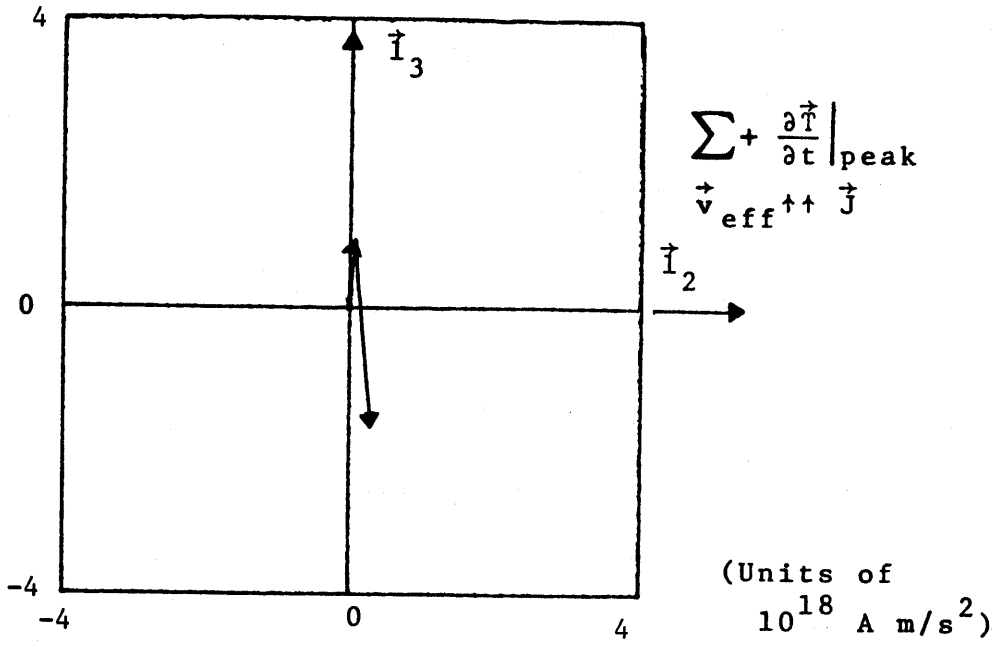

Effective reconstruction of positive streamer

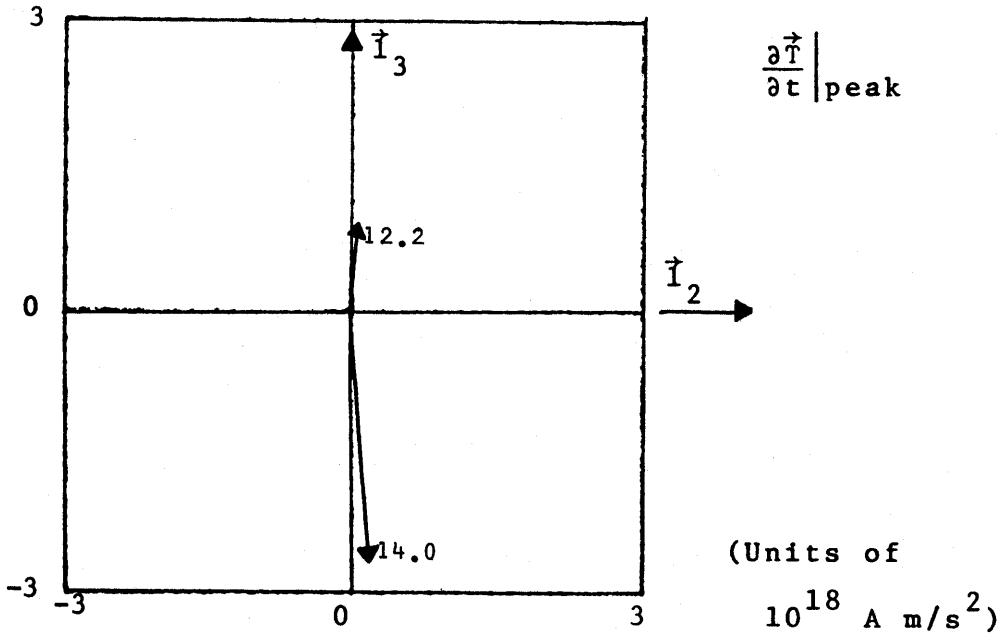

Peaks of $\partial\vec{T}/\partial t$

ϕ = 232° θ = 75° r = 786 m Set 2

Date: 79230 M.S.T.: 13:15:17

Figure 6.9.7A.2 $\partial\vec{T}/\partial t$ for midrange return stroke

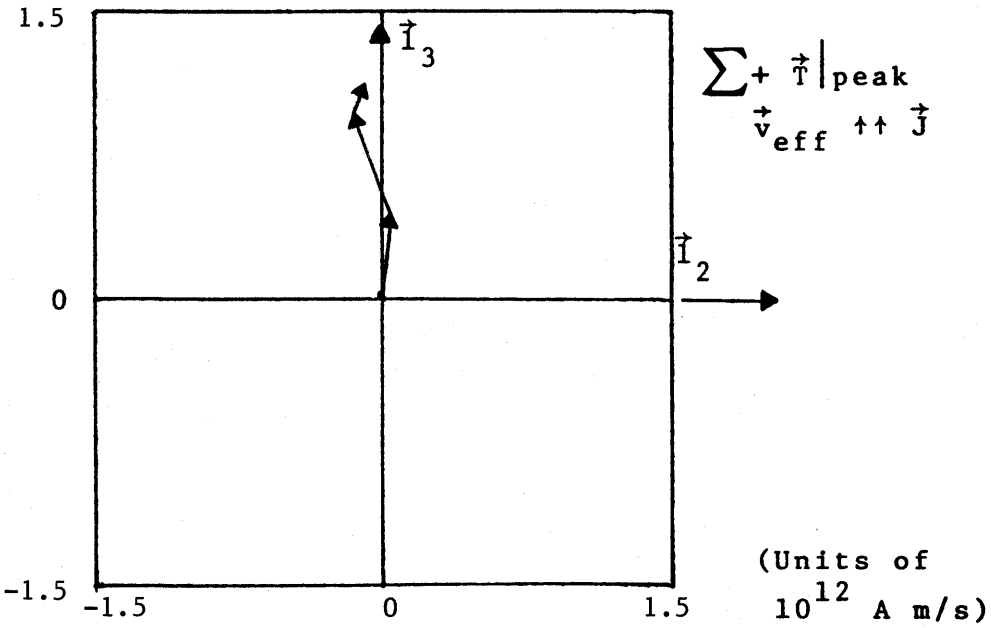

Effective reconstruction of positive streamer

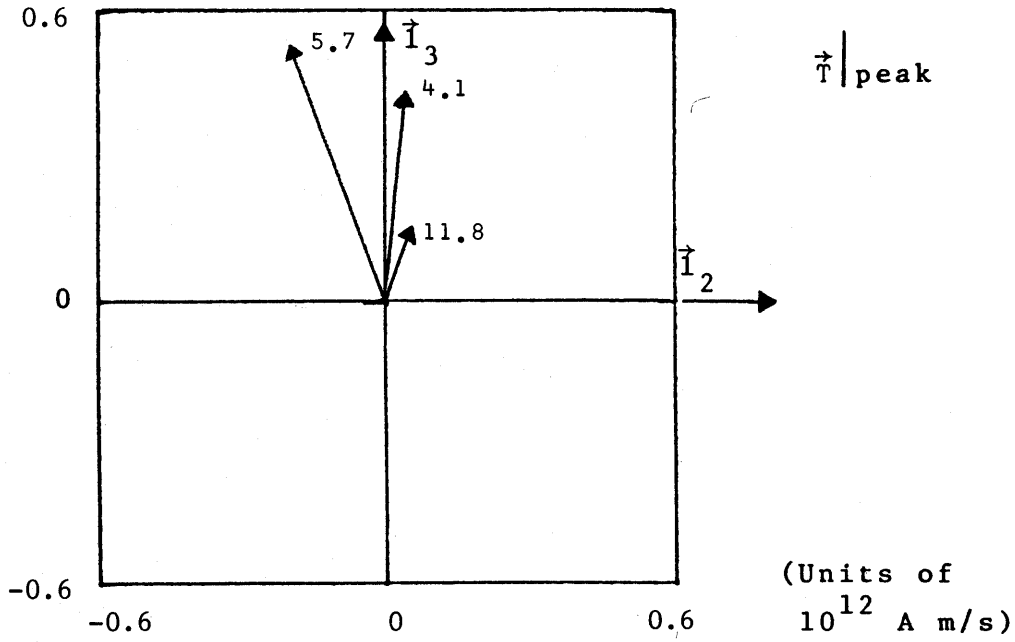

Peaks of $\vec{T}$

ϕ = 207° θ = 75° r = 786 m Set 1

Date: 79230 M.S.T.: 13:15:17

Figure 6.9.7B.1 $\vec{T}$ for midrange return stroke

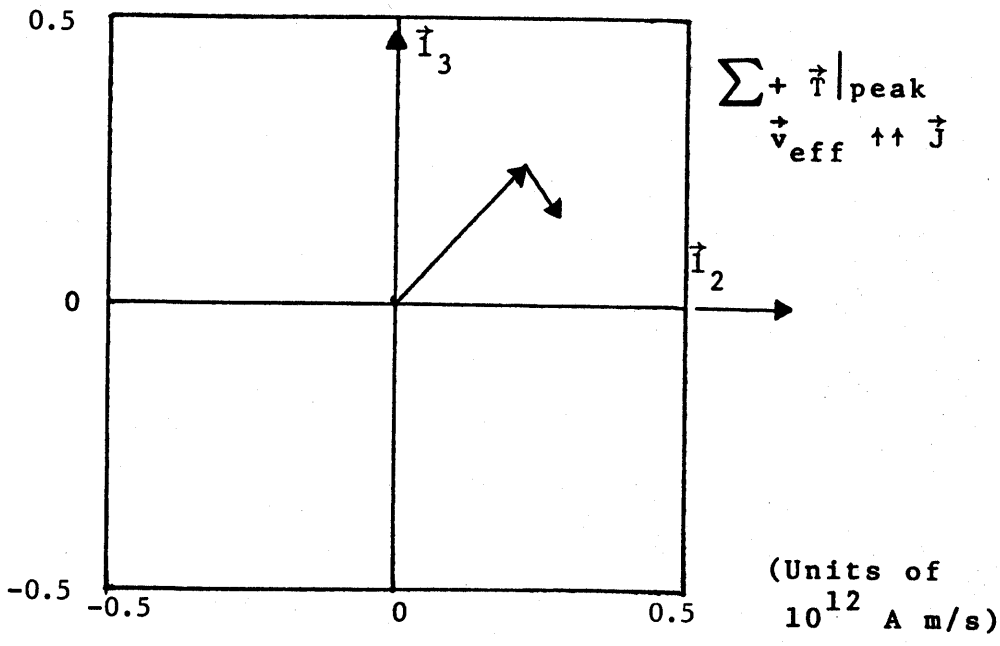

Effective reconstruction of positive streamer

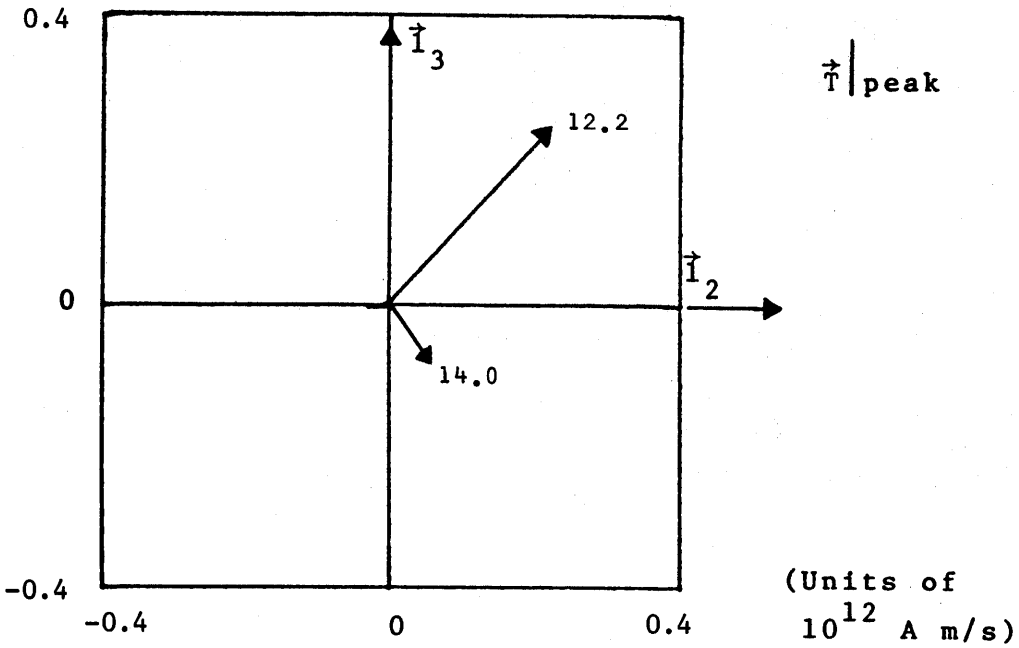

Peaks of $\vec{T}$

ϕ = 235° θ = 75° r = 786 m Set 2

Date: 79230 M.S.T.: 13:15:17

Figure 6.9.7B.2 $\vec{T}$ for midrange return stroke

VII. Some Comments Concerning the Data

These nine examples give representative characteristics of lightning near South Baldy peak. From the examples given the values of $\dot{T}$ have magnitudes (from transverse components) of about 2×10^{12} Am/s for return strokes to about 5×10^{11} Am/s for leader-like sources (noting order of magnitudes and directions of streamers toward (or away from) the observer at the Kiva). Assuming a v_{eff} of about 10^8 m/s gives 20 kA for return strokes and 5 kA for leader-like pulses. These are very variable and the number is quite approximate. Further analysis of the data may shed more insight into such results.

For these data all the lightning events represent negative charge being, in effect, lowered to earth. It would be interesting to see what would occur in the rare event of positive charge being lowered to earth.

In the recordings for the three components of field time derivative at the Kiva the peaks did not occur at exactly the same time. The separation of the sensors on the ground plane was about 11 ns, and the difference in cable transit times was about 14 ns, giving a maximum time shift of about 25 ns. This resulted in peaks on the digital printout having a relative time displacement of up to three time intervals, or 30 ns, as was observed. For the present analysis the actual peaks of the individual components, regardless of time, were used.

Unfortunately the trigger signal for the Biomation recorders was not recorded on magnetic tape in 1979, whereas it had been so recorded in 1978. This would have given even more definitiveness to the interpretations of the 3-component 1979 data. However, analysis of 1978 waveforms does indicate that to the 1 ms tape resolution, the waveforms all correspond to the first return stroke or the leader-like anticipation of this return stroke.

VIII. Summary

As the foregoing data and associated data analysis has indicated, fast nuclear-EMP related sensors and appropriate fast transient recorders have much to offer for the measurement and associated understanding of lightning electromagnetic environments. The lightning and nuclear EMP phenomena have some similar characteristics because of their common nature as transient electromagnetic phenomena.

In this report we have discussed some of the results obtained concerning lightning environments from our measurements using such instrumentation on South Baldy peak. Three electromagnetic field components (one electric, two magnetic) were measured on a ground plane with 10 ns resolution for recording times of about 20 μs. By comparing the three field components to each other, and by the use of acoustic ranging, the lightning electromagnetic sources were approximately located and their characteristics were studied.

The individual lightning waveforms yielded information concerning the temporal characteristics of leader electromagnetic fields. Pulse widths of the electromagnetic-field individual pulses varied from about half a microsecond to less than 100 ns. Characteristic times for the rise (peak field divided by peak derivative) varied from something approaching 100 ns to something less than 30 ns; rise times were a little longer than these characteristic times for the rise.

Information was also obtained concerning the temporal characteristics of return-stroke electromagnetic fields. Pulse widths (of the magnetic field) of the order of 1 μs were observed, and rise times less than 100 ns were also observed. Characteristic times for the rise of the order of 50 ns were observed.

Comparing the fast electromagnetic-field pulses from leaders and return strokes at comparable distances from source to observer shows that the return stroke field waveforms have generally larger amplitudes than those for leaders. However, for the time derivatives of the electromagnetic fields, the amplitudes for the leaders and return strokes are quite comparable.

Combining the three electromagnetic-field time-derivative waveforms (or their time integrals) one can obtain for each pulse a relation between θ and ϕ giving a contour in the θ, ϕ "plane." Intersections of such contours can give approximate (θ, ϕ) values for source location providing the corresponding pulses originate from nearly the same locations. With location, source orientation (current density transverse polarization) can then be determined. Acoustic data can be used to estimate distances to these sources. The source vectors $\overleftrightarrow{I}_t \cdot \vec{\uparrow}$ (their peaks or peak time derivatives) can then be plotted to see how the current direction changes from pulse to pulse. Connecting these vectors end to end gives a crude picture of the tortuousity of the leader path. From the magnitudes of the components of $\vec{\uparrow}$ one can obtain some information concerning currents and streamer speeds by giving these components the form Iv_{eff}. Typical current values of less

than to greater than 10 kA are consistent with streamer speeds of the order of 10^8 m/s for leader strokes and return strokes respectively.

This data has some implications concerning the formulation of criterion lightning electromagnetic environment(s). The pulses encountered are significantly faster than a microsecond in their rise characteristics, even less than 100 ns. In terms of frequency spectrum this means much more high frequency content for the individual pulses. A detailed frequency spectral analysis of these kinds of pulses would be quite useful for the formulation of lightning electromagnetic criteria. One should note that these waveforms are not strictly applicable for direct-strike lightning since measurements were not made in such an environment. One may expect some of the presently observed environmental characteristics to apply in the direct-strike case, but this is not a full description.

The measurements reported here were made on South Baldy peak. Measurements at other geographical locations with different atmospheric conditions might reveal some differences in the electromagnetic waveforms from those obtained here. Future measurements may also obtain more complete lightning waveform information by finer time resolution, longer recording time windows, and/or additional and/or more accurate tie-ins with other physical phenomena.

REFERENCES

1. Baum, C.E.: Emerging Technology for Transient and Broad-Band Analysis and Synthesis of Antennas and Scatterers, Interaction Note 300, November 1976, and Proc. IEEE, November 1976, pp. 1598-1616.

2. Longmire, C.L.: On the Electromagnetic Pulse Produced by Nuclear Explosions, IEEE Trans. Antennas and Propagation, January 1978, pp. 3-13, and IEEE Trans. Electromagnetic Compatibility, February 1978, pp. 3-13.

3. VanBladel, J.: Some Remarks on Green's Dyadic for Infinite Space, IRE Trans. Antennas and Propagation, November 1961, pp. 563-566.

4. Winn, W.P., C.B. Moore, C.R. Holmes, and L.G. Byerley III,: Thunderstorm on July 16, 1975, Over Langmuir Laboratory: A Case Study, J. Geophysical Research, vol. 83, no. C6, June 20, 1978, pp. 3079-3092.

5. Baum, C.E., E.L. Breen, C.B. Moore, J.P. O'Neill, and G.D. Sower: Electromagnetic Sensors for General Lightning Application, Symposium on Lightning Technology, NASA Conf. Pub. 2128, FAA-RD-80-30, April 1980, pp. 85-118.

6. Baum, C.E., E.L. Breen, J.P. O'Neill, C.B. Moore, and D.L. Hall: Measurement of Electromagnetic Properties of Lightning with 10 Nanosecond Resolution, Symposium on Lightning Technology, NASA Conf. Pub. 2128, FAA-RD-80,30, April 1980, pp. 39-82. This is an earlier version of the present paper.

7. Baum, C.E., E.L. Breen, F.L. Pitts, G.D. Sower, and M.E. Thomas: The Measurement of Lightning Environmental Parameters Related to Interaction with Electronic Systems, IEEE Trans. EMC, Special Issue on the subject of lightning and its interaction with aircraft, to be published in 1982.

☆U.S. GOVERNMENT PRINTING OFFICE : 1982–576-115/523